UNDERSTANDING IODINE (I/III) CATALYSIS: FROM RACEMIC TO ENANTIOSELECTIVE TRANSFORMATIONS

Eric Cots Fargas

UNIVERSITAT
ROVIRA i VIRGILI

Understanding Iodine(I/III) catalysis: From racemic to enantioselective transformations

Èric Cots Fargas

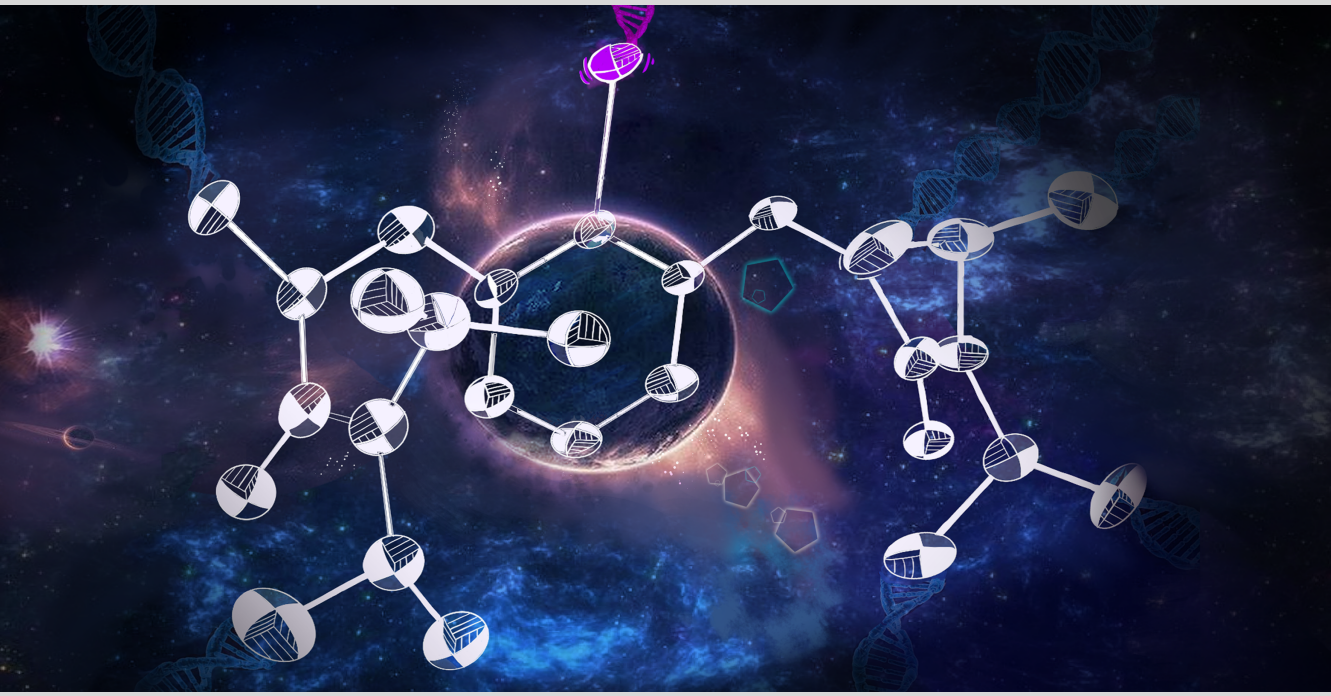

DOCTORAL THESIS
2021

PhD Thesis

“Understanding iodine (I/III) catalysis: From racemic to enantioselective transformations”

Èric Cots Fargas

Supervised by Prof. Dr. Kilian Muñiz and Prof. Dr. Marcos G. Suero

Tarragona

December 2021

Prof. Dr. Marcos G. Suero, Group Leader at the Institute of Chemical Research of Catalonia (ICIQ),

I STATE that the present Doctoral Thesis, entitled "**Understanding iodine I(I/III) catalysis: from racemic to enantioselective transformations**" presented by Èric Cots Fargas to receive the degree of Doctor, has been carried out under the supervision of Prof. Kilian Muñiz, in memoriam, and under my supervision at the Institute of Chemical Research of Catalonia (ICIQ).

Tarragona, November 2021

Doctoral Thesis Supervisor
Marcos G. Suero

Per a la meva família

“I wish it need not have happened in
my time,” said Frodo.
“So do I,” said Gandalf, “and so do all
who live to see such times. But that is not for them to decide. All we
have to decide is what to do with the time that is given us.”

J.R.R. Tolkien – The Fellowship of
The Ring (1954)

Acknowledgments

First, I would like to thank Kilian for choosing me to join his group. The way you left is not at all fair for any of us. Kilian, you and I were quite opposites in almost everything we ever spoke about. However, I will keep good memories of long football, politics and chemistry talks in the lab. As a boss, you were tough, but you always believed in us. In me. Any problem we'd encounter could be solved with more reactions. You never thought it was a question of ability but of time, patience, and a lot of lab work.

Since 2017 my goal was to prove to you that I could finish my thesis and that I was worthy of the trust you had put in me. This will never be fulfilled. You cannot imagine the void this has created in me. Another scar that we must carry.

You were a wonderful teacher. Probably one of the best I have ever had. I can state without any doubt that you have taught me most of the chemistry I now know. In a way, I have to thank you for letting me meet most of the people that will follow these lines. My time in Tarragona has been quite the adventure, with your passing and COVID-19. Altoghether, it was a bumpy ride, but I would never change a single thing. I can say with pride that I was a member of your group, and I like to think that you would be proud of all of us.

Rest in peace, Kilian.

We remember you.

En segundo lugar, quiero agradecer a Marcos que me acogiera en su grupo. Desde el principio me he sentido muy cómodo siendo tu estudiante y creo que eres un muy buen guía para el final de este viaje. Has estado muy atento conmigo y he aprendido muchísimo. Tengo que agradecerte los consejos y el tiempo que has invertido en mí, así como las largas charlas que tenemos. Gracias de corazón, Marcos, por aceptarme en tu grupo y todo lo que has hecho para mí (y esta tesis). Si no fuera por ti nunca podría haber terminado.

També vull agrair l'ajuda del Fernando i del Jeroen per a la col·laboració que hem tingut durant els últims dos anys. Aquesta tesi no hagués estat el mateix sense vosaltres, moltes gràcies per tot.

Gracias, Sorania, por ser una secretaria de primera que ha cuidado de mí durante estos cuatro años. Más que una compañera de trabajo te has convertido en una amiga y un pilar para mí en el ICIQ.

I want to thank all the current members of The Muñiz Group.

Eleni, thanks for your patience with me. You have become a good companion for the end of the journey. I will not forget our long talks and the good times in the lab. I will miss you now that you are leaving me alone.

Aliénor, you are a wonderful labmate and friend. I have always believed you have one of the purest hearts I've ever seen. Thanks for being always there for me and for this beautiful friendship we have. Also for your patience with me, I know I can be a little bit too intense sometimes…

Jiayu, you are a nice, lovable soul that has always made me smile. Thank you.

Everyone who left the group paved the way for me to go on. I believe it is one of the hardest parts of the PhD. Here there are some of them:

Belén, gracias por hacerme sonreír siempre. Echo un poco de menos la bachata a todo volumen en el laboratorio…

Mario, qué decirte a ti, *chaval*. Fuiste uno de mis mayores soportes cuando empecé en el ICIQ. Te echo mucho, mucho de menos. Todos lo hacemos, porque tienes un corazón enorme. Pienso mantener mi promesa de ir a verte. Tenlo claro. Por suerte, ahora tengo cerca a Bruno que también me apoya y ayuda mucho. Gracias a los dos, *boludos*.

Sebastian, I have missed you since the moment you left. You are and will be a true friend. Thanks for being so supportive of me and teaching me that the best time to start a column is 16:00. Come back soon, we need to party like we used to.

Julien, you are a one-of-a-kind person. The time we spent together in Tarragona was probably one of the best in my life, and you were always the companion by my side. You took care of me since the beginning, you cheered me up when the chemistry was not working, and most importantly, you taught me that the south of France is the best region in the whole world. Thank you for all of this, I truly miss you, *mec.*

Andrea, quina companya de viatge. Se'm va trencar el cor quan vas marxar, el 2.5 no ha tornat mai a ser el mateix després de que te n'anessis. Et vull donar

les gràcies per tots els moments que hem passat junts, per tot el suport que ens hem donat, totes les festes, els balls al laboratori... Ets una gran persona, I m'has marcat per sempre. Sé que vas triar el camí correcte i que ets feliç, però sempre t'he trobat a faltar a Tarragona. *Ay*, Andrea.

I want to thank Ana Mateo and Aslihan Baykal for being two excellent labmates, even if their time in the lab was short, I enjoyed your company very much. Keep going girls. You are amazing.

I want to thank my greek friend Anda for always being there for me. I am very glad you are back in Tarragona. Keep this positive energy of yours that makes everyone enjoy your company. I hope that we can keep on drinking white wine for many years. También quiero agradecerle a Martín su apoyo científico en el desarrollo de esta tesis y la corrección del primer capítulo.

Thanks to Dr. Kang Chen for his counsel and his positivity in the lab. Chen, you are such a nice and funny person. It was a pleasure to work alongside you.

Quiero darle las gracias también a Daniel Bafaluy. Bafa, básicamente eres una de las personas con las que más cosas he compartido en el laboratorio. No sólo dentro del laboratorio, sino que fuera de él hemos hecho realidad sueños como ver a grupos míticos en directo, o tocar juntos en un grupo nuestros temas favoritos. Eres un muy buen compañero de laboratorio y un químico increíble, y me has ayudado mucho a lo largo de estos cuatro años, pero sobretodo eres un gran amigo y compañero de aventuras. He sido muy feliz haciendo todo esto contigo, y espero que sean muchas más las aventuras que nos quedan por vivir.

Another of the best chemists that I know is Thomas Duhamel. My friend, you have helped me countless times and were always interested in my projects. I will never forget everything that you have done for me. Also, we have lived together many good times. All the Christmas dinners and parties where we laughed an enjoyed so much. Tarragona misses you, and so do I. Thanks for being the way you are and make other people happy around you.

Ay, Estefi. Qué bonita amistad hemos ido forjando. Tengo que agradecerte todos los momentos graciosos que hemos vivido en el lab, así como todos los consejos que me has dado. También por ser la promotora de todas las salidas del grupo al principio, sin ti seguro que no hubiéramos hecho ni la mitad de las cosas. A

parte, has demostrado al mundo lo fuerte y valiente que eres y que puedes llegar donde te propongas. No cambies nunca, Estefi.

Finally I want to thank Anastasia for her support and company in the 2.5 lab. Thanks for everything, Nastya.

The members of the Suero group have also played a big role in the development of this thesis: Pau, company de terra i company de cerveses. Estic molt content d'haver vingut al teu grup, en part perquè hi ets tu. No només ets un gran químic, sinó que també ets un gran cerveser i arribaràs allà on tu et proposis. Gràcies per tots els bons moments que hem compartit durant aquests quatre anys. Espero que la nostra amistat duri molt més temps. *Salut!*

Vull també donar les gràcies a l'Eric i el Leo, pels cafès i les converses de després de dinar. Al Valero i Alessio, per ser molt bones incorporacions al grup que han aportat des del minut zero.

Finally, I want to thank Liyin, Hangfei and Teo for their support during the last year of my thesis.

A part dels dos grups de recerca, l'ICIQ m'ha donat l'oportunitat de fer música amb persones meravelloses: Marcos, Bafa, Joan, Ana i Paula, gràcies per fer les estones al local d'assaig úniques. Voldria agrair a la Cristina Maquilón tot el suport mutu que ens hem donat aquests anys. Gràcies per la teva manera de ser.

Òbviament, vull agrair a la meva família. A les dues dones de la meva vida, l'Aina i la meva mare, per ser com són i fer-me feliç sempre que estem junts, per donar-me tot el seu suport durant aquests quatre anys. A tu, Papa, que has sigut capaç de superar un càncer. Ets i seràs un lluitador de primera i t'he de donar les gràcies per tot el que fas i has fet per mi. Ets el meu exemple a seguir.

He tingut molta sort a la vida i en sóc conscient. Cap gràcies que pugui articular serà suficient. Us estimo, família.

Por último, quiero agradecer a Ana su apoyo incondicional desde 2019. Has tenido que aguantar muchos llantos de tu *crying PhD*, pero al final todo llega. Sin ti nada hubiera sido lo mismo y me hubiera costado mucho recuperarme de los baches que he pasado durante la tesis. Eres una persona increíble que hace que mis días sean geniales. Te quiero Ana. Eskerrik asko.

Financial Support

The present doctoral thesis has been made possible thanks to funding received from AEI/MINECO (HalOx - Diseño de sistemas de oxidación basados en haluros para la formación de enlaces C-N, Ministerio de Ciencia e Innovación Ref: CTQ2017-88496-R) and the Institute of Chemical Research of Catalonia (ICIQ) (CERCA Programme/Generalitat de Catalunya).

UNIVERSITAT ROVIRA i VIRGILI

ICIQ Institut Català d'Investigació Química

EXCELENCIA SEVERO OCHOA

GOBIERNO DE ESPAÑA
MINISTERIO DE ECONOMÍA, INDUSTRIA Y COMPETITIVIDAD

Unión Europea
Fondo Europeo de Desarrollo Regional
"Una manera de hacer Europa"

Generalitat de Catalunya
Departament d'Economia i Coneixement

Curriculum Vitae

Èric Cots Fargas was born on August 18, 1994 in Manresa (Barcelona). He studied chemistry at IQS (Institut Químic de Sarrià), from 2012 to 2016. Afterwards, he moved to the University of Barcelona where he obtained in 2017 his MSc. in Organic Chemistry. In October of the same year, he started his PhD thesis in ICIQ (Tarragona) under the supervision of Prof. Kilian Muñiz, who passed away in March 2020. After this sad event, he joined the group of Prof. Marcos G. Suero in April 2020, where he continued to develop his work in enantioselective I(I/III) catalysis.

List of Publications

The following publications are based on the work described in this thesis:

1. Cots, E.; Rintjema, J.; Bravo, F.; Muñiz, K.
Deciphering the Keys for High Enantioselectivity in Hypervalent Iodine-Catalyzed 1,2-Difunctionalization: Improved Synthesis of Ishihara–Muñiz Precatalysts
Org. Lett. **2021**, 23 (16), 6429–6434.
https://doi.org/10.1021/ACS.ORGLETT.1C02252

2. Cots, E.; Flores, A.; Romero, R. M.; Muñiz, K.
A Practical Aryliodine(I/III) Catalysis for the VicinalDiamination of Styrenes
ChemSusChem **2019**, 12 (13), 3028–3031.
https://doi.org/10.1002/cssc.201900360

3. Flores, A.; Cots, E.; Bergès, J.; Muñiz, K.
Enantioselective Iodine(I/III) Catalysis in Organic Synthesis
Adv. Synth. Catal. **2019**, 361 (1), 2–25.
https://doi.org/10.1002/adsc.201800521

Patent Application:

4. Bravo, F.; Cots, E.; Rintjema, J. **METHOD FOR THE PREPARATION OF PRE-CATALYSTS FOR HYPERVALENT IODINE CATALYSIS** European Patent Application EP21382640.7, 15th July 2021.

Table of Contents

Preface

The work presented in this dissertation has been performed at the Institute of Chemical Research of Catalonia (ICIQ), during the period of October 2017 until September 2021 under the supervision of Professors Kilian Muñiz and Marcos G. Suero. This thesis is divided into six sections: a general introduction of the thesis, three research chapters, a chapter in which the overall conclusions of the work are presented and the references section. Each of the research chapters includes a brief introduction on the topic, followed by the collected results and their discussion, the main conclusions, and finally a detailed experimental section.

List of abbreviations

In this doctoral thesis, the abbreviations and acronyms most commonly used in organic chemistry are based on the recommendations of the ACS "Guidelines for authors". Additional abbreviations are listed below:

Phth .....Phthaloyl
Ac.....Acetyl
Ar .....Aryl
Cbz.....Benzylcarbamoyl
DAIB..... (Diacetoxyiodo)benzene
DBU..... 1,8-Diazabicyclo[5.4.0]undec-7-ene
DCM .....Dichloromethane
DFT.....Density functional theory
DIAD.....Diisopropyl azodicarboxylate
DMAP..... 4-(Dimethylamino)pyridine
DMF.....Dimethylformamide
DMSO.....Dimethylsulfoxide
EDA complex.....Electron donor-acceptor complex
ee.....Enantiomeric excess
Equiv. .....Equivalent
FT-IR.....Fourier-transform infrared spectroscopy
hfacac .....Hexafluoroacetylacetonate
HFIP..... 1,1,1,3,3,3-Hexafluoroisopropanol
HPLC .....High performance liquid chromatography
HRMS .....High resolution mass spectrometry
*i*Pr..... Isopropyl
IUPAC..... International Union of Pure and Applied Chemistry
m.p. .....Melting point
MALDI.....Matrix-assisted laser desorption ionization
*m*CPBA .....*meta* Chloroperbenzoic acid
MHz .....Megahertz
Ms .....Methanesulfonyl
MTBE .....Methyl *tert*-butyl ether
NFSI.....*N*-Fluorosuccinimide
NMR .....Nuclear magnetic resonance
ºC .....Celsius degree
Ph .....Phenyl
Phth .....Phthaloyl
PIDA..... (Diacetoxyiodo)benzene
PIFA..... [Bis(trifluoroacetoxy)iodo]benzene
PivO .....Pivalate
Py .....Pyridine

RT.....Room temperature
SET .....Single electron transfer
SFC ..... Supercritical Fluid Chromatography
TADDOL α,α,α,α-Tetraaryl-2,2-disubstituted-1,3-dioxolane-4,5-dimethanol
TEA.....Triethylamine
TFE 2,2,2-Trifluoroethanol
THF.....Tetrahydrofurane
TMS .....Trimethylsilyl
TS.....Transition state
Ts 4-Toluenesulfonyl
UPC2.....Ultraperformance convergence chromatography
UV.....Ultraviolet

Summary of the thesis

This thesis is focused on racemic and enantioselective I(I/III) catalysis for vicinal diamination of styrenes. Pre-catalyst rational design and enantioinduction are main issues throughout the thesis. The manuscript is divided into an introduction and three experimental sections:

1.- A practical aryliodine(I/III) catalysis for the vicinal diamination of styrenes

2.- Improved Synthesis of Ishihara–Muñiz Pre-catalysts

3.- C_1-Symmetry in aryliodine catalyzed diaminations: A proof of concept

The first experimental part describes the finding of a suitable pre-catalysts for a racemic styrene diamination. After trying commercially available aryliodines and demonstrate their inefficacy, an efficient pre-catalyst was developed based on an earlier asymmetric pre-catalyst for the enantioselective diamination. The newly developed pre-catalyst yielded moderate to good yields of the desired diamines, demonstrating that the design was adequate for the diamination reaction. Additionally, bistosylimides were identified as additionally suitable nucleophiles for the reaction.

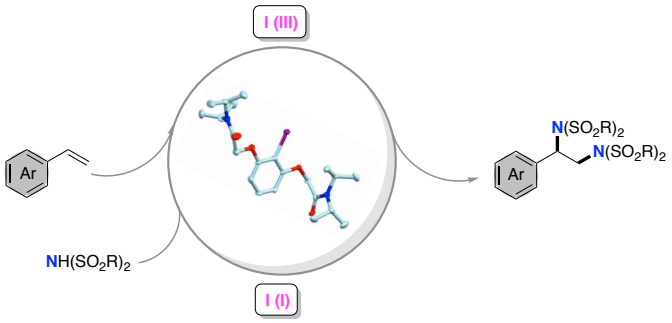

For the second project, the synthesis of three Ishihara-Muñiz pre-catalysts were upscaled. In the course of this upscaling, a *meso*- form of the Muñiz

pre-catalyst for the asymmetric diamination was identified. Its independent preparation confirmed its formation in the synthesis of this pre-catalyst. The suppression of tryethilamine as auxiliary base in the final amidation reaction of the synthesis yielded the pre-catalyst in 99% *ee*. This was translated into the highest enantioinduction ever observed for this diamination reaction reaching up to 99.5% *ee*. Moreover, a pre-catalyst without *para*- substitution in the aryl core was proved to be suitable for the reaction with comparable yields and *ee*.

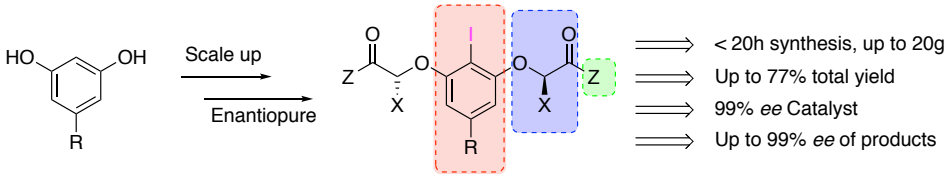

Finally, a proof of concept was developed involving C_1-symmetric pre-catalysts for the asymmetric diamination reaction. The idea to use a C_1-symmetric design to elaborate a pre-catalyst that suited the requirements of the reactions was proved. The yields of the diamination reaction were comparable to the obtained using the previously developed C_2-symmetric pre-catalysts. The stereochemical outcome of the reaction proved that the reaction can reach high enantiomeric excesses when only one stereocenter is present in the pre-catalyst.

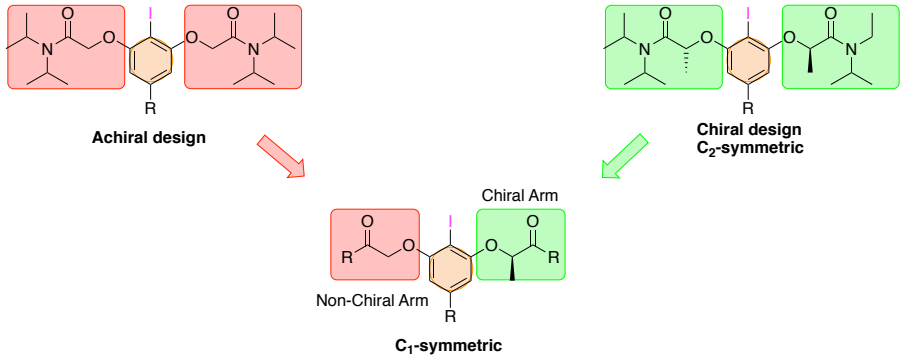

Chapter I – General Introduction

1. Chapter I – General Introduction

1.1 Diamines

1,2- difunctionalized molecules have a conspicuous relevance in nature, being vicinal diamines one of the most frequent motifs.[1] Several diamines are significant for their biological role, such as the antibiotics penicillin and cephalosporin.[2] Notably, vitamin H (Biotin) also contains a vicinal diamine, a molecule which has many functions as genetic stimulation for glucose regulation processes or as a carboxylase prosthetic group, related for example to fatty acid biosynthesis and gluconeogenesis (Figure 1).[3,4]

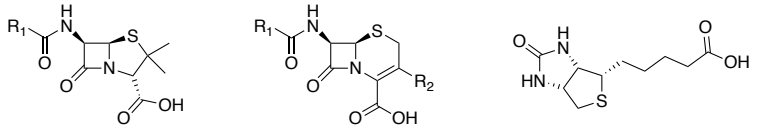

Figure 1. Naturally ocurring vicinal diamines

Many 1,2-diamines have biological activity and thus have significance for the pharmaceutical industry. Some examples are depicted in Figure 2: Asimadoline and ICI-199,411 are kappa opioid agonists, being the first a drug candidate for irritable bowel syndrome and rheumatic disorders,[5,6] while Antazoline is an antihistamine drug used to prevent redness and itching in allergic conjunctivitis.[7] Another example of a pharmacologically active diamine used as a treatment for worm infections in animals is Levamisole.[8] Mirtazapine is a well-known antidepressant, a racemic molecule showing a seven-membered ring and a diamine. [9] The (*S*)-enantiomer of Mirtazapine, called Esmirtazapine, has also use as treatment for some menopause problems as insomnia or hot flashes.[10] Oseltamivir, commercialized under the name of Tamiflu is an aliphatic diamine, an antiviral for treatment of the flu (influenzas A and B) while Oxaliplatin is used for colorectal cancer chemotherapy.[11,12]

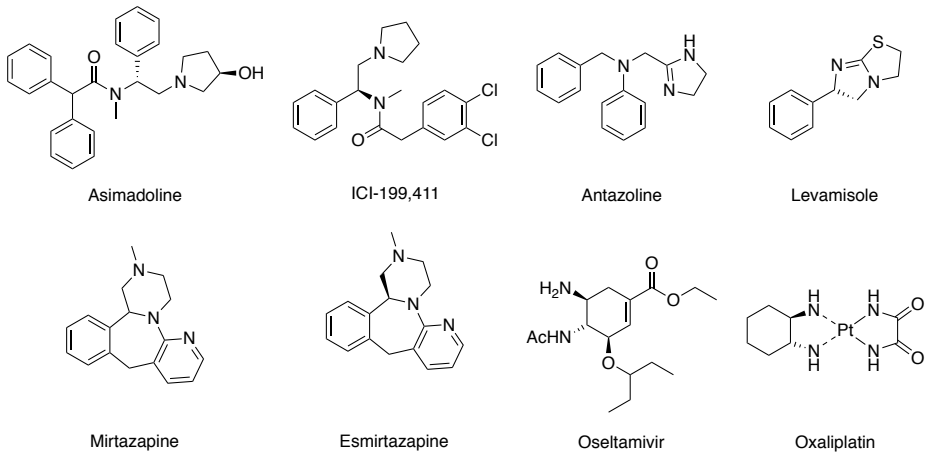

Figure 2. Diamines with pharmacological relevance

In organic synthesis, 1,2-diamines have received special attention, particularly enantiopure diamines. These can be used as chiral auxiliaries, ligands, or catalysts for asymmetric transformations.[2]

One of the most known examples is the Jacobsen-Katsuki epoxidation, mediated by a [Mn-(Salen)] catalyst, used in oxidative asymmetric transformations.[13] These catalysts show a structural resemblance to the metal-porphyrins, known for being involved in asymmetric oxidations in biological contexts.[14] As shown, the chiral non-racemic 1,2-diiminated cyclohexane moiety coordinates to the metal centre, playing an important role in the transformation (Figure 3).[14] Both Jacobsen and Katsuki described the epoxidation of substituted styrenes to yield the corresponding epoxide in high *ee* (Scheme 1).[15–17]

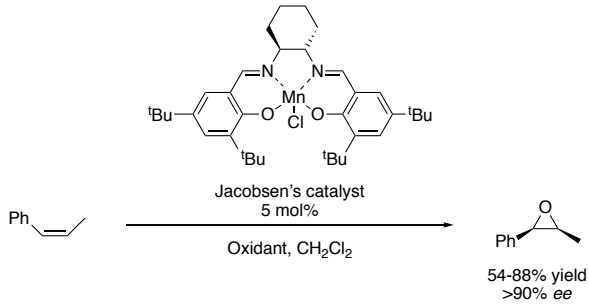

Scheme 1. Jacobsen-Katsuki epoxidation of styrenes

Another example of vicinal enantiopure amines in organic synthesis can be found in Noyori's catalyst for asymmetric hydrogenations. When treated with Ruthenium catalyst **I** and hydrogen in basic conditions, aromatic ketones can be transformed to alcohols in good to excellent *ee*.[18] For the transfer hydrogenation reaction, catalyst **II** employs ^{i}PrOH as the source of hydride. In these two examples, the diamine is one of the two ligands used to induce enantioselectivity in this asymmetric reaction and thus has crucial importance in the reaction (Scheme 2).[19]

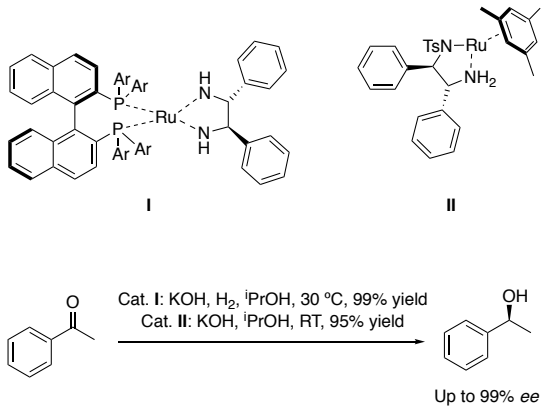

Scheme 2. Noyori asymmetric hydrogenation and transfer hydrogenation

1.2. 1,2-Diamine Synthesis from alkenes

One pioneering work in diamination reactions came from Barluenga in 1974, when they developed a diamination reaction using $Tl(OAc)_3$ and aromatic amines as nucleophiles.[20] In the following years, Sharpless and Bäckvall both developed diamination chemistry with osmium (VIII) and Palladium (II/IV) respectively, opening the door to the metal-catalyzed diamination of olefins.[21,22]

With this background, the group of Professor Muñiz started developing new vicinal diaminations of alkenes. His first contribution to the field was the diamination of esters with imidoosmium (VIII) complexes. Using chiral

information in the alkoxy group, specifically an (-)-8-phenylmenthol resulted in the successful selective diamination, with up to 95:5 d.r. of the major isomer (Scheme 3).[23,24] Two years later, another chiral auxiliary, Ti-TADDOLate was also found to be useful in the same reaction, reaching the same levels of selectivity as in the previous case.[25]

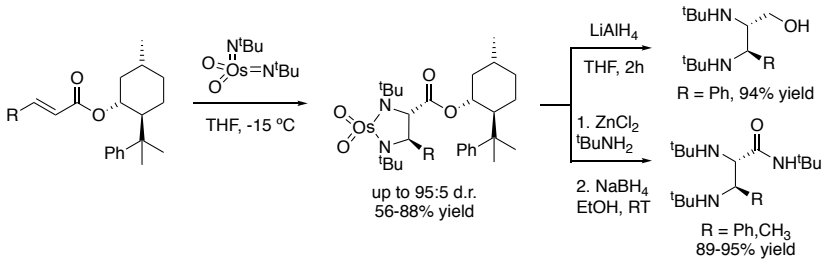

Scheme 3. Muñiz diamination with imidoosmium (VIII) complexes

Some years later, the focus was put on catalytic diamination. Several metal-catalyzed transformations were developed by Muñiz, including palladium, gold, nickel and platinum-based intramolecular reactions.[26–29] Particularly, tethered diamines were used as substrates, as they were found to be very suitable to react with the mentioned metals, and the free amine could be released after the catalyzed reaction finished (normally by reductive treatment like $LiAlH_4$). A general reaction mechanism can be elucidated, in which the alkene is aminometallated, followed by oxidation with a terminal oxidant, like PIDA. After proton extraction from a base, a nucleophilic attack from the second amine takes place, yielding the final diamine (Scheme 4).

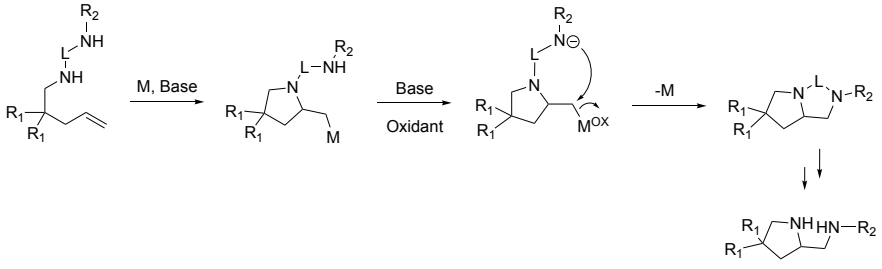

Scheme 4. General mechanism for metal-mediated diamination

Notably, the use of gold and palladium showed different stereoselectivity, making the final diamine *anti* and *syn* respectively (Scheme 5a). The main difference between the outcome of both metals was the ability of palladium to coordinate the second amine after the first aminopalladation, which is the crucial step for the stereochemical outcome of the reaction.[29,30] Furthermore, nickel catalysis can yield sulfamide-tethered diamines, as well as another combination of palladium with $CuBr_2$ as oxidant, in which the halogenated intermediate plays a significant role (Scheme 5b).[28,31]

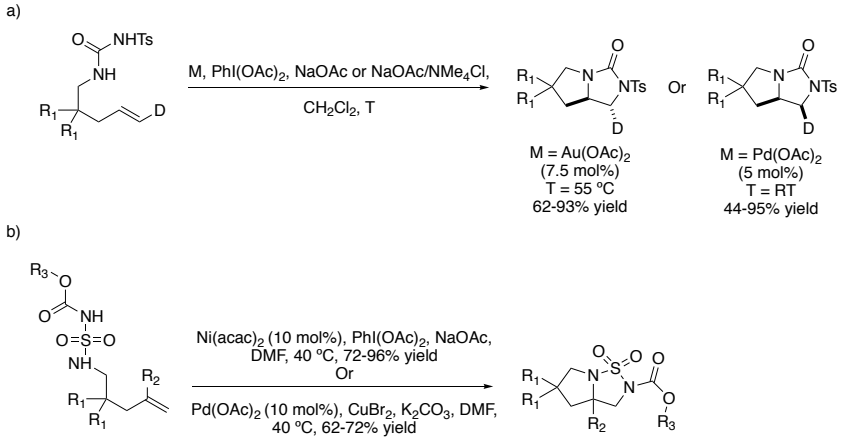

Scheme 5. Au, Pd and Ni catalyzed reactions

A relevant Pd-catalytic untethered diamination was also explored by the group during the same time, yielding the diamine motif (Scheme 6). By this strategy bisindolines, annelated indolines, and bipyrrolidines could be readily synthesized. The elucidated mechanism consists in a first *anti*-aminopalladation, followed by oxidation of the metal centre, and subsequent de-palladation and C-N bond formation leaving the two amines in *syn* disposition.[32]

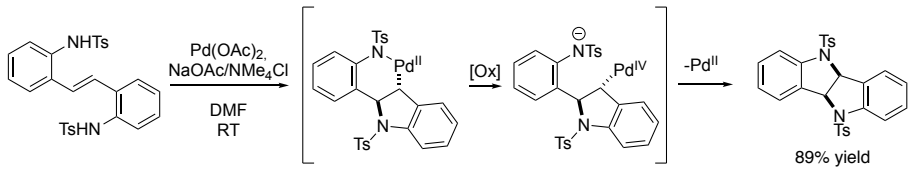

Scheme 6. Formation of Bisindoline core

Moving to further intermolecular amination, one of the first reports was in 2010, when olefin diamination was developed by our group, adding saccharin and $HNTs_2$ as nucleophiles. The suitable oxidant for the reaction was $PhI(O_2C^tBu)_2$ (Scheme 7a).[33]

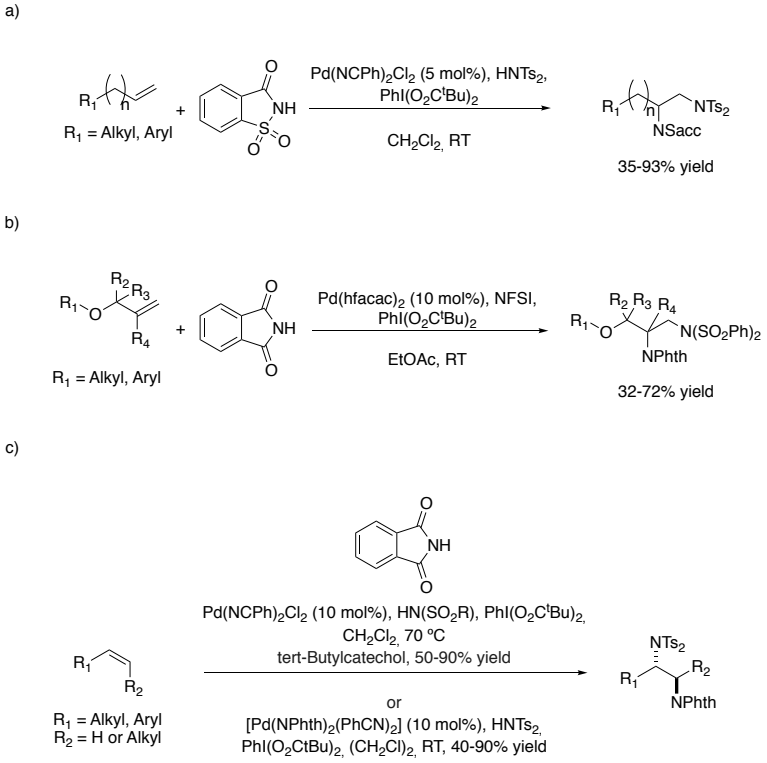

Scheme 7. Pd-Catalyzed diaminations using saccharin and phtalimide as nucleophiles

A similar transformation was carried out with allyl esters as substrates. phtalimide was the nucleophile and the hypervalent iodine oxidant was combined with with N-Fluorobenzenesulfonimide (NFSI), which was used as the second nucleophile (Scheme 7b).[34]

Afterwards, these works were further broadened by our group with a parallel aminooxygenation of the same ethers with saccharin.[35] Similarly, several diaminations of internal styrenes and terminal olefins could be achieved. Two main reaction modes can be identified: forming the active catalyst *in situ*, which required adding *tert*-butylcathecol as a polymerisation inhibitor or the preformation of the $[Pd(NPhth)_2(PhCN)_2]$ species, which also proved useful (Scheme 7c).[36,37]

More recent ways of synthesizing diamines from alkenes and other substrates include molecular iodine catalysis,[38] photocatalysis,[39] or combined electrophotocatalytical methods.[40]

1.3. Hypervalent Iodine (III)

1.3.1. λ^3-iodanes and λ^5-iodanes

Hypervalent species are those of the periodic groups 15-18 that have other valences than 3, 2, 1 and 0 respectively. Due to this fact, they need donor atoms, which makes them exceed their classical octet-rule fulfilling valences.[41] In the case of iodine, two main hypervalent types of compounds are described by IUPAC: λ^3-iodanes and λ^5-iodanes. The most common structures are aryl-λ^3-iodanes and aryl-λ^5-iodanes, which have oxidation state +3 and +5 respectively, and 10 or 12 electrons around the iodine centre respectively (Figure 3a). Aryl-λ^3-iodanes present a *pseudo*-trigonal bipyramid molecular geometry, in which the aryl group and the lone pairs of electrons are in the equatorial positions and the ligands in the apical positions. Due to this fact, λ^3-iodanes have been known to have a "T" shape, with the aryl group and the ligands in perpendicular planes. The electrophilicity of these compounds can be explained by molecular orbital theory. The ligand-iodine bond can be described by a 3-centre-4-electron (3*c*-4*e*) bond. This fact makes 2 electrons to be placed in the bonding orbital and 2 electrons in the non-bonding orbital (HOMO). Resulting from this overlap between the 5p orbital of the iodine and the orbitals of the ligands, a node is present in the HOMO (Figure 3b).[42]

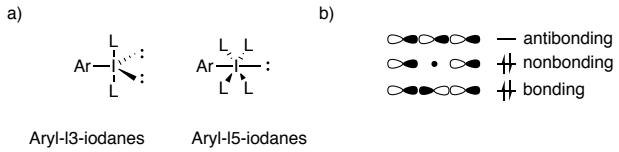

Figure 3. a) Aryl-λ^3-iodanes and Aryl- λ^5-iodanes b) Electronic configuration of iodanes

The first hypervalent iodine III ever made was (dichloroiodo)benzene, discovered in 1886 by the german chemist Conrad Willgerodt while reacting chlorine gas with iodobenzene in a solution of chloroform.[43]

Nowadays, due to their broad reactivity and applicability, hypervalent iodine compounds are relevant in synthesis. Many complex molecules have been synthesized using the chemistry of iodine (III) and (V).[44–46]

Some of the most used hypervalent iodine (V) compounds for oxidation are 2-iodoxybenzoic acid (IBX) and Dess-Martin periodinane (DMP) (Figure 4).[47–49]

In the case of hypervalent iodine (III), phenyliodine (III) diacetate or PIDA and its analogue with Trifluoroacetate as ligand, PIFA have been increasingly used in the last years in many different types of reactions.[44,50]

Another type of reagents such as Togni and their derivatives and Koser reagents are usually used in a broad range of transformations.[51–53] More recently, hypervalent I(III) compounds such as a modified benziodoxolone and a *pseudo*cyclic analog have been developed by Suero.[54]

These compounds have acquired a privileged status for their efficiency, availability and also for being environmentally friendlier than other related methodologies.

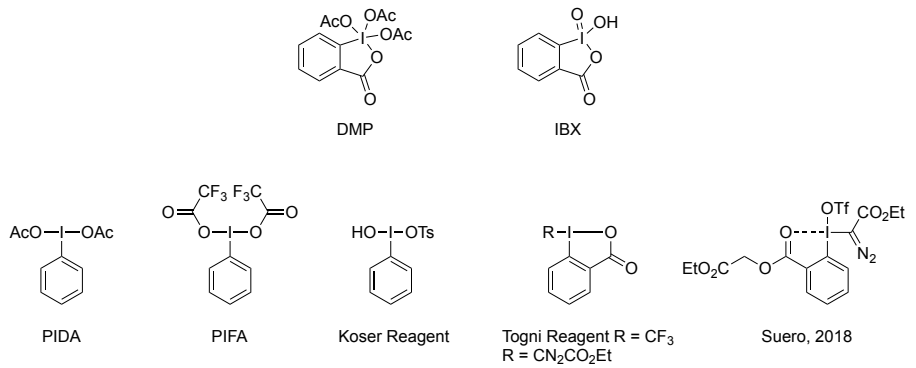

Figure 4. Hypervalent iodine V and III used in synthesis

Halogenations have become relevant in the last few years, but also diaminations and oxygenations have been successfully developed by many authors. For these purposes, different types of λ^3-iodanes have become relevant in the recent years, which bear as ligands adequate nucleophiles for their uses. Furthermore, several species, such as iodonium salts, iodonium ylides and iminoiodines have also been developed and used in synthetic organic chemistry (Figure 4). [55,56]

1.3.2. Reactivity of hypervalent iodine (III) compounds

1.3.2.1. Ligand Exchange

One of the main ways in which the iodine (III) compounds react is ligand exchange. Two main pathways have been classically proposed within this context: in one case, a ligand dissociates, creating a cationic aryliodonium (III) species, which is then prone to react with the nucleophile. In the other case, the nucleophile attacks the iodine (III) centre, which provokes the dissociation of one of the original ligands. These two pathways have been labelled dissociative and associative, respectively (Figure 5a).[55] By this and other methods many hypervalent iodine (III) species can be synthesized and used in different types of reactions, generating a wide range of compounds that can be classified by their ligands (Figure 5b).

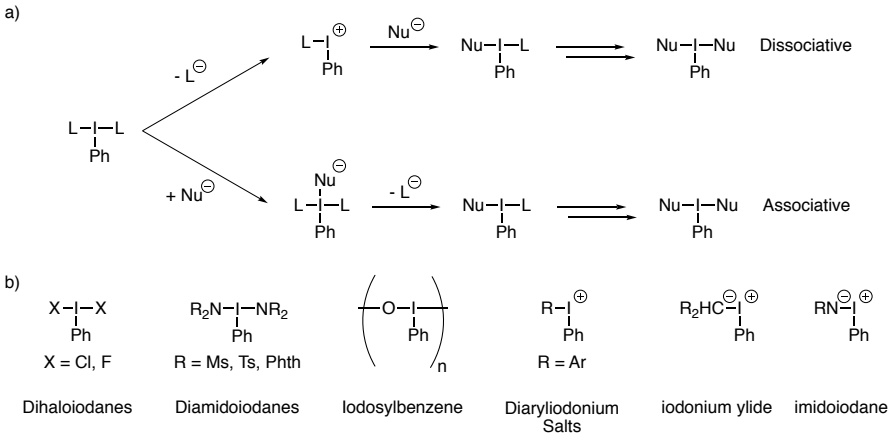

Figure 5. a) Ligand exchange for iodine (III) compounds b) Relevant iodanes in organic synthesis

1.3.2.2. Reductive elimination, substitution and ligand coupling

The reductive elimination is by far the most common reaction over the years for hypervalent iodine (III) compounds and can be used for ligand transfer from the iodanes to many substrates. The driving force in these reactions is the reduction of the λ^3-iodanes to the more stable monovalent iodine state, making the process completely favoured in terms of energy. In fact, some authors describe these species as Hypernucleophuges: their leaving group ability is even higher than superleaving groups as triflate groups (OTf).[57] Some species were found to be 10^6 times better leaving groups than OTf.[58]

Due to the great electrophilicity of the iodine (III) centre, ligand exchange for a nucleophile is a facile step (as previously described).

Generally, when an R-group is coordinated with the I(III), a substitution takes place, enabled by reductive elimination. This reaction can be understood as an *umpolung* in most cases, since the R-group needs to have a certain nucleophilicity (Scheme 8a). Ligand coupling occurs when

the two coordinated species of the iodine (III) are bonded through a concerted mechanism.[55,57]

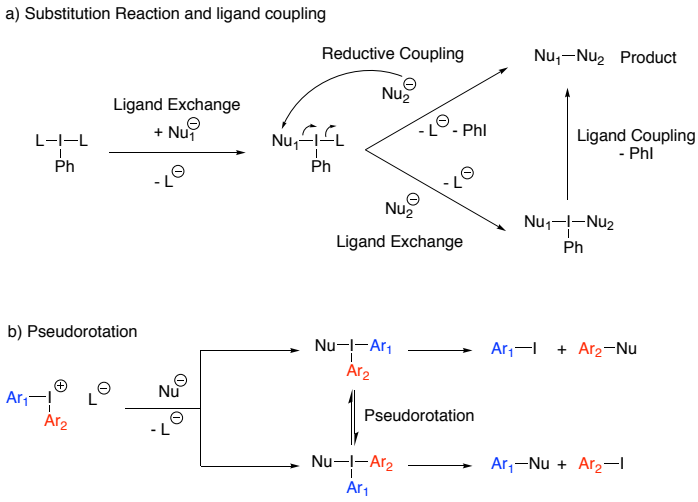

Scheme 8. a) Substitution of iodanes and ligand coupling b) Pseudorotation of diaryliodonium salts

Diaryliodonium salts are known for reacting by ligand coupling. A fast equilibrium described by Berry, called *pseudo*rotation allows two different intermediates, which are interconvertible species. This way, both aryls can be transferred, but the one that will be coupled to the nucleophile is in the adjacent apical position (Scheme 8b).[59] When non-symmetrical diaryliodonium salts are used, the preferred configuration will be the one where the nucleophile is next to the most electrophilic aryl group. Therefore, the major product is usually the one which this is coupled with the more electron-deficient aryl.[60] Sterics also can play a role in this equilibrium, changing the configuration of the intermediate.[61,62]

1.3.2.3. Radical Reactions and SET

Another type of transformations involving hypervalent iodine (III) are radical reactions. Light or temperature can homolytically cleave the I(III) – L bond of λ^3-iodanes, promoting the release of radicals into a reaction mixture. Again, the formation of more stable iodine (I) species drives this reactivity. In 1968, di-tertbutylperoxide ligands were shown to react in a radical manner in order to form polyoxides.[63] This reaction opened the door to modern radical chemistry using hypervalent iodine (III) species. Magnus and Kita developed radical azidations using $TMSN_3$. In both cases, homolytic cleavage was induced by light, and then the radical transferred to a carbon atom, which after reaction with the azide gave the final product (Scheme 9). Similarly, Minisci developed carbon-centered radicals by homolytic cleavage of the I–O bond from (diacyloxyiodo)arenes which generated radicals through decarboxylation.[64–66]

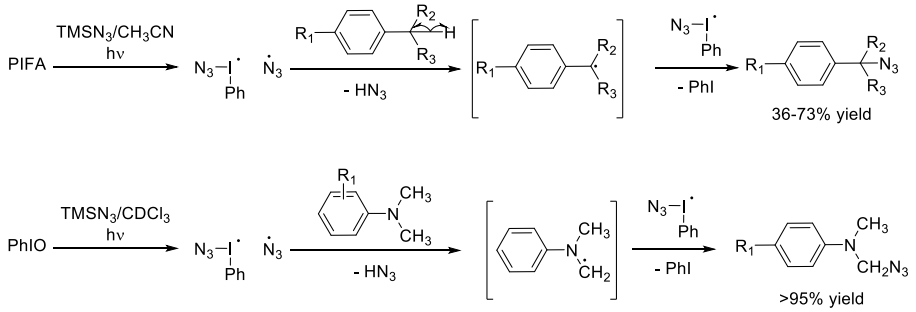

Scheme 9. Kita and Magnus azidations

A relevant C-H functionalization of alkaloids was reported by Breslow, using an internal aryliodine(I) that when oxidized to I(III) behaves as a directing group for the radical proton abstraction. This species oxidized the iodinated template in the molecule, an aryliodine, to an iodine-

centered radical. By homolytic cleavage, the radical was transfered to an accessible aliphatic carbon, which was finally functionalized with several groups.[67] This procedure is still used nowadays in the remote C–H functionalizations of alkaloids (Scheme 10).[68]

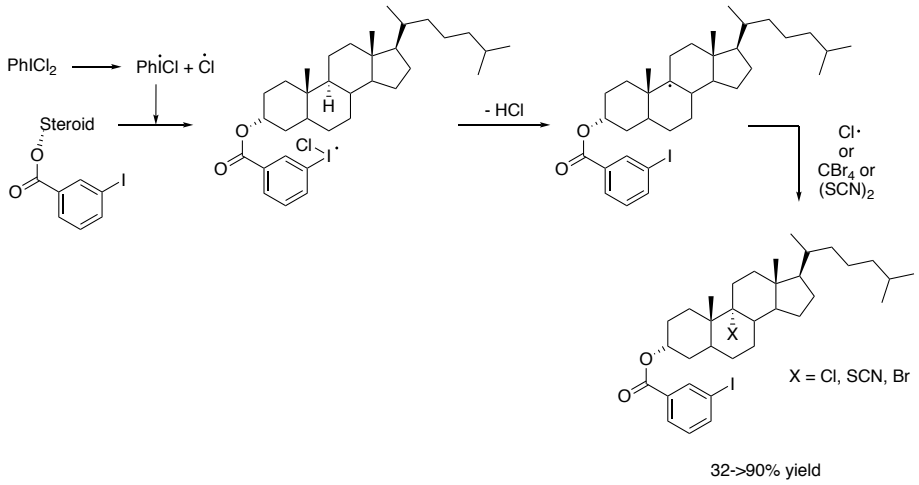

Scheme 10. Steroid functionalization by Breslow

Single-Electron Transfer (SET) are radical reactions in which one electron is transferred from a donor to an acceptor, starting the radical reaction. The first example of this reaction type using I(III) compounds was uncovered by Kita *et al.* in a first azidation of aromatic compounds that preceded other nucleophilic substitutions.[69,70] $BF_3{\cdot}OEt_2$ and TMSOTf were both used to activate the iodanes and facilitate the SET reaction (Scheme 11). Some years later, in the decade of 2000, aryl couplings were found to be feasible by SET, using PIFA or PIDA.[71] Several authors broadened the scope to other C-C, C-N and C-S bonds in the following years.[72]

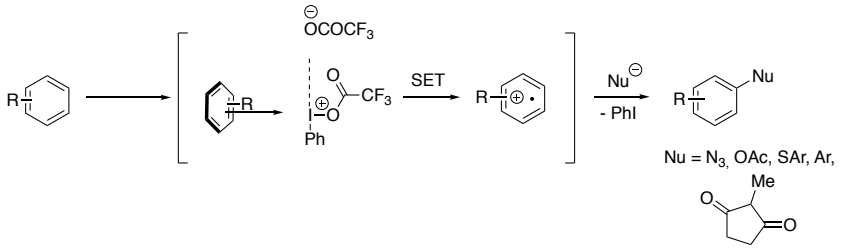

Scheme 11. SET in hypervalent iodine (III) chemistry

1.3.2.4. Reductive β–elimination and α–elimination

β–elimination is one of the most used reactions when oxidizing substrates with iodanes, particularly alcohol oxidations to ketone. Once again, the formidable leaving group ability of iodine (III) compounds is the driving force of these type of reactions. When an oxygen, nitrogen or carbon atom with labile protons in their β position coordinate with the iodine (III) centre, this proton can eliminate to yield a C=C, C=O or C=N bond. Parallel reactivity is observed by most of the λ^5-iodanes (which yield in turn their respective λ^3-iodanes), used in organic synthesis for the same transformations (Scheme 12).

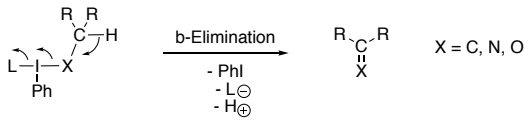

Scheme 12. β-elimination of I^3-iodanes

In a similar manner, α–elimination is used to yield carbenes when a proton is in an α position. A base is necessary to take the proton from the carbon adjacent to the I(III) centre, and the reductive elimination allows the formation of the carbene. In 1991, Ochiai described the dual reactivity of carbenes derived from (*Z*)-[β-(phenylsulfonyl)alkenyl]iodonium tetrafluoroborates, which showed predominance for 1,5-insertion rather than 1,2-shift to form an alkyne (Scheme 13).[73,74]

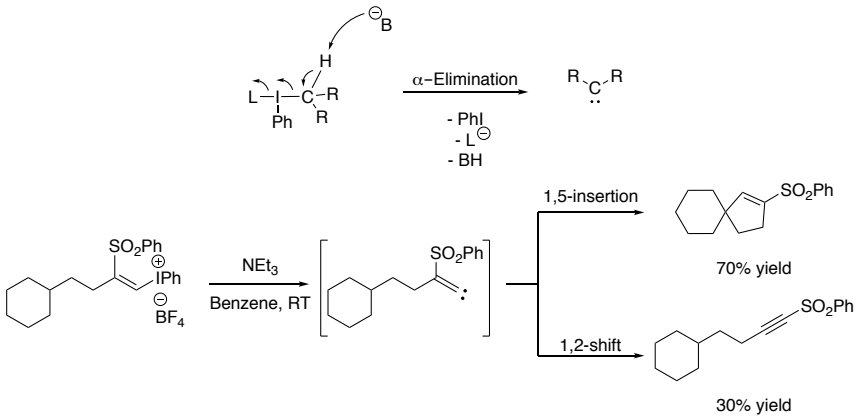

Scheme 13. α–elimination of λ^3-iodanes

1.3.3. Chiral hypervalent iodine (III) reagents

In 1907, Pribram is suspected to have synthesized the first chiral hypervalent iodine (III) species derived from *L*-tartaric acid and iodosobenzene (Figure 6).[75] No key structural determination was available at that time, which made Merkushev *et al.* in 1975 the first confirmed approach to a chiral λ^3-iodane. In this case, the species were synthesized by ligand exchange using protected amino acids and PIDA.[76]

Chiral hypervalent iodine (III) reagents have been developed continuously since the decade of 1990. Their classification can be summarized by their structure and the nature of the hypervalent iodine (III) (seen previously in Figure 5), but also one can establish two main kinds of reagents: the ones bearing chiral centres in the ligands and the ones that have the chiral information in the backbone (the substituents) of the aryl group (generally known as aryliodines) (Figure 6).

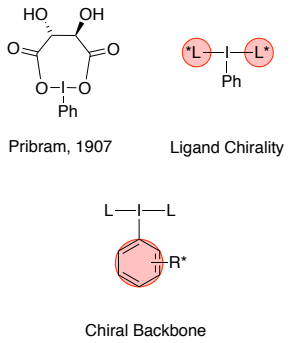

Figure 6. The chiral information can be in the ligands or in the aryl backbone

1.3.3.1. Chiral ligands in hypervalent iodine (III) reagents

As stated above, the two first examples of chiral iodanes contained asymmetric centres in the ligands. This fact is not surprising given that hypervalent iodine (III) species are very prone to ligand exchange (as seen in section 1.3.2.1). Even if there are only a few examples of chiral ligands in iodanes, they represented the beginning of the state-of-the-art stoichiometric asymmetric chemistry we know today. A pioneering author who worked on this type of reagents was Imamoto, who in 1986 came up with iodanes derived from tartaric anhydrides, similar to Pribram's work (Scheme 14). These were found to be useful in asymmetric sulfide oxidation, to give enantioenriched sulfoxides.[77] Working with the same compounds, Koser first derivatized his reagents with a chiral menthol moiety, achieving higher selectivity than previously reported.[78] He later postulated a polymer as the active species of Imamoto's previous reaction.[79]

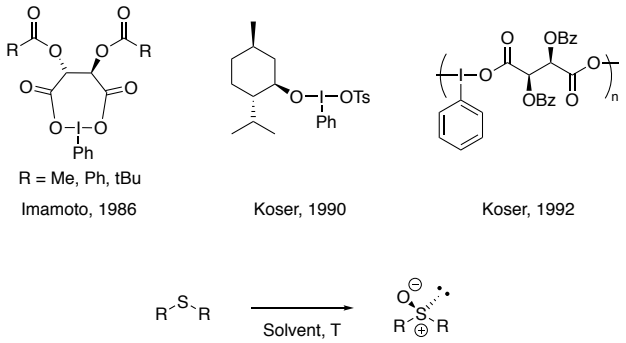

Scheme 14. Chiral ligands in iodanes for sulfide oxidation

In another context, Zhdankin developed in 2004 a reagent class using PIDA and benzyl-protected amino acids. These reagents allowed for the *anti* 1,2-iodoesterification with aminoacids, using cyclohexene or dihydropyran as substrates. The diversification was performed by the synthesis of various iodanes with some amino acids, which provided the reaction scope (Scheme 15).[80]

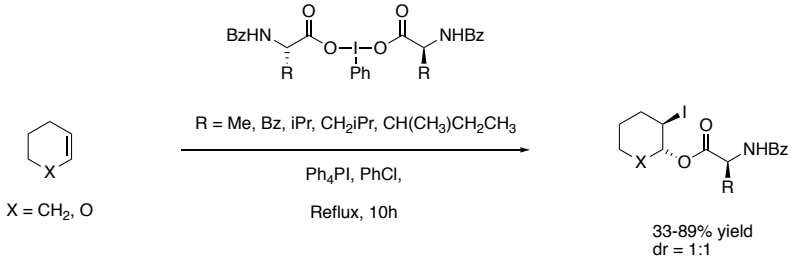

Scheme 15. Zhdankin iodoesterification with amino acids

1.3.3.2. Backbone chirality in hypervalent iodine (III) reagents

Contrary to the I-Ligand bond, the Ar-I bond is not dissociated and thus if chiral information is inserted in this part of the compounds, it will always remain attached to the iodine centre. This fact makes backbone chirality a better chance for enantioinduction than in the case of enantiopure ligands.

In 1990, Ochiai described the first C_2-symmetric chiral λ^3-iodanes, based on the binaphthyl moiety. Three different classes were synthesized, a mono-iodanediacetate, a bi-iodanediacetate which decomposed to a bridged μ-oxo-diiodinane. Also, a TFA analog to the latter was additionally described.[81] The first enantioselective reaction was developed by the same authors in 1999, when they transformed the aforementioned reagents into their corresponding diaryliodonium salts and accomplished phenylation of β-ketoester enolates, with up to 53% *ee* (Scheme 16).[82]

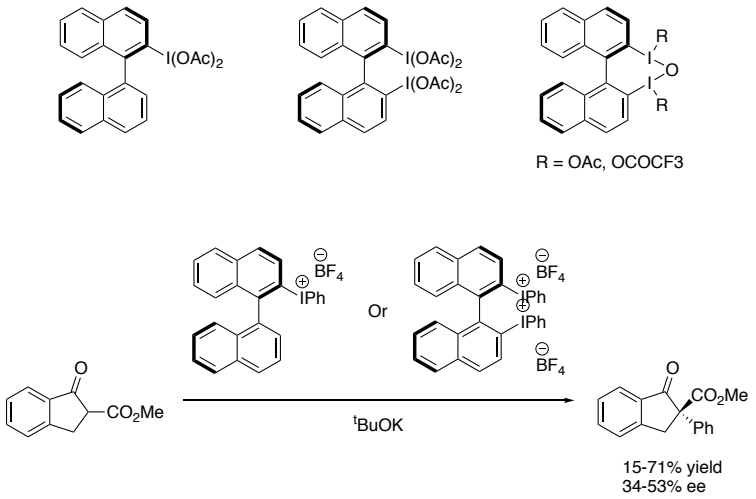

Scheme 16. First C_2-symmetric I(III) reagents and enantioselective phenylation

Following this work, during the last half of the 1990s decade and beginning of the 2000s, Wirth presented a series of chiral hypervalent iodine (III) reagents which were used for α-tosylation of ketones and 1,2-dioxygenation of alkenes. These compounds remind the structure of Koser's reagent, implementing a chiral carbon *ortho* to the iodine in the aryl ring. In 1997, two different reagents were tried, containing either one or two chiral alkyl moieties in *ortho* position.[83] In 1998, the use of electron-richer aryls gave better results.[84] Finally in 2001, the *ee* was ameliorated by the use of an *ortho*-ethyl reagent.[85] In all these cases, yields were moderate for the α-tosylation reaction, and the *ee* did not exceed 40%. It

was in the dioxytosylation of alkenes where the authors got a higher *ee* (65%, with most yields not reported), proving that enantioselective stoichiometric reactions were advancing in that time (Scheme 17).

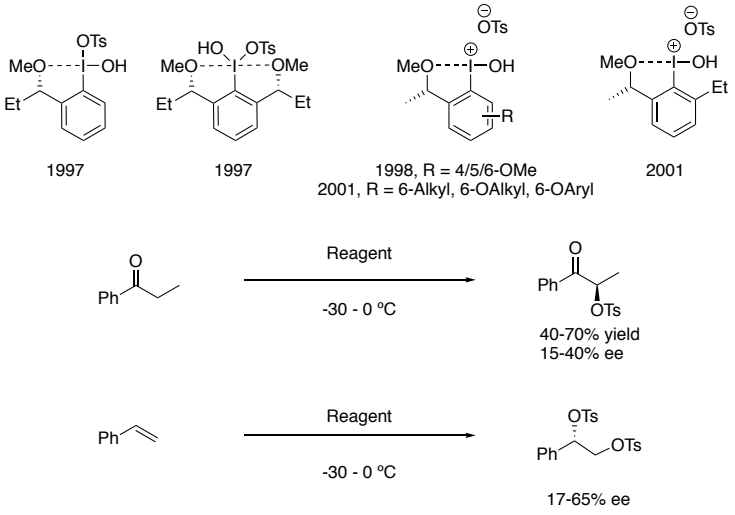

Scheme 17. Chiral reagents for tosylation from Witrth

In 2003, the same authors developed the first intramolecular cyclization reaction using 4-phenyl-4-pentenoic acid as substrate. Even if the enantiomeric excess is minor, the reaction is relevant as it precedes most of the intramolecular enantioselective chemistry that can be performed with hypervalent iodine (III) (Scheme 18).

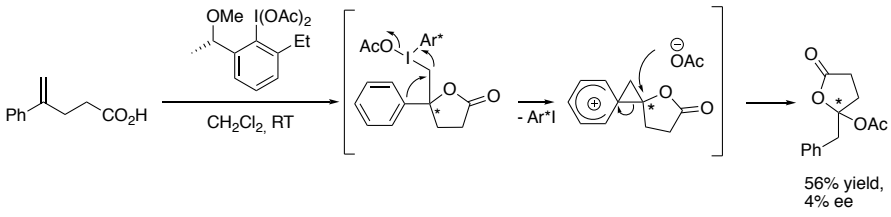

Scheme 18. First enantioselective intramolecular reaction developed by Wirth

In the context of intramolecular reactions, the most important contribution in the decade of 2000 was made in 2008 by Kita, and depicted

enantioselective phenol dearomatizations. This enantioselective reaction had already been tried by Pelter (using Imamoto's reagent) in 1999, but without any success in terms of *ee*.[86] The crucial importance of this work resides in the facts that not only it was the first time an *ee* higher than 85% was reported, but also that it would become one of the most studied and well-known reaction using asymmetric I(III) chemistry, reffered to as *Kita dearomatization* or *Kita Oxidation* (Scheme 19).[87]

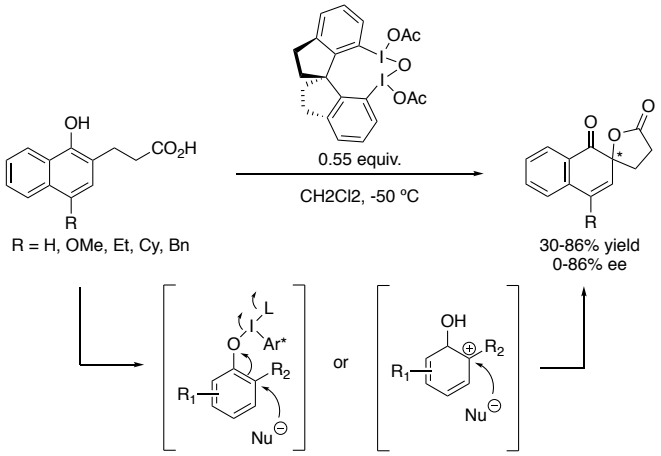

Scheme 19. First enantioselective dearomatization by Kita

In this transformation, the use of a rigid 1,1'-spirobiindane backbone allowed for a much more selective reaction. Mechanistically, two hypotheses were presented: an associative and a dissociative path. They were supported by solvent correlation to the *ee*, determining that the more polar the solvent the less *ee* was observed, suggesting that cation **B** could be involved in polar systems (Scheme 18).[88]

So far, the design of the reagents had proved to be the utmost key for enantioinduction in stoichiometric systems. From 2007, a series of reagents were developed by Fujita that became fundamental to the current chemistry. The base of their design represented a turning point for enantioinduction in iodine (III) mediated reactions, inspiring others to work

on similar structural features that ultimately lead to a huge increase in the *ee* of the products.

In this first work, intramolecular tetrahydrofuranylation of but-3-enylcarboxylates was developed. The hypervalent iodine (III) species was able to promote a first attack of the ester group into the double bond forming a 1,3-dioxan-2-yl cation, which undergoes water nucleophilic attack, yielding an orthoester. Its opening and subsequent re-cyclization yields the observed tetrahydrofuran bearing the ester moiety (Scheme 20).[89]

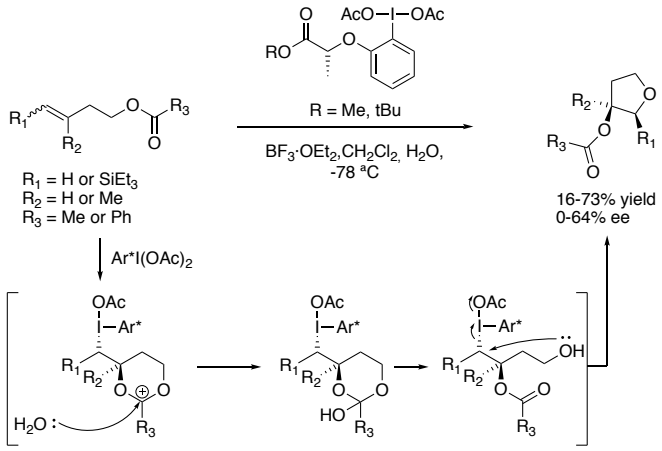

Scheme 20. First tetrahydrofuranylation from Fujita

In 2010, new lactate-derived Aryl-λ^3-iodanes were used by Fujita, this time containing another moiety in the 6- position of the aryl ring, again *ortho* to the iodine (III) centre. First, some alkyl and aryls were tried, but the best results were accomplished with a symmetrical double O-alkylated reagent, synthesized from resorcinol and methyl lactate (which will later be a recurrent base structure, especially in catalytic design). The reaction studied was the oxylactonization of styrenes, with high yields and an *ee* reaching an astounding 97%. In this case, the mechanism was elucidated through a first coordination of the *Si* face of the alkene and subsequent

nucleophilic attack of either a tosylate or an acetate, giving rise to two different *endo*-product types (Scheme 21).[90]

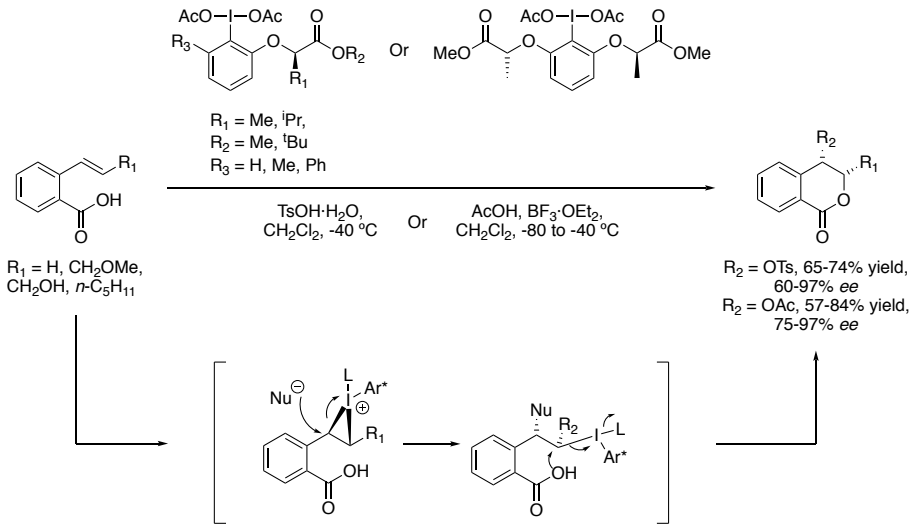

Scheme 21. Enantioselective oxylactionization using lactate-derived Aryl-λ^3-iodanes

After the parallel work from ishihara – who worked on enantioselective aryliodine pre-catalysts based in the resorcinol/lactate structure (See next sections),[91] several authors described reagents inspired in his work for stoichiometric reactions.

The first important example came from Nevado in 2013, when her group achieved aminofluorinations of alkenes. 2-fluoropiperidines and azepans were synthesized using selectfluor as an oxidant, $Et_3N{\cdot}HF$and a lactate-based difluoro aryliodine (III). This combination yielded moderate to high yields and *ee* of the products. In the case of azepans, the addition of [2-PicAuNTf$_2$] as a lewis acid was required to form the more challenging 7-membered ring. The mechanistic proposal suggested an activation of the amine group, which prompts an aziridination of the double bond in order to achieve the systematic reductive elimination of the aryliodine(III) (Scheme 22).[92]

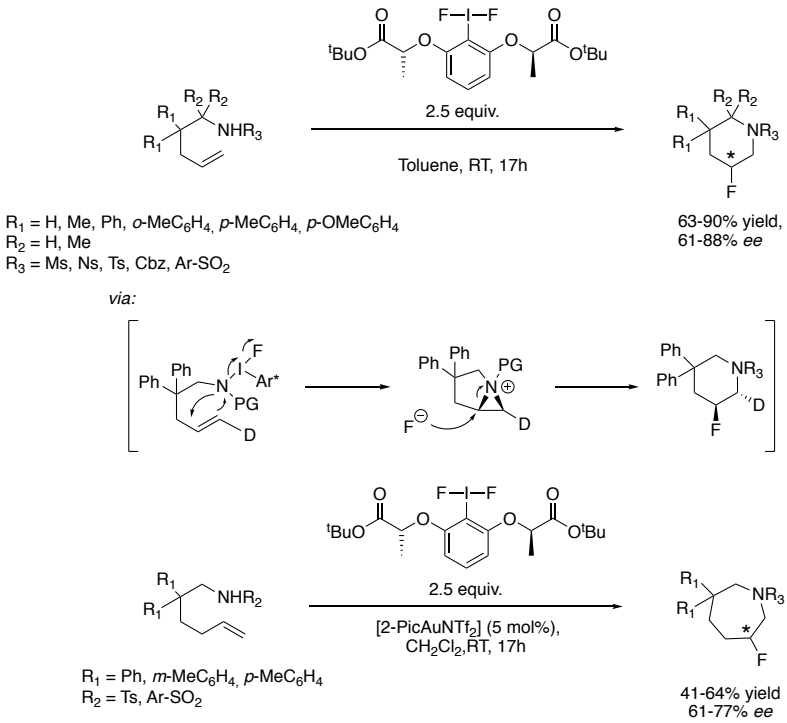

Scheme 22. Aminofluorination of alkenes to provide fluoropiperidines and fluoroazepans

Other examples were provided by Wirth during 2013-2017. By the use of the chiral reagents derived from Ishihara's catalyst (See next section), several important reactions were developed.

First, α-unsaturated ketones were submitted to Fujita's chiral lactate-based reagent seen above, and the rearrangement was observed with low to good yields and moderate to good *ee*. The use of TMSOTf or TfOH as lewis acid activator proved to be important for the reaction's enantioinduction. The reaction was thought to proceed through the nucleophilic attack of the alcohol to the iodine (III) intermediate (formed by ligand exchange), displacing the aryl group into the α-position of the ketone (Scheme 23a).[93] In second place, the *umpolung* of cyclic ketones with the same iodine (III) reagent enabled their nucleophilic functionalization. A first enolization to a functionalized silyl enol ether and

a latter treatment with the chiral hypervalent iodine (III) reagent provided a wide range of α-aminated and oxygenated ketones with high yields and *ee* (Scheme 23b).[94] Using the same reagent, arylketones could also be converted to α-arylesters in moderate yields and *ee* in 2016.[95]

Finally, an interesting alkene rearrangement to α-arylketones was discovered in 2016, when using a chiral aryliodine(III) reagent in 1,1-substituted olefins. The reaction relies on the use of $TsOH \cdot H_2O$ as activator, and MeOH as the nucleophile that will add into the iodonium intermediate generated in the first place. Then, after bond rotation, reductive elimination of the iodine (III) moiety allows for the observed rearrangement. A wide range of substrates could be submitted successfully to these conditions, obtaining up to 92% *ee* of the products (Scheme 23c).[96]

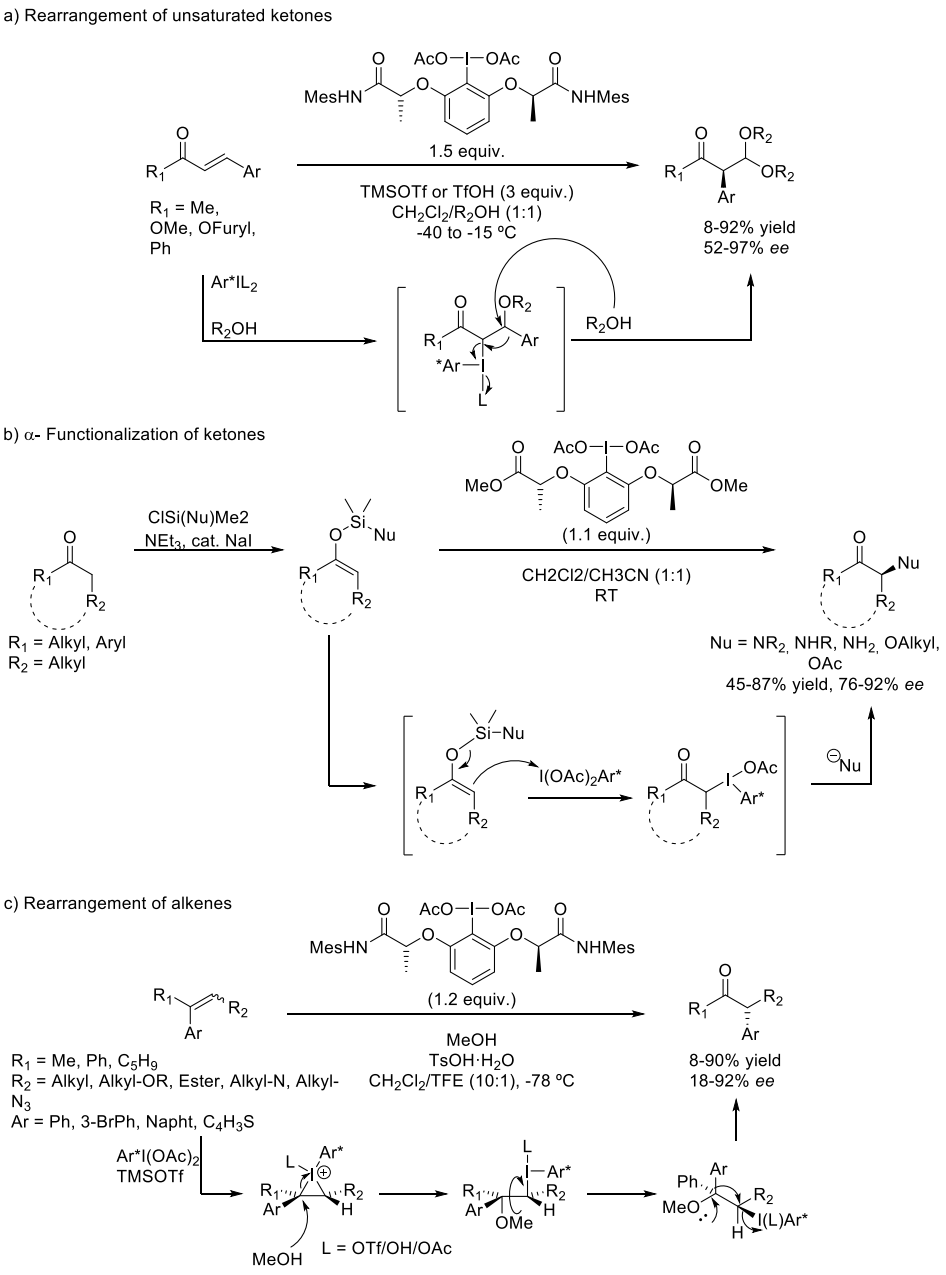

Scheme 23. a) Rearrangement of unsaturated ketones b) α-functionalization of ketones c) Alkene rearrangement to aryl ketones

1.4. Iodine (I/III) catalysis

1.4.1. The development of Iodine (I/III) catalysis

Given the broadness of the reactivity spectra presented in section 1.3.2, the idea of turning hypervalent iodine (III) chemistry into a new type of catalytic chemistry was thoroughly sought. The main reasons for this include the obvious atom economy that can be achieved by the catalytic concept, but also the further expansion of the field, as by that moment the inherent instability of some I(III) species was well known.

The concept of iodine (I/III) catalysis needs a suitable oxidant that reacts with an initial iodine (I) species (pre-catalyst). This will give rise to an oxidized I(III) (active catalyst) which contains the two ligands previously introduced in the reaction media, sometimes via ligand exchange or contained in the oxidant. Then, the substrate will react with this active species and form the product (Scheme 24).

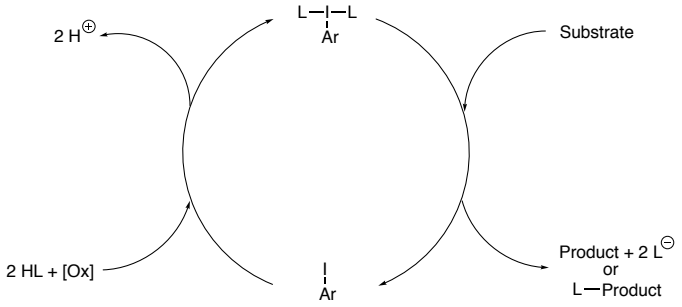

Scheme 24. Concept of Aryliodine (I/III) catalysis

It is therefore clear that the initial main obstacle that this concept faced was the selection of both oxidants and substrates which cannot react with each other. This problem was relatively fast to solve, but to date not many different oxidants are used in the field, with a great prevalence of peroxides.

Several groups reached the desired catalytic reactions in the beginning of

the decade of 2000. Among these, the first contribution was an intermolecular α-acetoxylation of ketones by Ochiai. The authors were successful in catalytically oxidizing iodobenzene to PIDA by *m*-CPBA/acetic acetic and its posterior reactivity with ketones. They used $BF_3 \cdot OEt_2$ as an activator for both the initial enolization of the ketone substrate and PIDA formation, and also reported 5 equivalents of water as necessary in order to achieve moderate to good yields of the final acetoxylated ketones (Scheme 25).[97]

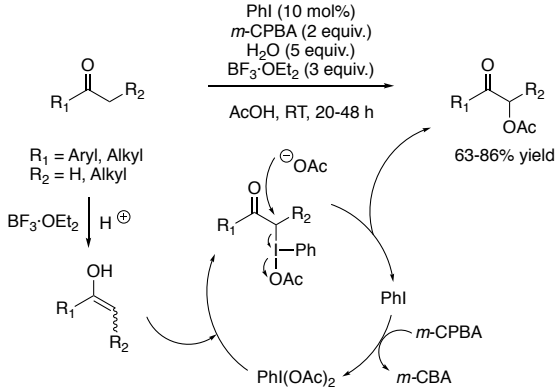

Scheme 25. First intermolecular reaction using I(I/III) catalysis

In the same year, Kita published the first catalytic intramolecular dearomatization reaction of phenols. In this case, a phenol was converted in good yields to a spirolactonized di-unsaturated ketone, by the action of 4-iodotoluene as pre-catalyst. The oxidation was also achieved with *m*-CPBA, and TFA was used as an additive. In the same paper, Kita *et al.* described also the first catalytic C-C bond formation by iodine (I/III) catalysis (Scheme 26).[98]

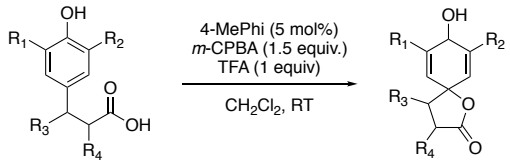

R_1 = H, Me, Br
R_2 = H, Me, Br
R_3 = H, Me, =CH-CH=CH-CH=
R_4 = H, Me, =CH-CH=CH-CH=

66-91% yield

Scheme 26. First catalytic Kita Dearomatization

These two examples set very important precedents for both intra and intermolecular reactions using iodine (I/III) catalysis, especially for the use of *m*-CPBA which would see an exponential increase in its use for this chemistry.[99]

1.4.2. Enantioselective iodine (I/III) catalysis

The challenge after the development of I(I/III) catalysis was the upgrade to both asymmetric and catalytic transformations. As seen above, the first chiral λ^3-iodanes date from 1975, and for this reason many authors wanted to apply the catalytic fashion to previously developed reactivity. Furthermore, many new reactions were developed since, in both stochiometric and catalytic manner at the same time.

The design of pre-catalysts has an utmost importance for the induction of enantioselectivity of the products. Even though some of them are inspired in previously developed chiral I(III) reagents, catalysis brought many new important structural features that would then even feed back into stochiometric reactions. The advent of this technology presented many advantages in terms of synthesis compared to the initial stoichiometric reagents as the stability issues of the corresponding I(III) can be mostly disregarded, being the species generated in situ. This fact further facilitates the modification of the aryliodine's backbones, as no isolation of the active species is required, which may be challenging in some cases.

The catalytic upgrade had also an effect on the scale of the synthesis of the pre-catalysts (See Chapter III). All these reasons brought enantioselective I(I/III) catalysis the popularity it has today, with new imputs generated constantly around the world.[100]

1.4.2.1. Structures and synthesis of pre-catalysts

As it can be extracted from the section 1.3.3.2, the aryliodine (I) backbones play a great role in the induction of enantioselectivity in the reactions with iodine (III) reagents, and by extension in the I(I/III) catalysis. Pre-catalyst can be classified depending on their symmetry, being C_2-symmetry and C_1-symmetry the most common. C_2-symmetrical biaryls have been widely developed, being the first ever developed and very useful for intramolecular chemistry. Other catalysts present one substituent in the *ortho* position of the aryl core, which contains one or more pre-installed chiral centres (C_1-symmetry) (Figure 7).

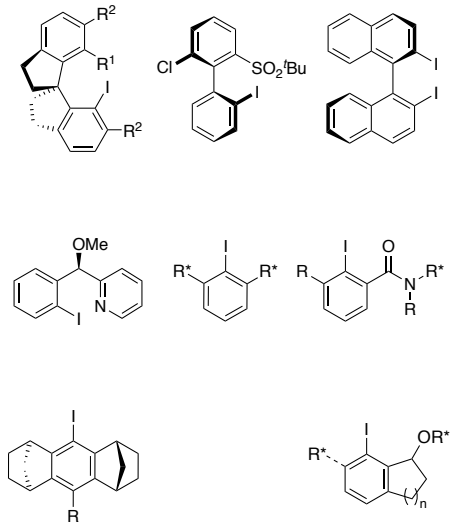

Figure 7. Common chiral pre-catalysts structures

A wide range of designs have been tried over the years, and the main strategies rely on alkyl substituents, annelated rings or chiral pool-derived moieties to promote enantioinduction.

The main quality of any given aryliodine(I) pre-catalyst resides in their ability to generate a suitable chiral pocket. This feature will *block* one of the enantiotopic faces of the substrate, allowing for the nucleophilic displacement of the I(III) (and its subsequent reductive elimination) to happen from the *free* enantiotopic face. The chiral pocket of Ishihara-Muñiz aryliodines will be discussed in the next sections.

1.4.2.2. Dearomatization reactions

One of the first examples of an enantioselective reaction was shown by Kita in 2008, in a work where both stochiometric and catalytic scenarios were developed (See section 1.3.3.2). In this starting point, where enantioselective catalysis was still under initial development, the maximum *ee* reported for naphtol dearomatization reactions was 69%, whilst the stochiometric variant went up to 86% *ee*.[88] In 2013, a modification of the same catalyst with ethyl groups in *ortho* position allowed for a much higher enantioinduction in the reaction, reaching up to 92% *ee* of the spirolactonized products. By extending the equatorial positions and screening different alkyl and ether groups, the authors could generate a successful pre-catalyst (Scheme 27).[101]

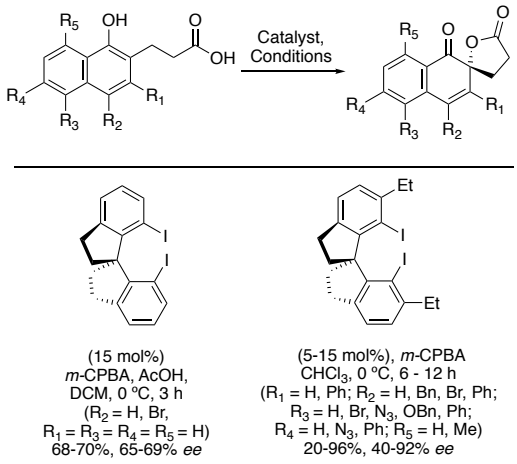

Scheme 27. Kita's catalytic enantioselective dearomatizations in 2008 and 2013

This was a very good example of how much pre-catalyst design matters: one basic structure can be slightly modified to highly amplify the *ee* of a given reaction, showing the capabilities of the catalytic upgrade.

Based on the X-Ray of the oxidized catalyst, the mechanism of the reaction was proposed to proceed through a nucleophilic attack of the carboxylic acid upon the less-hindered *Re*-face of the *ipso* carbon of the naphtol. This gives as product the *R*-enantiomer of the newly formed spiro-lactonized product (Scheme 28).[101]

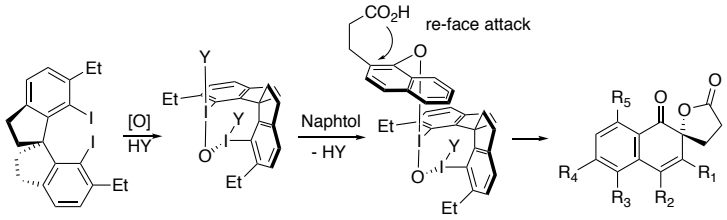

Scheme 28. Mechanism proposed by Kita in 2013

Another approach to the same reaction was developed by Ishihara in 2010. The pre-catalyst his group developed would later become the foundation for many other catalysts and thus is usually referred to as *Ishihara's Catalyst*. The basic C_2-symmetric structure of these pre-catalysts reminds the initial one of Fujita's reagents, but in this case

another moiety was introduced, a terminal mesitylene amide chained to the lactate.[91] This fact set the founding stone for the *modular* nature of these type of pre-catalysts, that will be thoroughly described throughout this thesis (See next chapters). In the seminal publication, Ishihara *et al.* described the same reaction as above (Scheme 29), reaching up to 92% *ee*, the same one achieved by Kita three years later in 2013.[101]

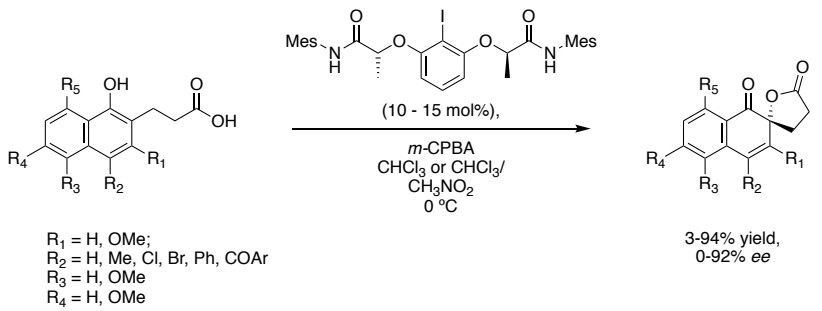

Scheme 29. First application of the lactate-based catalyst from Ishihara

The same group described their *second-generation* catalyst. Based on the same modular structures, they added a -CH_2- and also inverted the original lactate amide, being in this case the mesityl group the one bearing the carbonyl moiety and not the amine. Thus, the synthesis of this catalyst involves a 2-aminoalcohol instead of the former methyl lactate precursor. The rational design of this catalyst is of note as the underlying reasons for its enantiodifferentiation were shown: the folding of the active catalyst was found to be a chiral helix (Helical) configuration, helped by the H-bonding between the amide and the ligand in the I(III) centre (See chapters III and IV).

This catalyst was submitted to the aforementioned dearomatization reaching up to 98% *ee*. For the first time, the products of the dearomatization were subsequently submitted to a Diels-Alder reaction in a one-pot procedure, yielding the final bi- or tri-cyclic molecules in up to 97% *ee* (99% after recrystallization) using 1-10 mol% of the pre-catalyst (Scheme 30).[102]

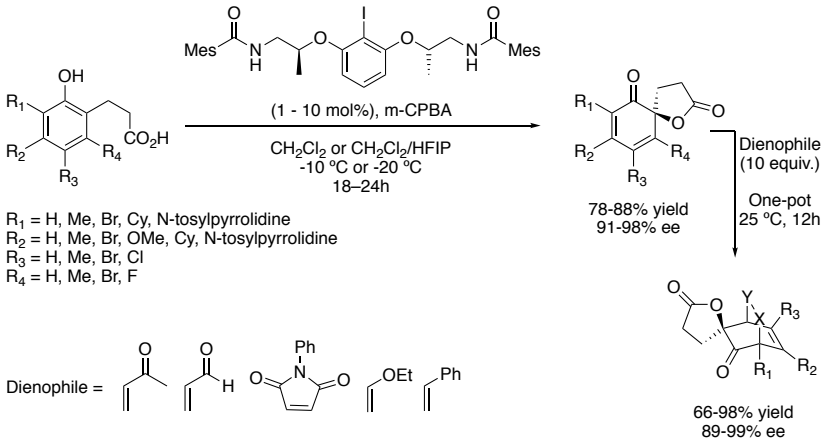

Scheme 30. One pot dearomatization/Diels-Alder reaction using Ishihara's second-generation catalyst

The same pre-catalyst was used in 2017 in order to dearomatize 2-naphtols, just in the adjacent position of the naphtol bridgehead. The reaction was successfully applied, with enantiomeric excesses reaching up to 95% *ee* and moderate to high yields (Scheme 31).[103]

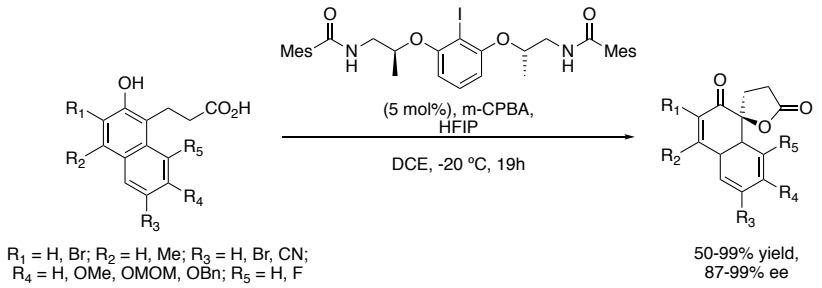

Scheme 31. Enantioselective dearomatization of 2-naphtols

To conclude with the classic naphtol substrates, two reactions were developed in 2015 and 2017 by Ibrahim and Kita respectively. In the first one, an original octahydrodimethanoanthracene structure was used with a *para*-methyl moiety, producing up to 67% *ee* of the spirolactonized products.[104] Similar *ee* were obtained by Kita by modyfing his original binaphtyl structure (Scheme 32).[105]

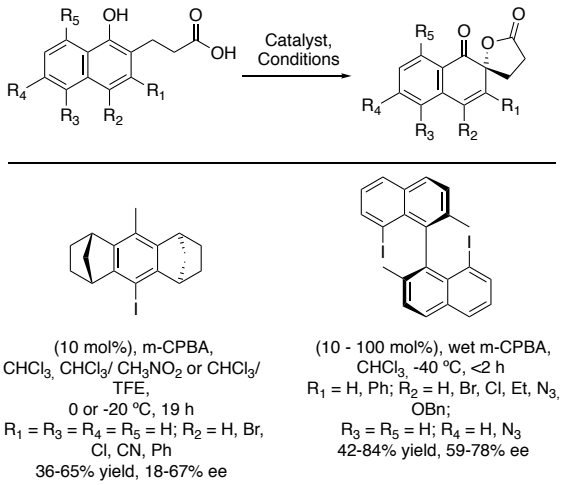

Scheme 32. Dearomatizations by Ibrahim and Kita

Besides the usual spirolactonization, the dearomatization reaction was expanded to terminal alcohols and amines by Ciufolini using a similar pre-catalyst, modified with *tert*-butyl groups at the chiral centres (Scheme 33 top).[106]

Harned also provided a spiroetherification with a different type of aryliodine, containing a tartaric bisamide. In this case, the ee values remained relatively low. One of the reasons for this fact can be due to the further *para*-dearomatization, which occurs at a longer distance from the I(III) centre than in the case of *ortho*-dearomatization (Scheme 33b).[107]

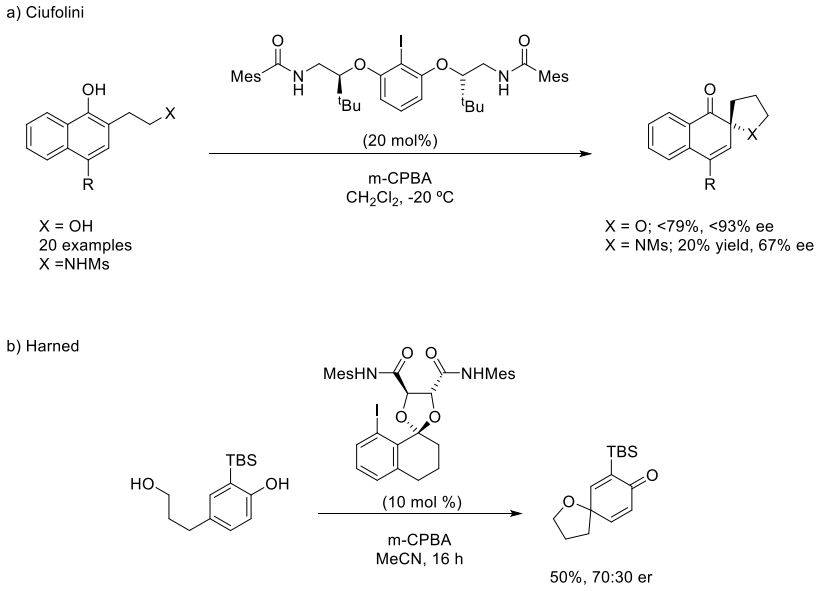

Scheme 33. a) Dearomatization by Ciufolini b) Harned's *para*-dearomatization

Another type of substrates submitted to dearomatization are the so-called *masked* quinones. Ishihara's pioneering work continued in 2017 with the development of these reactions. On one side, the reaction yielding *ortho*-quinones could be achieved in moderate to high yields and *ee*. This ecpanded the potential of Ishihara's second-generation pre-catalyst and showed good tolerance to more substrates (Scheme 34a).

On the other side, the *para*-quinones again presented much more difficulty due to the higher distance between the I(III) centre (attached to the phenol) and the site of the nucleophilic attack. This forced the authors to use the previously developed lactate-based catalyst and to enlarge the terminal aromatic amide, incorporating a chain of five consecutive

aromatic rings. Finally, the *ee* obtained for the substrates peaked at 89%, proving that the developed pre-catalyst could promote high enantioinduction (Scheme 34b).[108]

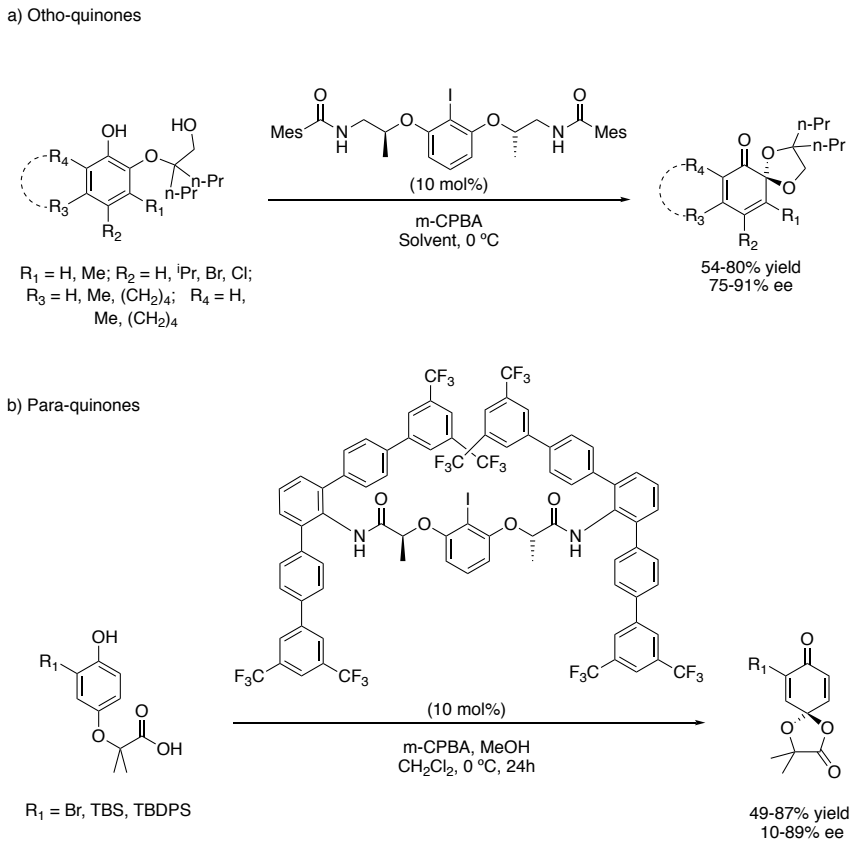

Scheme 34. a) *Ortho*-quinone synthesis b) *Para*-quinone synthesis

In 2015 a dearomatization was reported by Gong *et al.* forming for the first time an all-carbon chiral centre as a result of the dearomatization reaction. Using the first-generation Ishihara catalyst,[91] the enantiomeric excesses observed reached 92% *ee* and the yields were moderate. TFE was added in order to reduce the dissociation ability of the substrate (diminishing the electron-density of the I(III) centre). The mechanism of the reaction was proposed to proceed through the attack onto the *Si* face of the substrate,

while the *Re* face was hindered by the nearby terminal N-mesylamide of the catalyst (Scheme 35).[109]

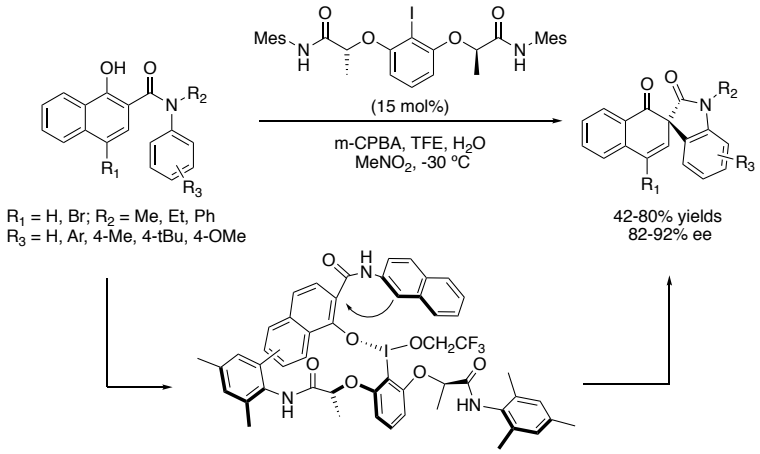

Scheme 35. All-carbon stereogenic centre formation from a dearomatization

One of the main upgrades in the recent years for the dearomatization reactions has been the development of intermolecular reactions. Even though they are still under progress, several examples can be outlined for their importance. The first asymmetric intermolecular dearomatization was successfully performed by Quideau in 2009. This reaction proved to be much more challenging than the previous intramolecular one: Firstly, two species – an *ortho*-quinol and an *ortho*-quinol epoxide – can be obtained from the reaction depending on the aryliodine loading. Secondly, the *ee* observed remained relatively low, reaching only 50% *ee* for the *ortho*-quinols and 29% *ee* for the *ortho*-quinol epoxides (Scheme 36a).[110]
Harned also worked on this chemistry later on, and used his aryliodine (I) with a chiral bis-amide structure in order to induce up to 60% *ee* in the products (Scheme 36b).[111] Additionally, in 2017 our group also developed an enantioselective intermolecular *para*-dearomatization of phenols, introducing new kinds of substrates such as tosylated anilines (See chapter III).[112]

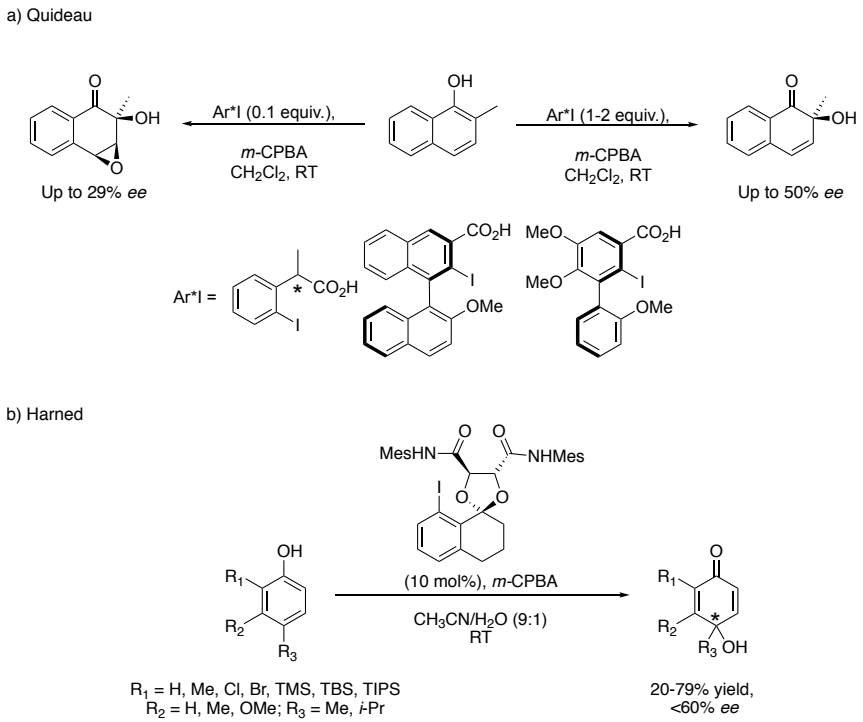

Scheme 36. a) Quideau's first intermolecular dearomatization b) *Para*-Dearomatization by Harned

Finally, the highest *ee* for an intermolecular dearomatization reaction was reported by Maruoka. The designed aryliodine (I) pre-catalyst was indanol-based and a methyl lactate moiety was also added. With this mixed structure, the enantiomeric excesses went up to 84% *ee* even though the yields remained moderate (Scheme 37).[113]

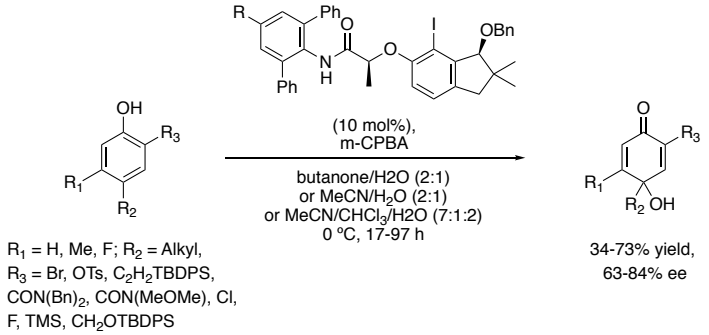

Scheme 37. Maruoka's *para*-dearomatization

1.4.2.3. α–Functionalization of carbonyls

The asymmetric α-functionalization of enolizable ketones represents a good strategy for the stereoselective synthesis of chiral ketone derivatives. Ishihara pioneered the racemic work, and Wirth its stochiometric enantioselective variant.[85,114]

Most of the reactions in this category proceed through an enolization at the beginning, and then the activated enol coordinates to the I(III) centre. A concerted nucleophilic attack and reductive elimination step allows several nucleophiles to be inserted at the α–position of the carbonyl.

The first and by far most common reaction is oxygenation. In 2010, Wirth developed the main conditions in which most enantioselective oxygenations would rely later, while trying a lactonization reaction. Even though this first attempt only produced up to 3% *ee* of the products, their conditions were kept to become a standard for this reaction (Scheme 38).[115]

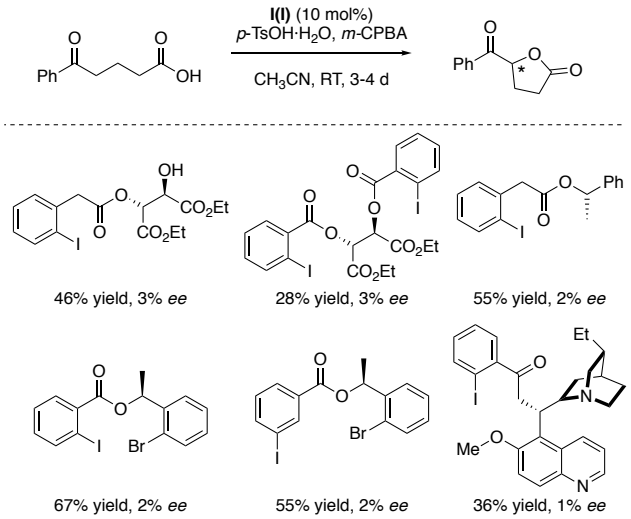

Scheme 38. First lactonization from Wirth

Another of the reactions where many pre-catalysts have been developed is the α-oxytosylation of ketones. Wirth presented the first enantioselective reaction in 2007 using a Koser-type aryliodine, even though the *ee* arrived only to 28%. When a menthyl ester was used in the structure of the pre-catalyst, the excess went up to 39% *ee,* but the use of the bromophenyl ester resulted in racemic products.[116]

Even higher results were achieved with the spirobiindane aryliodine pre-catalyst designed by Zhang and co-workers, who reached moderate yields and 58% *ee* for this transformation.[117]

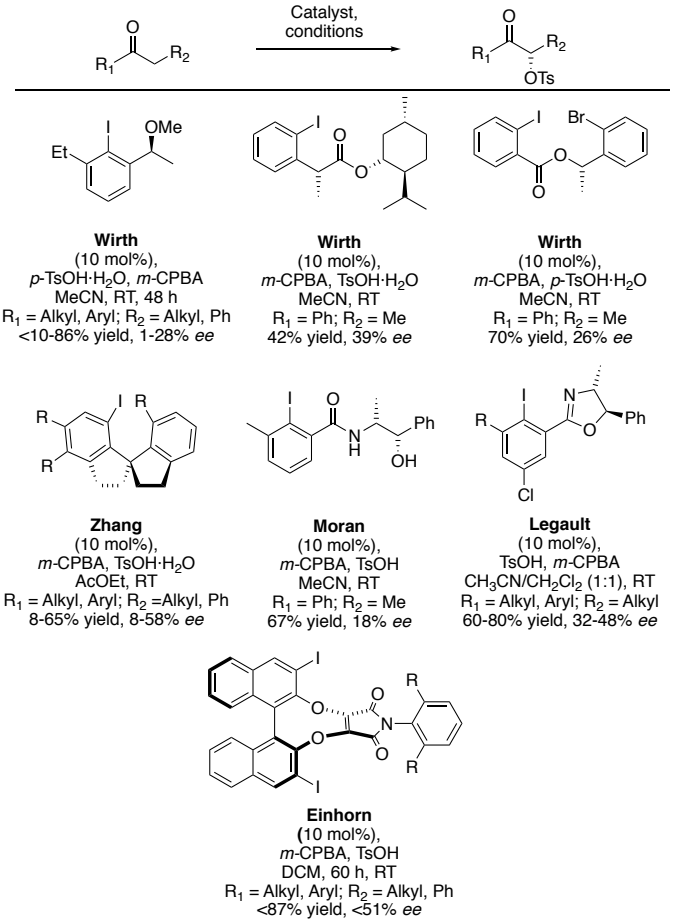

Scheme 39. Enantioselective oxytosylation of ketones

Other authors such as Moran, Legault and Einhorn also developed different pre-catalysts for the oxytosylation of ketones, getting a maximum of 48 and 51% *ee* respectively (Scheme 39).[118–120] All these efforts to design a better pre-catalyst for the reaction paid off in 2015 when Legault developed a lactate-based aryliodine (I) that reached a peak of 90% *ee* of the oxytosylated products. The key to this work resided in the fact that the authors used an acetyl enol ether instead of the traditional propiophenone as substrate. This fact led to a much higher enantioselectivity than using the ketones, which got only up to 5% *ee* (Scheme 40a).[121]

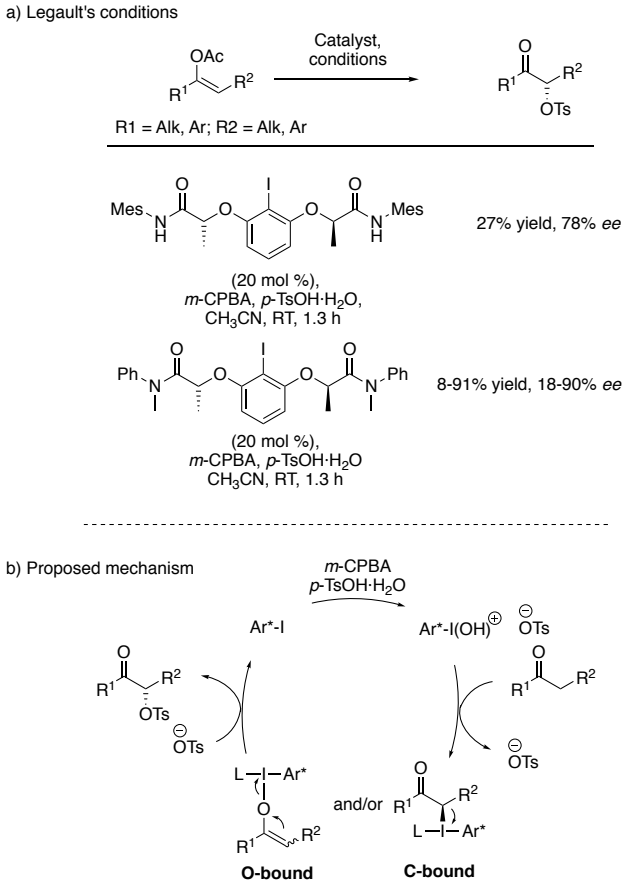

Scheme 40. a) Legault oxytosylation b) Proposed mechanism

When looking into the mechanism of the reaction, two different intermediates have been proposed generally to get the resulting oxygenated molecules. One of them includes the I(III) centre coordinated to the oxygen and the other one is C-coordinated to the α–position of the carbonyl. Higher enantioinduction and yields have been observed when using acetyl enol ethers instead of free ketones as initial substrates (Scheme 40b).[122]

Other types of products that can be obtained by similar methodologies were presented by Masson *et al.* in 2017, including other sulfonyls and phosphoryls. The design of the catalyst was based in the traditional Koser-type reagent but adding an axially chiral moiety that made the authors reach the 94% *ee* milestone (Scheme 41).[123]

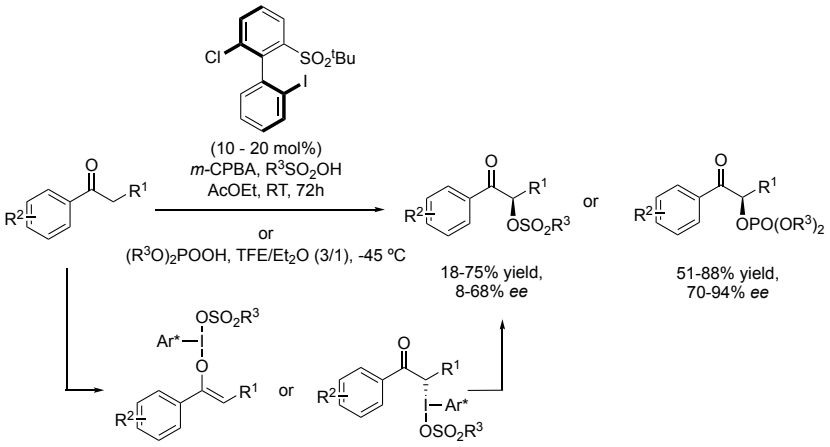

Scheme 41. Sulfuryl- and phosphorylation by Masson *et al.*

Another of the functionalizations in the α–position of the carbonyl that has started to gain importance is the enantioselective halogenation of ketones. One of the pioneers in this field was Kita, who in 2014 could fluorinate a β–dicarbonylic compound, using HF as the fluorine source and his axially chiral double iodinated aryliodine (I). The reaction proceeded with modearate yields and enantioselectivities (Scheme 42a).[124]

Later, Rueping *et al* successfully improved Kita's work by the use of a lactate-based aryliodine and $NEt_3 \cdot 5HF$ as a fluoride source. This combination proved to be as effective than the previous one, as the 90% *ee* was surpassed. The two pre-catalysts used for this transformation displayed menthyl esters as the main motif to induce this high enantiodifferentiation. It is noteworthy to mention that this specific design with a bi-phenyl system is not common in lactate-based pre-catalysts, and it provided in general higher selectivities than the "naked" lactate-containing aryliodine (I) (Scheme 42b).

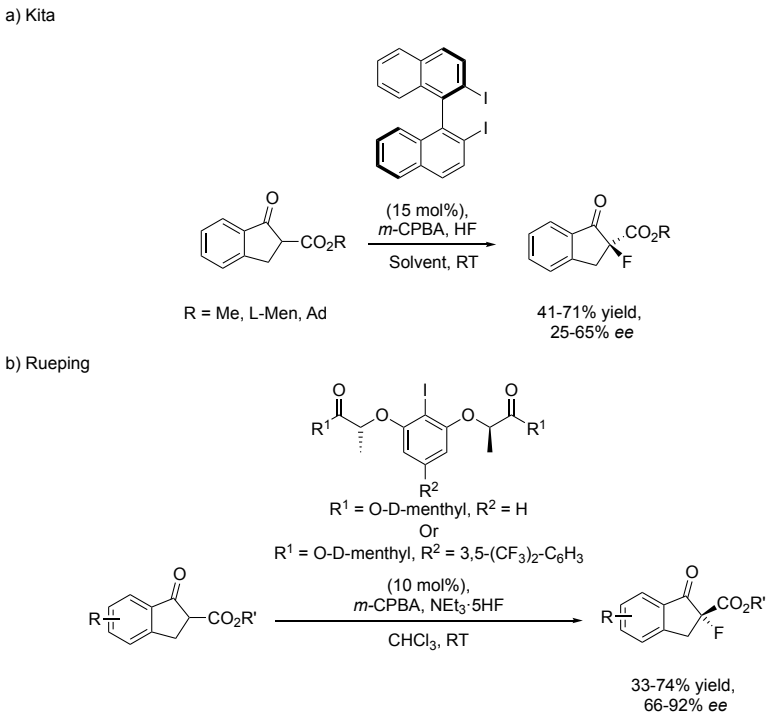

Scheme 42. a) Kita's enantioselective Fluorination b) Rueping's modification

In order to understand the mechanism of the reaction, DFT calculations were carried out by the authors. These suggested that a first I-O bond formation can be formed. Afterwards, proton abstraction by the HF could form an enolized structure, which ultimately leads to the transfer of the

I(III) to the α-position of the carbonyl. This intermediate would be the calculated enantioselectivity-determining step. Afterwards, a double inversion of the stereochemistry takes place: First, an hemiacetal is formed after the oxygen in the carbonyl displaces the I(III) moiety and second when a *trans*-selective opening from a nucleophilic fluoride takes place and generates the preferred (*R*)-enantiomer observed (Scheme 43).[125]

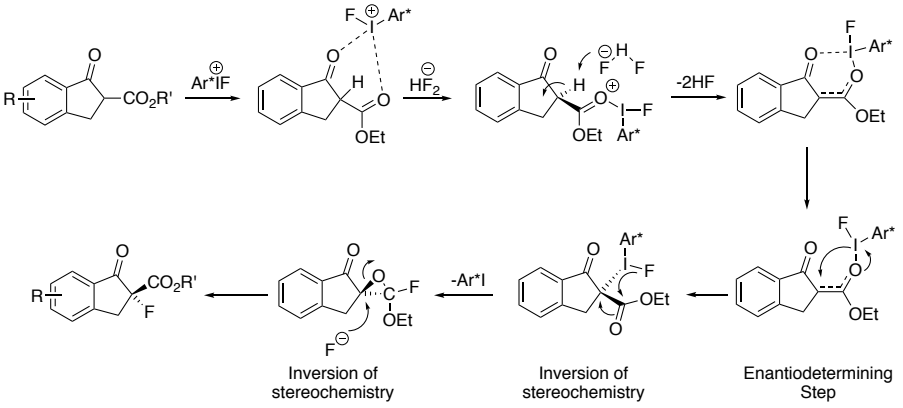

Scheme 43. Proposed mechanism supported by DFT calculations

Continuing with α–halogenations of carbonyls, in 2016 Legault followed a contrary strategy: He achieved the formation of α–chloro ketones from chloroalkenes instead of ketones. His experiments were successful but only reached a 27% *ee* of the α–chlorinated products. The use of TsOH·H_2O proved key in order to introduce the oxygen of the final ketones into the substrates.[126]

Finally, a prominent example of a formal α–functionalization was developed by Gong *et al.* while investigating the formation of *spiro*

compounds: a C(sp^2)-C(sp^3) bond formation. This group also used a resorcinol and methyl lactate-based pre-catalyst, bearing terminal proline esters as amides. The reaction was successful, albeit the yields can be considered moderate but also with up to 90% *ee* of the desired enantiomers of the products.[127]

Sometime after, Hadad, Sunoj *et al.* suggested that the I(III) generates an I-O bonded species, which undergoes proton abstraction and generates an enamine. A migration of the I(III) centre could then provide a C-iodonium intermediate, which the authors consider the enantiocontrolling step. Then, an S_N2 takes place between the methylenic carbon and the next aromatic carbon, creating the first new bond. A similar path is followed to afford the second C-C bond. The enantioselectivity of the reaction relies on this step as the chiral information is lost through the enamine formation (Scheme 44).[128]

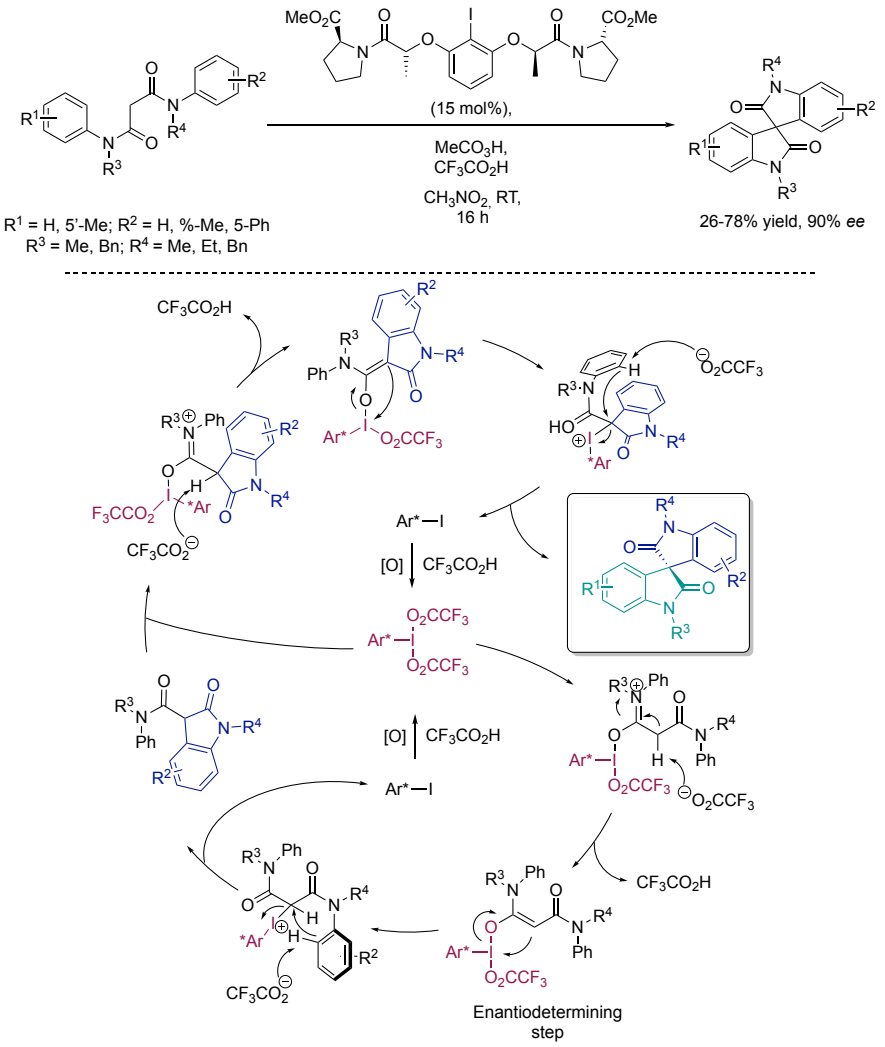

Scheme 44. Gong's C-C bond formation and mechanistic proposal

1.4.2.4. Alkene difunctionalization

Alkenes are perfect matches for Iodine (III) catalyzed reactions due to the electron-density of their π orbitals. This fact makes them a moiety with facile coordination with electrophilic I(III) active catalysts and subsequently a good fit for reactivity. Many difunctionalizations of alkenes have been developed throughout the history of contemporary chemistry

(see previous sections), but enantioselective I(I/III) catalysis is thought to give a synthesis a more environmentally friendly aspect. One requirement that these alkenes need is the preferential reactivity with the active I(III) species than with the usual peroxide oxidants generally used in these reactions. Therefore, a clear selectivity for the oxidation of the aryliodine (I) or a kinetic preference over the background oxidations is needed for the viability of these reactions. One of the first alkene difunctionalizations came from Fujita's group who designed in 2012 a range of pre-catalyst based on their previous I(III) reagents (See section 1.3.3.2) and used peracetic acid as co-oxidant.

From all of them, a pre-catalyst with a terminal menthyl ester was selected for its very high enantioinduction. Two main products from the catalysis arose from the reaction and two racemic ones belong to background reactions (not shown), with their combined yields remained below 70% and the enantioselectivity of the products reached up to 98% *ee* (Scheme 45).[129] In the same year, the group applied their methodology using I(III) reagents for the synthesis of enantiopure hydroxymonocerins.[130]

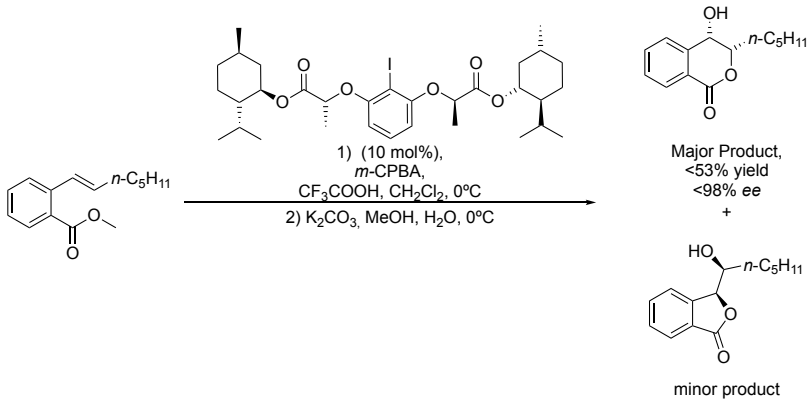

Scheme 45. Fujita's alkene deoxygenation

Another type of combined intra/intermolecular reactivity using I(I/III) catalysis was developed by Moran in 2015, which produced oxazolines in high yield and moderate *ee*. The cyclization of unsaturated amides

produced five- and six-membered rings by the use of a lactate-based aryliodine (I) and Selectfluor as co-oxidant. The mechanism was thought to proceed through a first intramolecular attack followed by a nucleophilic oxygenation that triggered the reductive elimination leaving a 1,2-dioxygenated final product (Scheme 46).[131]

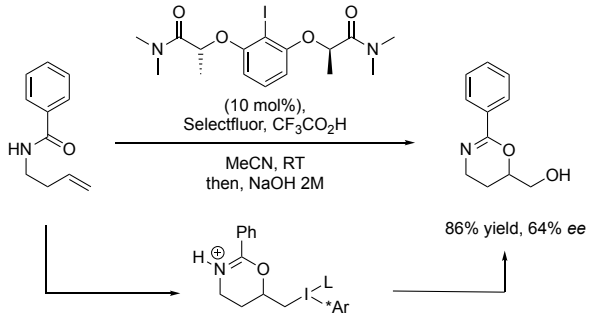

Scheme 46. Moran cyclization of N-alkenamides in 2015

In 2017, Masson further expanded the field by the development of an enantioselective lactonization of alkenes coupled with the introduction of a sulfonyl or a phosphoryl group into 4-pentenoic acids. In the case of the phosphorylation, moderate to high yields were reported and up to 94% *ee* of the products. However, the sulfonylation resulted in lower yields and enantiomeric excesses. The catalyst used in this case was Ishihara's first generation pre-catalyst,[91] which promoted the high *ee* observed in the final products. The proposed mechanism for this reaction involved the initial coordination of the active I(III) species to the alkene, and the enantioselective lactonization step by the neighbouring carbonyl. The catalyst effectively blocked the *Si* face of the substrate in this step, and finally the subsequent nucleophilic displacement of the I(III) from either a sulfonyl or a phosphoryl group yielded the final product (Scheme 47).[132]

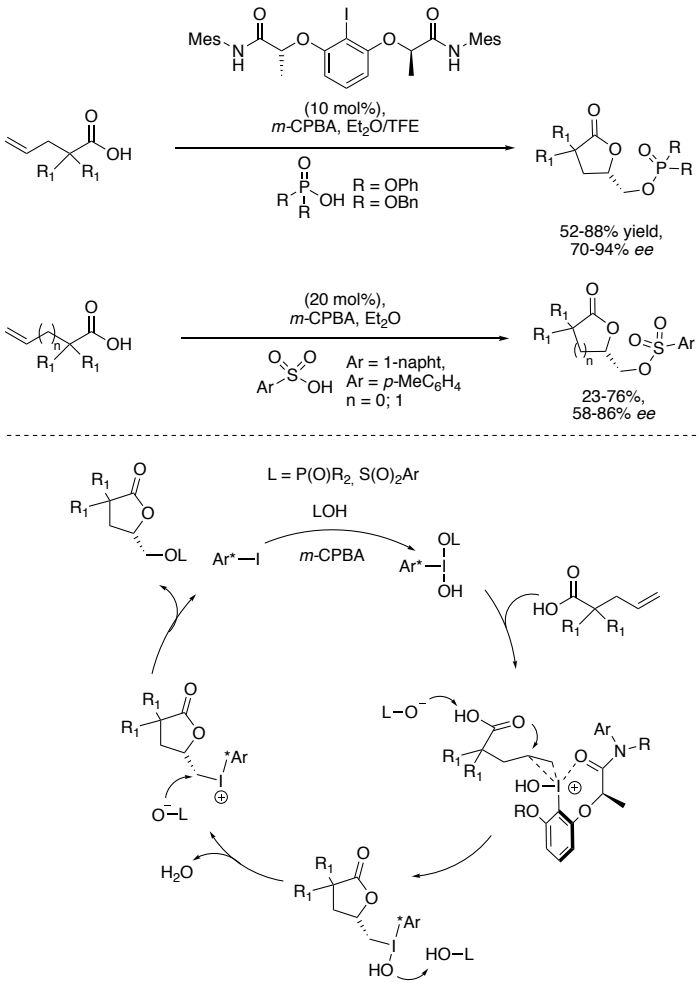

Scheme 47. Difunctionalization by Masson in 2017

Another reaction type of interest similar to these examples is the diacetoxylation of alkenes. Our group has developed in 2016 two enantioselective diacetoxylations that are described in Chapter III, reaching high yields and *ee*.[133,134] Important diaminations have also been developed by our group, which are described in the introduction of Chapter II.[135]

One of the first examples of racemic, I(III)-mediated aminofluorination was developed in 2012 by Li [136] One year later, the Nevado group developed

the enantioselective version of this reaction (Seen above in section 1.3.3.2), using a di-fluorinated version of a lactate-based I(III) reagent.[92] These two projects inspired Kita and Shibata to come up a catalytic, enantioselective version of the reaction, which was developed in 2014. Employing their already developed axially chiral biaryl, a 70% *ee* was obtained. Even though the yields and enantiomeric excesses were relatively lower than in the stochiometric version, their work inspired others to explore similar reactivity. The most prominent examples came from the group of Jacobsen in 2018, where the authors could obtain α–Fluoroaziridines from aminostyrenes. The pre-catalyst used was an ester derived from the mentioned lactates, but with the notable modification: the introduction of an ester in the *para*-position of the aryl core. With this design, the authors could reach remarkable yields and enantiomeric excesses, reaching up to 97% *ee*. The newly formed aziridines were further derivatized by ring-opening and substitution giving access to a wide range of highly enantiopure, derivatized fluoroamines. The main limitation of this reaction was the formation of mainly 3-membered rings and only one 5-membered ring, lacking the formation of 6-membered rings. While 3-membered rings formation presented a *syn* product, the 5-membered ring was in *anti* disposition, this difference was thought to indicate that both reactions proceed through different pathways (Scheme 48).[137]

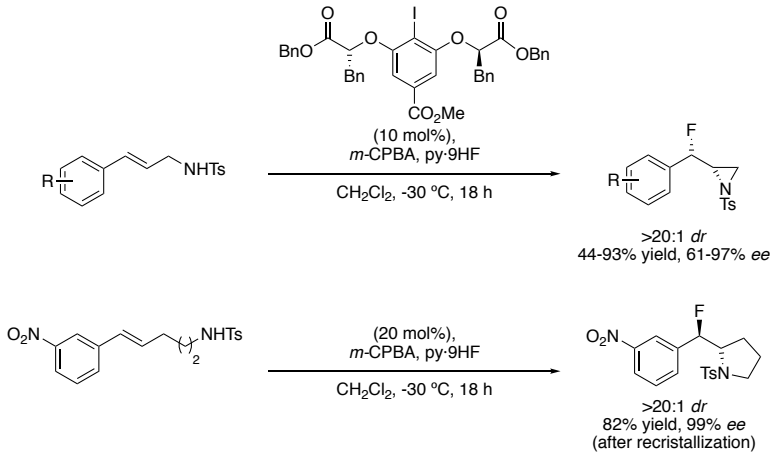

Scheme 48. Jacobsen's aminofluorination

A similar aryliodine was previously developed by the same group in order to promote the catalytic enantioselective fluorolactonization of 2-unsaturated methyl benzoates, resulting in the formation of 4-fluoroisochromanones.The yields remained mainly moderate but the enantioselectivity of the reaction proved to be very high with examples with up to 96% *ee*. Even though most of the substitution was very well tolerated, when using more electron-deficient substitution a drop in yields and *ee* were observed (Scheme 49).[138]

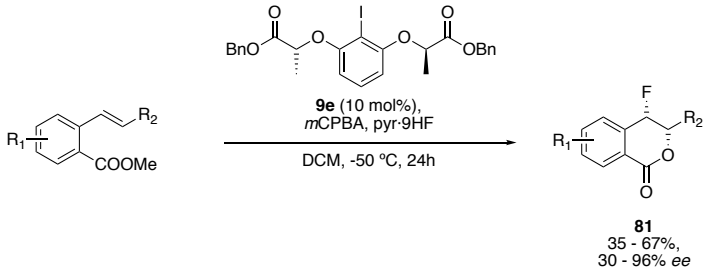

Scheme 49. Formation of 4-fluoroisochromanones

Additionally to the development of fluorooxygenation and fluoroamination reactions, an enantioselective difluorination was also developed. Several top-tier publications by the groups of Jacobsen and Gilmour have made I(III)-mediated reactions popular within the context of fluorination

chemistry. In 2016, Gilmour developed an a racemic vicinal difluorination of styrenes. They used the Ishihara's 2nd generation catalyst obtaining up to 22% *ee* of difluorinated compounds and 41% *ee* of oxyfluorinated compounds. One of the main novelties they introduced were the use of selectfluor as terminal oxidant with a combination of $Et_3N{\cdot}3HF$ and Py·HF as fluorine sources, which proved effective for the desired transformation (Scheme 50).[139]

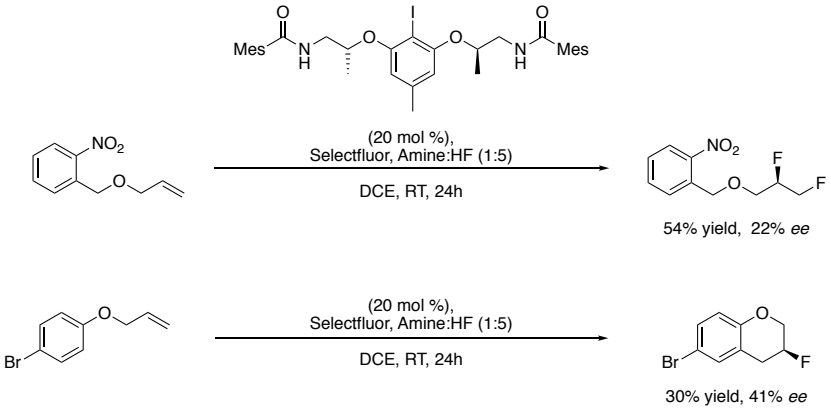

Scheme 50. Gilmour's first enantioselective difluorination and oxyfluorination

Simultaneously, Jacobsen introduced two different fluorinations with his newly developed catalyst. Even though the difluorination of alkenes was racemic in this initial work, the 1,2-difluorination of *o*-nitrostyrenes and β–substituted acrylamides could be performed in an enantioselective fashion. This first publication relied on the use of 20 mol% of the catalyst in combination with Py·HF as a fluorine source and *m*-CPBA as terminal oxidant, and produced the target difluorinated molecules in up to 93% *ee*. Mechanistically, the role of both the *o*-nitro and the amide groups was thought to be key as the authors propose that the *anti*-difluorination observed is the consequence of the anchimeric assistance of these moieties within the reaction pathway. In the case of amides, it is the carbonyl moiety which displaces the I(III) species, generating an oxiraniminium intermediate which fluoride attacks (Scheme 51).[140] Some

years later a similar procedure was found to be also effective in the enantioselective vicinal difluorination of *N-tert*butyl Cinnamides in an analogous work from Jacobsen.[141]

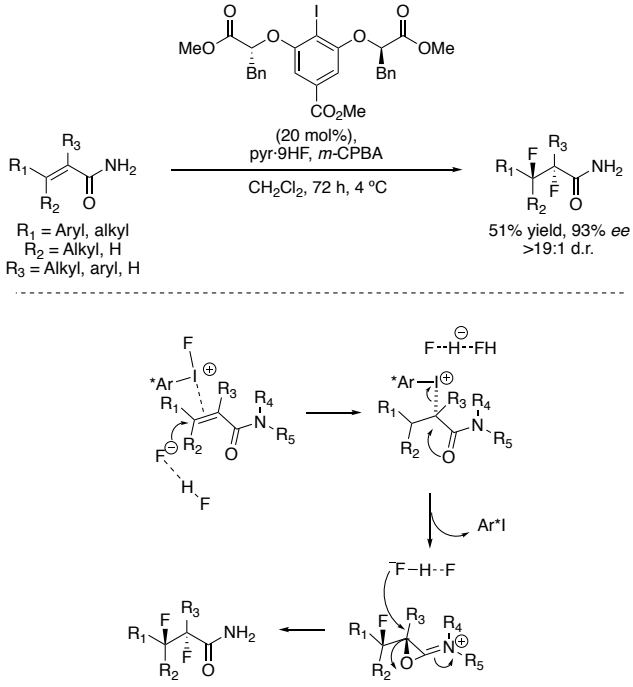

Scheme 51. Enantioselective vicinal difluorination of acrylamides by Jacobsen

The second work provided a much general geminal difluorination of styrenes, employing the same pre-catalyst. Amides and esters were well tolerated by the methodology developed, reaching moderate to high yields and up to 97% *ee*. Mechanistically, the removal of the alkyl R_3 substituent of the previous reaction (See scheme 51) makes a drastic change in reactivity. In this case, the neighbouring aryl ring migration is proposed as the responsible for the displacement of the I(III). The resulting phenonium ion intermediate causes the rearrangement of the cyclopropane ring and a nucleophilic attack upon the previously substituted carbon finally results in the 1,1-difluorinated products (Scheme 52).[142]

Finally, Gilmour published the enantioselective 1,2-difluorination of

styrenes in 2018 using a C_2-symmetric pre-catalyst secondary amide, based on an orcinol core and bearing two mesytils α to the carbonyl.

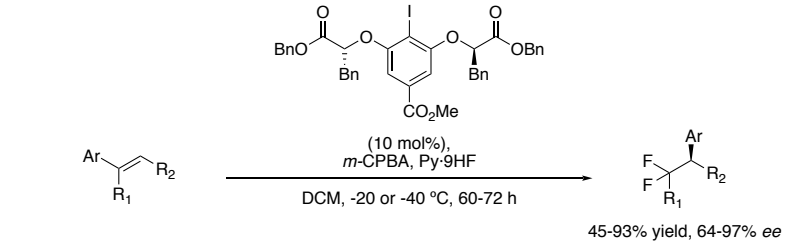

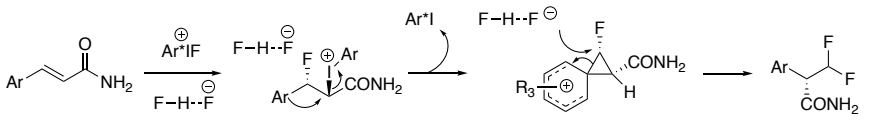

Scheme 52. Jacobsen's enantioselective geminal difluorination

By their previously developed methodology using both Py·HF and Et_3N·HF along with selectfluor, up to 88% *ee* of the vicinal difluorinated compounds was obtained. For the mechanism of the reaction, the authors proposed the double displacement of the I(III) by a nucleophilic addition to the aryliodonium intermediate by the fluoride (Scheme 53). Additionally, the geminal product by Jacobsen was also observed, as the mechanism of the reaction can also involve the one described above.[143]

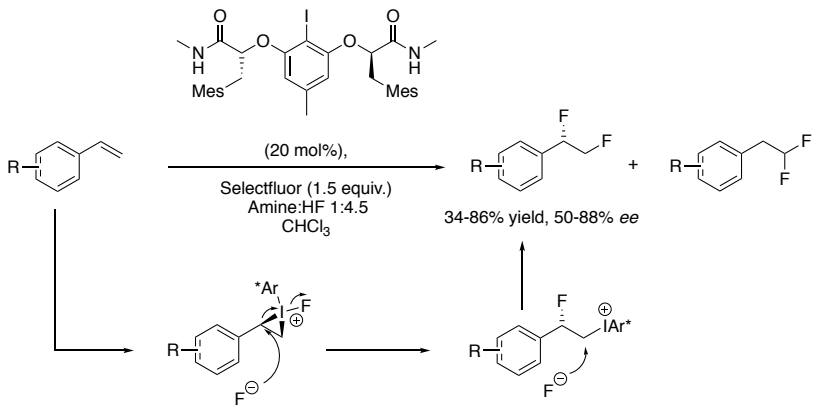

Scheme 53. Difluorination by Gilmour

1.5. Overall Aims

Our group has always put the focus in the development of new methods for oxidative amination required to obtain aminated and diaminated compounds. Indeed, most of the published work from the Muñiz group revolves around the formation of new C-N bonds with several tools.

As presented throughout this introduction, I(I/III) catalysis has become a state-of-the-art field in the recent years, showing they are both effective and green alternatives to transition-metal catalysis. Moreover, the introduction of enantioselective reactions by the design of new catalysts has had a prominent impact on general organic synthesis and methodology.

For some years, our group has designed and developed new pre-catalysts and reactions, and several major breakthroughs have been achieved. In several publications, the importance of the design of the pre-catalysts has been highlighted as one of the major crucial points for enantioinduction in I(I/III) catalysis. Thus, bearing these two concepts in mind – diaminations and I(I/III) catalysis, this thesis intends to design new catalysts for diamination reactions and also to go as deep as possible into unknown points of aryliodine (I/III) catalysis.

First, the catalytic racemic diamination of styrenes is presented containing two types of amine nucleophiles.

Then a scale-up of the pre-catalysts for enantioselective diamination reaction was performed and brought insights on how to maximize the enantiomeric excess of these reactions.

Finally, a new unsymmetrical aryliodine(I/III) pre-catalyst was developed, showing a high performance and giving information on the importance of the pre-catalysts' side chains in the diamination reaction.

Chapter I – General Introduction

Chapter II – A practical aryliodine (I/III) catalysis for the vicinal diamination of styrenes

2. Chapter II – A practical aryliodine(I/III) catalysis for the vicinal diamination of styrenes

Chapter II – A practical aryliodine (I/III) catalysis for the vicinal diamination of styrenes

2.1. Introduction: Alkene diamination reactions using I(III) or I(I/III) catalysis

2.1.1. Nitrogen sources

In contrast with other reactions in organic chemistry, there are not any equivalent direct biochemical routes for vicinal diamination, which has always forced chemists to come up with novel, non-biomimetic methodologies. Apart from metal transition catalysis developed by many authors during the last 20 or 30 years, diamines have been also synthesized in the last decade using hypervalent iodine chemistry. When thinking of a given diamination, one of the most important features consists in the selection of suitable nitrogen sources for the active species in the reaction. The fact that sulfonamides were already successfully introduced in alkenes in combined Pd-I(III) methodologies previously was the hint that they could represent a proper fit for metal-free diaminations.[33,37]

The acidity of the NH proton is key for the successful formation of I(III) species both in stochiometric reactions and *in situ* oxidations of I(I). This is a consequence of the effect of the two sulfonamides that grant the nitrogen atom a sp^2 character. Hence, sulfonamides and bissulfonamides were identified as very suitable ligands (Figure 8) for hypervalent iodine (III)-mediated reactions.[144]

Along these lines saccharins, phtalimides and succinimides have also been used as ligands for I(III)-mediated reactions since the 1980s (Figure 8). However, their N-I bonds are stronger and thus the reactivity differs from the one shown by sulfonamides or bissulfonamides.[145,146]

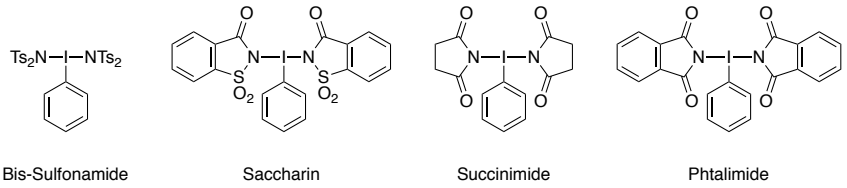

Figure 8. N-bonded hypervalent Iodine (III) species

2.1.2 Racemic diaminations of alkenes

Several diaminations of alkenes using hypervalent Iodine(III) have been developed during the last decades. In 1986, Moriarty developed the first vicinal diazidation by the use of iodosylbenzene (PhIO) and $NaNO_3$, and AcOH as solvent. By reduction of the products of the reaction, vicinal diamines can be obtained, but azides are known for their explosive nature, which makes difficult the application of this reaction (Scheme 54).[147]

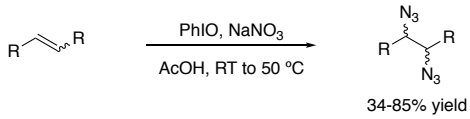

Scheme 54. Diazidation by Moriarty

One of the first relevant contributions came from Muñiz and Barluenga in 2008. When studying the cyclization of ω-alkenyl ureas with Pd(II)/Cu(II) catalysis, the authors found that the application of the hypervalent reagent IPy_2BF_4 resulted in the formation of the product without the need of metal catalysis (Scheme 55). The obtained amines were *anti* when using *E* alkenes, due to a first *anti* aminoiodination and a subsequent S_N2 reaction.[31]

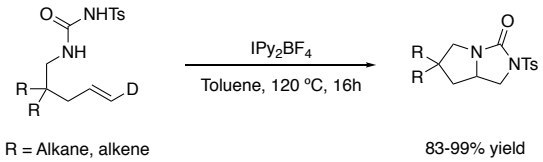

Scheme 55. Cyclization of w-alkenyl ureas by Muñiz and Barluenga

Chapter II – A practical aryliodine (I/III) catalysis for the vicinal diamination of styrenes

From 2010, the Muñiz group has been focused in the diamination of styrenes, starting with a pioneering work: the enantioselective diamination with stoichiometric chiral I(III) reagents (See section 2.1.3).[148] This work was also supported by observations during the mechanistic studies of metal-catalyzed diaminations, where the major product of the Pd-mediated reaction was a bistosylimide. This was interpreted as a product of an I(III)-mediated reaction as no phtalimide was introduced (Scheme 56).[37]

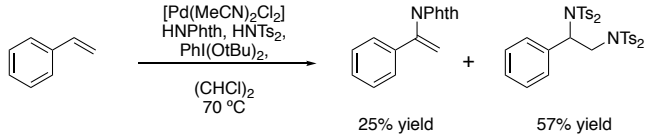

Scheme 56. Formation of a major bistosylimide showing an alternative I(III) mediated pathway for the diamination

The racemic, stochiometric versions of this reaction were then developed, and allowed for an insightful knowledge we nowadays have. By the use of PIDA and a sulfonamide, a broad range of alkenes were explored. Most functionalities were well tolerated, with the exception of high electron density styrenes (like *p*-methoxystyrene) which gave an enimide instead. Two types of sulfonamides were introduced as nucleophiles: Bistosylimides and Bismesylimides. (Scheme 57a).

Additionally, this methodology was extended to terminal and internal olefins with very different moieties, showing moderate to good yields (Scheme 57b). When using internal *E* or cyclic olefins, an *anti* product was observed, but *Z* alkenes led to *syn* products or mixtures. [149] The mechanistic proposals at that time suggested an active I(III) species containing an acetate and a sulfonamide Nonetheless, subsequent investigations showed that most probably the active species of the reaction is a bis-sulfonamidated I(III) species (Scheme 57c).

Chapter II – A practical aryliodine (I/III) catalysis for the vicinal diamination of styrenes

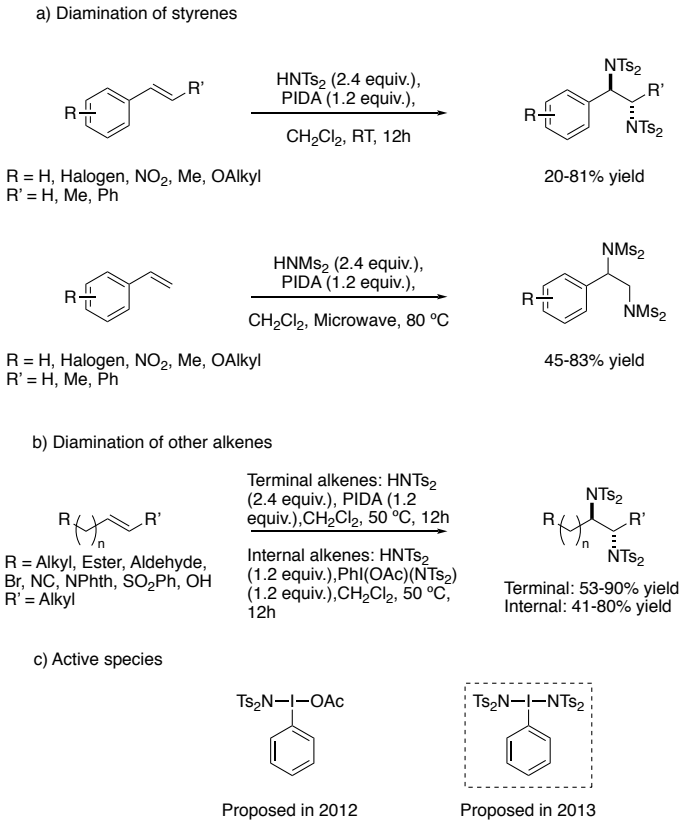

Scheme 57. a) Diamination of styrenes b) Diamination of unactivated alkenes c) Active species

Notably, this compound is stable at room temperature and was subsequently used directly for the diamination of styrenes, α-amination of ketones and even aromatic amination.[150] Other relevant uses include diamination of dienes and trienes[151], allylic amination[152], acetylenic amination[153] and amination of allenes.[154] Thus, the conditions for the styrene diamination were improved in terms of yields but mostly in terms of reaction time (Scheme 58).

Chapter II – A practical aryliodine (I/III) catalysis for the vicinal diamination of styrenes

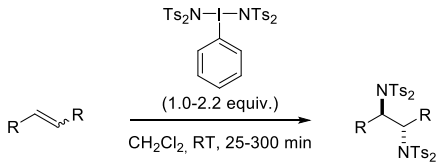

Scheme 58. Improved diamination using $PhI(NTs_2)_2$

The discovery of stable bisimidoiodanes helped understand the mechanism of the reaction, which was postulated in 2016. In this publication, our group collaborated with theoretical chemists to propose a calculated mechanism for the reaction. In the first place, after coordination of the I(III) to the styrene, it is the oxygen of the sulfonamide that is incorporated in the styrene (which was confirmed experimentally). This is followed by a five-membered transition state similar to the Woodward-Prévost intermediate when dihidroxylating alkenes.[155] Ring opening by reaction with another bismesylimide molecule displaces the oxygen tethering and yields the final product (Scheme 59).[156]

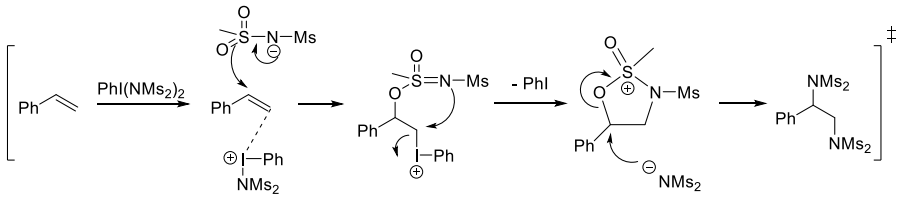

Scheme 59. Calculated mechanism for the diamination reaction using $PhI(NMs_2)_2$

When studying the structural design of the bistosylimido reagents, our group found that the best *para*-substituents for the reaction were R = H or R = Me, and that electron-withdrawing *para*-substitution lowers the conversion of the diamination reaction.[157]

2.1.3 Enantioselective diaminations of Styrenes

In 2011 a major development of metal-free diamination chemistry took place when our group developed the first ever I(III)-mediated enantioselective diamination. The chiral I(III) reagent from Fujita[90] was used in combination with a sulfonamide in CH_2Cl_2 at 0 ºC and a wide scope of styrenes were diaminated reaching up to 95% *ee* (Scheme 60).[148]

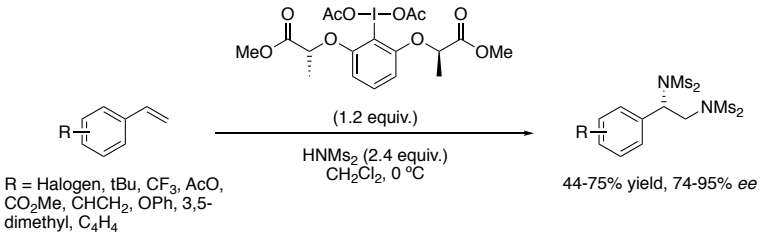

Scheme 60. I(III)-mediated enantioselective diamination of styrenes

Some years later, this reaction was upgraded to the catalytic version. This facilitated the reaction as the active species is generated *in situ*, and the scope of the reaction was further broadened. Thanks to the previous studies, the design of the pre-catalysts was thought as a mixture of all the enhancing structural features that worked previously. By changing the terminal amides from Ishihara's pre-catalyst[134] to isopropylamines and adding a *para*-methyl moiety in the aryl core, the best results were obtained (Figure 9).[135]

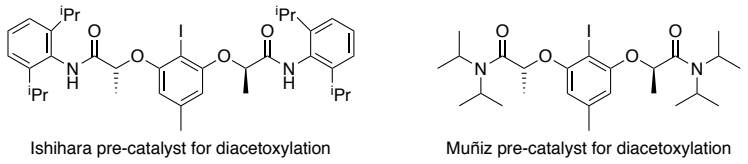

Figure 9. Design of pre-catalysts for diacetoxylation and diamination

The scope of the catalytic diamination comprised more than 25 different products, internal and terminal all of them with excellent *ee* (91-98% *ee*).

In terms of yield, most were moderate to good with a clear preference for terminal over internal styrenes (Scheme 61).

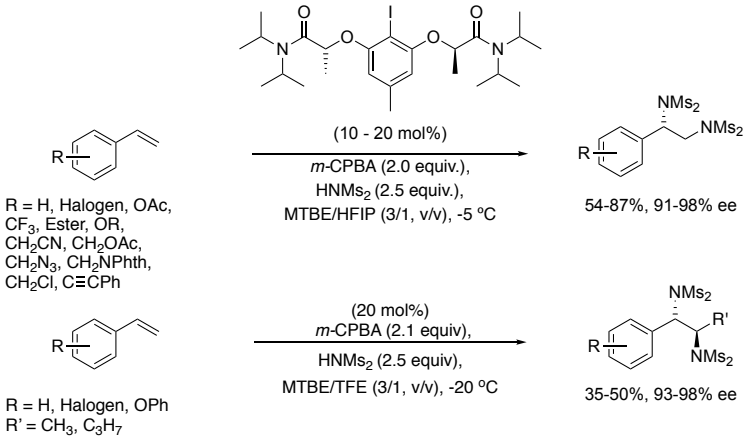

Scheme 61. Scope of the asymmetric diamination using I(I/III) catalysis

Thanks to the *P*-helical configuration of the active species of the catalyst and the folding of the side arms this high enantioinduction is possible (Figure 10) .[158]

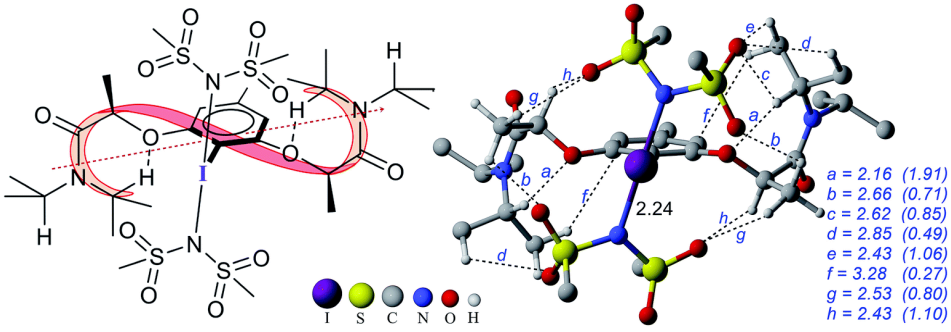

Figure 10. Calculated Folding of the active species

The best reaction conditions were *m*-CPBA as oxidant, $HNMs_2$ as nitrogen source and a mixture of MTBE and HFIP (3:1, v/v) as solvent. This system favours the formation of the diaminated product but also prevents the background reaction between the alkene and *m*-CPBA that generates an epoxide. Its opening with bismesylimide yields an aminoalcohol (Figure 11).[135] Thanks to the *P*-helical configuration of the active species of the

catalyst and the folding of the side arms this high enantioinduction is possible.

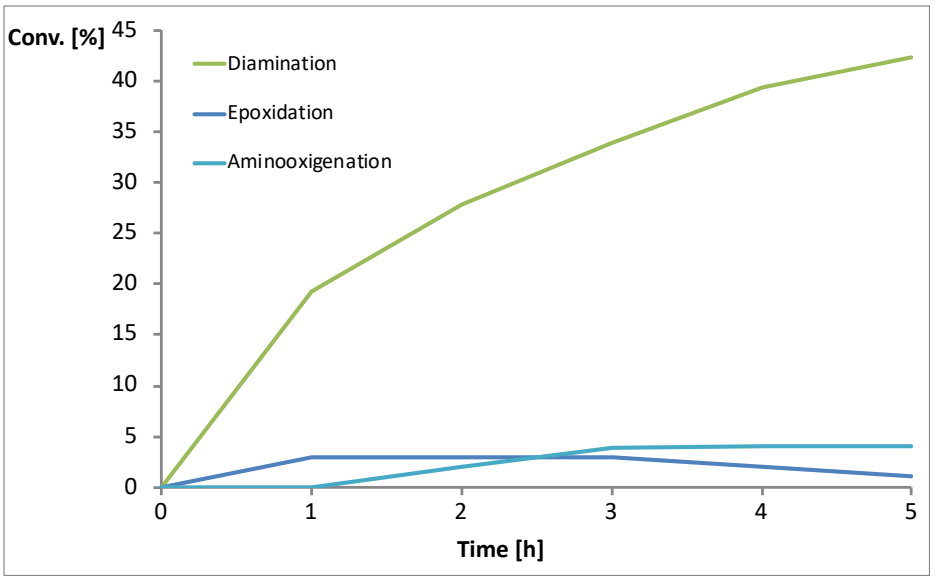

Figure 11. Reaction kinetics showing inhibition of byproducts formation

The proposed mechanism of the reaction included a first formation of the active species analogous to $PhI(NMs_2)_2$ with *m*-CPBA and $HNMs_2$. Then, thanks to the helicity displayed by the hypervalent iodine(III) intermediate, an adequate discrimination of the enantiotopic faces of the alkene takes place after its coordination. N-attack of the bismesylimide provokes the shift of the I(III) to the non-benzylic position (an *anti*-iodoamination). Finally, the Woodward-Prévost-like intermediate is formed when the I(III) centre is displaced by the oxygen from the sulfonamide, undergoing reductive elimination to I(I). A second sulfonamide nucleophile yields the diaminated product with the observed diastereoselectivity (Scheme 62).

Chapter II – A practical aryliodine (I/III) catalysis for the vicinal diamination of styrenes

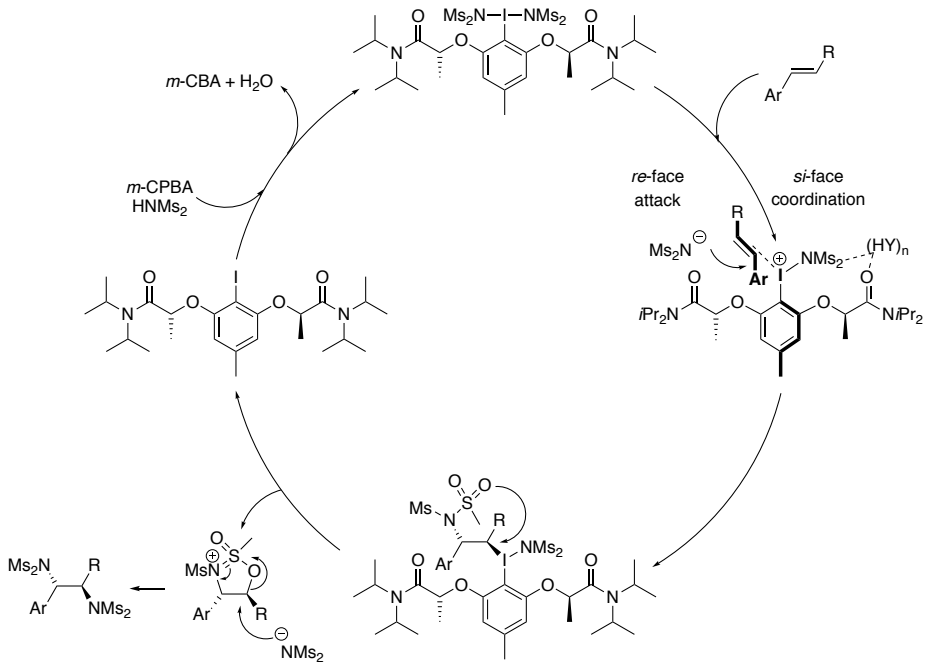

Scheme 62. Diamination mechanism proposed by Muñiz and calculated by Sunoj

Contrary to the racemic diamination, the O-attack of the sulfonamide to the benzylic position cannot occur in this case.[156] The Muñiz catalyst for diamination gives the same enantiomer as the original Ishihara pre-catalyst in the diacetoxylation reaction, then the postulated mechanism would apply (Scheme 63 top). Taking this into account, the same O-attack for the diamination reaction would yield the opposite enantiomer than the observed one (Scheme 63 middle).

Thus, the only possible explanation for the stereochemical output of the reaction is that a first N-attack takes place according to the mechanism above (Scheme 63 bottom).[134] Moreover, in 2019 Sunoj *et al.* performed DFT calculations on the mechanism of the reaction, which further confirmed the initial hypothesis from our group.

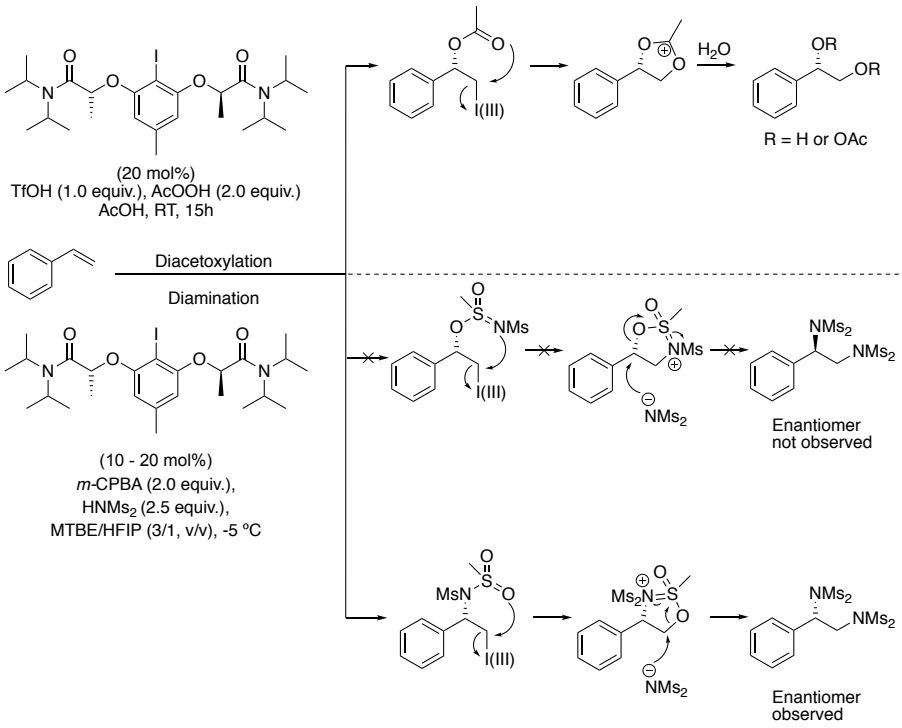

Scheme 63. Stereochemical rationale of the enantioselective diamination reaction and expected products for O- and N-attack

The assistance of HFIP makes possible the N-attack pathway due to an increased charge in the nitrogen and nucleophilicity (Scheme 64). In the same work, the authors calculated the free energy of the transition states of the proposed mechanism and found to be in agreement with the experimentally observed facts.[158]

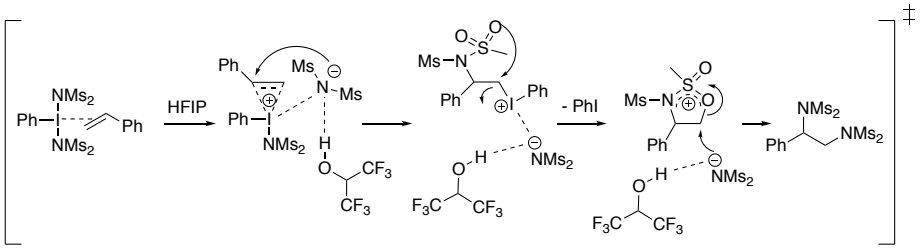

Scheme 64. Sunoj's calculation of the HFIP-assistance in the reaction mechanism

Chapter II – A practical aryliodine (I/III) catalysis for the vicinal diamination of styrenes

2.2. Results and discussion

2.2.1. Pre-catalyst design and reaction conditions

In view of this successful development of a catalytic enantioselective reaction, it appeared of general interest to render the racemic diamination reaction in catalytic fashion as well. In order to devise conditions for such a productive homogeneous iodine(I/III) catalysis for the vicinal diamination of styrenes, we applied findings from our earlier works. These had previously demonstrated a significantly reduced rate for the background reaction of styrene epoxidation with the terminal oxidant *m*-CPBA (3-chloro perbenzoic acid) and MTBE/HFIP (3:1, v/v) as solvents. Much to our surprise, submitting commercially available iodoarenes **1**-**2** to the diamination reaction led to styrene degradation without any or only little product being detected (Scheme 65 top).

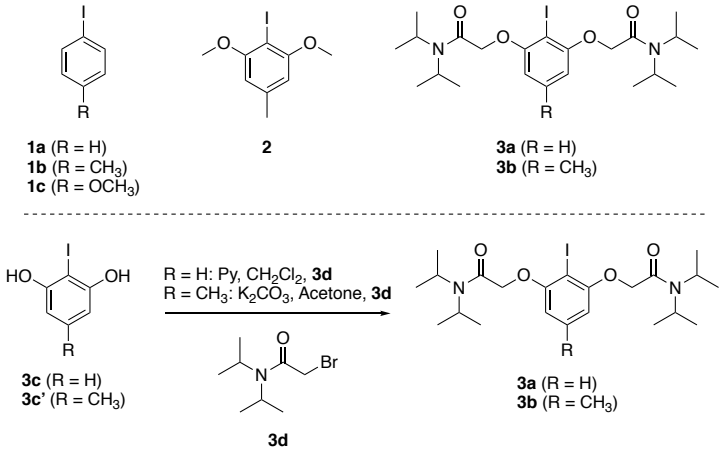

Scheme 65. Pre-catalysts tried in the racemic diamination and synthesis of **3a** and **3b**

In order to accomplish a suitable reactivity and reaction rate, the acetamide derivatives **3** were synthesized. Following an earlier related outline from our group[134], these compounds are conveniently prepared from the free 2-iodo resorcinols **3c** upon condensation with known *N*,*N*-

diisopropyl 2-bromo acetamide **3d** (Scheme 65 bottom).[159] The pre-catalysts **3** in this case were designed to mimic the chiral arms found to be effective in the enantioselective version of the reaction.

Table 1. Screening of pre-catalyst and conditions for the racemic diamination catalysis

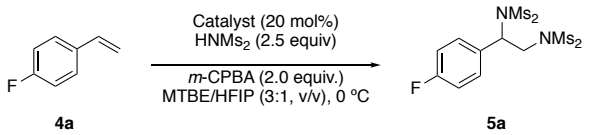

4a **5a**

Entry	Catalyst	Deviation from standard conditions	5a NMR Yield (%)
1	**1a**	None	<10%
2	**1b**	None	<10%
3	**1c**	None	<10%
4	**1c**	CH_2Cl_2 as solvent	<10%
5	**2**	None	<10%
6	**2**	–10 ºC	<10%
7	**3a**	None	68[a]
8	**3a**	–5 ºC	48[a]
9	**3a**	EtOAc/HFIP	54[a]
10	**3b**	None	71[a]

[a] Isolated yields

Throughout all exploration with aryliodines **1**-**2**, product formation to **5a** was rarely observed and, when detectable, corresponded only to minor amounts of product. Instead, styrene decomposition and/or polymerization appeared to be dominant.

Changing the reaction conditions, in particular, the solvent combination resulted in the appearance of styrene oxide as the major product, as expected after Sunoj's input to the reaction mechanism.

Chapter II – A practical aryliodine (I/III) catalysis for the vicinal diamination of styrenes

Using **3a** as catalyst resulted in an immediate change in reaction selectivity providing the desired diamination product **5a** in 68% isolated yield (entry 7). At lower temperature, the reaction did not reach completion and the isolated yield dropped (entry 8).

The same was observed for a change in solvent to a mixture of ethyl acetate and HFIP (entry 9). Although the expected complete chemoselectivity in favor of diamination was still obtained, the reaction rate dropped. Finally, a related outcome was obtained for the 4-methyl derivative **3b**, which provided diamination product **5a** in 71% isolated yield (entry 10).

2.2.2. Reaction kinetics

In order to further investigate the reaction when submitting styrene **4a** to pre-catalysts **1**-**3**, several kinetic profiles were developed. In the case of **1b**, almost no evolution of the starting material was observed, possibly due to the formation of the iodoso polymer formed by the oxidation of the pre-catalyst (Figure 12).[160–162]

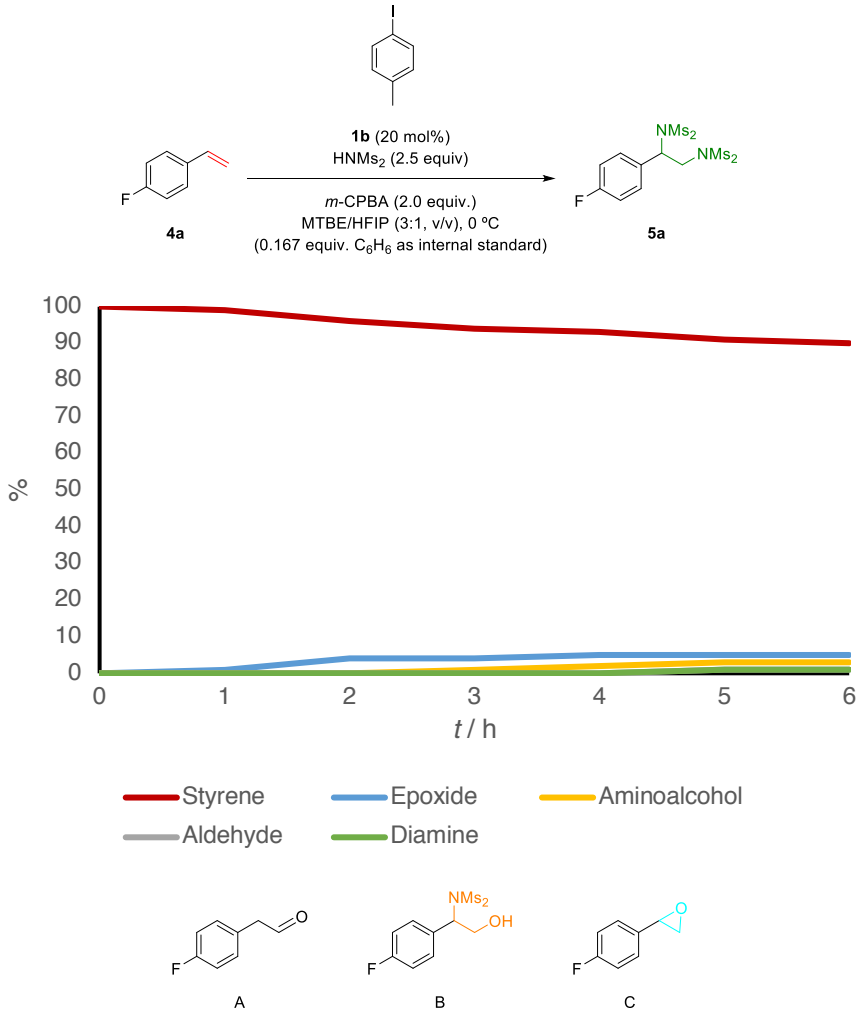

Figure 12. Kinetic profile of the diamination reaction using **1b**

When using **2** in the reaction, the transformation of the starting material takes place, but as seen in Figure 12, mostly background products are

observed by ^{19}F NMR in the course of 7 h. In this case can be seen clearly that the introduction of two O-alkylated groups has an effect, although the wanted reactivity is still not reached. To achieve a good conversion and no background reaction, the design of the pre-catalyst is crucial. Furthermore, this proves that not only the solvent combination helps avoid this background reactions but also a suitable pre-catalyst is needed (Figure 13).

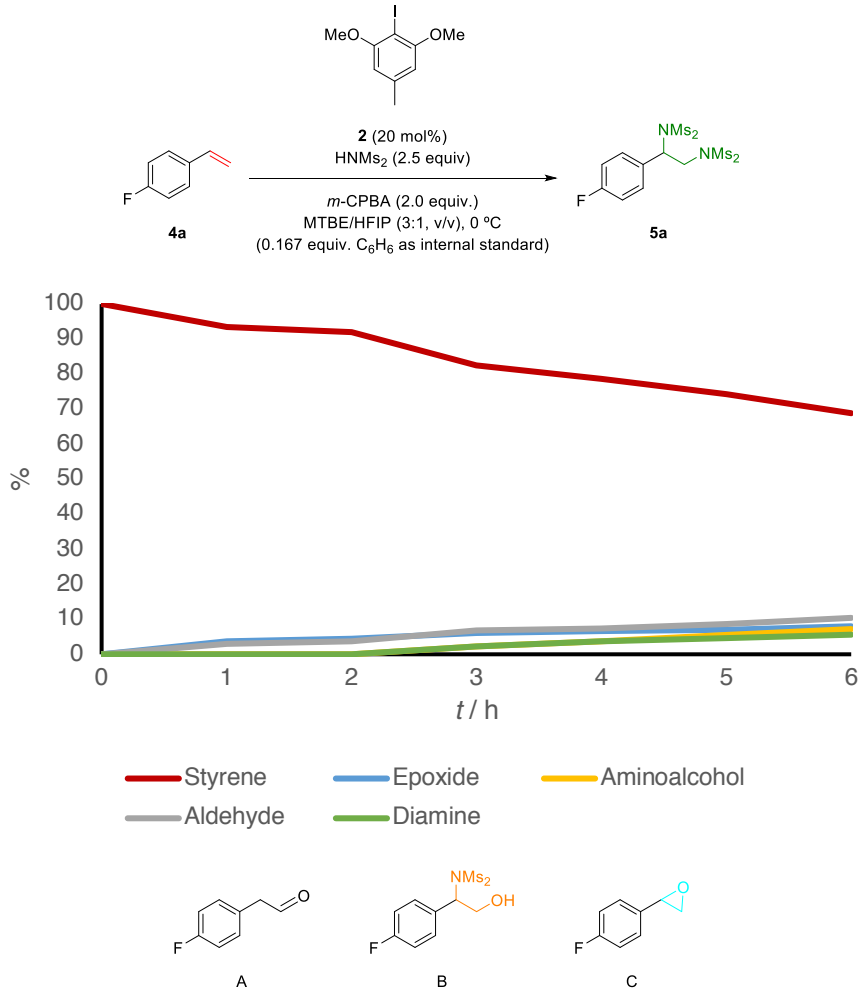

Figure 13. Kinetic profile of the diamination reaction using **2**

Finally, use of **3b** in the reaction mixture resulted in an unequivocally different scenario, where in the course of 7 h the diamine product formation is already around 50% by NMR. The conversion of the starting material is 58%, being this 7% a combination of the background reaction products (2% aldehyde **A**, 4% aminoalcohol **B** and 1% epoxide **C**, Figure 15). This provides a significantly more selective reaction outcome, producing diamine **5a** with an initial turnover frequency of 0.4 h^{-1}.

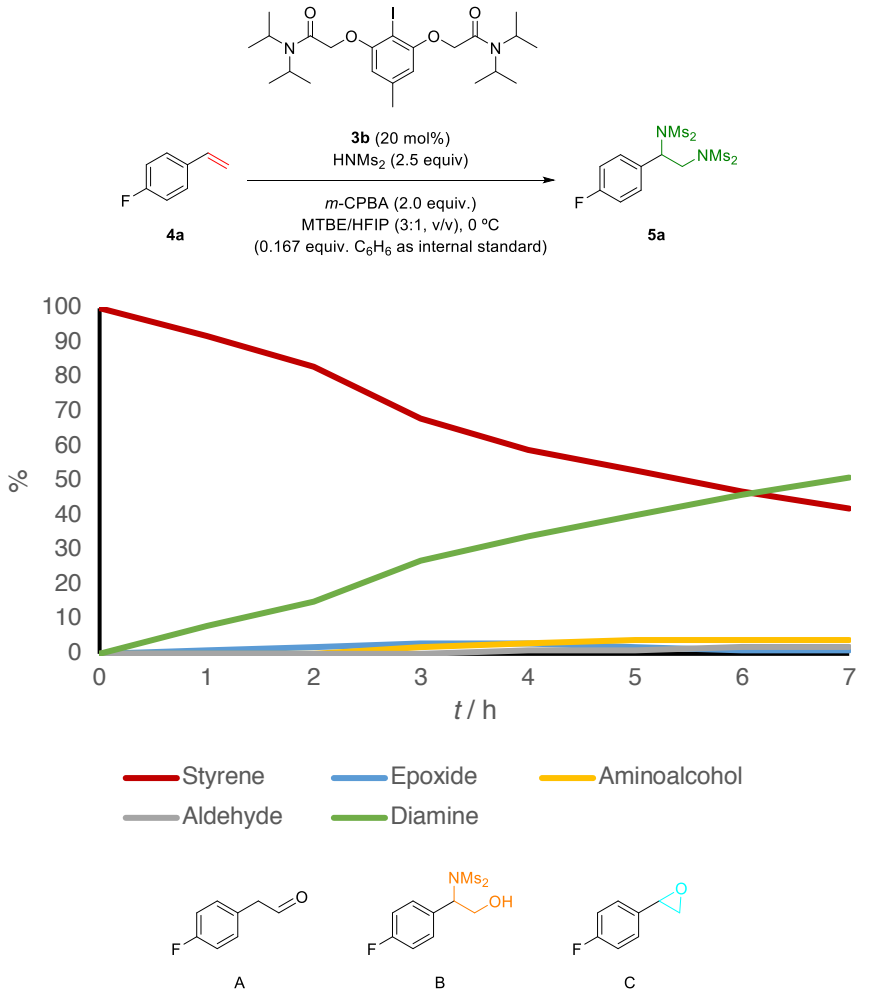

Figure 14. Kinetic profile of the diamination reaction using **3b**

2.2.3. Scope of the Reaction

Under the optimized conditions, a number of styrenes were tested for diamination with bismesylimide and bistosylimide respectively as nitrogen sources.

In the case of bismesylimide, both **3a** and **3b** were tested in the same substrates, in order to know the effect of the R group in *para* to the iodine. As a general comment, **3b** was slightly better at yielding diamines than **3a**, but for some specific examples like **5c**, **5d** and **5i** the opposite was observed (Scheme 66). This same tendency was observed in the previously developed enantioselective catalysis, when choosing the best catalyst. The more electron-donating methylated group in *para*- to the iodine moiety seems to have a slightly better effect in most substrates, even if the difference between them never exceeds 8% yield.

As for the comparison between substrates, one can determine than sterically demanding substrates like **4c**, **4f**, **4i** and **4j-k** present much less yield than the rest of them. This is probably due to a spatial limitation in the pocket generated by the active catalyst. If electronic effects are compared, in general EWG groups such as halogens, CF_3 and esters are better tolerated than EDG groups, but also depending on the steric congestion for each substrate.

The higher conversion was obtained by a *p*-CO_2Me moiety, reaching 81% yield with pre-catalyst **3b** and 77% yield with **3a**.

Chapter II – A practical aryliodine (I/III) catalysis for the vicinal diamination of styrenes

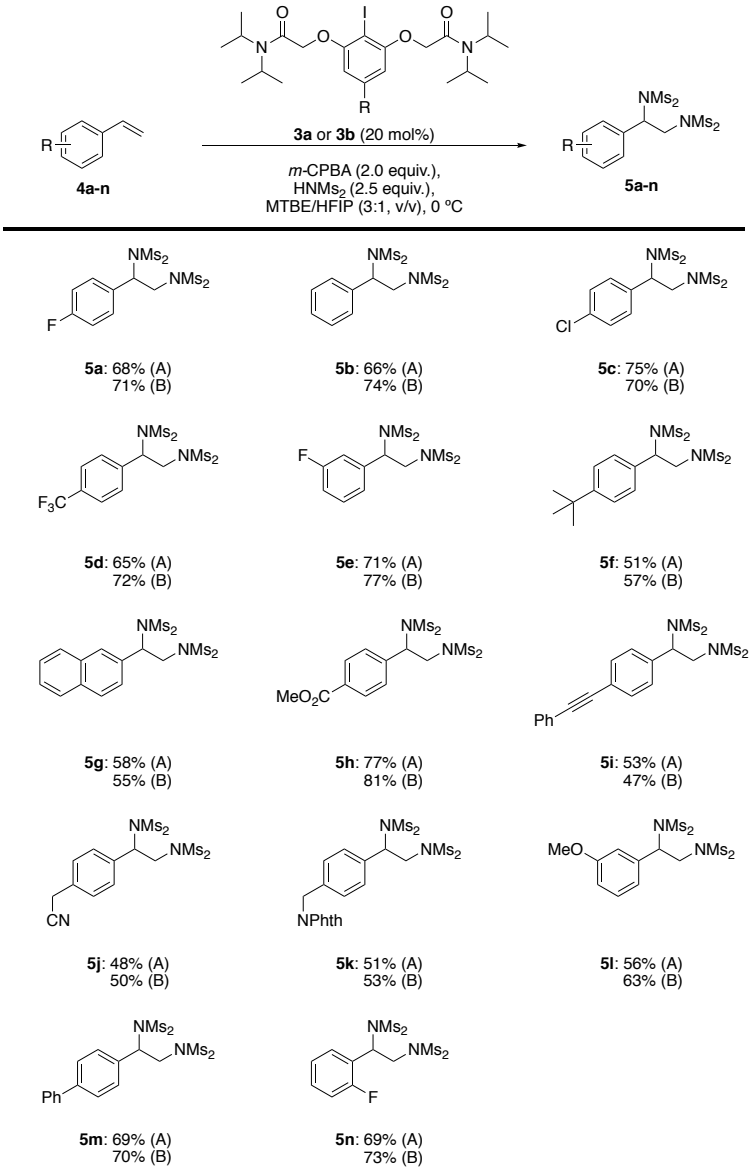

Scheme 66. Scope of the racemic diamination with bismesylimide. Method A: **3a** as catalyst. Method B: **3b** as catalyst

Chapter II – A practical aryliodine (I/III) catalysis for the vicinal diamination of styrenes

Moreover, bistosylimides were also tested in the reaction, which previous reports indicated would turn into lower yields (Scheme 67).[135] The main difference between the two of them is that NTs_2 possesses a much bigger tolyl group instead of NMs_2's terminal methyl, therefore creating an active species with inherently more steric limitations.

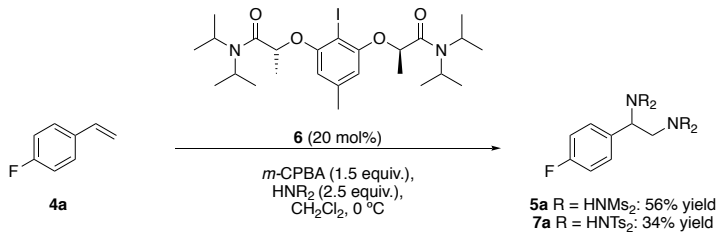

Scheme 67. Preliminary results of the catalytic enantioselective diamination with $HNTs_2$ and $HNMs_2$

This way, it was initially expected to obtain much lower yields than actually observed (Scheme 68). In this case, the reaction was only explored with **3b** as catalyst and again selectively provided the diamination products **7a-i**. To our surprise, the reaction worked equally well with bistosylimides. The transformation included compatibility with *ortho*-, *meta*-, and *para*-substitution.

As to an additional substrate scope, (*E*)-stilbene underwent a moderate formation of the corresponding diamine **7j** whereas allylbenzene **4t** generated the corresponding diamine **7k** in very good yield (the highest even compared to the $HNMs_2$ diamination).

Again, in general halogens were very well tolerated and gave generally good yields, but some EDG substitution like *para*- or *ortho*-methyl only yielded moderate diamines.

Chapter II – A practical aryliodine (I/III) catalysis for the vicinal diamination of styrenes

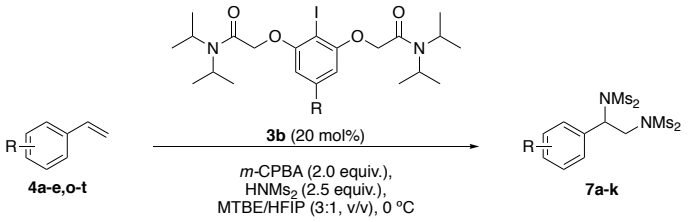

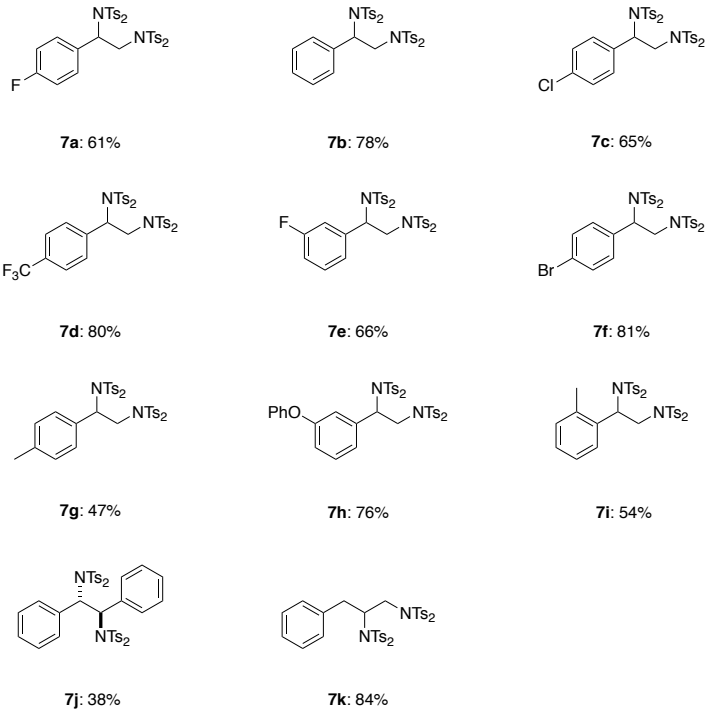

Scheme 68. Scope of the racemic diamination with bistosylylimide

2.2.4. Mechanistic proposal and active species

The basic catalytic cycle for the vicinal diamination with catalysts **3a** and **3b** is depicted in Scheme 69. This is obviously based on the previous insights from the enantioselective diamination reaction. The reaction starts with an oxidation of the iodine(I) **3a,b** to an iodine(III), which upon coordination of the bisimido groups provides the active bisimidoiodine(III) catalyst state **A**. It is important to note that formation of **A** should proceed via the corresponding iodoso intermediate and subsequent reaction with the protic bissulfo-nimides. As Sunoj *et al.* calculated, HFIP-assistance in **B** is a requirement for this reactivity, so the depicted mechanism has been updated to include this fact.[158,163] Finally, **B** is iodoaminated in *anti*-fashion and **C** gives way to the Woodward-Prévost-like step.

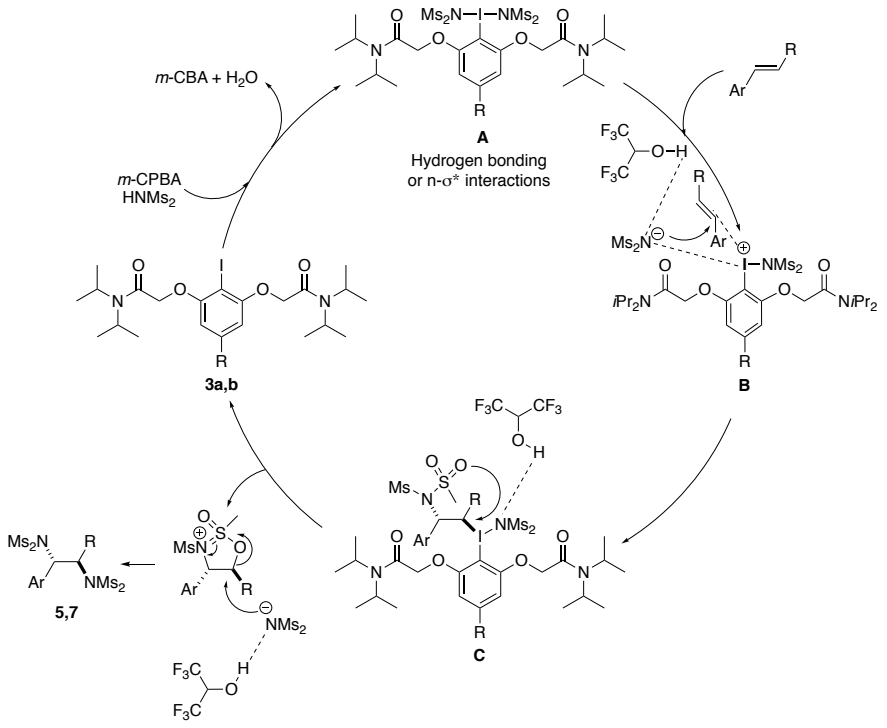

Scheme 69. Mechanistic proposal based on the enantioselective version of the reaction

A positive effect of the bulky ortho-substituents may be the prevention of polymeric derivatives formed at the iodoso state, as insightfully designed

by Zhdankin and co-workers.[160,162,164] However, this should not be the only factor in the present case in light of the inactivity of the related compound **2**. It is therefore more appropriate to assign an active participation of the two ortho-substituents throughout the reaction as previously discussed for the related chiral side-chain derivatives.

This assignment is also in agreement with an observation during the diacetoxylation studied by Shimogaki et *et al.* This study demonstrated that 2,6-dialkoxy-substituted iodoarenes were readily oxidized by mCPBA, and that the interacting side chains prevented the electron-rich iodoarene catalyst from decomposing to a diaryliodonium salt.[129] This interaction should be in form of a chelation with the catalytically active iodine(III) centre and may involve either n–σ*interactions or hydrogen bonding within agglomerates of protic HFIP solvent molecules or water (Figure 15).

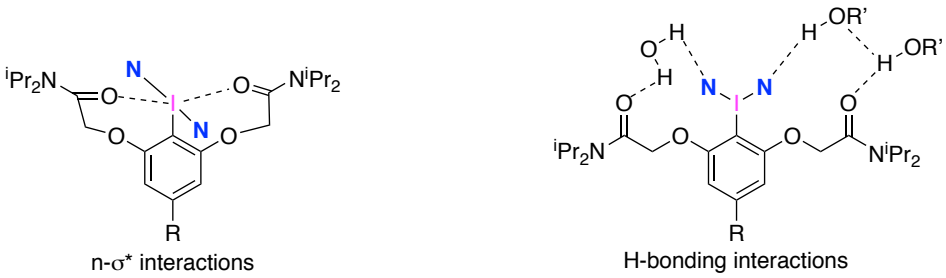

Figure 15. Proposed interactions forming the catalysts' pocket

For catalyst **3a**, a crystal structure analysis (Figure 15b) confirms its expected molecular constitution. Interestingly, in contrast to the structure of the related chiral catalyst **6** the present achiral derivative shows a significantly more pronounced spatial arrangement towards the creation of a pocket around the central iodine. In contrast, the crystal structure of catalyst **3b** shows a molecular constitution that is widely in agreement with the one from chiral catalyst **6**. However, it appears that the orientation of the side chains in these structures does not predetermine the subsequent

catalysis performance because both **3a** and **3b** give comparable performances (Figure 16).

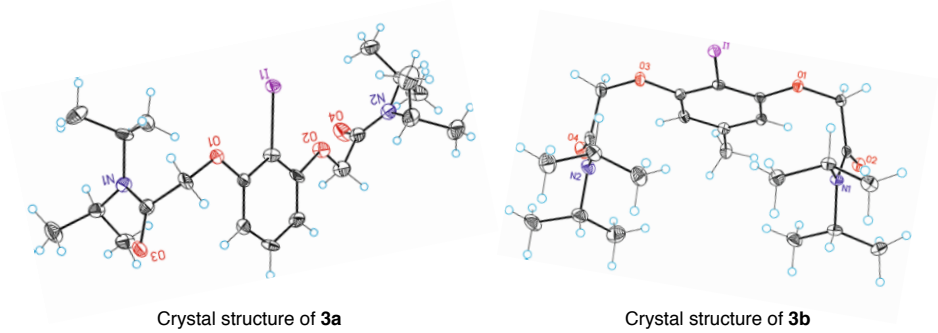

Crystal structure of **3a** Crystal structure of **3b**

Figure 16. Crystal structures of **3a** (CCDC 1895651) and **3b** (CCDC 1898343)

Additionally, a theoretic model by Xue and co-workers invokes arene π-stacking as a stabilizing element within aryliodine(III) catalysts. Nonetheless, calculations by Sunoj *et al*. note that it is the side chain of the active catalyst that interacts with the substrate.[158,165]

2.3. Conclusions

In conclusion, a new pair of achiral aryliodine(I) pre-catalysts **3a** and **3b** that enable a rapid and productive vicinal diamination of styrenes under sustainable iodoarene catalysis has been described. These compounds outperform standard aryliodine pre-catalysts commonly employed in iodine(I/III) catalysis. Even if **3b** has a slightly better effectiveness, both catalysts are comparable in terms of yields.

A total of 25 products have been synthesized by this methodology that combines the group's generated knowledge on the field during the last decade.

One of the main points of this section is to remark the utmost importance of pre-catalyst design, as the reaction is not feasible without the suitable *ortho*-O-alkylated chains. Thus, the designed pre-catalysts comply with the demands of the reaction from the structural point of view. The analogous (non-chiral) pocket to the chiral version of the pre-catalyst **6** is thought to be generated by **3a** and **3b** as well for their chemical constitution.

Besides the known diamination with $HNMs_2$, the reaction has been successfully extended to $HNTs_2$ as nucleophile for 11 substrates, showing that these nucleophiles are also suitable for I(I/III) catalysis.

2.4. Experimental section

2.4.1. General remarks

All solvents were commercially available and were used as received. Column chromatography was performed with silica gel (Merck, type 60, 0.063-0.2 mm). NMR data were recorded in deuterated solvents at 23 ºC on a Bruker Advance 400 Ultra Shield (400 MHz for ^{1}H, 100 MHz for ^{13}C and 376 MHz for ^{19}F) and Bruker 300 Ultrashield (300 MHz for ^{1}H and 75 MHz for ^{13}C) spectrometers. IR spectra were taken in a Bruker Alpha instrument in the solid or liquid state. Chemical shifts (δ) are reported in parts per million (ppm) and referenced to residual solvent. The following calibrations were used: $CDCl_3$ δ = 7.26 and 77.16 ppm. Coupling constants (*J*) are reported in Hertz (Hz). Mass Spectra were recorded on a Bruker Daltonics Autoflex (MALDI) spectrometer within the services centre at ICIQ. *m*-CPBA (≤77% purity) was purchased from Sigma Aldrich and used as received. The following compounds were commercially available and used as received: 4- fluorostyrene, 4-chlorostyrene, 4-bromostyrene, 4-tert-butylstyrene, 4-(trifluoromethyl)styrene, 4-vinylbiphenyl, 4-vinyltoluene, (4-vinylphenyl)acetonitrile, 3-fluorostyrene, 3-methoxystyrene, 2-fluorostyrene, 2-vinyltoluene, 2-vinylnaphtalene, styrene, (*E*)-stilbene and allylbenzene. The following compounds were synthesized according to a modified literature procedure.[166] The spectral data of the individual compounds matches the ones from literature reports: methyl-4-vinylbenzoate[167], 3-phenoxystyrene[168]. 4-(Phthaloylmethylenyl)styrene was prepared according to a known procedure.[169]

2.4.2. General Procedures

Synthesis of Catalyst 3a. To a stirred solution of 2-iodobenzene-1,3-diol **3c** (0.944 g, 4 mmol) in 25 mL of dry dichloromethane at

room temperature were added anhydrous pyridine (5 mL) and 2-bromo-*N,N*-diisopropylacetamide **3d** (1.11 g, 5 mmol). After 37 hours the reaction was diluted with dichloromethane (50 mL) and washed by careful addition of 6N HCl aqueous solution (3 x 25 mL). The organic layer was dried over $NaSO_4$, filtered and concentrated under reduced pressure. The residue was purified by flash chromatography on silica gel using hexane/AcOEt (5/1, v/v). The product was isolated as a white solid (1.9 g, 3.67 mmol, 91.7%). Colorless crystals for X-ray analysis were grown from methanol solution.

Synthesis of Catalyst 3b. To a stirred solution of 2-iodo-5-methylbenzene-1,3-diol **3c'** (0.125 g, 0.5 mmol) in 5 mL of dry acetone at room temperature was added anhydrous K_2CO_3 (0.173 g, 1.25 mmol) and stirring was continued for 1 hour. 2-Bromo-*N,N*-diisopropylacetamide **3d** (0.277 g, 1.25 mmol) was then added to the reaction mixture and the reaction was heated to reflux. After 12 hours the solvent was evaporated, water was added and it was extracted using CH_2Cl_2. The organic layers were dried over $NaSO_4$, filtered and concentrated under reduced pressure. The residue was purified by flash chromatography on silica gel using hexane/AcOEt (8/1 to 3/1, v/v). The product was isolated as a white solid (75%, 0.2 g, 0.375 mmol). Colorless crystals for X-ray analysis were grown from methanol solution.

General Protocol for the Vicinal Diamination of Styrenes. In a sealed pyrex tube, styrene **4** (0.5 mmol) was added to a mixture of $HNMs_2$ (2.5 equiv), catalyst **3a** or **3b** (0.1 mmol, 20 mol%) and

*m*CPBA (1 equiv) in HFIP (0.45 mL) and MTBE (1.3 mL) at 0 ºC. After 16 h of reaction, another portion of *m*CPBA (1 equiv) was added and the final mixture was stirred for additional 24 h. After a total of 40 h reacting, the mixture was quenched with $NaHCO_3$ and extracted with DCM (3x), dried over Na_2SO_4 and evaporated under reduced pressure. The final crude product was purified by chromatography (silica gel, *n*-hexane/ethyl acetate, 85/15, v/v to 2/1, v/v) to give the pure diaminated product.

2.4.3. Kinetic reaction profile

a) Using compound 1b as pre-catalyst

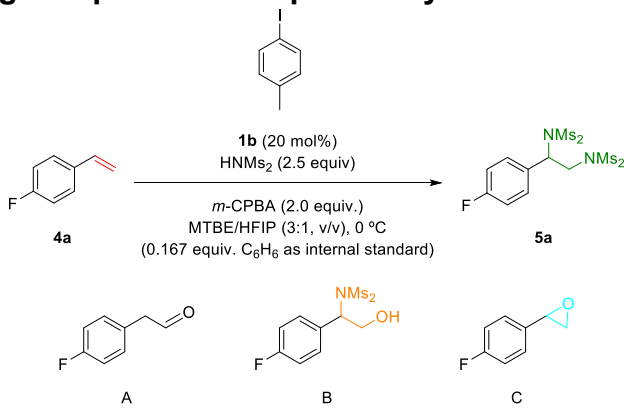

In a sealed Pyrex tube, 4-fluorostyrene **4a** (0.167 mmol) was added to a mixture of $HNMs_2$ (2.5 equiv.), 4-iodotoluene **1b** (0.2 equiv.), *m*CPBA (2 equiv.) and C_6F_6 (0.167 equiv.) in HFIP (0.15 mL) and MTBE (0.43 mL) at 0 ºC. The reaction was followed by ^{19}F-NMR by taking samples from the reaction mixture each hour (including t = 0) over a period of time of 6 hours using $CDCl_3$ as solvent for the acquisition.

Table 2. Kinetic profile using pre-catalyst **1b** (NMR yields)

t / h	**4a** (%)	**A** (%)	**B** (%)	**C** (%)	**5**[a] (%)
0	100	0	0	0	0
1	99	0	0	1	0
2	96	0	0	4	0
3	94	0	1	4	0
4	93	0	2	5	0
5	91	1	3	5	1
6	90	1	3	5	1

b) Using compound 2 as pre-catalyst

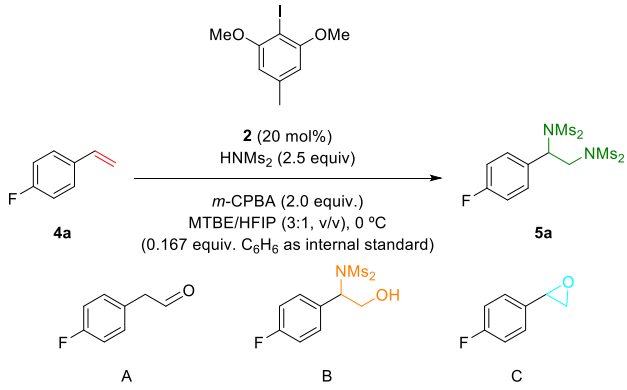

In a sealed Pyrex tube, 4-fluorostyrene **4a** (0.167 mmol) was added to a mixture of $HNMs_2$ (2.5 equiv.), 4-iodo-1,3-dimethoxytoluene 2 (0.2 equiv.), *m*CPBA (2 equiv.) and C_6F_6 (0.167 equiv.) in HFIP (0.15 mL) and MTBE (0.43 mL) at 0 ºC. The reaction was followed by ^{19}F-NMR by taking samples from the reaction mixture each hour (including t = 0) over a period of time of 6 hours using $CDCl_3$ as solvent for the acquisition.

Table 3. Kinetic profile using pre-catalyst **2**

t (h)	**4a** (%)	**A** (%)	**B** (%)	**C** (%)	**5**[a] (%)
0	100	0	0	0	0
1	93	3	0	4	0
2	92	4	0	4	0
3	82	7	2	6	2
4	79	7	4	7	4
5	74	9	5	7	5
6	69	10	7	8	6

c) Using compound 2 as pre-catalyst

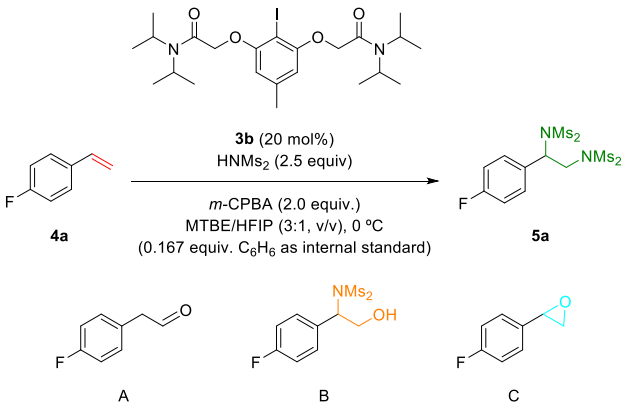

In a sealed Pyrex tube, 4-fluorostyrene (0.5 mmol) was added to a mixture of $HNMs_2$ (2.5 equiv.), 2,2'-((2-iodo-5-methyl-1,3-phenylene)bis(oxy))bis(*N*,*N*'-diisopropylacetamide) **3b** (0.2 equiv.), *m*CPBA (2 equiv.) and C_6F_6 (0.167 equiv.) in HFIP (0.45 mL) and MTBE (1.3 mL) at -5 ºC. The reaction was followed by ^{19}F-NMR by taking samples from the reaction mixture each hour (including t = 0) over a period of time of 7 h using $CDCl_3$ as solvent for the acquisition.

Table 4. Kinetic profile using pre-catalyst **3**

t / h	**4a** (%)	**A** (%)	**B** (%)	**C** (%)	**5ª** (%)
0	100	0	0	0	0
1	92	0	0	1	8
2	83	0	0	2	15
3	68	0	2	3	27
4	59	1	3	3	34
5	53	1	4	2	40
6	47	2	4	1	46
7	42	2	4	1	51

2.4.4. Characterization of catalysts 3

2,2'-((2-iodo-1,3-phenylene)bis(oxy))bis(*N*,*N*'-diisopropylacetamide) 3a:

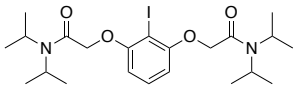

^{1}H-NMR ($CDCl_3$, 300 MHz): δ 1.20 (d, *J* = 6.6 Hz, 12H), 1.39 (d, *J* = 6.7 Hz, 12H), 3.36-3.45 (m, 2H), 4.20-4.27 (m, 2H), 4.69 (s, 4H), 6.61-6.64 (m, 2H), 7.17-7.23 (m, 1H) ppm.

^{13}C-NMR ($CDCl_3$, 75 MHz): δ 20.3, 21.2, 46.2, 48.8, 70.7, 105.8, 130.8, 158.2, 166.3 ppm.

IR ν(cm^{-1}): 767, 1094, 1226, 1256, 1335, 1452, 1584, 1627, 2970.

HRMS (MALDI+): calcd. $[M+H]^+$ $C_{22}H_{36}IN_2O_4$: 519.1714; found: 519.1717.

2,2'-((2-iodo-5-methyl-1,3-phenylene)bis(oxy))bis(*N*,*N*'-diisopropylacetamide) 3b:

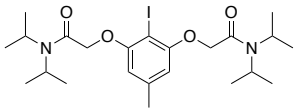

^{1}H-NMR (500 MHz, $CDCl_3$): δ 1.15 (d, *J* = 6.7 Hz, 12H), 1.35 (d, *J* = 6.7 Hz, 12H), 2.24 (s, 3H), 3.36 (m, 2H), 4.20 (m, 2H), 4.62 (s, 4H), 6.41 (s, 2H) ppm.

^{13}C-NMR (125 MHz, $CDCl_3$): δ 20.3, 21.1, 21.9, 46.2, 48.9, 70.7, 73.6, 106.9, 140.7, 157.9, 166.5 ppm.

IR ν(cm^{-1}): 729, 1022, 1118, 1263, 1346, 1445, 1579, 1625, 2962.

HRMS (MALDI+): calcd. for $[M+Na]^+$ $C_{23}H_{37}IN_2O_4Na$: 555.1690; found: 555.1692.

2.4.5. Characterization of diamines 5

***N,N'*-(1-(4-Fluorophenyl)ethane-1,2-diyl)bis(*N*-(methylsulfonyl)methanesulfonamide) 5a:**

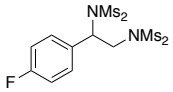

Isolated as a white solid in 68% (Method A) and 71% (Method B) yield.

Mp: 237-239 ºC.

^{1}H-NMR (300 MHz, $CDCl_3$): δ = 2.31-2.87 (bs, 3H), 3.24 (s, 6H), 3.28-3.76 (bs, 3H), 4.52 (dd, *J* = 6.4, 15.4 Hz, 1H), 4.77 (dd, *J* = 5.6, 15.3 Hz, 1H), 5.88 (*pst*, *J* = 6.0 Hz, 1H), 7.10-7.19 (m, 2H), 7.64 (dd, *J* = 5.2, 8.7 Hz, 2H) ppm.

^{13}C-NMR (75 MHz, $CDCl_3$): δ = 43.3, 44.6, 50.9, 62.8, 116.2 (d, *J* = 21.5 Hz), 129.8 (d, *J* = 3.5 Hz), 132.2 (d, *J* = 8.3 Hz), 163.2 (d, *J* = 251.0 Hz) ppm.

^{19}F NMR (376 MHz, $CDCl_3$): δ = -111.74 (d, *J* = 3.6 Hz), -110.33 (d, *J* = 3.6 Hz) ppm.

***N,N'*-(1-Phenylethane-1,2-diyl)bis(*N*-(methylsulfonyl)methanesulfonamide) 5b:**

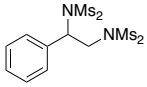

Isolated as a white solid in 66% (Method A) and 74% (Method B) yield.

Mp: 184-186 ºC.

^{1}H-NMR (300 MHz, $CDCl_3$): δ = 2.25-2.87 (bs, 3H), 3.24 (s, 6H), 3.30-3.84 (bs, 3H), 4.57 (dd, *J* = 6.8, 15.3 Hz, 1H), 4.79 (dd, *J* = 5.2, 15.3 Hz, 1H), 5.84-5.95 (m, 1H), 7.39-7.48 (m, 3H), 7.57-7.65 (m, 2H) ppm.

^{13}C-NMR (75 MHz, $CDCl_3$): δ = 43.2, 44.5, 50.7, 63.4, 129.1, 129.8, 130.2, 133.8 ppm.

***N,N'*-(1-(4-Chlorophenyl)ethane-1,2-diyl)bis(*N*-(methylsulfonyl) methanesulfonamide) 5c:**

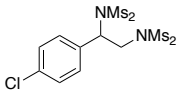

Isolated as a white solid in 75% (Method A)[a] and 70% (Method B)[b] yield.

Mp: 212-213 ºC.

^{1}H-NMR (300 MHz, $CDCl_3$): δ = 2.23-2.98 (bs, 3H), 3.25 (s, 6H), 3.30-3.94 (bs, 3H), 4.52 (dd, *J* = 6.5, 15.3 Hz, 1H), 4.75 (dd, *J* = 5.5, 15.3 Hz, 1H), 5.85 (pst, *J* = 6.0 Hz, 1H), 7.42 (d, *J* = 8.6 Hz, 2H)., 2H), 7.58 (d, *J* = 8.5 Hz, 2H) ppm.

^{13}C-NMR (75 MHz, $CDCl_3$): δ = 43.3, 44.5 (bs), 50.7, 62.8, 129.4, 131.6, 132.4, 136.0 ppm.

***N,N'*-(1-(4-(Trifluoromethyl)phenyl)ethane-1,2-diyl)bis(*N*-(methylsulfonyl)methanesulfonamide) 5d:**

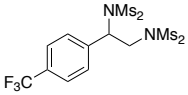

Isolated as a white solid in 65% (Method A) and 72% (Method B) yield.

Mp: 223-225 ºC.

^{1}H-NMR (300 MHz, $CDCl_3$): δ = 2.37-3.03 (bs, 3H), 3.27 (s, 6H), 3.32-4.34 (bs, 3H), 4.60 (dd, *J* = 6.7, 15.3 Hz, 1H), 4.77 (dd, *J* = 5.2, 15.4 Hz, 1H), 5.93 (dd, *J* = 5.2, 6.6 Hz, 1H), 7.71 (d, *J* = 8.5 Hz, 2H), 7.77 (d, *J* = 8.6 Hz, 2H) ppm.

^{13}C-NMR (75 MHz, $CDCl_3$): δ = 43.2, 44.6, 50.4, 62.7, 123.7 (d, *J* = 273.7 Hz), 126.0 (q, *J* = 3.7 Hz), 130.6, 131.9 (d, *J* = 32.9 Hz), 138.0 ppm.

^{19}F-NMR (376 MHz, $CDCl_3$): δ = -63.0 ppm.

_N_,_N_'-(1-(3-Fluorophenyl)ethane-1,2-diyl)bis(_N_-(methylsulfonyl)methanesulfonamide) 5e:

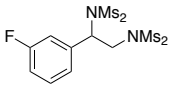

Isolated as a white solid in 71% (Method A) and 77% (Method B) yield.

Mp: 162-164 ºC.

^{1}H-NMR (300 MHz, $CDCl_3$): δ = 2.38-3.00 (bs, 3H), 3.27 (s, 6H), 3.30-3.68 (bs, 3H), 4.56 (dd, *J* = 6.7, 15.4 Hz, 1H), 4.73 (dd, *J* = 5.2, 15.3 Hz, 1H), 5.87 (dd, *J* = 5.3, 6.6 Hz, 1H), 7.09-7.16 (m, 1H), 7.33-7.38 (m, 1H), 7.41-7.46 (m, 2H) ppm.

^{13}C-NMR (75 MHz, $CDCl_3$): δ = 43.2, 44.6 (d, *J* = 2.9 Hz), 50.6, 62.8, 116.9 (d, *J* = 20.6 Hz), 117.3 (d, *J* = 22.4 Hz), 125.9 (d, *J* = 3.1 Hz), 130.7 (d, *J* = 8.2 Hz), 136.3 (d, *J* = 6.9 Hz), 164.4 ppm.

^{19}F NMR (376 MHz, $CDCl_3$): δ = -110.49 ppm.

(1-(4-(*tert*-Butyl)phenyl)ethane-1,2-diyl)bis(_N_-ethylsulfonyl)methanesulfonamide) 5f:

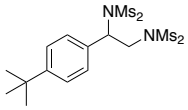

Isolated as a white solid in 51% (Method A) and 57% (Method B) yield.

Mp: 153-155 ºC.

^{1}H-NMR (300 MHz, $CDCl_3$): δ = 1.31 (s, 9H), 2.19-2.90 (bs, 3H), 3.24 (s, 6H), 3.28-3.78 (bs, 3H), 4.57 (dd, *J* = 7.0, 15.3 Hz, 1H), 4.76 (dd, *J* = 5.2, 15.3 Hz, 1H), 5.89 (dd, *J* = 5.1, 6.9 Hz, 1H), 7.44 (m, 2H), 7.52 (m, 2H) ppm.

^{13}C-NMR (75 MHz, $CDCl_3$): δ = 31.3, 34.9, 43.2, 44.5 (bs), 50.8, 63.2, 126.0, 129.9, 130.7, 153.2 ppm.

***N*,*N*'-(1-(Naphthalen-2-yl)ethane-1,2-diyl)bis(*N*-(methylsulfonyl) methanesulfonamide) 5g:**

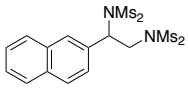

Isolated as a white solid in 58% (Method A) and 55% (Method B) yield.

Mp: 166-168 ºC.

^{1}H-NMR (300 MHz, $CDCl_3$): δ = 2.23-2.77 (bs, 3H), 3.25 (s, 6H), 3.29-3.83 (bs, 3H), 4.67 (dd, *J* = 6.6, 15.3 Hz, 1H), 4.94 (dd, *J* = 5.2, 15.3 Hz, 1H), 6.05-6.10 (m, 1H), 7.51-7.60 (m, 2H), 7.70 (dd, *J* = 1.9, 8.6 Hz, 1H), 7.81-7.88 (m, 1H), 7.88-7.93 (m, 2H), 8.09-8.11 (m, 1H) ppm.

^{13}C-NMR (75 MHz, $CDCl_3$): δ = 43.3, 44.4 (bs), 50.8, 63.6, 126.9, 127.2, 127.6, 127.8, 128.7, 129.1, 129.9, 130.9, 132.8, 133.4 ppm.

***N*,*N*'-(1-(4-Methoxycarbonyl)phenyl)ethane-1,2-diyl)bis(*N*-(methylsulfonyl)methanesulfonamide) 5h:**

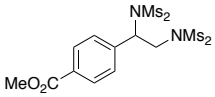

Isolated as a white solid in 77% (Method A) and 81% (Method B) yield.

Mp: 225-227 ºC.

^{1}H-NMR (300 MHz, $CDCl_3$): δ = 2.27-2.85 (bs, 3H), 3.26 (s, 6H), 3.31-3.74 (bs, 3H), 3.94 (s, 3H), 4.59 (dd, *J* = 6.8, 15.4 Hz, 1H), 4.77 (dd, *J* = 5.2, 15.4 Hz, 1H), 5.91-5.94 (m, 1H), 7.71 (d, *J* = 8.3 Hz, 2H), 8.11 (d, *J* = 8.3 Hz, 2H) ppm.

^{13}C-NMR (75 MHz, $CDCl_3$): δ = 43.2, 44.6 (bs), 50.4, 52.6, 62.9, 130.2, 131.4, 138.7, 166.2 ppm.

***N*,*N*'-(1-(4-(Phenylethynyl)phenyl)ethane-1,2-diyl)bis(*N*-(methylsulfonyl)methanesulfonamide) 5i:**

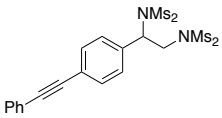

Isolated as a white solid in 53% (Method A) and 47% (Method B) yield.

Mp: 111-114 ºC.

^{1}H-NMR (300 MHz, $CDCl_3$): δ = 2.3-2.9 (bs, 3H), 3.26 (s, 6H), 3.27-3.75 (bs, 3H), 4.54 (dd, *J* = 6.5, 15.4 Hz, 1H), 4.80 (dd, *J* = 5.5, 15.4 Hz, 1H), 5.88-5.92 (m, 1H), 7.34-7.38 (m, 3H), 7.51-7.55 (m, 2H), 7.58-7.64 (m, 4H) ppm.

^{13}C-NMR (75 MHz, $CDCl_3$): δ = 43.3, 44.6 (bs), 50.6, 63.1, 88.3, 91.4, 122.8, 125.0, 128.6, 128.9, 130.2, 131.8, 132.2, 133.6 ppm.

***N*,*N*'-(1-(4-(Cyanomethyl)phenyl)ethane-1,2-diyl)bis(*N*-(methylsulfonyl)methanesulfonamide) 5j:**

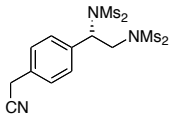

Isolated as a white solid in 48% (Method A) and 50% (Method B) yield.

Mp: 225-226 ºC.

^{1}H-NMR (300 MHz, $CDCl_3$): δ = 2.39-2.89 (bs, 3H), 3.27 (s, 6H), 3.33-3.67 (bs, 3H), 3.79 (s, 2H), 4.57 (dd, *J* = 6.7, 15.3 Hz, 1H), 4.76 (dd, *J* = 5.3, 15.3 Hz, 1H), 5.87-5.91 (m, 1H), 7.43 (d, *J* = 8.1 Hz, 2H), 7.66 (d, *J* = 8.2 Hz, 2H) ppm.

^{13}C-NMR (75 MHz, $CDCl_3$): δ = 23.6, 43.3, 44.6 (bs), 50.6, 62.9, 128.7, 131.0, 131.8, 134.0 ppm.

***N*,*N*'-(1-(4-((1,3-dioxoisoindolin-2-yl)methyl)phenyl)ethane-1,2-diyl)bis(*N*-(methylsulfonyl)methanesulfonamide) 5k:**

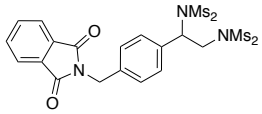

Isolated as a white solid in 51% (Method A) and 53% (Method B) yield.

Mp: 215-216 ºC.

^{1}H-NMR (300MHz, $CDCl_3$): δ = 2.57 (bs, 3H), 3.25 (s, 6H), 3.48 (bs, 3H), 4.56 (dd, *J* = 6.8, 15.3 Hz, 1H), 4.72 (dd, *J* = 5.2, 15.3 Hz, 1H), 4.88 (s, 2H), 5.88 (dd, *J* = 5.3, 6.7 Hz, 1H), 7.47 (d, *J* = 8.2, 2H), 7.59 (d, *J* = 8.3 Hz, 2H), 7.76 (dd, *J* = 5.5, 3.0, 2H), 7.85-7.91 (m, 2H) ppm.

^{13}C-NMR (75 MHz, $CDCl_3$): δ = 41.2, 43.2, 44.6 (bs), 50.7, 63.1, 123.7, 128.8, 130.5, 132.1, 133.4, 134.4, 138.2, 168.1 ppm.

***N*,*N*'-(1-(3-(methoxyphenyl)ethane-1,2-diyl)bis(*N*-(methylsulfonyl)methanesulfonamide) 5l:**

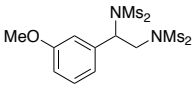

Isolated as a white solid in 56% (Method A) and 63% (Method B) yield.

Mp: 102-104 ºC.

^{1}H-NMR (300 MHz, $CDCl_3$): δ = 2.32-2.92 (bs, 3H), 3.24 (s, 6H), 3.29-3.70 (bs, 3H), 3.83 (s, 3H), 4.51 (dd, *J* = 6.5, 15.3 Hz, 1H), 4.81 (dd, *J* = 5.5, 15.4 Hz, 1H), 5.87 (*p*st, *J* = 6.0 Hz, 1H), 6.94 (ddd, *J* = 1.0, 2.6, 8.3 Hz, 1H), 7.16-7.23 (m, 2H), 7.34 (t, *J* = 9.4 Hz, 1H) ppm.

^{13}C-NMR (75 MHz, $CDCl_3$): δ = 43.3, 44.4 (bs), 50.8, 55.6, 63.3, 115.4, 115.6, 122.5, 130.2, 135.1, 160.0 ppm.[a]

***N*,*N*'-(1-([1,1'-Biphenyl]-4-yl)ethane-1,2-diyl)bis(*N*-(methylsulfonyl)methanesulfonamide) 5m:**

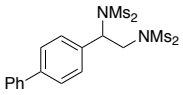

Isolated as a white solid in 69% (Method A) and 70% (Method B) yield.

Mp: 159-162 ºC.

^{1}H-NMR (300 MHz, $CDCl_3$): δ = 2.24-3.14 (bs, 3H), 3.27 (s, 3H), 3.32-3.90 (bs, 3H), 4.60 (dd, *J* = 6.7, 15.3 Hz, 1H), 4.83 (dd, *J* = 5.3, 15.3 Hz, 1H), 5.95 (dd, *J* = 5.3, 6.7 Hz, 1H), 7.35-7.42 (m, 1H), 7.43-7.50 (m, 2H), 7.56-7.64 (m, 2H), 7.6 (s, 4H) ppm.

***N*,*N*'-(1-(2-Fluorophenyl)ethane-1,2-diyl)bis(*N*-(methylsulfonyl)methanesulfonamide) 5n:**

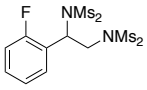

Isolated as a white solid in 69% (Method A) and 73% (Method B) yield.

Mp: 224-226 ºC.

^{1} H-NMR (300 MHz, $CDCl_3$): δ = 2.39-3.34 (bs, 6H), 3.41 (s, 6H), 4.48 (dd, *J* = 3.0, 15.0 Hz, 1H), 4.79 (ddd, *J* = 1.1, 9.1, 15.0 Hz, 1H), 6.14 (dd, *J* = 3.0, 9.1 Hz, 1H), 7.12-7.26 (m, 2H), 7.39-7.47 (m, 1H), 7.54 (td, *J* = 1.7, 7.7 Hz, 1H) ppm.

^{13}C-NMR (75 MHz, $CDCl_3$): δ = 42.9, 44.4 (bs), 50.2 (d, *J* = 1.96 Hz), 56.6, 116.2 (d, *J* = 21.7 Hz), 121.3 (d, *J* = 13.0 Hz), 124.5 (d, *J* = 3.7 Hz), 131.5 (d, *J* = 2.7 Hz), 131.7 (d, *J* = 8.6 Hz), 161.1 (d, *J* = 251.8 Hz) ppm.

^{19}F NMR (376 MHz, $CDCl_3$): δ = -111.49 ppm.

2.4.6. Characterization of diamines 7

***N,N'*-(1-(4-fluorophenyl)ethane-1,2-diyl)bis(4-methyl-N-tosylbenzenesulfonamide) 7a:**

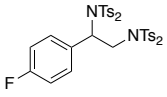

Isolated as a white solid in 61% yield.

Mp: 206-209 ºC.

^{1}H-NMR (400 MHz, $CDCl_3$): δ = 2.40 (s, 12H), 3.72 (dd, *J* = 14.4, 4.0 Hz, 1H), 5.52 (dd, *J* = 14.4, 11.6 Hz, 1H), 6.07 (dd, *J* = 11.5, 4.0 Hz, 1H), 6.70-8.40 (bs, 8H), 6.82 (t, *J* = 8.7 Hz, 2H), 7.18 (d, *J* = 8.4 Hz, 4H), 7.44 (dd, *J* = 8.6, 5.4 Hz, 2H), 7.64 (d, *J* = 8.3 Hz, 4H) ppm.

^{13}C-NMR (125 MHz, $CDCl_3$): δ = 21.8, 50.1, 61.4, 114.8 (d, J_{CF} = 21.2 Hz), 128.3, 128.6 (bs), 129.1 (d, J_{CF} = 3.2 Hz), 129.4 (bs), 129.6, 133.0 (d, J_{CF} = 8.3 Hz), 136.7, 145.1, 162.8 (d, J_{CF} = 248.8 Hz) ppm.

^{19}F-NMR (376 MHz, $CDCl_3$): δ = -113.1 ppm.

***N,N'*-(1-phenylethane-1,2-diyl)bis(4-methyl-*N*-tosylbenzenesulfonamide) 7b:**

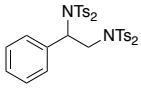

Isolated as a white solid in 78% yield.

Mp: 202-205 ºC.

^{1}H-NMR (300 MHz, $CDCl_3$): δ = 2.39 (s, 12H), 3.74 (dd, *J* = 4.0, 14.5 Hz, 1H), 5.58 (dd, *J* = 11.4, 14.4 Hz, 1H), 6.10 (dd, *J* = 3.9, 11.3 Hz, 1H), 7.0-8.0 (bs, 8H), 7.1-7.2 (m, 7H), 7.46 (d, *J* = 8.3 Hz, 2H), 7.60 (d, *J* = 8.4 Hz, 4H) ppm.

^{13}C-NMR (75 MHz, $CDCl_3$): δ = 21.8, 49.9, 62.2, 127.8, 128.0, 128.2, 128.4 (bs), 129.5 (bs), 131.1, 136.6, 144.9 ppm.

***N,N'*-(1-(4-chlorophenyl)ethane-1,2-diyl)bis(4-methyl-*N*-tosylbenzenesulfonamide) 7c:**

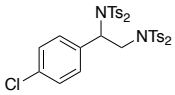

Isolated as a white solid in 65% yield.

Mp: 222-223 ºC.

^{1}H-NMR (300 MHz, $CDCl_3$): δ = 2.40 (s, 12H), 3.72 (dd, *J* = 4.0, 14.4 Hz, 1H), 5.51 (dd, *J* = 11.6, 14.4, Hz, 1H), 6.05 (dd, *J* = 4.0, 11.5 Hz, 1H), 6.80-8.40 (bs, 8H), 7.06 (d, *J* = 8.5 Hz, 2H), 7.18 (d, *J* = 8.3 Hz, 4H), 7.34 (d, *J* = 8.6 Hz, 2H), 7.65 (d, *J* = 8.4 Hz, 4H) ppm.

^{13}C-NMR (75 MHz, $CDCl_3$): δ = 21.8, 50.0, 61.2, 128.1, 128.3, 128.6 (bs), 129.4 (bs), 129.6, 131.7, 132.4, 134.7, 136.6, 145.1 ppm.

***N,N'*-(1-(4-(trifluoromethyl)phenyl)ethane-1,2-diyl)bis(4-methyl-*N*-tosylbenzenesulfonamide) 7d:**

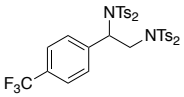

Isolated as a white solid in 80% yield.

Mp: 202-204 ºC.

^{1}H-NMR (400 MHz, $CDCl_3$): δ = 2.38 (s, 12H), 3.74 (dd, *J* = 4.0, 14.2 Hz, 1H), 5.58 (dd, *J* = 11.7, 14.2 Hz, 1H), 6.15 (dd, *J* = 4.0, 11.7 Hz, 1H), 6.8-7.6 (bs, 4H), 7.15 (d, *J* = 8.2 Hz, 4H), 7.29 (d, *J* = 8.2 Hz, 2H), 7.49 (d, *J* = 8.1 Hz, 2H), 7.68 (d, *J* = 8.4 Hz, 4H), 7.70-8.30 (bs, 4H) ppm.

^{13}C-NMR (125 MHz, $CDCl_3$): δ = 21.7, 49.9, 60.6, 124.0, (q, J_{CF} = 3.7 Hz), 124.8 (q, J_{CF} = 3.7 Hz), 128.2, 128.6 (bs), 129.4 (bs), 129.6, 130.3, 131.0, 136.7, 136.9, 137.2 (bs), 145.2 ppm.

^{19}F-NMR (376 MHz, $CDCl_3$): δ = -62.89 ppm.

***N,N'*-(1-(3-fluorophenyl)ethane-1,2-diyl)bis(4-methyl-*N*-tosylbenzenesulfonamide) 7e:**

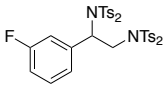

Isolated as a white solid in 66% yield.

Mp: 178-180 ºC.

^{1}H-NMR (400 MHz, $CDCl_3$): δ = 2.42 (d, *J* = 17.7 Hz, 12H), 3.76 (dd, *J* = 4.0, 14.4 Hz, 1H), 5.54 (dd, *J* = 11.5, 14.3 Hz, 1H), 6.03 (dd, *J* = 3.9, 11.5 Hz, 1H), 6.94 – 6.84 (m, 2H), 7.18 (d, *J* = 8.2 Hz, 5H), 7.31 (d, *J* = 8.1 Hz, 4H), 7.41 (dt, *J* = 1.1, 7.8 Hz, 1H), 7.67 (d, *J* = 8.4 Hz, 4H), 7.88 – 7.83 (m, 4H) ppm.

^{13}C-NMR (125 MHz, $CDCl_3$): δ = 21.8, 21.8, 50.0, 61.2, 115.4 (d, J_{CF} = 21.0 Hz), 118.0 (d, J_{CF} = 22.3 Hz), 126.5, 128.0, 128.3, 129.6, 129.9, 135.4 (d, J_{CF} = 7.4 Hz), 136.7, 136.8, 145.1, 145.2, 162.4 (d, J_{CF} = 246.3 Hz) ppm.

^{19}F NMR (376 MHz, $CDCl_3$): δ = -112.98 ppm.

***N,N'*-(1-(4-bromophenyl)ethane-1,2-diyl)bis(4-methyl-*N*-tosylbenzenesulfonamide) 7f:**

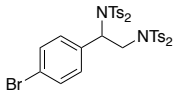

Isolated as a white solid in 81% yield.

Mp: 228-231 ºC.

^{1}H-NMR (300 MHz, $CDCl_3$): δ = 2.41 (s, 12H), 3.71 (dd, *J* = 4.0, 14.4 Hz, 1H), 5.51 (dd, *J* = 11.6, 14.3 Hz, 1H), 6.04 (dd, *J* = 4.0, 11.5 Hz, 1H), 6.8-8.3 (bs, 8H), 7.15-7.23 (m, 6H), 7.24-7.30 (d, 2H), 7.65 (d, *J* = 8.4 Hz, 4H) ppm.

^{13}C-NMR (75 MHz, $CDCl_3$): δ = 21.8, 49.9, 61.2, 122.9, 128.3, 128.6 (bs), 129.4 (bs), 129.6, 131.1, 132.1, 132.6, 136.6, 145.1 ppm.

***N,N'*-(1-(p-tolyl)ethane-1,2-diyl)bis(4-methyl-*N*-tosylbenzenesulfonamide) 7g:**

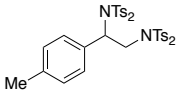

Isolated as a white solid in 47% yield.

Mp: 198-201 ºC.

^{1}H-NMR (300 MHz, $CDCl_3$): δ = 2.34 (s, 3H), 2.39 (s, 12H), 3.74 (dd, *J* = 3.9, 14.5 Hz, 1H), 5.52 (dd, *J* = 11.3, 14.5 Hz, 1H), 6.05 (dd, *J* = 4.0, 11.2 Hz, 1H), 6.7-8.3 (bs, 8H), 6.95 (d, *J* = 7.9 Hz, 2H), 7.15 (d, *J* = 8.2 Hz, 4H), 7.31 (d, *J* = 8.1 Hz, 2H), 7.60 (d, *J* = 8.3 Hz, 4H) ppm.

^{13}C-NMR (75 MHz, $CDCl_3$): δ = 21.3, 21.8, 50.0, 62.3, 128.4, 128.7, 129.2 (bs), 129.5, 130.2, 131.1, 136.7, 138.5, 144.9 ppm.

***N,N'*-(1-(3-phenoxyphenyl)ethane-1,2-diyl)bis(4-methyl-*N*-tosylbenzenesulfonamide) 7h:**

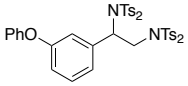

Isolated as a white solid in 76% yield.

Mp: 195-196 ºC.

^{1}H-NMR (300 MHz, $CDCl_3$): δ = 2.39 (s, 6H), 2.41 (s, 6H), 3.80 (dd, *J* = 4.0, 14.4 Hz, 1H), 5.52 (dd, *J* = 11.3, 14.4 Hz, 1H), 6.02 (dd, *J* = 4.0, 11.3 Hz, 1H), 6.7-6.77 (m, 2H), 6.81 (*pst*, *J* = 2.3 Hz, 1H), 6.87 (ddd, *J* = 0.9, 2.5, 8.16 Hz, 1H), 7.01-7.14 (m, 1H), 7.12-7.23 (m, 8H), 7.24-7.31 (m, 3H), 7.44-7.46 (m, 1H), 7.6-8.3 (bs, 4H), 7.68 (d, *J* = 8.4 Hz, 4H) ppm.

^{13}C-NMR (75 MHz, $CDCl_3$): δ = 21.8, 21.8, 50.1, 61.8, 118.5, 119.2, 121.9, 123.3, 125.9, 128.4, 128.8 (bs), 129.4, 129.6, 129.8, 135.1, 136.6, 145.1, 156.8, 157.0 ppm.

***N,N'*-(1-(o-tolyl)ethane-1,2-diyl)bis(4-methyl-*N*-tosylbenzenesulfonamide) 7i:**

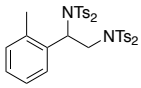

Isolated as a white solid in 54% yield.

Mp: 212-214 ºC.

^{1}H-NMR (300 MHz, $CDCl_3$): δ = 1.70 (s, 3H), 2.39 (s, 12H), 3.88 (dd, *J* = 4.3, 14.0 Hz, 1H), 5.49 (dd, *J* = 11.6, 14.0 Hz, 1H), 6.23 (dd, *J* = 4.3, 11.6 Hz, 1H), 6.52 (d, *J* = 7.5 Hz, 1H), 7.05-7.15 (m, 9H), 7.21 (t, *J* = 7.6 Hz, 1H), 7.35-7.95 (bs, 4H), 7.65 (d, *J* = 8.1 Hz, 4H), 8.04 (d, *J* = 7.9 Hz, 1H) ppm.

^{13}C-NMR (75 MHz, $CDCl_3$): δ = 19.9, 21.8, 49.9, 58.8, 125.9, 128.0, 128.8, 129.1, 129.3, 129.5, 130.3, 131.7, 136.9, 139.8, 144.7 ppm.

***N,N'*-(1,2-diphenylethane-1,2-diyl)bis(4-methyl-*N*-tosylbenzenesulfonamide) 7j:**

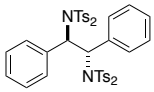

Isolated as a white solid in 38% yield.

Mp: 186-188 ºC.

^{1}H-NMR (300MHz, $CDCl_3$): δ = 2.30 (d, *J* = 3.5 Hz, 12H), 6.89 (d, *J* = 8.5 Hz, 8H), 6.95 (d, *J* = 8.6 Hz, 4H), 7.03 (t, *J* = 7.6 Hz, 4H), 7.10-7.17 (m, 4H), 7.36 (d, *J* = 7.9 Hz, 4H), 7.76 (bs, 4H) ppm.

^{13}C-NMR (75MHz, $CDCl_3$): δ = 21.6, 21.7, 66.5, 127.9, 128.4, 128.5, 128.7, 129.0, 129.2, 135.4, 135.8, 138.7, 144.0, 144.3 ppm.

***N,N'*-(3-phenylpropane-1,2-diyl)bis(4-methyl-*N*-tosylbenzenesulfonamide) 6k:**

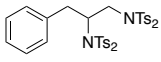

Isolated as a white solid in 84% yield.

^{1}H-NMR (300 MHz, $CDCl_3$): δ = 2.42 (s, 3H), 2.46 (s, 9H), 3.04 (dd, *J* = 5.4, 14.9 Hz, 1H), 3.18 (dd, *J* = 9.7, 14.9 Hz, 1H), 4.11 (dd, *J* = 5.1, 15.1 Hz, 1H), 4.51 (dd, *J* = 9.5, 15.1 Hz, 1H), 5.04 (tt, *J* = 5.3, 9.9 Hz, 1H), 6.69-6.76 (m, 2H), 7.01 (tt, *J* = 1.8, 6.6 Hz, 2H), 7.05-7.15 (m, 3H), 7.23-7.32 (m, 6H), 7.66-7.59 (m, 2H), 7.81-7.89 (m, 4H), 7.91-7.99 (m, 2H) ppm.

^{13}C-NMR (75 MHz, $CDCl_3$): δ = 21.8, 35.4, 50.2, 62.9, 126.1, 128.2, 128.8, 128.8, 129.0, 129.2, 129.4, 129.5, 129.7, 135.7, 136.0, 137.0, 138.6, 145.0, 145.3 ppm.2.4.7.

2.4.7.X-Ray Analysis of compounds 3

2,2'-((2-iodo-1,3-phenylene)bis(oxy))bis(*N*,*N*'-diisopropylacetamide) 3a:

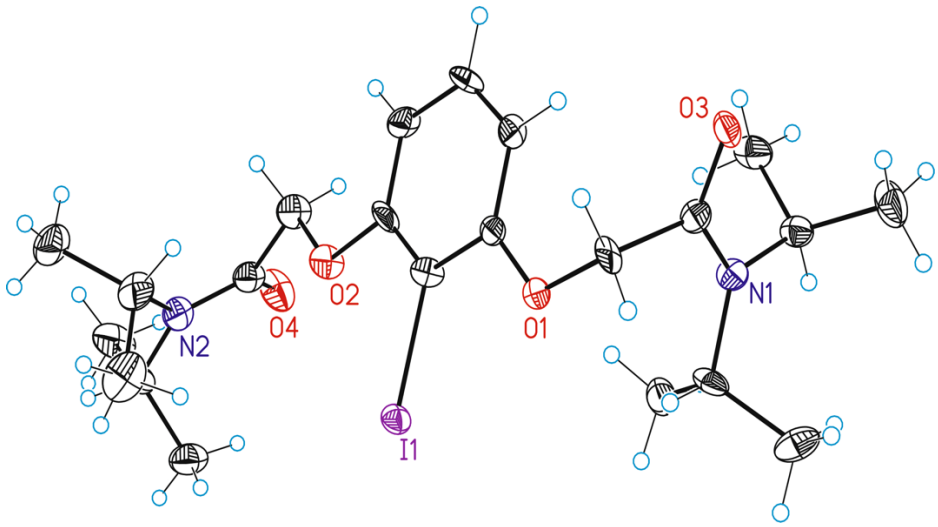

Table S-1. Crystal data and structure refinement for compound **3a**.

Identification code	CCDC 1895651
Empirical formula	C22 H35 I N2 O4
Formula weight	518.42
Temperature	100(2) K
Wavelength	0.71073 Å
Crystal system	Monoclinic
Space group	P2(1)/c
Unit cell dimensions	a= 21.275(3)Åα = 90º.
	b= 8.1422(11)Å β = 110.298(5)º.

	c = 14.8744(19)Å γ = 90º.
Volume	2416.6(6) $Å^3$
Z	4
Density (calculated)	1.425 Mg/m^3
Absorption coefficient	1.353 mm^{-1}
F(000)	1064
Crystal size	0.20 x 0.15 x 0.01 mm^3
Theta range for data collection	2.702 to 25.727º.
Index ranges	-25<=h<=24,0<=k<=9,0<=l<=18
Reflections collected	4590
Independent reflections	4590[R(int) = ?]
Completeness to theta =25.727∞	99.299995%
Absorption correction	Multi-scan
Max. and min. transmission	0.987 and 0.759
Refinement method	Full-matrix least-squares on F^2
Data / restraints / parameters	4590/ 0/ 271
Goodness-of-fit on F^2	1.085
Final R indices [I>2sigma(I)]	R1 = 0.0627, wR2 = 0.1432
R indices (all data)	R1 = 0.1090, wR2 = 0.1782
Largest diff. peak and hole	0.971 and -1.464 e. $Å^{-3}$

Chapter II – A practical aryliodine (I/III) catalysis for the vicinal diamination of styrenes

2,2'-((2-iodo-5-methyl-1,3-phenylene)bis(oxy))bis(*N*,*N*'-diisopropylacetamide) 3b:

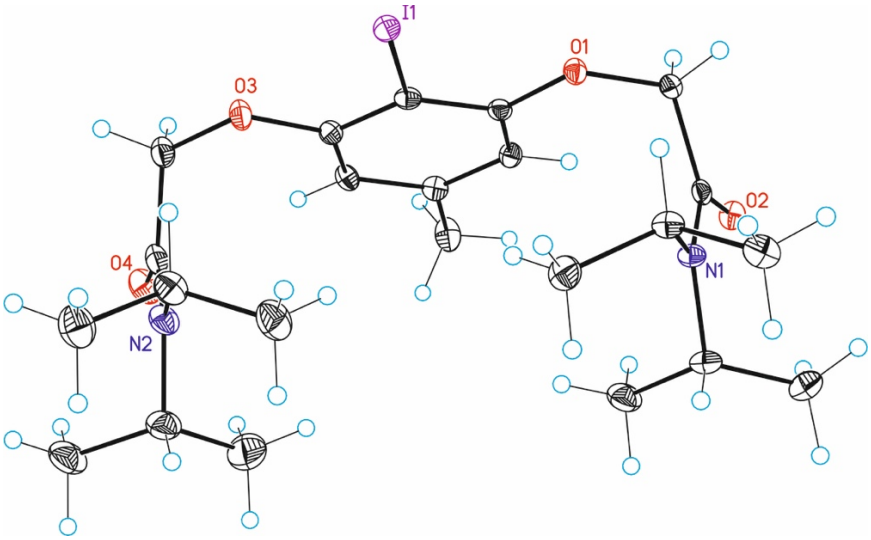

Table S-2. Crystal data and structure refinement for compound **3b**.

Identification code	CCDC 1898343
Empirical formula	C23 H37 I N2 O4
Formula weight	532.44
Temperature	100(2) K
Wavelength	0.71073 Å
Crystal system	Monoclinic
Space group	P2(1)/c
Unit cell dimensions	a = 19.8520(6)Å α= 90°.
	b = 8.4876(2)Å β = 104.0217(8)°.
	c = 15.4763(5)Å γ = 90°.
Volume	2529.99(13) Å^3
Z	4
Density (calculated)	1.398 Mg/m^3

Absorption coefficient	1.294 mm^{-1}
F(000)	1096
Crystal size	0.40 x 0.20 x 0.15 mm^3
Theta range for data collection	2.115 to 27.526°.
Index ranges	-20<=h<=25,-11<=k<=7,-19<=l<=20
Reflections collected	16888
Independent reflections	5738[R(int) = 0.0171]
Completeness to theta =27.526°	98.7%
Absorption correction	Multi-scan
Max. and min. transmission	0.830 and 0.638
Refinement method	Full-matrix least-squares on F^2
Data / restraints / parameters	5738/ 0/ 281
Goodness-of-fit on F^2	1.066
Final R indices [I>2sigma(I)]	R1 = 0.0168, wR2 = 0.0421
R indices (all data)	R1 = 0.0182, wR2 = 0.0428
Largest diff. peak and hole	0.479 and -0.334 e.$Å^{-3}$

Chapter II – A practical aryliodine (I/III) catalysis for the vicinal diamination of styrenes

3. Chapter III - Improved Synthesis of Ishihara–Muñiz Pre-catalysts

3.1. Introduction

Asymmetric catalysis for oxidative transformations has become an increasingly important topic in recent years, especially for those involving 1,2-functionalizations (See section 1.1) and dearomatizations (See section 1.4.2.2).[13,142,170–173] In this matter, hypervalent iodine reagents and aryliodine pre-catalysts have remained an unchallenged source of innovation due to their broad reactivity and sustainability.[174–178] Similarly, oxidative transformations using these compounds have presented themselves as state-of-the-art, conveying a high applicability in modern organic synthesis.[161,179] The principal attribute for iodine reagents to have gained this status is their high reactivity and reliability, combined with good site-selectivity and broad applicability in many transformations within organic synthesis.[45,164] On the other hand, the main reasons for aryliodines to have spread in the chemistry of vicinal transformations nowadays is a consequence of their facile and adaptable synthesis. This fact allows for the modular construction of fit-for-purpose pre-catalysts. Departing from the aryliodine core, many different pre-catalysts can be synthesized through direct paths, creating a wide variety of pre-catalysts. The different key structural features showed to make a large impact upon the yield and stereoselectivity of a given reaction (Figure 17).[107,180]

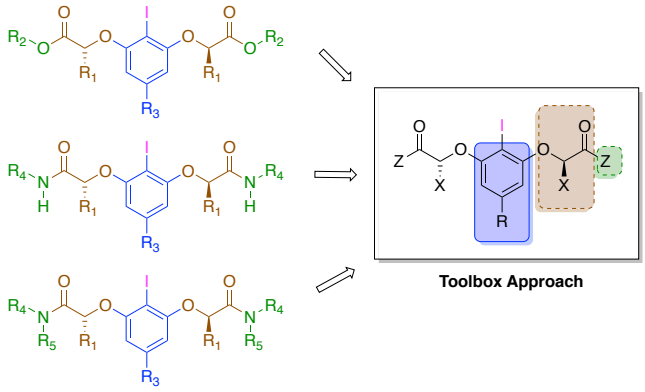

Figure 17. Modular nature of Aryliodine pre-catalysts

Throughout the first two chapters of this thesis, many transformations have been presented, with special emphasis in diaminations and fluorination reactions using I(III) either in stochiometric or catalytic modes. Various reactions rely on the catalysts developed by our group, which will be shown in the next sub-sections.

3.1.1. Diacetoxylation reaction

One of the most important transformations to be presented yet in this thesis is the enantioselective vicinal diacetoxylation of styrenes. Not only its pre-catalyst design but the mechanistic implications (which have already been mentioned in the previous chapter) had a big impact on related I(III)-mediated reactions. In 2012, Meng, Li *et al.* described a racemic methodology for the first diacetoxylation reaction using I(I/III) catalysis. Even though not enantioselective, the transromation showed a clear predominance for *syn* products. The mechanism involving a Woodward-Prévost step was then proposed for the first time to justify this fact (Scheme 70).[181]

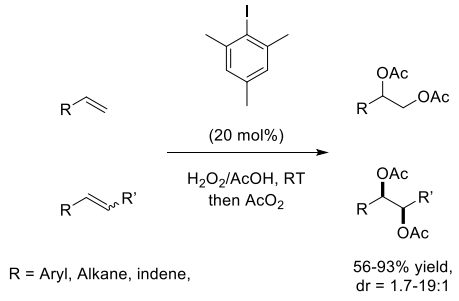

Scheme 70. First racemic diacetoxylation by Meng and Li in 2012

Later on, Ishihara and our group upgraded this reaction to the enantioselective fashion, by the modification of Ishihara's ishiharation pre-catalyst.[91] This consisted in the introduction of a terminal 2,6-

diisopropylphenylamide and the introduction of a *para*-methyl group in the central aromatic core. X-ray analysis of the diacetate I(III) derivative showed for the first time the importance of the side-chains in the pre-catalyst's design, as they interact with the ligands in the active centre.
This fact was later noted for the design of other catalytic systems, such as the diamination reaction.

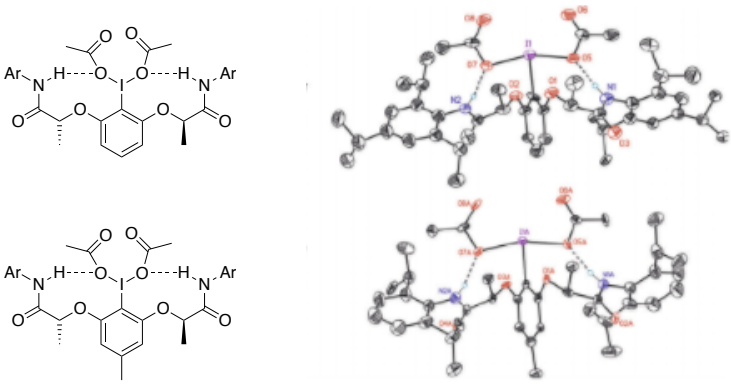

Figure 18. Intramolecular H-bonding in Aryliodine pre-catalysts. Ar = 2,6-diisopropylphenyl

When the mentioned structure was used in an improved procedure for styrenes diacetoxylation, its performance was up to 94% *ee* and 93% yield. This enantioselective procedure also involved the use of AcOOH as oxidant and TfOH as additive. A wide variety of substrates were tolerated, with enantioseletivities ranging from 63% to 94 % *ee* for a total of 24 examples (Scheme 71).[134]

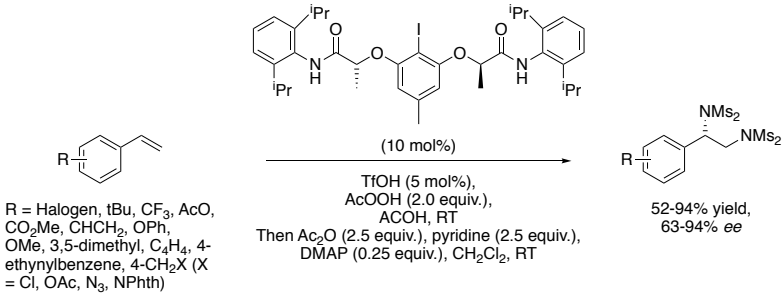

Scheme 71. Diacetoxylation reaction by Muñiz and Ishihara in 2016

As for the proposed mechanism, it was very similar to the initial suggestion of Meng and Li, but with the introduction of the chiral arms and TfOH. As depicted in Scheme 72, a first formation of the active species **A** is followed by a ligand exchange with the triflate anion (**B**). Then, coordination of the alkene and an *anti*-acetoxyiodination (**C**) precedes the suggested Woodward-Prévost intermediate (**D**). Upon water introduction and addition of acetic anhydride, it finally gets converted into the final 1,2-diacetoxylated compound **E**.

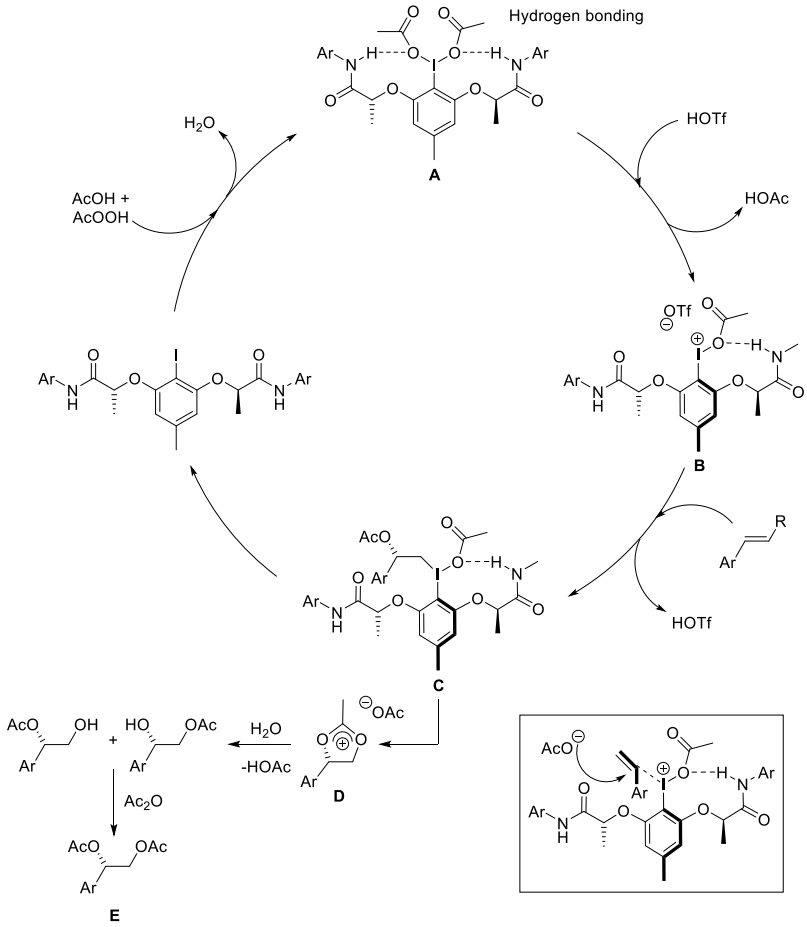

Scheme 72. Diacetoxylation suggested mechanism

3.1.2. Dearomatization reaction

One of the initial reactions in the I(III) chemistry was the dearomatization reaction (See section 1.4.2.2.). Nowadays, the main challenge for this field is the development of enantioselective intermolecular reactions, as most intramolecular variants have been thoroughly optimized and achieved excellent stereoselectivities. Our group developed in 2017 an enantioselective intermolecular reaction employing the pre-catalyst used in the diacetoxylation reaction. Even if the yields were moderate to excellent, the *ee* values were not over 50%. Besides, a new tosylaniline substrate was oxidized to the corresponding imine with 34% *ee*, expanding the synthetic application of this transformation (Scheme 73).

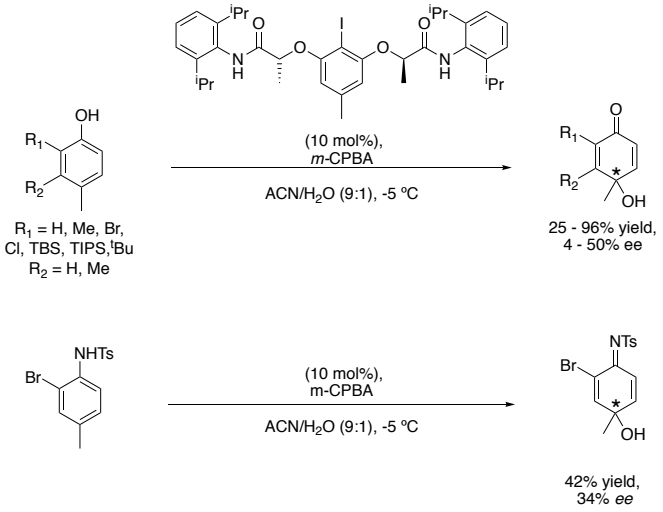

Scheme 73. Intermolecular dearomatization by Muñiz in 2017

The mechanistic suggestion followed what was postulated beforehand for this pre-catalyst. Thisinvolves a first conversion to the active I(III) species, an O-coordination of the substrate and an attack from the water nucleophile (Figure 19). Subsequent investigations from Maruoka in 2018 and 2021 showed that an indanol-based pre-catalyst is able to yield up to excellent *ee* values (95% *ee*) for both products.[113,182]

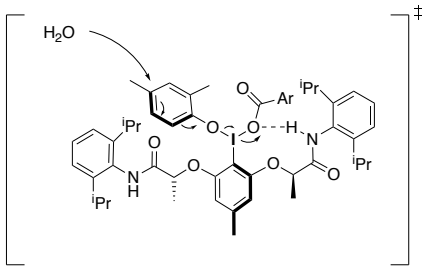

Figure 19. Proposed mechanism for the *para*-dearomatization

3.1.3. α-Acetoxylation of ketones

Even if this reaction type has been already presented in section 1.4.2.3, it is of note that in 2020 Wirth used the Ishihara-Muñiz pre-catalyst in his α-Acetoxylation of ketones. In this work, the authors found this structure to be among the best *ee*-inducing - with up to 85% *ee* - of the corresponding acetoxylated products when used in stoichiometric amounts. When the reaction was tested in a catalytic fashion, the best pre-catalyst was the one containing a *para*-methyl moiety. Not only the *ee* was maintained in similar values but rose to 88% *ee*. Moreover, the use of only 5 mol% of the pre-catalyst and the help of boron trifluoride as a lewis acid were crucial to the observed results.[180]

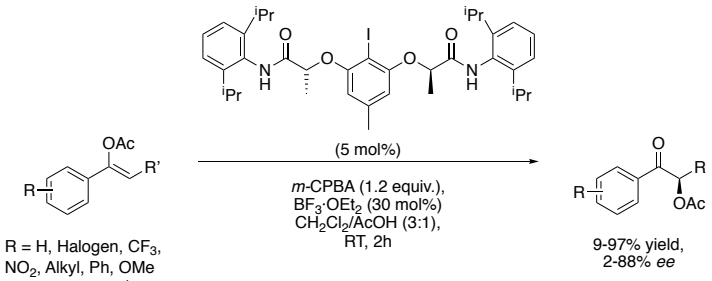

Scheme 74. α-Acetoxylation of ketones

3.1.4. Other reactions: Oxyaminations

Recently, another kind of reaction have been repeatedly developed with the involvement of I(III) and I(I/III) catalysis: Oxyamination reactions of alkenes. In this reaction, an alkene and an amide are reacted to form a 5-iminotetrahydrofuranyl ring. In this field, the first group to use the Muñiz pre-catalyst (made originally for the diamination reaction) were Yu and He in 2020, getting up to 53% *ee*. Their reaction reached 95% yield and 98% *ee* when the diisopropylamide moiety of the pre-catalyst was changed to a cyclohexylethylamide moiety.[183]

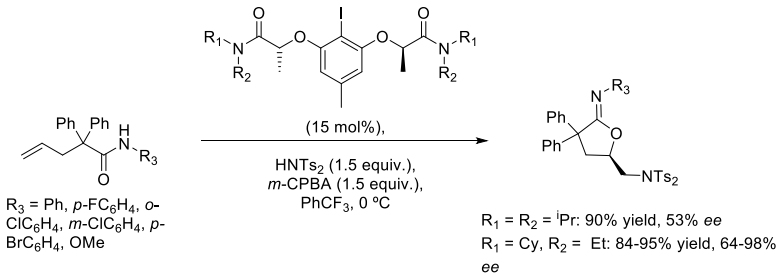

Scheme 75. Oxyamination of alkenes with sulfonamides

Next, Wei Li published another reaction to intermolecularly form oxazolines from alkenes and amides. This reaction switches reactivity depending on the acidity of the reaction media. If basic conditions are applied, a first O-nucleophilicity is observed, but if on the contrary a Lewis acid is added, it is the nitrogen atom that is first incorporated in the styrene moiety. This fact makes the reaction regiodivergent as depending on the conditions the regioisomer obtained changes. One of their experiments consisted in trying a chiral aryliodine pre-catalyst, and the Muñiz pre-catalyst gave 86% *ee* and 74% *ee* respectively when used in basic or acid conditions (Scheme 76).[184]

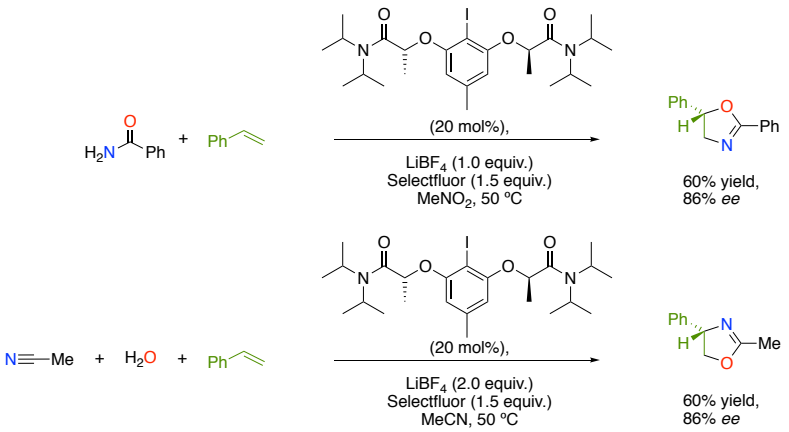

Scheme 76. Oxazoline formation using chiral Muñiz pre-catalyst

Finally, the group of Hashimoto developed another intermolecular oxyamination using alkenes and N-fluorosulfonylcarbamates. In this case, two different oxidants were employed: magnesium monoperoxyphthalate hexahydrate (MMPP) and Selectfluor. For electronically neutral styrenes , MMPP was used, and Selectfluor was convenient forelectron-deficient ones. Both methods gave moderate to good yields and 83-99% *ee*. A modification of the Muñiz pre-catalyst was generally used, which contained benzyl moieties instead of methyls, even if the original pre-catalyst was also used in some substrates with similar results (Scheme 77).[185]

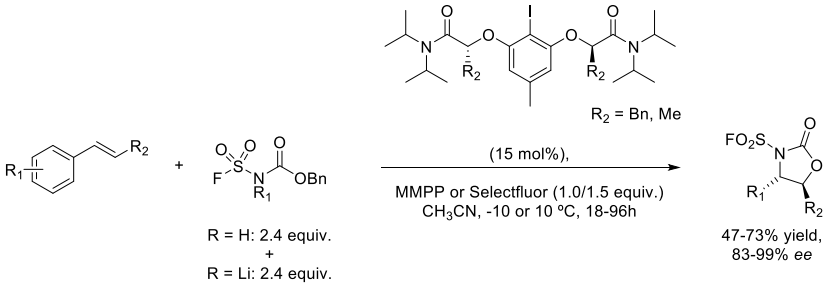

Scheme 77. Enantioselective oxyamination using benzyl N-(fluorosulfonyl)-

Carbamate

3.1.5. Previous pre-catalyst scale-ups

One fundamental limitation in this field is the lack of upscaling procedures for the pre-catalysts synthesis, this being to date limited to a 1-2 g scale for most of them. Moreover, all reported procedures involve various unoptimized and time-consuming purifications.[100] These facts severely hamper the use of large scale I(I/III)-catalyzed transformations at industrial level, or even for academic purposes when large screenings have to be performed.[180]

However, some efforts have been put in this direction. Recently, Ishihara brought focus on the scalability of his second-generation pre-catalyst and the dearomatization reaction it mediates (Scheme 78). This pre-catalyst was synthesized in 10 mmol scale (6.47 g). So far, this is the highest scale for a terminal amide aryliodine pre-catalyst.[186,187] Besides, a first generation variant also containing a terminal mesitylamide is commercially available.

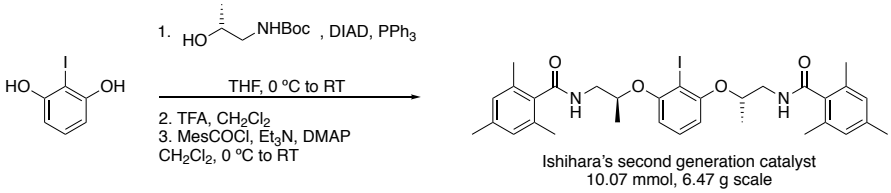

Scheme 78. Scaled synthesis of Ishihara's second-generation catalyst

Nevertheless, a unified, general and scalable synthesis for the first generation of these catalysts helping to generalize the use of Iodine I/III catalysis among the scientific community has been long overdue.

3.2. Results and discussion

The previous synthesis of Ishihara-Muñiz pre-catalysts started with the iodination of Resorcinol **8** or Orcinol **9**, following purification by chromatography or recrystallisation (Scheme 79). Next, a Mitsunobu reaction using L-methyl lactate (or the non-natural D-methyl lactate) enabled access to the corresponding diesters **10**-**11** after isolation by column chromatography. As in most Mitsunobu reactions, the presence of triphenylphosphine used in excess, triphenylphosphine oxide, DIAD, and its reduced form hamper the separation of the desired product. Following a saponification reaction involving a rather prolonged basic treatment (16 h), diacids **12** and **13** were synthesized. Lastly, an amidation yielded the final pre-catalysts **16**-**18** after another purification by column chromatography.

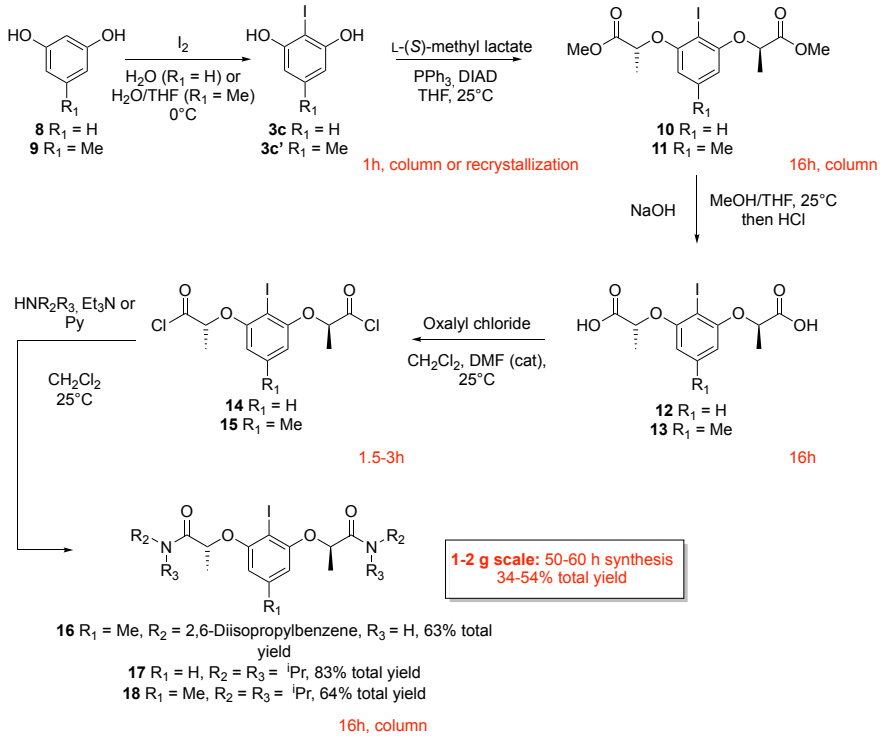

Scheme 79. Synthesis of Ishihara-Muñiz pre-catalysts

The total yields are moderate (34-54%) and pre-catalysts **16**, **17** and **18** can be synthesized on a 1-2 g scale in 4-5 days (50-60h), chromatographic purifications and work-ups included.

3.2.1. Initial scale-up of Ishihara-Muñiz pre-catalysts

When the scale-up of the procedure was planned, the general synthetic plan was not altered. Instead, a thorough optimization of the reactions and their associated work-ups, avoiding the isolation of some intermediates, was performed in order to provide an efficient synthesis. The intention was to significantly improve the synthesis in terms of time, required purifications and overall yield. During the optimization of the first iodination step we observed that, in the case of orcinol, the by-products formed could be largely avoided by simply reversing the order of reactants addition. These by-products mainly arise from diiodination, along with unreacted starting material (see Table 5). A screening was performed, changing the equivalents of iodine which reveals that 1.5 equiv. of I_2 gives the best result (Entry 3). Over 90% of selectivity towards the desired product can be obtained by this method and the crude product can be used without further purification.

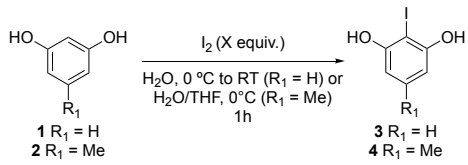

Scheme 80. Iodination reaction of Resorcinol **1** and Orcinol **2**

Table 5. Optimization for the iodination reaction scale-up

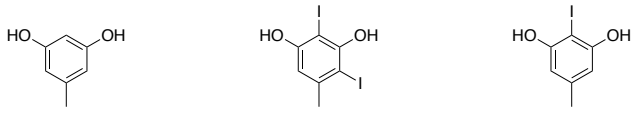

9 **19** **3c'**

Entry	Eq. I_2	%(NMR) 9	19	3c'
1	1.1	14	3	83
2	1.3	14	2	84
3	1.5	**3**	**6**	**91**
4	2.0	1	16	83

The Mitsunobu reaction was not modified further than decreasing the reaction time, but we developed a procedure to reduce the main byproducts of the reaction: $OPPh_3$ and reduced DIAD. We observed that most of the $OPPh_3$ can be precipitated by the addition of Cyclohexane to the crude. However, reduced DIAD and some residual $OPPh_3$ still remain in the crude of the upscaled reactions (Scheme 81).

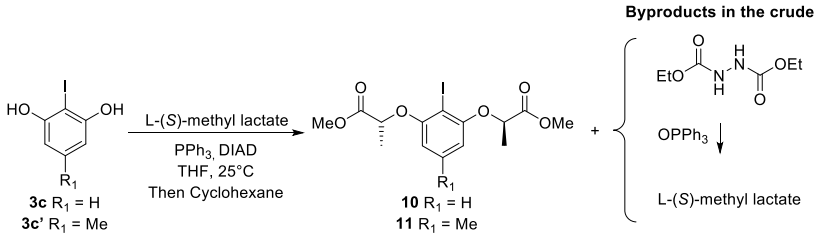

Scheme 81. Optimized Mitsunobu reaction and work-up to eliminate $OPPh_3$

We also found that the saponification step can be immediately performed with the crude mixture from the Mitsunobu reaction containing excess lactate, some $OPPh_3$ and reduced DIAD. Then, this crude was directly submitted to the saponification reaction with NaOH, MeOH and THF. The reaction time was reduced to 1h, as TLC showed the scaled-up reactions were smoothly completed. In contrast, 16h was the previously described

runtime for small scale reactions. While the lactate and residual PPh_3O are easily eliminated through an acid-base extraction, the removal of reduced DIAD proved more difficult. Finally, we found that dissolving the crude acid in EtOAc followed by addition of 10 volumes of cyclohexane led to precipitation of the acids **12-13** that were isolated as pure white solids after filtration (Scheme 82).

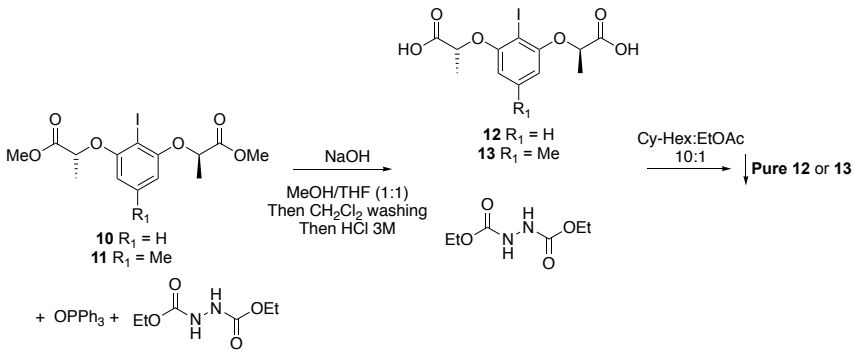

Scheme 82. Saponification reaction and work-up to remove by-products of the Mitsunobu reaction

For the final step, the diacid was dissolved in anhydrous dichloromethane and reacted with oxalyl chloride to produce the corresponding bis(acyl chloride) **14** and **15**, which was immediately submitted to amidation. In this last reaction, as previously reported, pyridine was used as an acid scavenger in the preparation of catalyst **16**, while triethylamine was used with the same purpose in the preparation of **17** and **18**. A final recrystallization using $MeOH/H_2O$ was performed instead of the previously reported column chromatography, but the reaction times were not yet modified.

The first upscaling of these syntheses were performed at 20 g scale with improved overall yields of 63% for **16**, 83% for **17** and 64% for **18**.

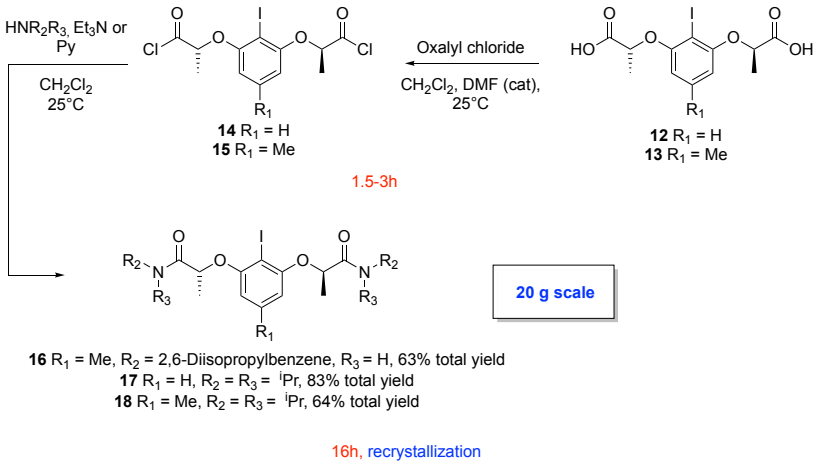

Scheme 83. Final step of the scaled pre-catalysts synthesis

3.2.2. Application to substrates: Racemic outcomes

In order to demonstrate that the new procedure provided the catalyst in equal purity as in the previous laboratory scale synthesis, we employed them in the reported diamination reaction.[135] To our surprise, the reaction with the above catalysts yielded almost racemic products, with up to 19% *ee* (Scheme 84, Figure 20). This fact was thoroughly investigated, as we did not conceive any notable changes in the synthesis, nor in the analysis of the final pre-catalysts by NMR, HPLC-MS or TLC compared to the literature data.

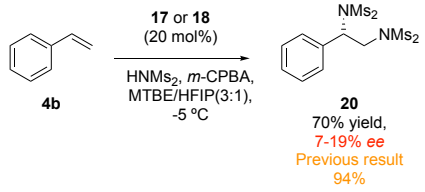

Scheme 84. Unexpected racemic formation of diamines with the upscaled pre-catalysts

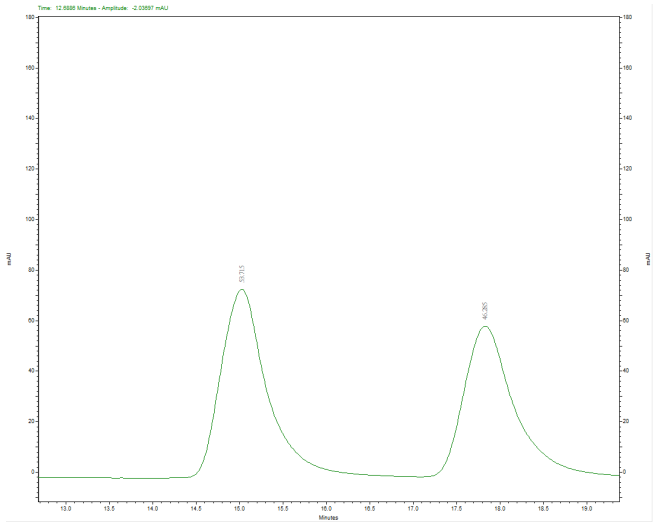

Figure 20. Chiral HPLC chromatography of one of the diamination reactions showing a product with 7.4% *ee*

To our surprise, Chiral Supercritical Fluid Chromatography (SFC) indicated that the upscaled procedure had led to the formation of the enantiomer *S,S* and a new species, which did not correspond to either the *R,R* or *S,S* forms of the catalyst.

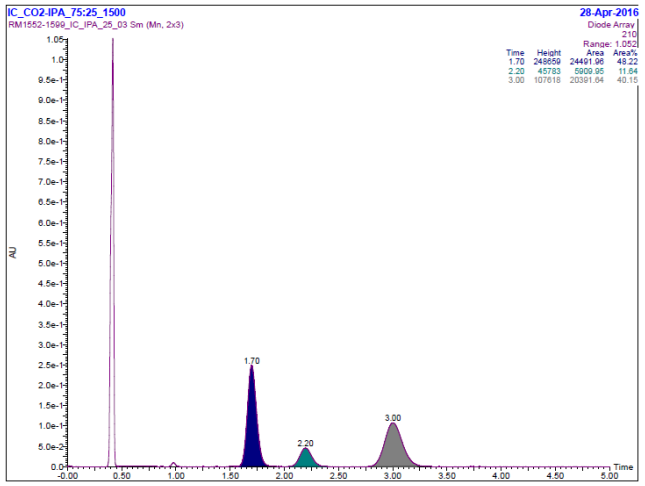

Figure 21. SFC spectra of racemic pre-catalyst **18** in 2017 showing three peaks *R,R;* meso and *S,S*

The occurrence of this third species was as high as 90% in some of the batches, which we assumed to be responsible for generating racemic products. Indeed, this species was already observed in the SFC spectra of the pre-catalyst **18** (Figure 21) when first published in 2017. The extra peak was observed in the racemic sample containing the *R*,*R* and *S,S* pre-catalysts, but also in the individual ones which had only one of the enantiomers, in amounts up to 12%. This fact brought us to one of the first hypotheses we proposed: that a *meso*-species was formed in a higher rate due to the upscaling of the pre-catalyst synthesis. This was supported by the fact that no other molecular ion could be detected by HPLC-MS. A *meso*-form of the pre-catalyst would be an achiral compound which would arise from the epimerization of one of the two chiral arms (Scheme 85). Later reports from Ishihara also identified a *meso*-compound in their *second-generation* catalyst.[186]

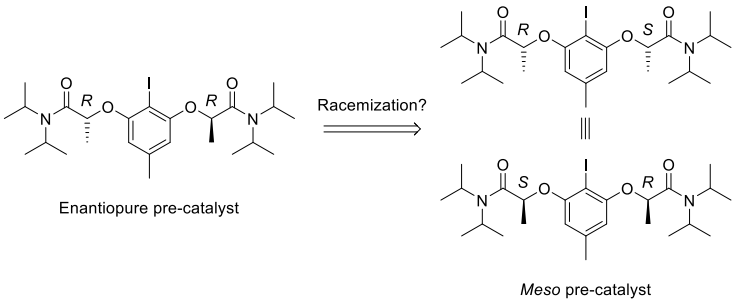

Scheme 85. Plausible racemization of the pre-catalyst to generate a *meso* compound

3.2.3. Synthesis of *meso*-species 26

To confirm the identity of the new peak, an independent synthesis was planned to generate the *meso* isomer of the catalyst and analyze it by SFC (Scheme 86). Following a procedure reported by Yoshida, 2-iodoresorcinol **3c** was first monoprotected with a methoxymethyl (MOM) group (**21**).[188]

Then, a Mitsunobu reaction allowed for the introduction of the *R* side-chain to form **22**. After deprotection of the MOM group with trifluoroacetic acid (TFA), and another Mitsunobu reaction to introduce the *S* arm, the diester **24** was synthesized.

Following the same procedure as for the pre-catalysts **17** and **18**, **24** was submitted to saponification affording diacid **25**. A final amidation without the use of Et_3N (See next section) was performed in order to obtain **26**. When injected in the SFC, we confirmed it to be the major species present in our catalysts. Unambiguous characterization was also achieved by X-Ray.

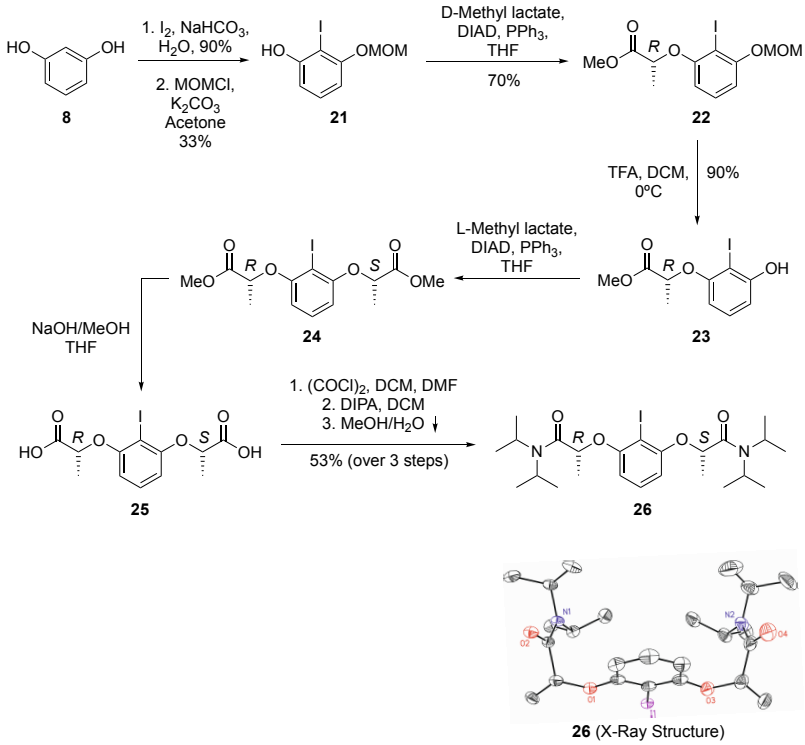

Scheme 86. Independent synthesis of the meso compound **26**

When the diamination reaction was carried out on styrene (**4b**) using pure **26** and with the same reaction time, the completely racemic product **5b** was obtained in comparable yield as with the pure *R*,*R* form, further

confirming the initial hypothesis and showing that the *meso* form has similar activity as the *R,R* or *S,S* enantiopure pre-catalysts.

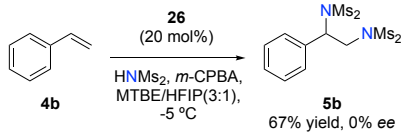

Scheme 87. Catalytic activity of **26** showing similar yields as **17** and **18**

3.2.5. Quest for *meso* formation

One of the two most important questions we asked ourselves about this *meso*-form were: *when?* and *why?* When was it epimerized? Why does it happen? And also: Why an increase epimerization was observed when upscaling the procedure?

In parallel with the synthesis of **26**, all the reactions from section 3.2.1. were repeated, but this time, chiral SFC or HPLC analysis wereperformed in order to identify the formation of **26** within our synthetic plan. Our first suggestion was that the epimerization could occur under the strongly basic conditions during the saponification step with aqueous NaOH.

To prove it, we undertook a systematic analysis to determine where the epimerization occurred. We started off with the commercial lactate; the specific batch of natural L-(*S*)-methyl lactate used during this synthesis has an *ee* of 99.6%. This lactate is subsequently used in the Mitsunobu reaction with the iodinated derivative from resorcinol **8** (or the orcinol derivative **9**). After chiral SFC analysis and comparison with the product of the same reaction but using (*rac*)-methyl lactate, the reaction product **10** turned out to be 99.3% *R*,*R*, with only a small amount of *meso* form (0.7%), indicating that epimerization did not occur in the conditions of the Mitsunobu reaction.

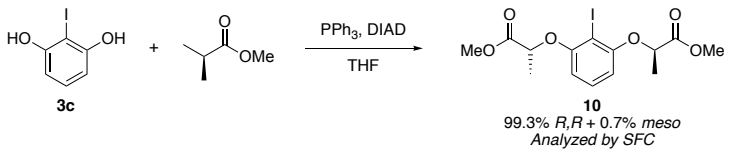

Scheme 88. Outcome of the Mitsunobu reaction showing no epimerization

Next, the saponification step to yield the diacid was analyzed. In this case, the product could not be analyzed by SFC, and chiral HPLC was used instead. This experiment and analysis showed that the epimerization leading to *meso* form did not originate in the saponification, as the diacid product **12** maintained its *ee* compared to the diester **10** (Scheme 89). The slight increase in *ee* was attributed to the change of equipment in this analysis, but not to a stereochemical modification of **12** by the NaOH.

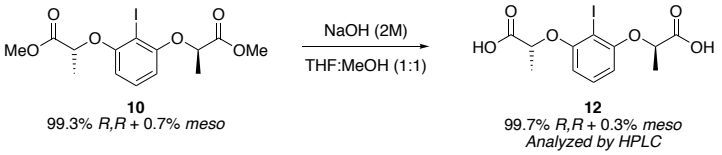

Scheme 89. The *ee* of the pre-catalyst is not affected by the saponification reaction

Indeed, it was not until the last two reactions, the chlorination of the diacid and the amidation, where the *meso*-form was detected for the first time (Scheme 90). Our hypothesis is that the fundamental reason for the racemization of the catalyst was the formation of a ketene species.[189]

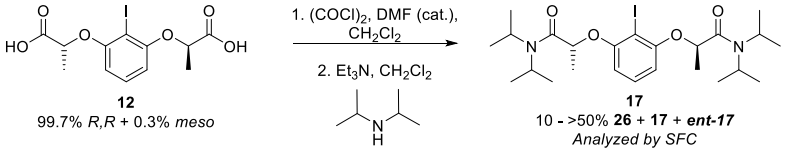

Scheme 90. Final step of the synthesis to give **17** and origin of the *meso*-form **26** observed

Because of the relatively low pKa of the α-carbonyl proton in **14**, base abstraction leads to the formation of ketene **27**. Afterwards, the non-face discriminating reaction with diisopropylamine opened the door to the formation of *meso* **26** and a minor amount of the *S,S* enantiomer. Small

increases in the reaction temperature and generation of local hotspots at this stage can be responsible for variable degrees of epimerization in the large-scale synthesis of **17**-**18**.

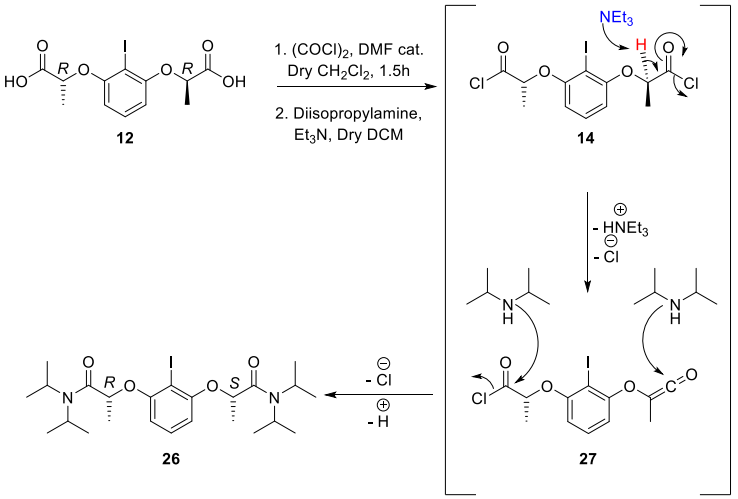

Scheme 91. Mechanistic proposal for the formation of meso **26**

3.2.5. Identification of the ketene intermediate

The colour observed during the amide formation can give some hint of the hypothesized ketene formation. When using Et_3N in the reaction, a red solution was observed, which could be attributed to the formation of the ketene. However, when no Et_3N was added, this red solution was not obtained. Instead, in these conditions the colour remained yellow (See Scheme 92a).

The acyl chloride intermediate was also stirred with triethylamine during 16h after which it was treated with either water (to revert to the acid) or diisopropylamine (to form the amidated product). Both should in theory give a mixture (of *meso*, *R,R and S,S* products), however, no product could be isolated in both cases and a polymeric material immediately was formed, which was not soluble in any solvent (Scheme 92b).

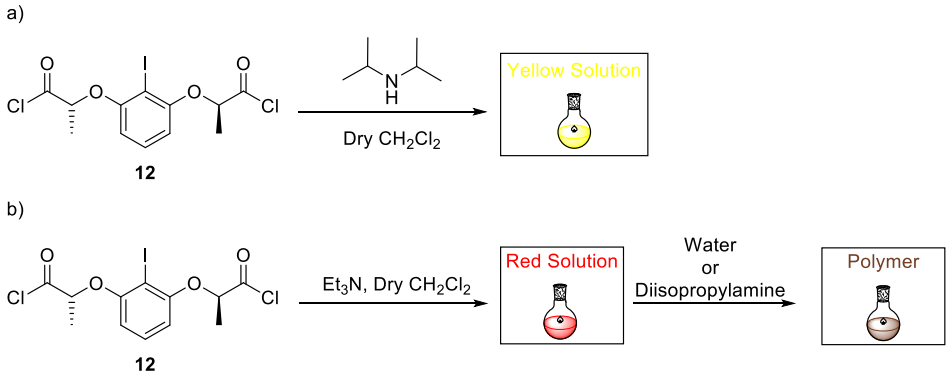

Scheme 92. a) Yellow solution obtained when using only diisopropylamine. b) Red solution and polymerization when using Et_3N

Variation of the conditions did not allow the isolation of the desired ketene intermediate. We turned our attention to the known reaction of ketenes, and we tried a [2+2] cycloaddition with both vinyl ethyl ether and methyl acrylate (Scheme 93). In both cases, as in previous observations, the formation of the insoluble solid, probably arising from the self-polymerization of the ketene, prevented us to demonstrate the formation of **27**.

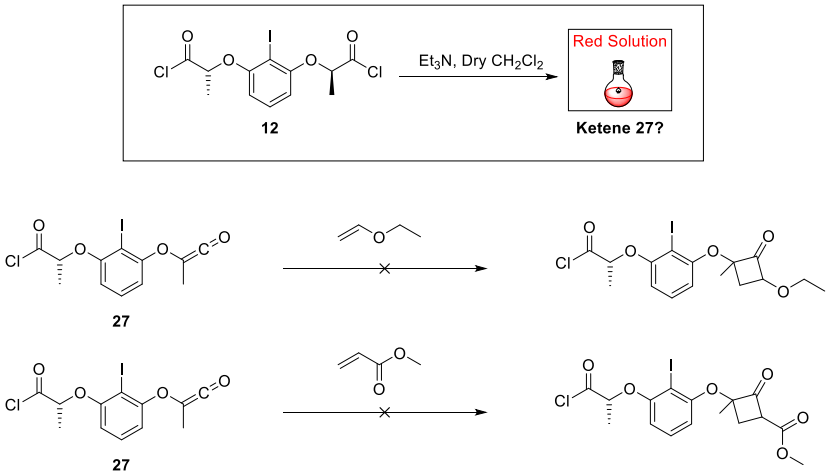

Scheme 93. Failed [2+2] cycloadditions with ethyl vinyl ether and methyl acrylate

With this background, we thought that the identification of significant IR peaks could be the easiest way to detect this intermediate, as the polymer is formed very quickly without the presence of a nucleophile. Using an ATR IR instrument, a drop of diacyl chloride **12** diluted in chlorobenzene (used as a non-volatile solvent) was positioned on the detector, and the analysis was started. Quickly, one drop of Et_3N was added to the previous drop. Peaks at 1779.8 and 2152.5 cm^{-1} were observed, suggesting that the conversion of the acid chloride into the ketene occurs under these conditions. After the analysis, the polymer obtained previously was again observed in the chlorobenzene droplets.

Figure 22. Two IR analysis of the supposed ketene species **27** in solution, after submitting **12** to Et_3N (Bottom)

Further experiments to observe the generality of the formation of the ketene were carried out with different tertiary amine and pyridine bases. Addition of 4-dimethylaminopyridine and N-methylpiperidine induced the immediate formation of a solid (which we interpreted like a polymer formation). In the latter case also accompanied by the generation of dense white fumes, likely due to condensation of the base hydrochloride in the headspace. Addition of diisopropylethylamine was accompanied by the immediate change of colour to a deep orange solution and the formation of dense white fumes, but in this case, we did not observe formation of polymer. Pyridine, in turn, provided very little change, the coloration of the solution not changing substantially after the addition and no evolution of fumes. However, it gradually faded to a more intense yellowish color, and after about 15-20 min, a solid was formed (Scheme 94). For this reason, one can assume that the formation of ketene **27** with pyridine is much slower than with DMAP or 4-methylpiperidine.

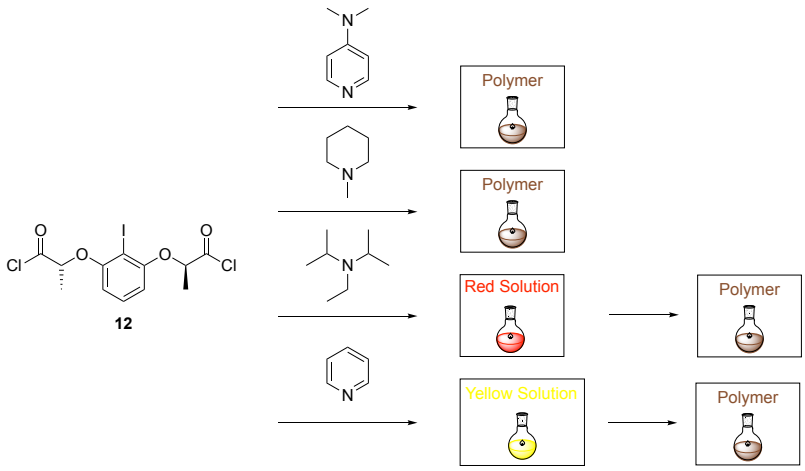

Scheme 94. Formation of polymers or changes of colour when adding different bases to the acyl chloride **12**

Analysis by ATR IR when using diisopropylethylamine seem to confirm the formation of the ketene intermediate, as can be observed in the spectrum of a diluted sample in Figure 23. Notably, in this case the signal at 2150 cm^{-1} is not as visible as when using Et_3N.

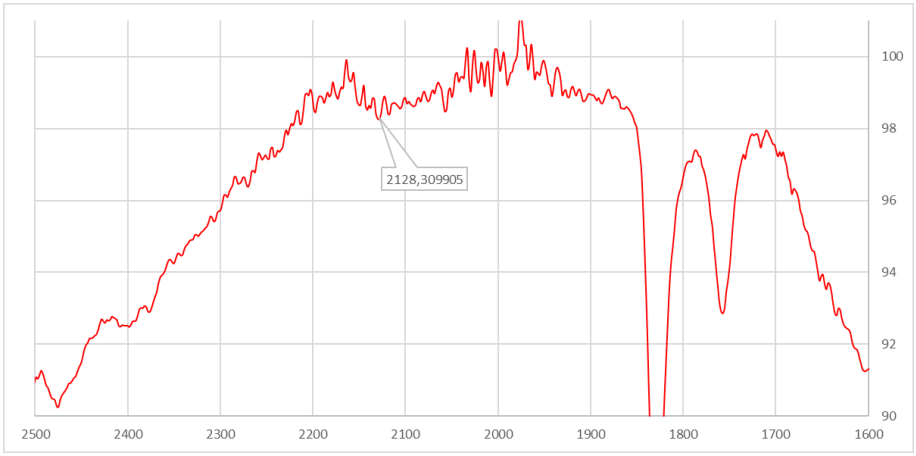

Figure 23. ATR IR spectrum of a diluted sample of the acyl chloride over which diisopropylethyamine has been added.

These observations are in agreement with the formation of **27** with all the bases tested if one assumes that the presence of solid is due to a polymerization induced by the ketene. Although the IR data confirms the presence of a peak attributable to the ketene **27** at 2150 cm^{-1} (very clear when using Et_3N), all other characterization methods failed due to rapid conversion to the insoluble solid.

3.2.6. Final scale-up and optimization of the amidation reaction

All the above findings brought us to explore other potentially milder coupling methods to carry out the amidation. As explained above, the epimerization occurs when the transformation is performed with Et_3N, with a minimum of 10% formation of *meso* **26** and also the *S,S* enantiomer of the pre-catalyst **17**. The impact on the enantiopurity of the pre-catalyst is massive, going down to even less than 10% *ee* (Table 6, entry 1).

The usual coupling agents used in peptide synthesis such as HBTU or EDC resulted either in significant epimerization (HBTU, Table 6 entry 2) or no reaction (EDC/HOBT, Table 6 entry 3).

Finally, the best solution was found by simply removing triethylamine and using a larger excess of the diisopropylamine (Table 6 entry 4). Considering the results described in the previous section, when submitting the reaction only to diisopropylamine, the solution did not seem to form the hypothesized ketene **26** (Scheme 92a). Instead, the reaction from **12** to **17** proceeded smoothly with only a slight decrease in yield. When submitting diacid **13** to the same conditions, the same effect in the *ee* of the pre-catalyst was observed, as (*R*,*R*)-**18** was obtained in >99% *ee* without significant drop in the yield.

Although the basicity of triethylamine and diisopropylamine are very similar, it would appear that the reaction rate towards nucleophilic amidation is much faster than proton abstraction in the absence of a tertiary amine base.[190]

When 4.5 equivalents of diisopropylamine were used, the reaction was finished within 30 mins and showed virtually no epimerization. The *ee* of the pre-catalyst **17** and **18** went up to more than 99%, thus fulfilling one of the main points of the scale-up of these compounds.

Table 6. Optimization of the amidation reaction

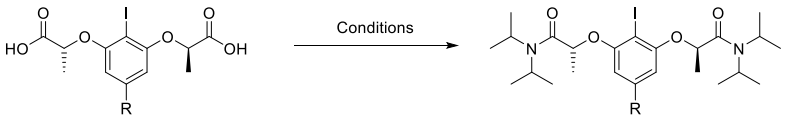

12 R = H
13 R = Me

17 R = H
18 R = Me

Analyzed by SFC

Entry	Compound	Conditions	Yield	*ee* (%) of (*R,R*) **17** or **18**
1	**17**	Et_3N, DIPA, DCM	99%	8% (29.6% *R,R*/49% **27**/21.4% *S,S*)
2	**17**	HBTU, DIPA, DCM	84%	10% (30% *R,R*/50% **27**/20%
3	**17**	EDC, HOBT, DIPA, DCM	-	-
4	**17**	DIPA, DCM	76%	>99% *R,R*
5	**18**	DIPA, DCM	90%	>99% *R,R*

In the case of pre-catalyst **16**, another peak, of about 5% integral was also detected in 20g-scale batches. One could easily think that the *meso*-compound analogous to **26** (**28**, Figure 24) cannot be avoided in this case, but the analytical data does not agree with this hypothesis. After suppressing pyridine and using only 2,6-diisopropylamine as both nucleophile and base, this second peak was still observed by SFC.

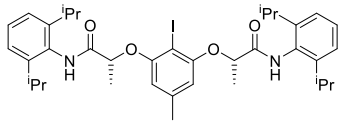

28

Figure 24. Meso compound from pre-catalyst **16**

After injecting the sample 16 along with a mixture synthesized with racemic lactate (containing **28**, **16** and ***ent*-16**) in the SFC, it became clear that the peak observed did not correspond to compound **28**. As it can be observed in figure 25, four peaks appeared in the SFC chromatogram of this mixture.

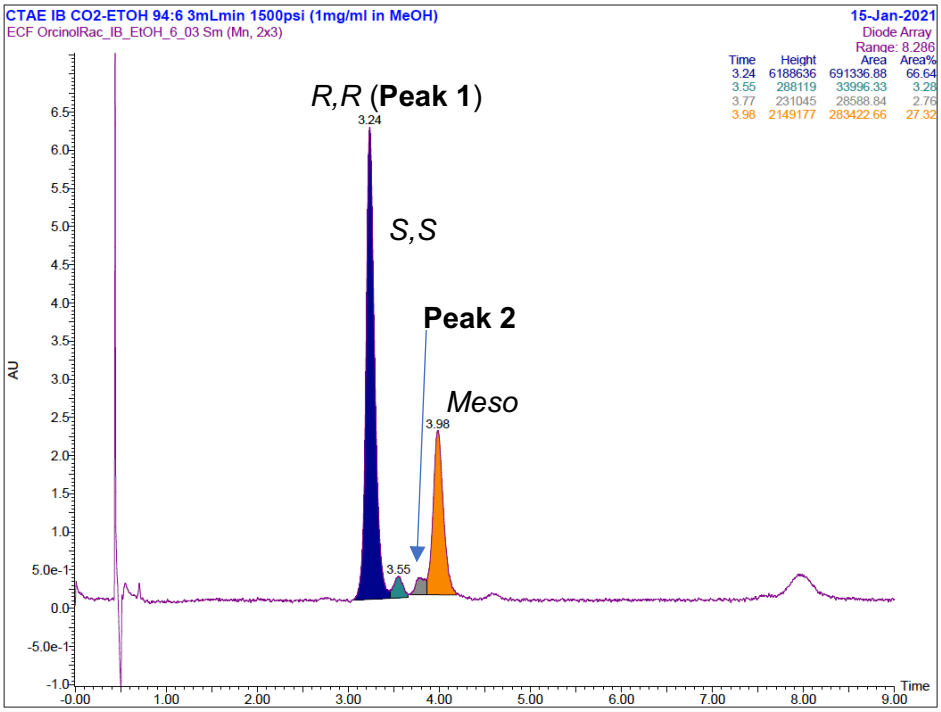

Figure 25. Chiral SFC of the mixture of (R,R)-**16** + pre-catalyst **16** formed from racemic methyl lactate

A chiral semi-preparative HPLC was performed in order to separate both peaks and proceed to its full analysis. Both compounds could be isolated, providing one single peak when reanalyzed by chiral SFC.

When submitted to nominal mass analysis, both peaks showed the same mass, indicating that peak 2 was an isomer of the catalyst.

We initially thought that either an iodine-regioisomer or a double-iodinated species could be present, so a crystallization of the iodination step was performed to provide pure monoiodinated compound **3c'**, and the

synthesis of the catalyst was repeated (Scheme 95). We ruled out these possibilities, as the peak 2 was still present in the final compounds' SFC analysis.

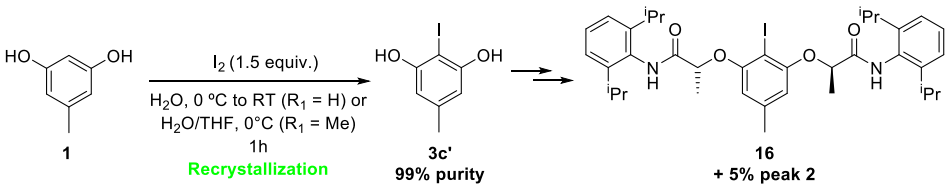

Scheme 95. Recrystallization of **3c'** also led to formation of a second peak in the SFC of **16**

When NMR analysis of both peaks was performed, a clear splitting of some signals was observed, both in ^{1}H and ^{13}C NMR (Scheme 26).

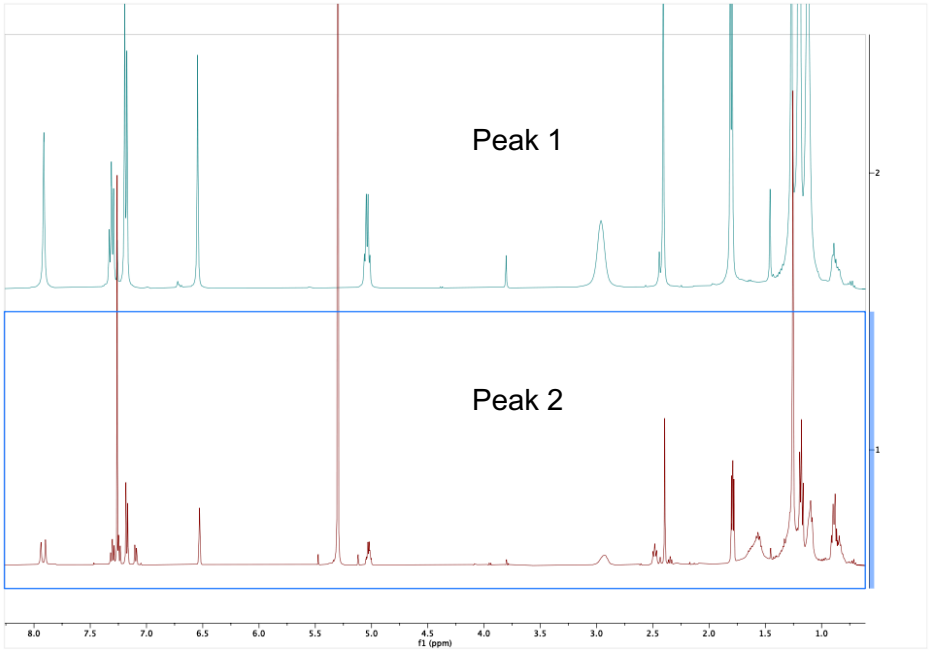

Figure 26. ^{1}HNMR of the two SFC peaks. Top: **16**, bottom: Peak 2

As widely known, secondary amides may have *E*/*Z* forms (Figure 27), so we performed a coalescence NMR experiment by warming both compounds independently (**16** and **16'**).

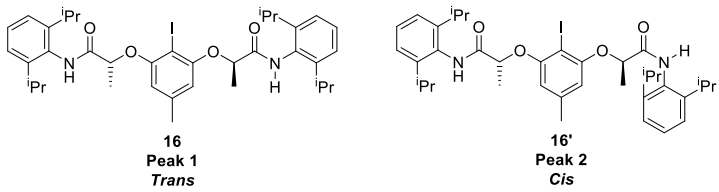

Figure 27. Cis- and Trans-amides of the pre-catalyst **16**

The signals of both compounds tended to coalescence into the same signals (Figure 28), which suggested that we were correct in our hypothesisthat this is a case of *E*/*Z* rotamers at the amide. For full details see experimental section.

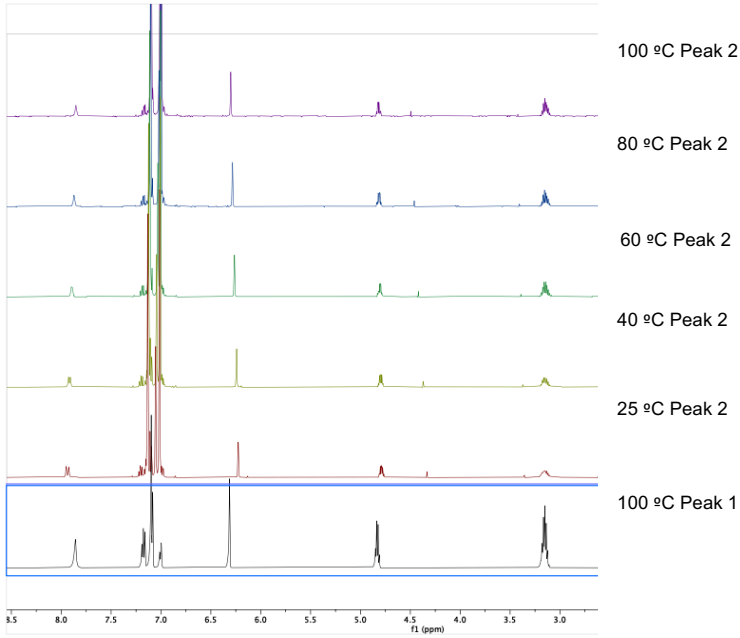

Figure 28. View of the ^{1}H NMR spectra (2.5-8.5 ppm) of the Peak 2 increasing from 25 to 100 ºC, and Peak 1 (catalyst **16**, *R,R)* at 100°C (bottom) showing the tendency to coalescence in one unique compound

Therefore, in this case one can consider that no *meso* **28** is formed using pyridine, taking into account that the only peak formed is **16'**.

In any case, the suppression of pyridine as a base in the synthesis of **16** and the exclusive use of 2,6-diisopropylaniline as both base and nucleophile gives a yield of 90% in the amidation reaction. The yield using 4.0 equivalents of pyridine and 4.0 of 2,6-diisopropylaniline is 87%,[134] which already represents an advantage from the point of view of atom economy but also in the reaction's price tag.

Taking all of this into account, the optimized and scaled procedure for the synthesis of Ishihara-Muñiz pre-catalysts is depicted in Scheme 96, with all the major changes to the procedure.

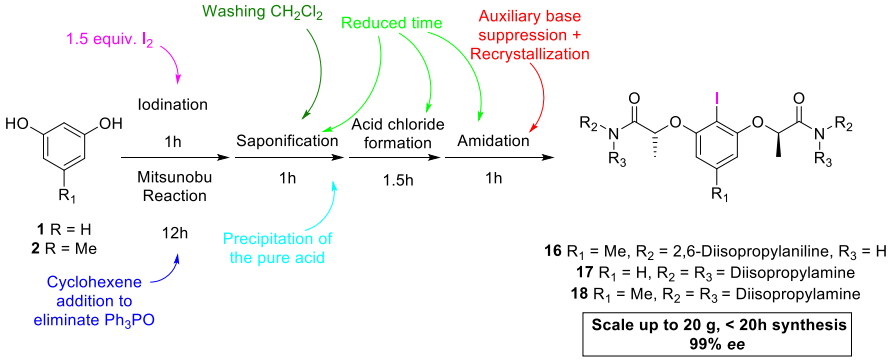

Scheme 96. Variation of the procedures to make possible the scale-up of **16**-**18**

As for the total yields, they were re-calculated after the modifications of the reactions (Scheme 97). The global yields went up from a minimum of 34 to a minimum of 63% total yield, showing the efficiency of the new upscaled method to obtain **16-18**. In the case of the acids **12-13**, the yields were 88% and 70% for small scale respectively, making it around 20% higher employing our new protocol.[134]

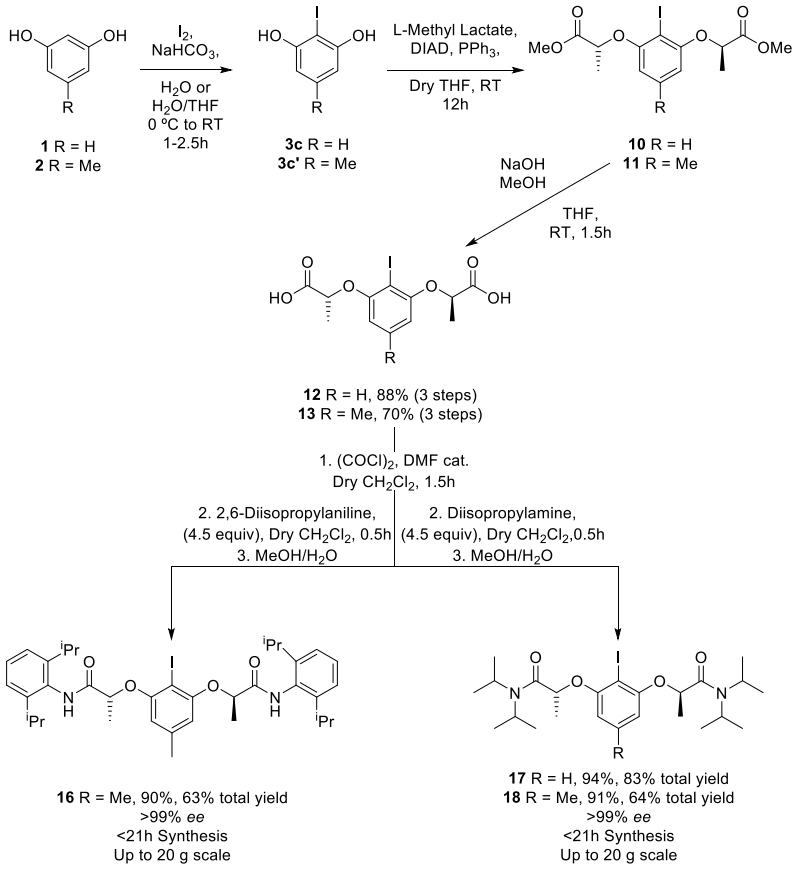

Scheme 97. Final upscaled procedure for the synthesis of **16-18**

3.2.7. Substrate scope

With this improved and scalable procedure at hand, we set out to try once again our catalysts and compare their performance with the already published results.[112,134] Firstly, we applied the Ishihara-Muñiz catalyst to the well-known diacetoxylation (Scheme 98), with a similar activity as when using a smaller-scale synthesis for the pre-catalysts. The diacetoxylated styrene **30** was converted to the free diol **31** in order to measure the *ee*.

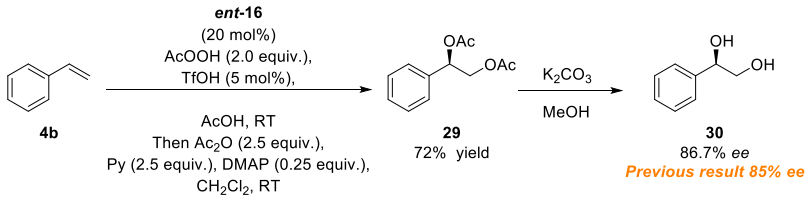

Scheme 98. Diacetoxylation performed with the upscaled batch of ***ent*-16**

Secondly, a intermolecular dearomatization reaction was also performedwhere the catalyst **11** from the upscaled batch showed the same catalytic activity as what was previously reported (Scheme 99).

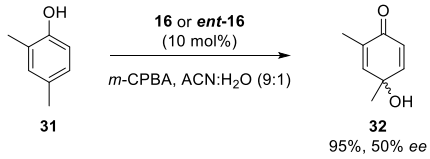

Scheme 99. Intermolecular dearomatization of **31**

Therefore, the new procedure provides a catalyst with at least the same performance than the originally reported small-scale one but benefitting from great synthetic simplification and allowing multigram (30 mmol) access to this catalyst.

Next, catalysts **17** and **18** were tried for the diamination reaction, using *m*-CPBA and $HNMs_2$ as oxidant and nucleophile, respectively (Scheme 100). To our delight, the diamination enantioselecitivity of naked styrene (**20a**) was >99% *ee* with a similar yield as previously observed. This is the first

time the Muñiz diamination has achieved the 99% *ee* milestone, with the previously reported enantioselectivity being 94%. We turned our attention to other previously reported diaminations to form compounds **20b** and **20c** where lower-than-optimal enantioselectivities had been previously reported. Both presented an improved enantioselectivity showing more than 99.0% *ee.* This is a general feature of the catalyst produced with this new, scalable route.

We hypothesize that this is a result of the complete removal of the *meso*-form from the catalyst. Thus, it might be possible that the presence of the *meso*-isomer had gone unnoticed when **17** and **18** were synthesized at smaller scale.

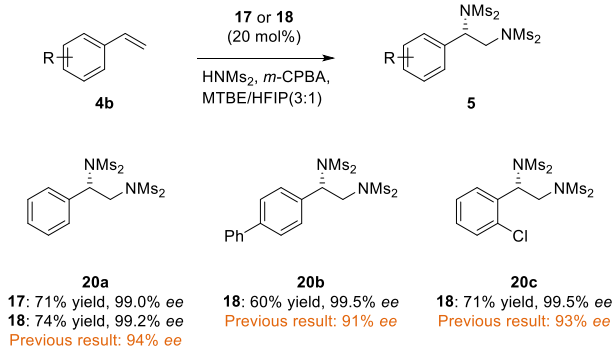

Scheme 100.

Additionally, catalyst **17**, derived from cheaper starting material resorcinol **8**, showed not only similar yield but as well the same increase in *ee*, making it worth to be included as an equally effective catalyst for this reaction.

3.3. Conclusions

In conclusion, a scale-up and optimization for the formation of three different aryliodine precatalysts has been performed, leading to an overall increased yield and shorter reaction times. Additionally, this synthesis has been made more industry-friendly, as all the time-consuming columns and purifications have been removed. All three catalysts **16**-**18** have been synthesized in higher yield than previously reported, and in a 20g scale.

For Ishihara−Muñiz precatalyst **16**, two reactions were reproduced in yield and *ee*, showing the validity of the new synthesis. A previously unknown *Z*-rotamer of the pre-catalyst has been identified by NMR and Mass spectrometry.

For Muñiz pre-catalysts **17** and **18**, upscaling involved variable levels of epimerization, as confirmed by the isolation and independent synthesis of the previously unknown *meso* pre-catalysts.

Because the synthetic route followed is the same as in the previously reported small scale preparations, it can be assumed that the formation of the *meso* compounds could also have taken place to some extent in those cases.

Once the origin of said epimerization was identified and an alternative synthesis was put in place to successfully avoid it, enantiomerically pure catalysts **17** and **18** could be synthesized. They showed improved, exquisite levels of enantioselectivity (99.0−99.5% ee) in the diamination reaction of originally somewhat problematic styrenes **20**.

The importance of reaching high levels of *enantiopurity* in aryliodine(I) pre-catalysts is clear at the end of this work, as the impact it could have on other reactions is unknown. For the diamination reaction, the maximum *ee* gained was around 8.5%, but other catalytic contexts may have much different stereochemical outcomes if the pre-catalyst is synthesized in >99% *ee*.

3.4. Experimental part

3.4.1. General Remarks

All solvents, reagents and all deuterated solvents were purchased from Merck, Fluorochem, Acros and TCI commercial suppliers, and used as received unless otherwise stated. Column chromatography was performed with silica gel (Merck, type 60, 0.063-0.2 mm). NMR spectra were recorded on a Bruker Avance 300 MHz, 400 MHz or 500 MHz spectrometer, respectively. All chemical shifts in NMR experiments were reported as ppm downfield from TMS. The following calibrations were used: The following calibrations were used: $CDCl_3$ δ = 7.26 and 77.16 ppm, DMSO-d6 δ = 2.50 and 39.52 ppm. MS (ESI-LCMS) experiments were performed using an Agilent 1100 HPLC with a Bruker micro-TOF instrument (ESI). A Supelco C8 (5 cm x 4.6 mm, 5 µm particles) column was used with a linear elution gradient from 100% H_2O (0.5% HCO_2H) to 100% MeCN in 13 min at a flow rate of 0.5 mL/min. HRMS measurements were performed on a UHPLC-MS-QqTOF (MaXis Impact, Bruker Daltonics) or HPLC-MS-TOF (MicroTOF II, Bruker Daltonics) within the ICIQ service department. IR spectra were taken in a Bruker Alpha instrument in the solid state. Ketene formation and detection experiments were conducted on a Cary 630 FTIR ATR instrument from Agilent Technologies. Specific optical rotation values were measured with a Polarimeter JascoP1030 equipped with a 100 mm cell. HPLC measurements were carried out on a Knauer Wellchrome (injection valve A0258, pump K-100, solvent organizer K-1500, UV-detector K-2600, detection at 220 or 254 nm) or on a Waters ACQUITY UPC2 SYSTEM (PDA photodiode array detector). The respective chiral stationary phase and exact conditions are specified for each individual compound within the

compound characterization section. Thin layer chromatography (TLC) was carried out using Merck TLC Silicagel 60 F254 aluminum sheets; components were visualized by UV light (λ = 254 nm) and stained with permanganate dip. HPLC to follow reactions was performed on a Agilent 1100 series, using a Luna 2 C18 column from Phenomenex, eluting with a gradient of water:acetonitrile containing 0.1% of formic acid as mobile phase.

3.4.2. Synthesis of Aryliodine Catalysts 16, 17 and 18 at 1 g scale

Published procedures were followed for the synthesis of the precatalysts **16**, **17** and **18**, starting from resorcinol (**8**) or orcinol (**9**). Spectroscopic data of the final compounds and intermediates are in agreement with the reported data.[134,135]

3.4.3. Quest for *meso* formation

While analyzing the final catalysts to determine their enantiomeric excess, we noticed that there was a significant amount of epimerization occuring, leading to formation of the *meso* form (and some of the *S*,*S* enantiomer) during the synthesis of the catalyst.

Natural L-(*S*)-methyl lactate used during this synthesis has an *ee* of 99.6%.

Mitsunobu reaction

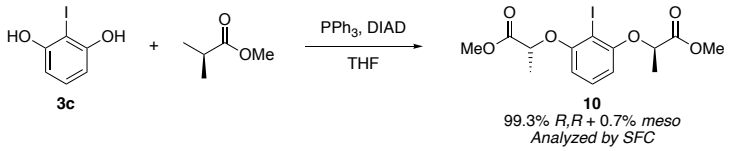

99.3% *R,R* + 0.7% *meso*
Analyzed by SFC

SFC (IB, CO_2/Ethanol = 90/10, flow rate = 3 mL/min, I = 240 nm) T_R = 0.92 min (*S*,*S*), 1.03 (*Meso*), 1.15 min (*R*,*R*).

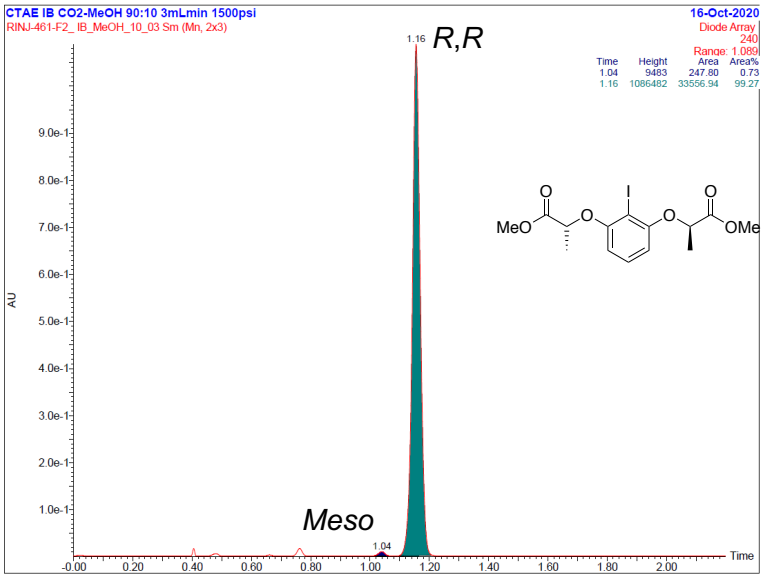

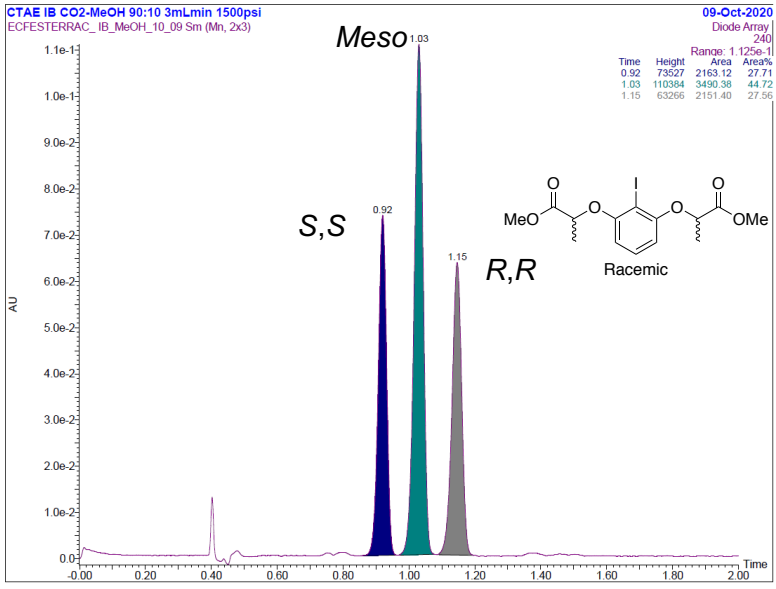

Saponification reaction

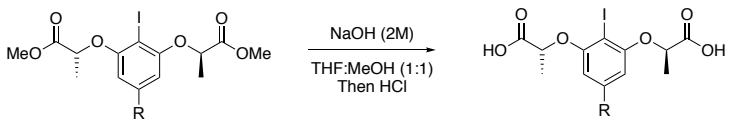

10
99.3% *R,R* + 0.7% *meso*

12
99.7% *R,R* + 0.3% *meso*

HPLC (IJ, ethanol/*n*-hexane/TFA = 80/20/1, flow rate = 1 mL/min, l = 254 nm) T_R = 6.67 min (*Meso*), 8.20 (*S*,*S*), 14.08 min (*R*,*R*).

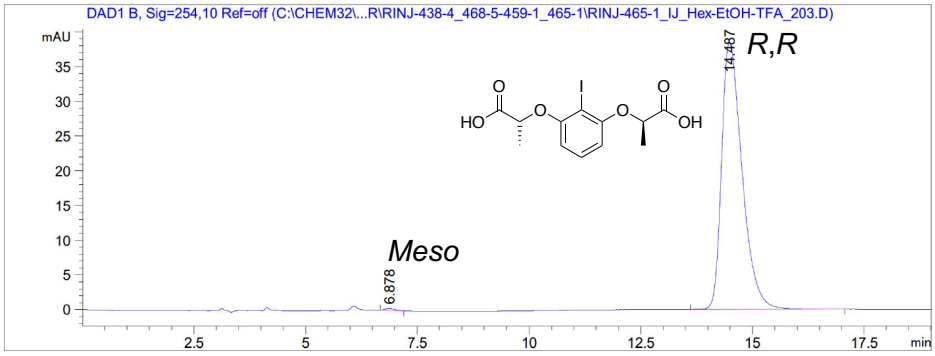

Peak #	RetTime [min]	Type	Width [min]	Area [mAU*s]	Height [mAU]	Area %
1	6.878	BB	0.1890	4.01721	3.23268e-1	0.3259
2	14.487	BB	0.4890	1228.72083	38.43350	99.6741

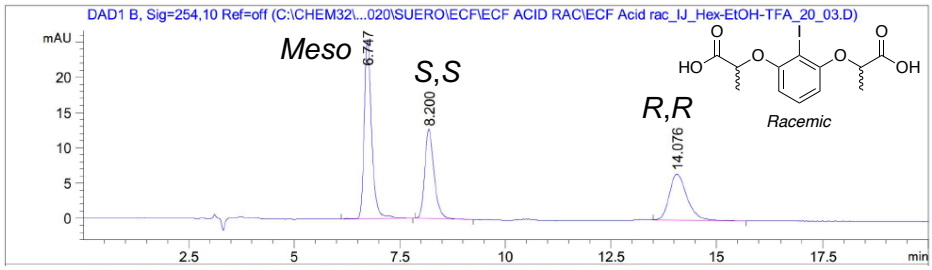

Peak #	RetTime [min]	Type	Width [min]	Area [mAU*s]	Height [mAU]	Area %
1	6.747	BB	0.2267	309.52878	24.62035	44.7953
2	8.200	BB	0.2440	193.46899	12.53876	27.9990
3	14.076	BBA	0.4475	187.98714	6.53619	27.2057

Amidation reaction

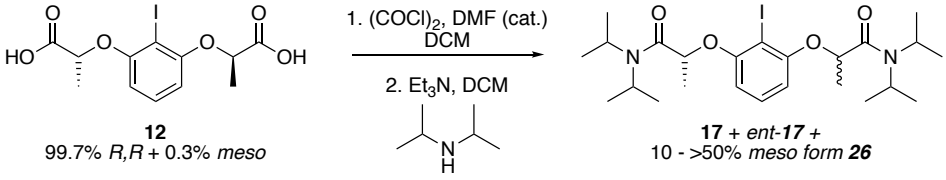

12
99.7% *R,R* + 0.3% *meso*

17 + *ent-**17*** +
10 - >50% *meso form **26***

SFC (ID, CO_2/Ethanol = 90/10, flow rate = 3 mL/min, l = 210 nm) T_R = 2.58 min (*R*,*R*), 2.97 (*meso*), 3.42 (*S*,*S*).

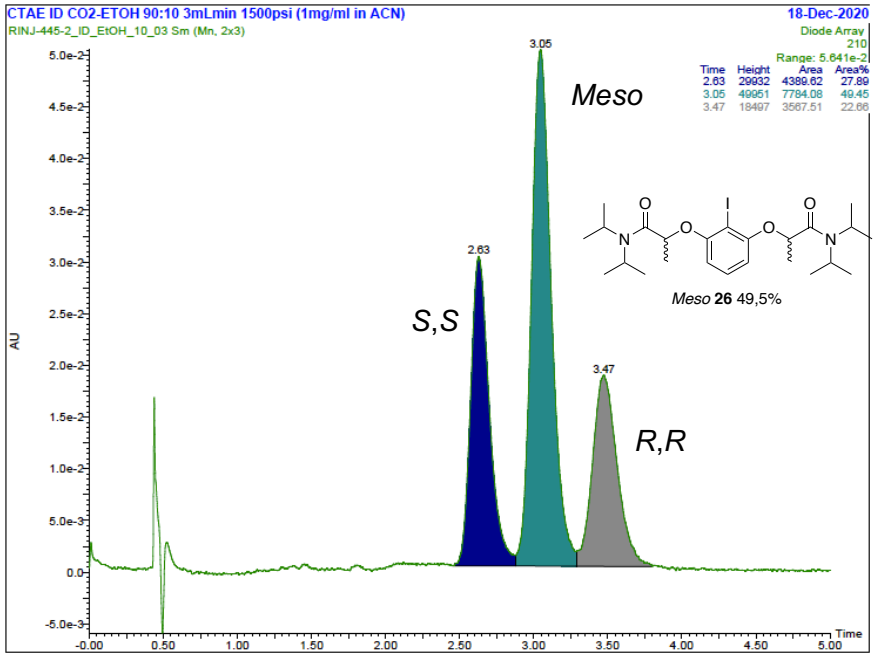

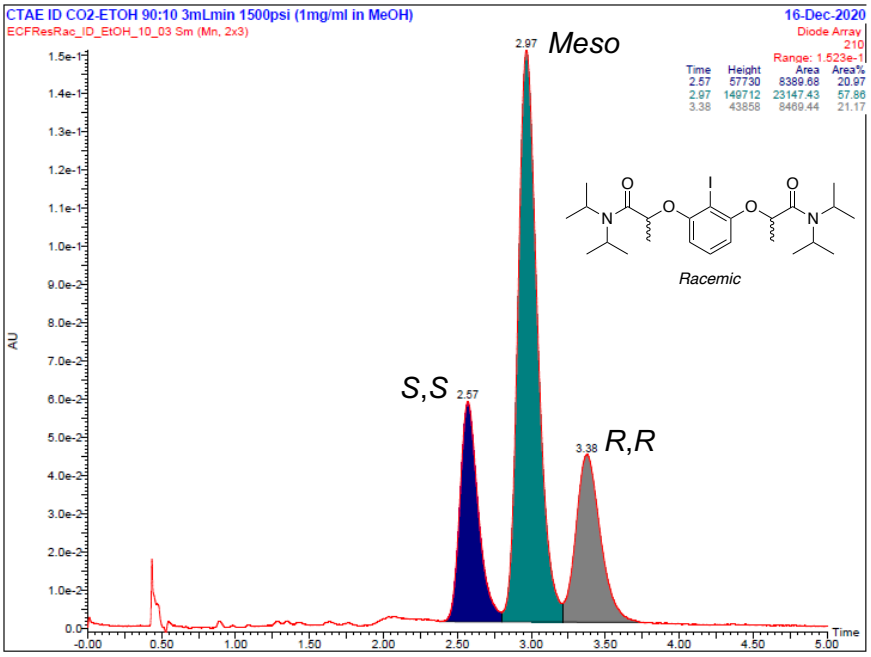

3.4.4. Synthesis of *meso* form 26

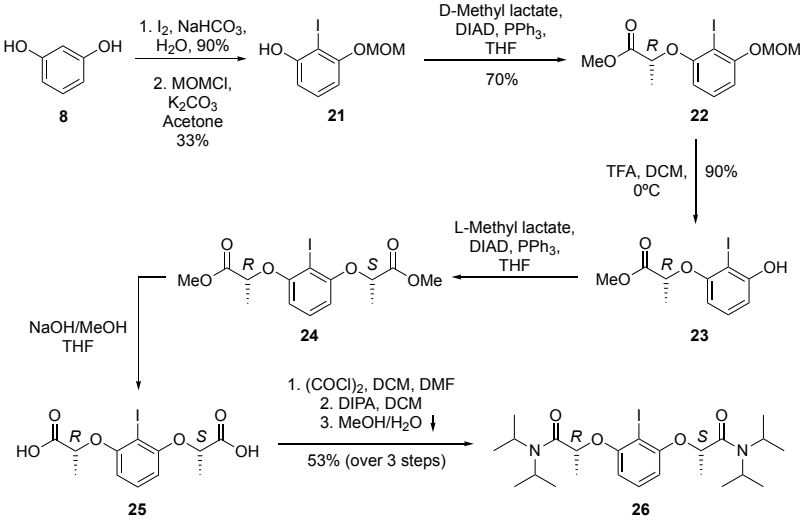

2-Iodo-3-(methoxymethoxy)phenol (21)

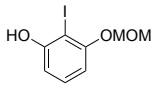

Following an adapted described procedure, MOMCl (1.26 mL, 15.35 mmol, 1.2 equiv.) was added to a stirred solution of 2-iodoresorcinol **1** (3.02 g, 12.78 mmol, 1.0 equiv.) and K_2CO_3 (2.30 g, 16.61 mmol, 1.3 equiv.) in acetone (31.5 mL) at room temperature and the resulting mixture was stirred at the same temperature for 24 h. The reaction was quenched by addition of H_2O and extracted with EtOAc, then dried over Na_2SO_4. After filtration and evaporation of the solvent under reduced pressure, the crude was purified by flash column chromatography (silica gel, hexane:EtOAc = 3:1, v/v) to give phenol **21** (1.61 g, 5.74 mmol, 33% yield). All analytical data matched the reported values.[191]

^{1}H-NMR (300 MHz, Chloroform-*d*): *δ* 7.16 (t, *J* = 8.2 Hz, 1H), 6.70 (dd, *J* = 8.2, 1.3 Hz, 1H), 6.62 (dd, *J* = 8.2, 1.3 Hz, 1H), 5.49 (s, 1H), 5.24 (s, 2H), 3.51 (s, 3H) ppm.

^{13}C-NMR (75 MHz, Chloroform-*d*): *δ* 156.7, 156.3, 130.3, 108.8, 106.7, 95.1, 79.6, 56.6 ppm.

Methyl (*R*)-2-(2-iodo-3-(methoxymethoxy)phenoxy)propanoate (22)

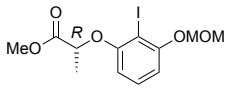

According to the reported procedure, DIAD (1.1 mL, 5.5 mmol, 1.3 equiv.) was added to a stirred solution of **21** (1.20 g, 4.3 mmol, 1.0 equiv.), Ph_3P (1.35 g, 5.1 mmol, 1.2 equiv.), and L-(*S*)-methyl lactate (0.446 mL, 4.7 mmol, 1.1 equiv.) in anhydrous THF (22 mL) at 0 °C and the resulting mixture was stirred at room temperature for 72 h. After evaporation of the solvent under reduced pressure, chiral ester **22** (1.13 g, 3.1 mmol, 70%

yield) was obtained as a crude product. All spectral analysis matched the reported data.[188]

^{1}H-NMR (400 MHz, Chloroform-*d*): δ 7.17 (t, J = 8.3 Hz, 1H), 6.74 (dd, J = 8.3, 1.1 Hz, 1H), 6.39 (dd, J = 8.3, 1.1 Hz, 1H), 5.24 (d, J = 0.9 Hz, 2H), 4.77 (q, J = 6.8 Hz, 1H), 3.75 (s, 3H), 3.51 (s, 3H), 1.70 (d, J = 6.8 Hz, 3H) ppm.

^{13}C-NMR (101 MHz, Chloroform-*d*): δ 172.3, 158.1, 157.8, 129.8, 108.7, 107.1, 95.2, 80.8, 74.4, 56.6, 52.5, 18.8 ppm.

Methyl (*R*)-2-(3-hydroxy-2-iodophenoxy)propanoate (23)

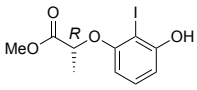

Following an adapted procedure, to a stirred solution of **22** (1.107 g, 3.0 mmol, 1.0 equiv.) in CH_2Cl_2 (30 mL) at 0 °C was slowly added TFA (1.15 mL, 15 mmol, 5.0 equiv.) and the resulting mixture was stirred at the room temperature for 5 h. The reaction was quenched by addition of H_2O and extracted with CH_2Cl_2, then dried over Na_2SO_4. After filtration and evaporation of the solvent under reduced pressure, the residue was purified by purified by flash column chromatography (silica gel, hexane:EtOAc = 4:1, v/v) to give phenol **23** (1.61 g, 5.74 mmol, 90% yield). All analytical data matched the reported values.[188]

^{1}H-NMR (300 MHz, Chloroform-*d*): δ 7.13 (t, J = 8.2 Hz, 1H), 6.68 (dd, J = 8.2, 1.2 Hz, 1H), 6.24 (dd, J = 8.2, 1.2 Hz, 1H), 5.47 (s, 1H), 4.78 (q, J = 6.8 Hz, 1H), 3.75 (s, 3H), 1.69 (d, J = 6.8 Hz, 3H).

^{13}C-NMR (126 MHz, Chloroform-*d*): δ 172.2, 157.3, 156.6, 130.3, 108.8, 104.8, 79.5, 74.2, 52.6, 18.7.

Methyl (*S)-2-(2-iodo-3-(((*R**)-1-methoxy-1-oxopropan-2-yl)oxy)phenoxy)propanoate (24)**

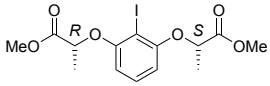

The same procedure as for molecule **22** was followed: DIAD (0.7 mL, 3.5 mmol, 1.3 equiv.) was added to a stirred solution of **23** (0.874 g, 2.7 mmol, 1.0 equiv.), Ph_3P (0.854 g, 3.2 mmol, 1.2 equiv), and methyl L-(*S*)-methyl lactate (0.29 mL, 3 mmol, 1.1 equiv.) in anhydrous THF (13.5 mL) at 0 °C and the resulting mixture was stirred at the room temperature for 72 h. After evaporation of the solvent under reduced pressure, the crude was used in the next reaction after precipitating most part of the PPh_3O with a 10:1 Cy-hex:EtOAc mixture.

(*S)-2-(3-((*R**)-1-carboxyethoxy)-2-iodophenoxy)propanoic acid (25)**

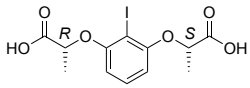

To a solution of **24** (0.564 g, 1.5 mmol, 1 equiv.) in THF (4 mL), a solution of sodium hydroxide (0.32 g, 4 mL, 2 molar, 3.73 equiv., 5.5 mmol) in MeOH (4 mL) was added, and the mixture was stirred for 0.5 h at 25 °C. Then, the organic solvents were removed under reduced pressure. The aqueous phase was washed with CH_2Cl_2 to remove PPh3O and some DIAD-H_2 and acidified with HCl 3M to pH 1. After that, the acidified phase was extracted with CH_2Cl_2 to give **25** + DIAD-H_2. The product was dried and evaporated to give crude **25** that was used in the following reaction without further purification.

(*S)-2-(3-(((*R**)-1-(diisopropylamino)-1-oxopropan-2-yl)oxy)-2-iodophenoxy)-*N*,*N*-diisopropylpropanamide (26)**

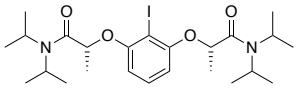

Following an adapted procedure, diacid 25 (0.564 g, 1 equiv., 1.5 mmol) was suspended in dry DCM (mL). After addition of oxalyl dichloride (0.947 g, 0.64 mL, 3.5 equiv., 5.25 mmol) and a catalytic amount of DMF the reaction mixture was stirred for 1.5 h at 25 °C and then concentrated in the rotavap. The crude product was re-dissolved in dry DCM (3.75 mL) followed by addition of diisopropylamine (0.687 g, 0.95 mL, 4.5 equiv., 6.75 mmol). The reaction mixture was stirred for 30 min at 25 °C and quenched by addition of aqueous HCl 3M (2 mL).

A solvent swap was carried out by adding 100 mL of MeOH and evaporating the DCM on the rotavap. A total of 50 mL of water were added to precipitate all of **26** after which it was isolated by filtration and washing with 50 mL of 2:1 MeOH:water. The final product was further dried overnight under vacuum at 50°C to give **26** as a white solid (0.790 g, 97% isolated yield). Crystallisation was achieved overnight by slow addition of 0.4 mL H_2O in 5 mL MeOH. SFC injection confirmed the stereochemical identity of **26** in our pre-catalyst **17**, with >99% enantiopurity.

HRMS (m/z): $[M+H]^+$ calcd for $C_{24}H_{40}IN_2O_4$, 547.2027; found, 547.2029.

$[\alpha]_D$ ^{25}: 0 (C = 1.00, $CHCl_3$)

^{1}H-NMR (500 MHz, Chloroform-*d*): δ 7.16 (t, *J* = 8.3 Hz, 1H), 6.56 (d, *J* = 8.3 Hz, 2H), 4.86 (d, *J* = 6.9 Hz, 2H), 4.55 (p, *J* = 6.6 Hz, 2H), 3.33 (p, *J* = 6.8 Hz, 2H), 1.69 (d, *J* = 6.9 Hz, 6H), 1.44 (d, *J* = 6.7 Hz, 6H), 1.32 (d, *J* = 6.8 Hz, 6H), 1.21 (d, *J* = 6.7 Hz, 6H), 0.93 (d, *J* = 6.5 Hz, 6H).

^{13}C-NMR (126 MHz, Chloroform-*d*): δ 169.7, 158.0, 130.1, 106.2, 78.0, 77.36, 47.8, 46.6, 21.0, 20.7, 20.6, 20.1, 18.1.

SFC (IC, CO_2/Isopropanol = 75/25, flow rate = 3.0 mL/min, l = 210 nm) T_R = 3.0 min (major).

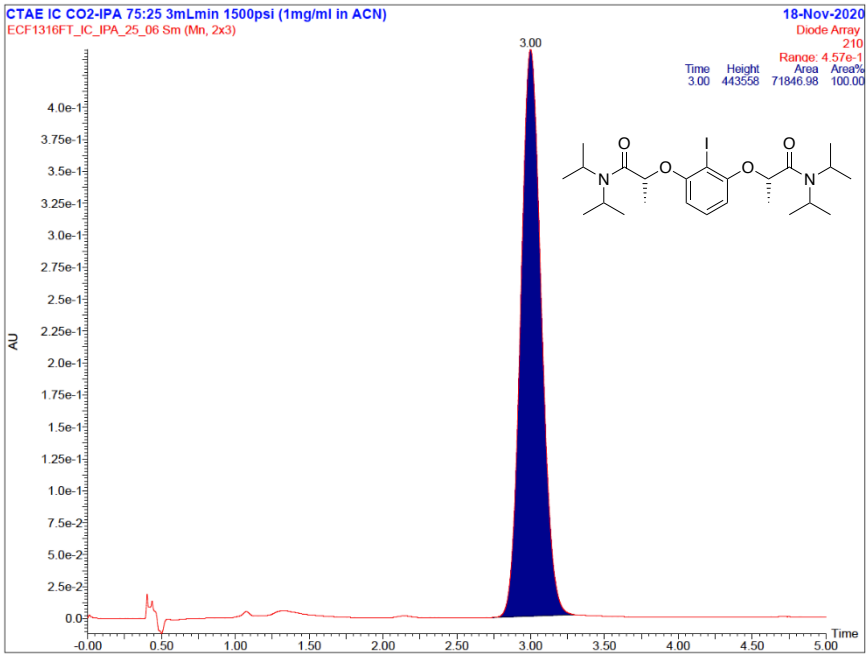

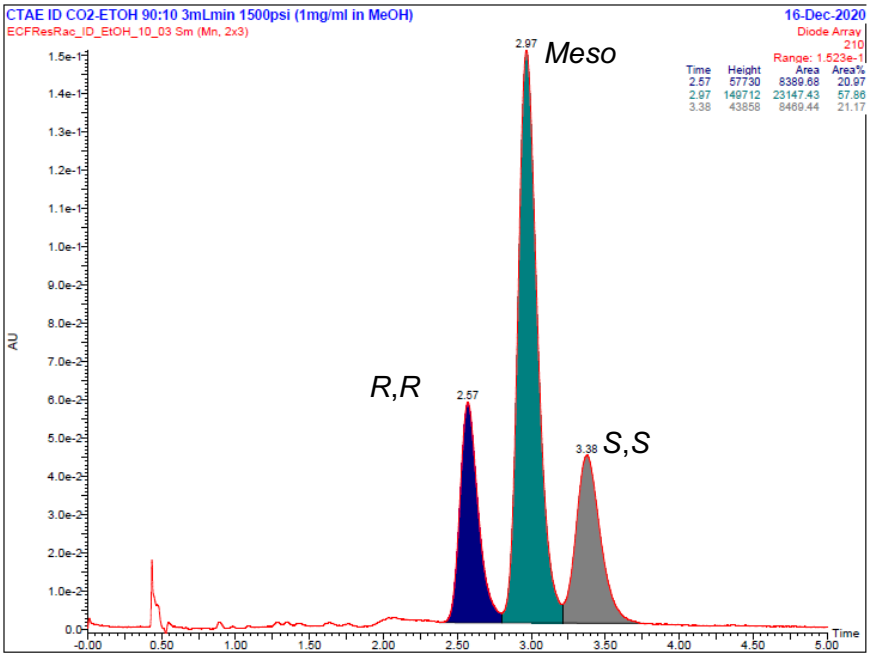

3.4.5. Synthesis of *meso* form 26

X-Ray data for compound 26

Single crystal of **26** were obtained by slow evaporation from a mixture of Methanol$_3$/*n*-hexane at RT. Single-crystal X-ray diffraction data were collected on a Rigaku MicroMax-007HF rotating anode diffractometer equipped with a Pilatus 200K hybrid pixel area detector using graphite-monochromated MoKα radiation (λ = 0.71073 Å) in the scan range 2.665< 2θ < 27.102°. The structure was solved with SIR2019 using the Modern Direct Methods algorithm and refined with SHELXL under the SHELXLE interface. Crystallographic data have been deposited in the Cambridge Crystallographic Data Centre as deposition number CCDC 2070374. Thermal probability ellipsoids are shown at the 50% probability level.

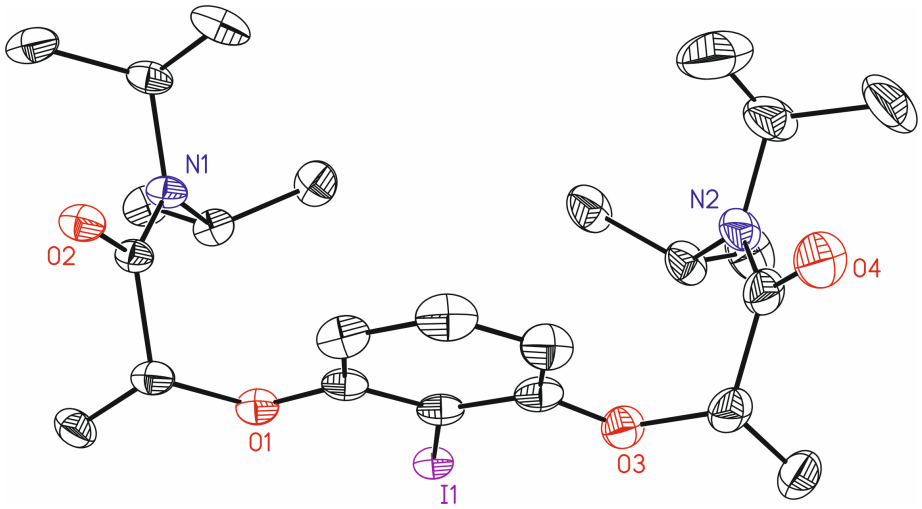

Table 7. Crystal data and structure refinement for CCDC 2070374

Identification code	CCDC 2070374

Empirical formula	C24.25 H41.50 I N2 O5
Formula weight	567.99
Temperature	100(2)K
Wavelength	0.71073 Å
Crystal system	monoclinic
Space group	C 2/c
Unit cell dimensions	a = 14.29958(15)Å α= 90°.
	b = 8.83314(8)Å β = 92.3856(8)°.
	c = 45.8980(4)Å γ = 90°.
Volume	5792.37(9) $Å^3$
Z	8
Density (calculated)	1.303 Mg/m^3
Absorption coefficient	1.138 mm^{-1}
F(000)	2352
Crystal size	0.100 x 0.100 x 0.020 mm^3
Theta range for data collection	2.665 to 27.102°.
Index ranges	-18<=h<=18,-11<=k<=11,-
58<=l<=58	
Reflections collected	83858
Independent reflections	6391[R(int) = 0.0424]
Completeness to theta =27.102°	100.0%
Absorption correction	Multi-scan
Max. and min. transmission	1.00 and 0.70
Refinement method	Full-matrix least-squares on F^2
Data / restraints / parameters	6391/ 32/ 328
Goodness-of-fit on F^2	1.523
Final R indices [I>2sigma(I)]	R1 = 0.0395, wR2 = 0.0741
R indices (all data)	R1 = 0.0400, wR2 = 0.0743

Largest diff. peak and hole	0.711 and -1.368 e.Å^{-3}

3.4.6. Scaled synthesis of Aryliodine catalysts (20 g scale)

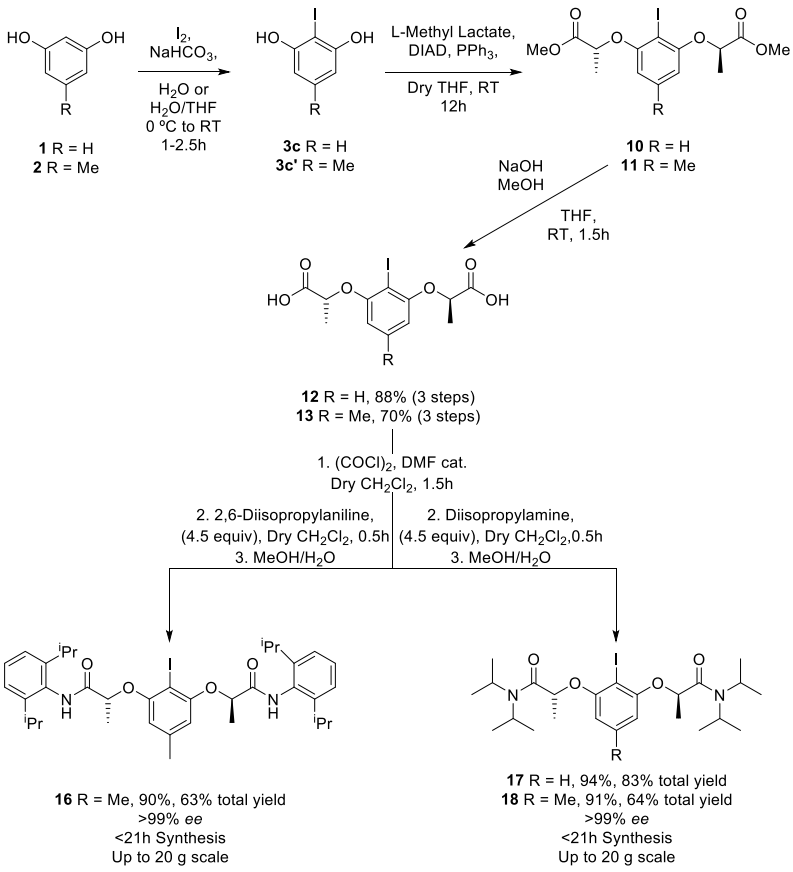

2-Iodobenzene-1,3-diol (3c)

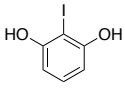

Resorcinol **1** (20.0 g, 181.6 mmol, 1.0 equiv) was dissolved in Water (80 mL). After cooling to 0 °C, diiodine (48.4 g, 190.7 mmol, 1.05 equiv.), was added followed by slow addition of a solution of sodium bicarbonate (16.8 g, , 199.8 mmol, 1.10 equiv.) in water (200 mL) via an addition funnel. After complete addition, the ice bath was removed and the reaction was allowed to warm to room temperature and stirred for an additional 60 min. After about 5 mins after complete addition of bicarbonate the mixture lost

the intense brown/purple color of iodine. The reaction was then quenched by addition of a solution of sodium sulfite (22.9 g, 181.6 mmol, 1.00 equiv.) in water (100 mL). After extraction with EtOAc (2x200 mL), the combined organic phases were washed with brine (50 mL), dried over anhydrous $MgSO_4$ and concentrated under reduced pressure. The final crude after evaporating most of EtOAc contains **3c** + around 7% of resorcinol **1**. Virtually no di- or tri-iodinated species could be detected.

2-iodo-5-methylbenzene-1,3-diol (3c')

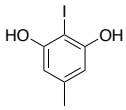

5-methylbenzene-1,3-diol **2** (orcinol; 20.0 g, 161.1 mmol, 1 equiv.) and sodium bicarbonate (40.6 g, 483.3 mmol, 3.0 equiv.) were dissolved in water (275 mL) and THF (80 mL). The mixture was cooled to 0 °C and a solution of diiodine (61.3 g, 241.7 mmol, 1.5 equiv.) in THF (195 mL) was added dropwise during 60 mins. The reaction mixture was further stirred at 0 °C for 60 min and was subsequently diluted with MTBE (160 mL). A solution of sodium sulfite (20.31 g, 161.1 mmol, 1 equiv.) in water (80 mL) was added slowly. The mixture was allowed to warm to room temperature and was stirred for 30 min until the effervescence had ceased. The mixture was extracted with MTBE (2 x 100 mL) and the combined organic phases were dried over MgSO4. The solvent was removed in vacuo.

Dimethyl 2,2'-((2-iodo-1,3-phenylene)bis(oxy))(2*R*,2'*R*)-dipropionate (10)

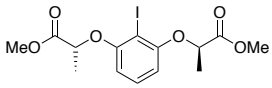

The previously obtained 2-iodobenzene-1,3-diol **3c** crude was divided into two equal portions (of about 80.5 mmol each, 1 equiv.), and each of them was treated with triphenylphosphine (49.1 g, 185 mmol, 2.3 equiv.) and dissolved in dry THF (120 mL) under an argon atmosphere. After addition of L-(*S*)-methyl lactate or D-(*R*)-methyl lactate (18.8 g, 17.3 mL, 177 mmol, 2.2 equiv.), diisopropyl (*E*)-diazene-1,2-dicarboxylate (DIAD; 41.6 g, 40.0 mL, 193 mmol, 2.4 equiv.) was added dropwise while cooling the mixture in a water bath. The water bath was removed and the reaction mixture was stirred for 12 hour hours at 25 °C.

The mixture was concentrated under reduced pressure, and 150 mL of cyclohexane were added to precipitate the PPh_3O, which was removed by filtration. The filtrate was concentrated on the rotavap to reduce the amount of cyclohexane. Crude **10** was used in the next step without purifying or isolating the product. No di- or tri-iodinated species could be detected in the crude.

Dimethyl 2,2'-((2-iodo-5-methyl-1,3-phenylene)bis(oxy))(2*R*,2'*R*)-dipropionate (11)

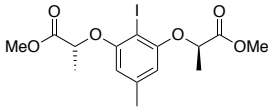

The previously obtained 2-iodo-5-methylbenzene-1,3-diol **3c'** crude was divided into two equal portions (of about 72.5 mmol each, 1 equiv.) and triphenylphosphine (49.1 g, 185 mmol, 2.3 equiv.) were dissolved in dry THF (120 mL) under an argon atmosphere. After addition

of of L-(*S*)-methyl lactate or D-(*R*)-methyl lactate (18.8 g, 17.3mL, 177 mmol, 2.2 equiv.), diisopropyl (*E*)-diazene-1,2-dicarboxylate (41.6 g, 40.0 mL, 193 mmol, 2.4 equiv.) was added dropwise while cooling the mixture in a water bath. The water bath was removed and the reaction mixture was stirred for 12 hour hours at 25 °C.

Full conversion of the starting material was achieved after 16h. The mixture was concentrated under reduced pressure. To this cyclohexane (150 mL) was added, in order to precipitate the PPh_3O, which was removed by filtration. The filtrate was concentrated on the rotavap to reduce the amount of cyclohexane. Crude **11** was directly used in the next step without further purification.

(2*R*,2'*R*)-2,2'-(2-Iodo-1,3-phenylene)bis(oxy)dipropanoic acid (12)

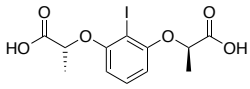

To the previous crude containing **10**, THF (120 mL) was added , followed by MeOH (120 mL) and sodium hydroxide (12.0 g, 150 mL, 2 molar, 300 mmol, 3.73 equiv.) and stirred for 1.5 h at 25 °C. Then, the organic solvents were removed under reduced pressure. The aqueous phase was washed with CH_2Cl_2 to remove PPh_3O and some of the reduced form of DIAD, and acidified with HCl 3M to pH 1. After that, the acidified phase was extracted with CH_2Cl_2 to give **12** contaminated with reduced DIAD. A mixture of 200 mL Cy-Hex:EtOAC 10:1 was added to give a white solid in a slightly yellow solution. The solid was isolated by filtration and washed with fresh Cy-Hex:EtOAc 10:1 (60 mL) to give an off-white powder. The product was further dried under vacuum at 50°C, thus furnishing diacid **12** (30.4 g, 88% isolated yield over 3 steps). All observed signals corresponded with the described ones in the literature.[134]

^{1}H-NMR (400 MHz, DMSO-d_6) δ 13.05 (bs, 2H), 7.21 (t, J = 8.3 Hz, 1H), 6.43 (d, J = 8.4 Hz, 2H), 4.85 (q, J = 6.7 Hz, 2H), 1.55 (d, J = 6.8 Hz, 6H).
^{13}C-NMR (101 MHz, DMSO-d_6) δ 172.7, 157.7, 129.7, 106.0, 79.6, 72.8, 18.3.
$[\alpha]_D^{25}$: -27.0 (C = 1.00 mg/mL, $CHCl_3$, *R*,*R*)

(2*R*,2'*R*)-2,2'-((2-Iodo-5-methyl-1,3-phenylene)bis(oxy))dipropanoic acid (13)

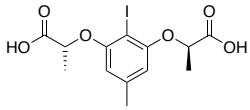

THF (120 mL) was added to the crude containing **11**, followed by MeOH (120 mL) and sodium hydroxide (12.0 g, 150 mL, 2 molar, 300 mmol, 3.85 equiv.). The resulting mixture was stirred for 1.5 h at 25 °C. Then, the organic solvents were removed under reduced pressure. The aqueous phase was washed with CH_2Cl_2 (100 mL) to remove PPh_3O and some of the reduced form of DIAD and acidified with HCl 3M to pH 1. After that, the acidified phase was extracted with CH_2Cl_2 (2x100 mL) to give **13** contaminated with reduced DIAD. Afterwards the crude product was concentrated and a mixture of 400 mL Cy-Hex:EtOAc 10:1 was added to give a pinkish solid in a slightly yellow solution. The solid was isolated by filtration and washed with fresh Cy-Hex:EtOAC 10:1 (60 mL) to give a slightly pink powder. The solid was dried under vacuum at 50°C, to furnish **13** (22.30 g, 70% isolated yield over 3 steps). All observed signals corresponded with the described ones in the literature.[134]
^{1}H NMR (400 MHz, Chloroform-*d*) δ 10.28 (bs, 2H), 6.29 (d, J = 0.8 Hz, 2H), 4.83 (q, J = 6.8 Hz, 2H), 2.30 (d, J = 0.8 Hz, 3H), 1.73 (d, J = 6.9 Hz, 6H).

^{13}C NMR (101 MHz, Chloroform-*d*) δ 175.1, 157.4, 140.9, 108.7, 77.2, 73.9, 22.0, 18.5.

$[\alpha]_D$ ^{25}: -7.0 (C = 1.00 mg/mL, $CHCl_3$, *R*,*R*)

(2*R*,2'*R*)-2,2'-((2-iodo-1,3-phenylene)bis(oxy))bis(*N*,*N*-diisopropylpropanamide) (17)

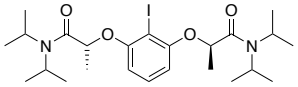

(2*R*,2'*R*)-2,2'-(2-Iodo-1,3-phenylene)bis(oxy)dipropanoic acid **12** or ent-**12** (15.0 g, 39.5 mmol, 1 equiv.), was suspended in anhydrous CH_2Cl_2 (200 mL), followed by oxalyl dichloride (17.5 g, 11.9 mL, 166 mmol, 3.5 equiv.). Then, a catalytic amount of DMF (1-2 drops) is added, observing some gas evolution and progressive dissolution of the solids. The reaction mixture was allowed to stir for 2 hours at 25 °C and then concentrated in vacuo in the rotavap. The crude product was re-dissolved in anhydrous CH_2Cl_2 (100 mL) followed by addition of diisopropylamine (18.0 g, 25.1 mL, 177 mmol, 4.5 equiv.). The reaction mixture was stirred for 30 min at 25 °C and quenched by addition of aqueous HCl 3M (40 mL).

A solvent swap was carried out by adding 200 mL of MeOH and evaporating the CH_2Cl_2 on the rotavap. A total of 100 mL of water were added to precipitate all of **17** after which it was isolated by filtration and washing with 100 mL of 2:1 MeOH/water. The final product was further dried overnight under vacuum at 50°C to give **17** or *ent*-**17** as a white solid (20.29 g, 94% yield).

All analytical data matched the reported values.[135]

^{1}H-NMR (400 MHz, Chloroform-*d*) *δ* 7.12 (t, *J* = 8.3 Hz, 1H), 6.52 (d, *J* = 8.4 Hz, 2H), 4.83 (q, *J* = 6.9 Hz, 2H), 4.53 (m *J* = 6.6 Hz, 2H), 3.30 (p, *J* = 6.8 Hz, 2H), 1.66 (d, *J* = 6.9 Hz, 6H), 1.41 (d, *J* = 6.8 Hz, 6H), 1.28 (d, *J* = 6.7 Hz, 6H), 1.18 (d, *J* = 6.7 Hz, 6H), 0.91 (d, *J* = 6.5 Hz, 6H).

^{13}C-NMR (100 MHz, Chloroform-*d*) δ 169.6, 157.9, 130.0, 106.1, 78.7, 78.0, 47.7, 46.6, 21.0, 20.7, 20.7, 20.0, 18.1.

SFC (ID, CO_2/Ethanol = 90/10, flow rate = 3 mL/min, l = 210 nm) T_R = 2.58 min (*R*,*R*), 2.97 (*meso*), 3.42 (*S*,*S*).

$[\alpha]_D^{25}$: -156.0 (C = 1.00 mg/mL, $CHCl_3$, *R*,*R*)

$[\alpha]_D^{25}$: +162.0 (C = 1.00 mg/mL, $CHCl_3$, *S*,*S*)

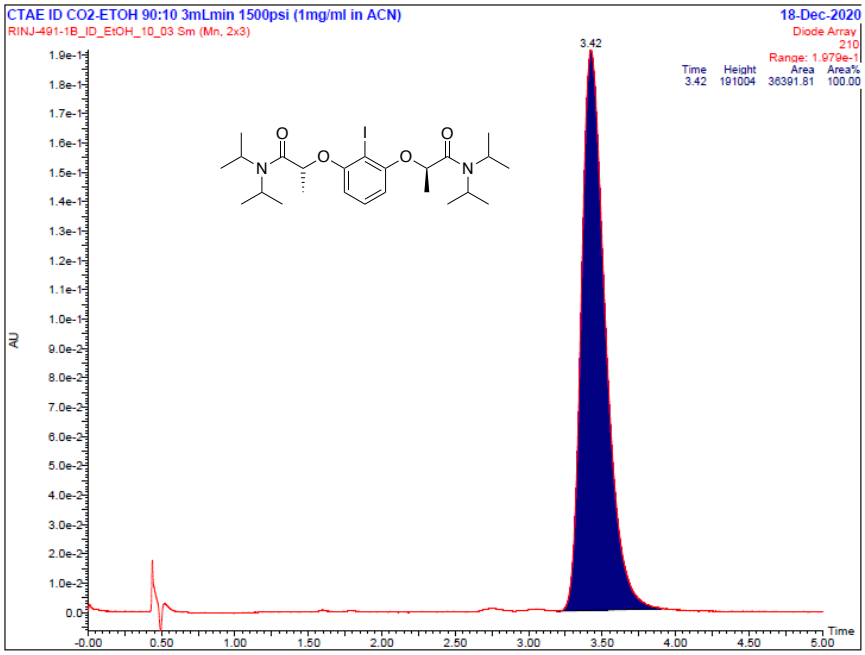

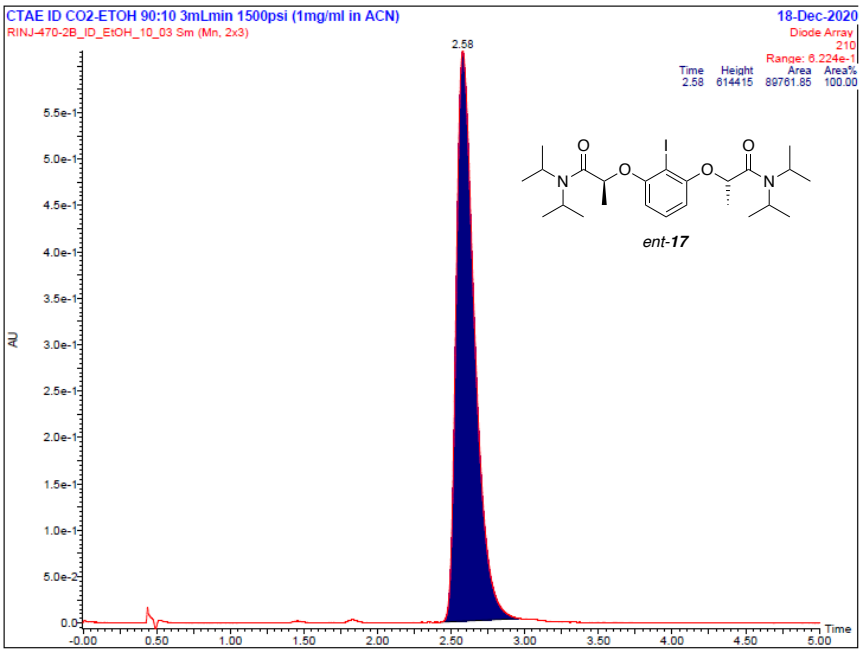
CTAE ID CO2-ETOH 90:10 3mLmin 1500psi (1mg/ml in ACN)
RINJ-470-2B_ID_EtOH_10_03 Sm (Mn, 2x3)
18-Dec-2020
Diode Array
210
Range: 6.224e-1
Time Height Area Area%
2.58 614415 89761.85 100.00
2.58
ent-17
AU
Time

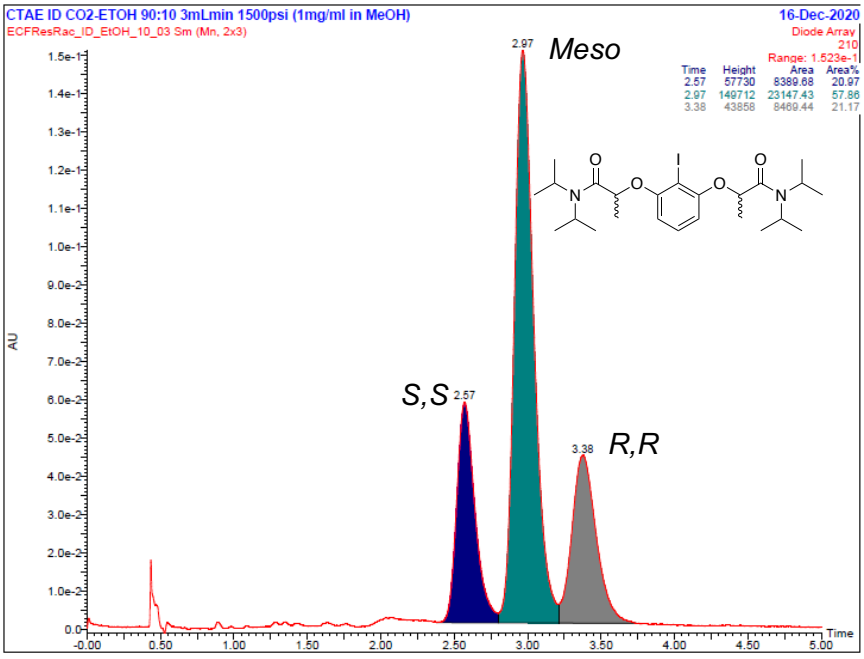
CTAE ID CO2-ETOH 90:10 3mLmin 1500psi (1mg/ml in MeOH)
ECFResRac_ID_EtOH_10_03 Sm (Mn, 2x3)
16-Dec-2020
Diode Array
210
Range: 1.523e-1
Time Height Area Area%
2.57 57730 8389.68 20.97
2.97 149712 23147.43 57.86
3.38 43858 8469.44 21.17
2.97
Meso
S,S 2.57
3.38
R,R
AU
Time

(2*R*,2'*R*)-2,2'-((2-iodo-5-methyl-1,3-phenylene)bis(oxy))bis(*N*,*N*-diisopropylpropanamide) (18)

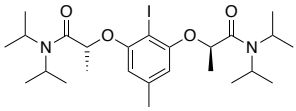

(2*R*,2'*R*)-2,2'-((2-iodo-1,3-phenylene)bis(oxy))dipropionic acid **11** or ***ent*-11** (16.0 g, 40.6 mmol, 1 equiv.), was suspended in anhydrous CH_2Cl_2 (200 mL). After addition of oxalyl dichloride (18.0 g, 12.2 mL, 166 mmol, 3.5 equiv.) and a catalytic amount of DMF the reaction mixture was stirred for 2 hours at 25 °C and then concentrated in vacuo on the rotavap. The crude product was re-dissolved in anhydrous CH_2Cl_2 (100 mL) followed by addition of diisopropylamine (18.5 g, 25.8 mL, 183 mmol, 4.5 equiv.). The reaction mixture was stirred for 30 min at 25 °C and quenched by addition of aqueous HCl 3M (40 mL).

A solvent swap was carried out by adding 200 mL of MeOH and evaporating the CH_2Cl_2 in the rotavap. A total of 100 mL of water were added to precipitate all of **18** after which it was isolated by filtration and washing with 100 mL of 2:1 MeOH/water. The final product was further dried overnight in the vacuum oven at 50°C to give **18** as a white solid (20.7 g, 91% yield). All analytical data matched the reported values.[135]

^{1}H NMR (400 MHz, Chloroform-*d*) δ 6.36 (d, J = 0.8 Hz, 2H), 4.83 (q, J = 6.9 Hz, 2H), 4.52 (m, J = 6.6 Hz, 2H), 3.30 (q, J = 6.8 Hz, 2H), 2.22 (s, 3H), 1.66 (d, J = 6.9 Hz, 6H), 1.42 (d, J = 6.7 Hz, 6H), 1.30 (d, J = 6.8 Hz, 6H), 1.19 (d, J = 6.7 Hz, 6H), 0.91 (d, J = 6.5 Hz, 6H).

^{13}C NMR (100 MHz, Chloroform-*d*) δ 169.9, 157.5, 140.7, 107.3, 77.8, 77.4, 47.8, 46.6, 21.1, 20.8, 20.6, 19.9, 18.1.

SFC (IC, CO_2/Ethanol = 75/25, flow rate = 3 mL/min, l = 210 nm) T_R = 1.70 min (*R*,*R*), 2.20 (*meso*), 3.00 (*S*,*S*).

$[\alpha]_D^{25}$: -159.8 (C = 1.00 mg/mL, $CHCl_3$)

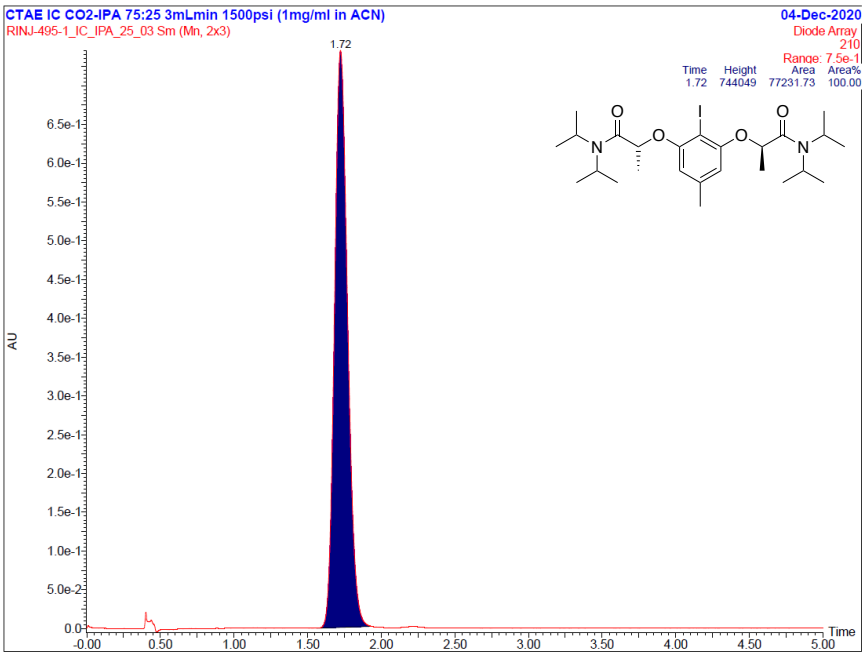
CTAE IC CO2-IPA 75:25 3mLmin 1500psi (1mg/ml in ACN)
RINJ-495-1_IC_IPA_25_03 Sm (Mn, 2x3)
04-Dec-2020
Diode Array
210
Range: 7.5e-1
Time Height Area Area%
1.72 744049 77231.73 100.00
1.72
AU
Time

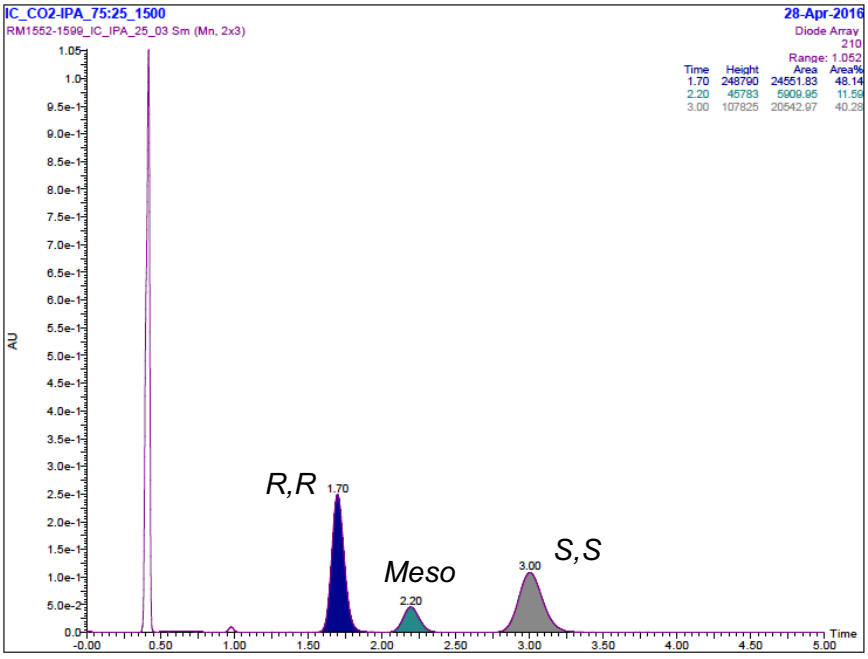
IC_CO2-IPA_75:25_1500
RM1552-1599_IC_IPA_25_03 Sm (Mn, 2x3)
28-Apr-2016
Diode Array
210
Range: 1.052
Time Height Area Area%
1.70 248790 24551.83 48.14
2.20 45783 5909.95 11.59
3.00 107825 20542.97 40.28
R,R
1.70
Meso
2.20
S,S
3.00
AU
Time

3.4.6. Synthesis of pre-catalyst 16 and identification of its isomeric form

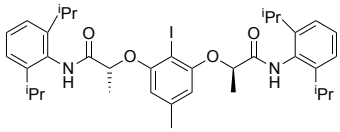

(2*R*,2'*R*)-2,2'-((2-iodo-1,3-phenylene)bis(oxy))dipropionic acid 11 (12.4 g, 31.5 mmol, 1 equiv.), was suspended in anhydrous CH_2Cl_2 (200 mL). After addition of oxalyl dichloride (14.0 g, 9.5 mL, 110.3 mmol, 3.5 equiv.) and a catalytic amount of DMF the reaction mixture was stirred for 2 hours at 25 °C and then concentrated in vacuo on the rotavap. The crude product was re-dissolved in anhydrous CH_2Cl_2 (100 mL) followed by addition of diisopropylamine (25.1 g, 26.7 mL, 141.8 mmol, 4.5 equiv.). The reaction mixture was stirred for 30 min at 25 °C and quenched by addition of aqueous HCl 3M (20 mL).

A solvent swap was carried out by adding 100 mL of MeOH and evaporating the CH_2Cl_2 on the rotavap. A total of 50 mL of water were added to precipitate all of compound **16** after which it was isolated by filtration and washing with 50 mL of 2:1 MeOH/water. The final product was further dried overnight under vacuum at 50°C to give **16** as a white solid (20.2 g, 90% yield).

^{1}H-NMR (400 MHz, Chloroform-*d*) δ 7.90 (s, 2H), 7.33 – 7.28 (m, 2H), 7.18 (d, *J* = 7.7 Hz, 4H), 6.53 (s, 2H), 5.03 (q, *J* = 6.7 Hz, 2H), 2.95 (bs, 4H), 2.40 (s, 3H), 1.79 (d, *J* = 6.7 Hz, 6H), 1.19 (d, *J* = 6.8 Hz, 12H), 1.11 (d, *J* = 6.8 Hz, 12H).

^{13}C-NMR (100 MHz, $CDCl_3$) δ 170.8, 157.0, 146.4, 141.7, 130.2, 128.8, 123.7, 108.3, 77.2, 76.2, 28.9, 23.7, 18.9.

$[\alpha]_D^{25}$: -32.5 (C = 1.00 mg/mL, $CHCl_3$)

SFC (IB, CO_2/Ethanol = 94/6, flow rate = 3 mL/min, l = 210). T_R= 3.3 min (major), 3.8 min (minor).

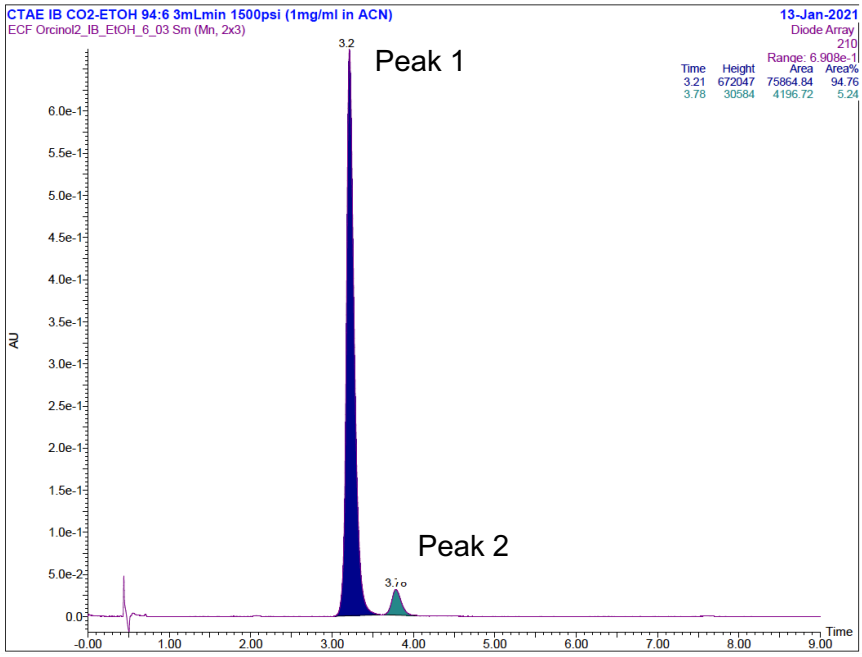

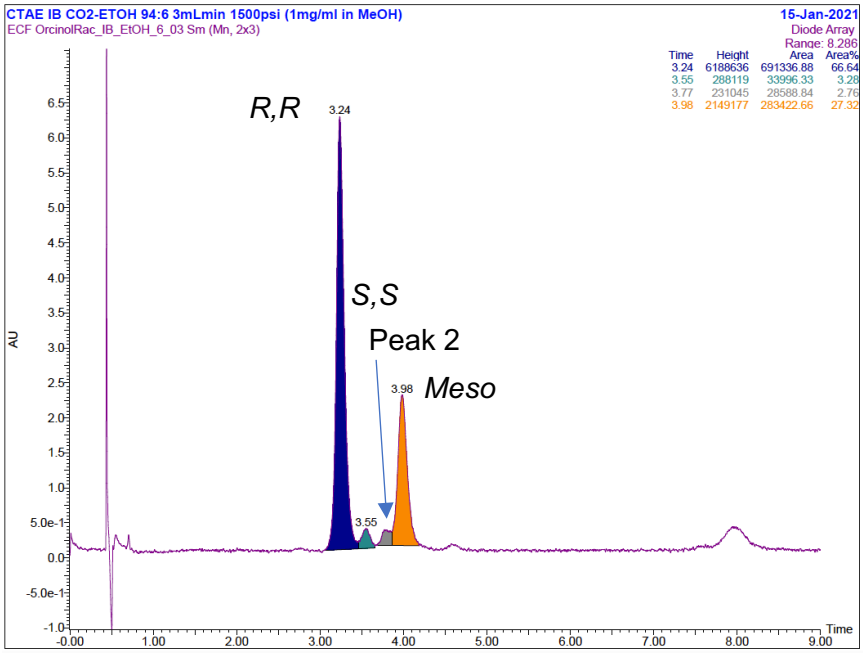

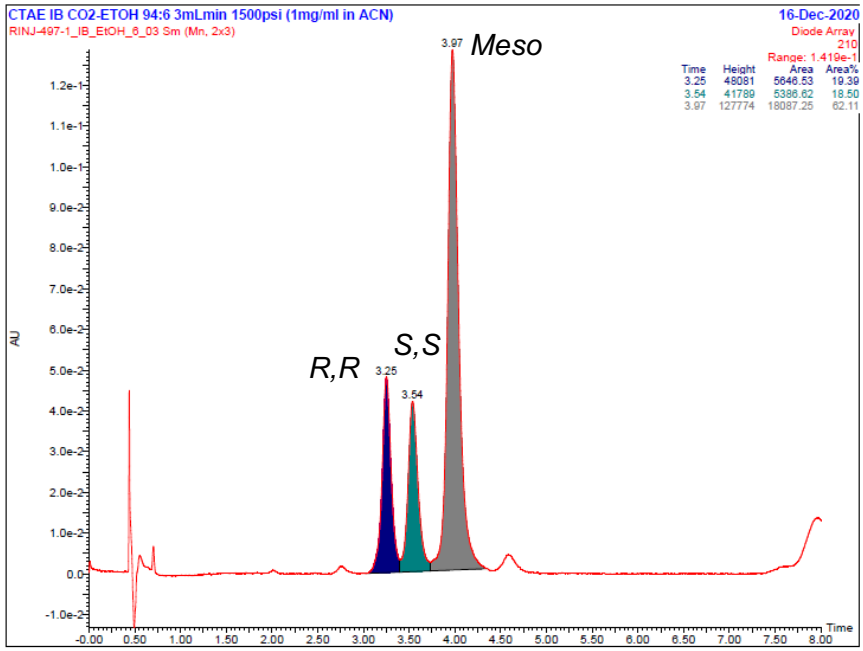

After chiral semi-preparative HPLC the two peaks were separated:

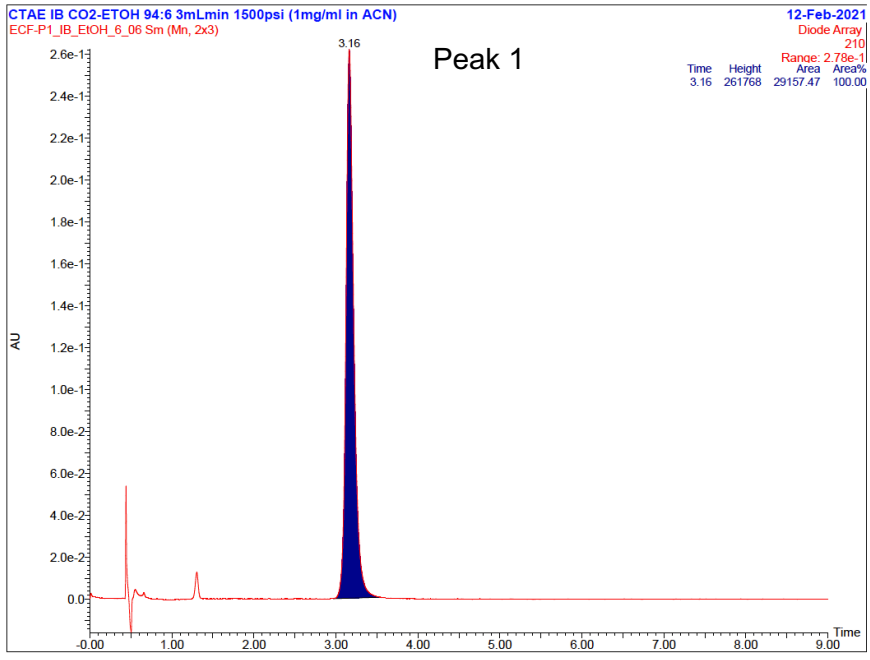

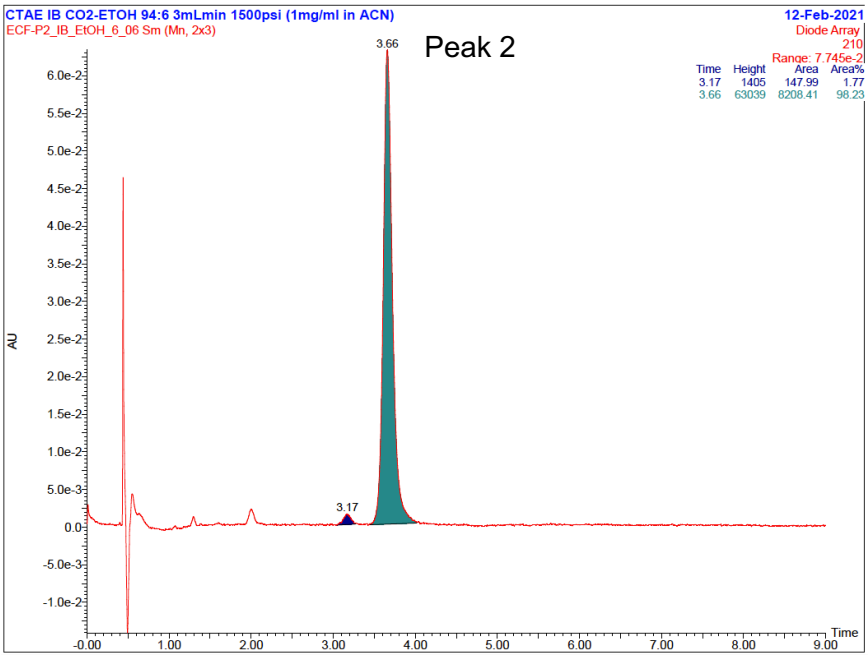

The two samples were analyzed by MS:

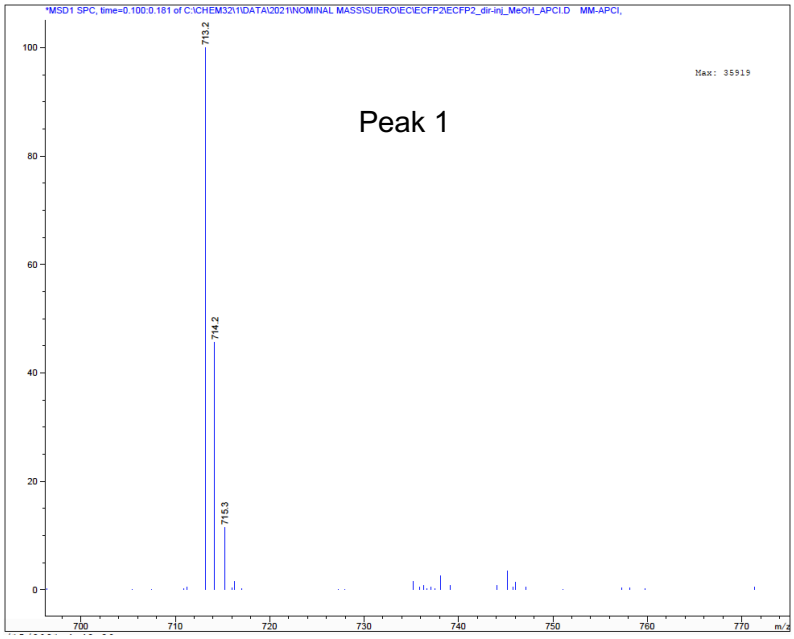

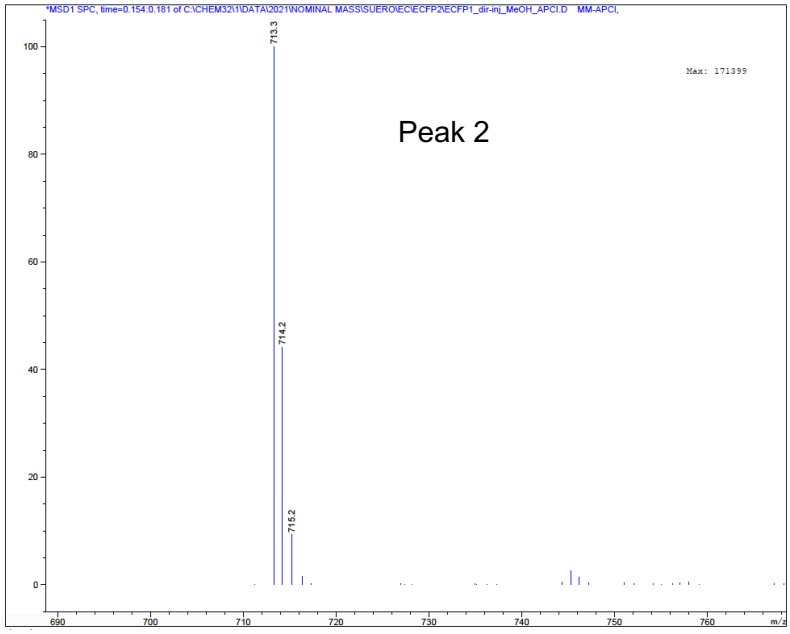

Full NMR spectra of the two peaks:

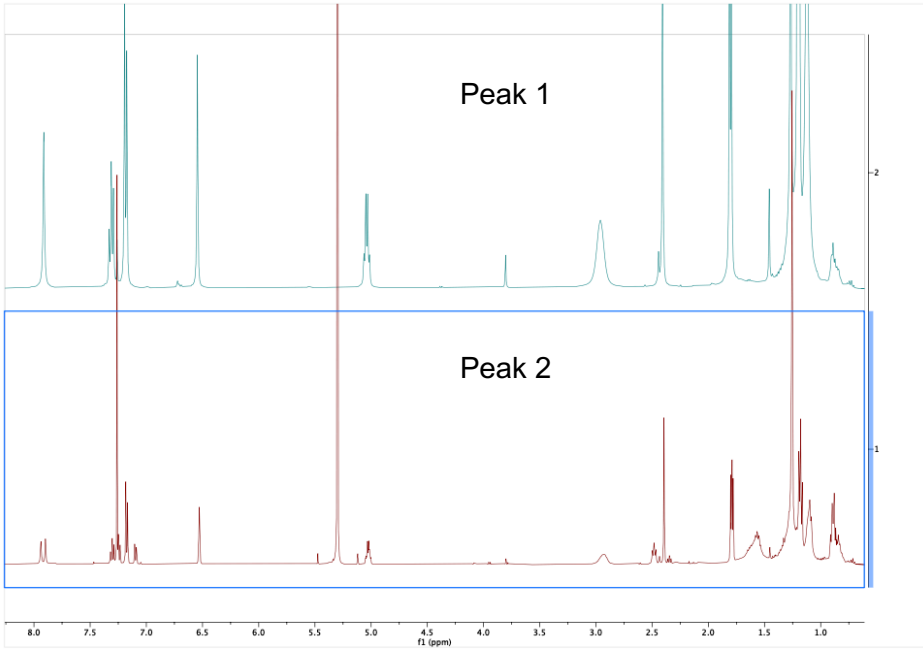

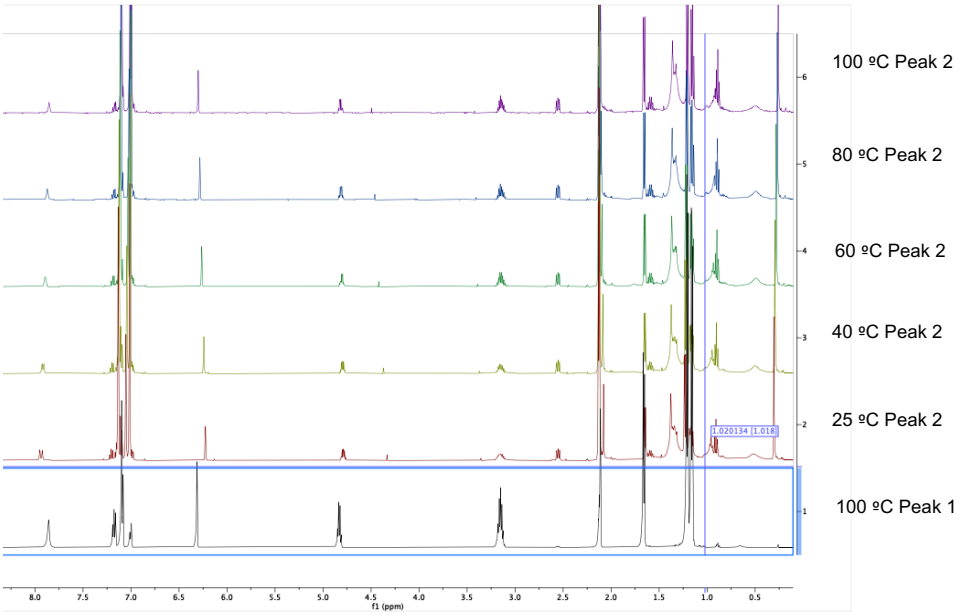

Aromatic signals (5.5-9.0 ppm):

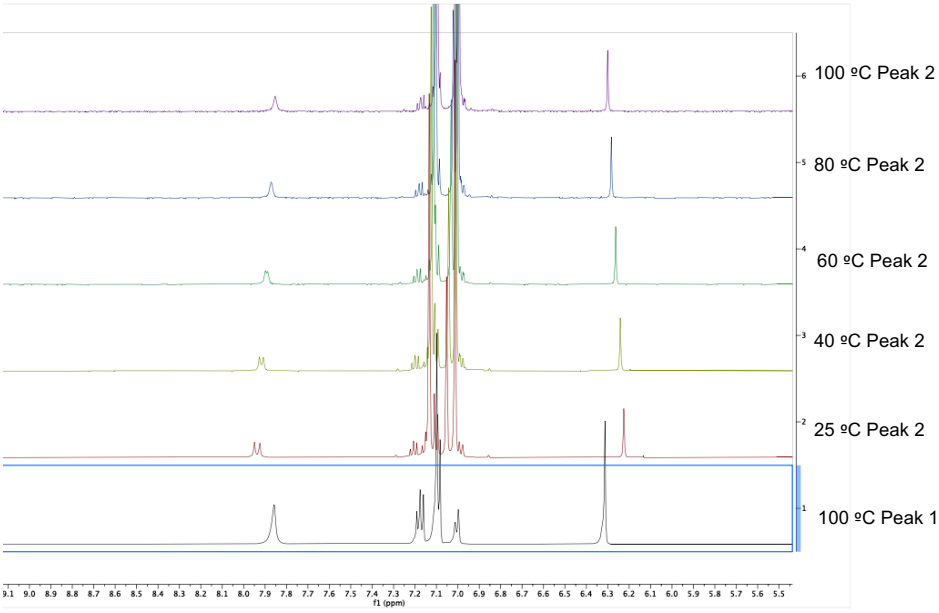

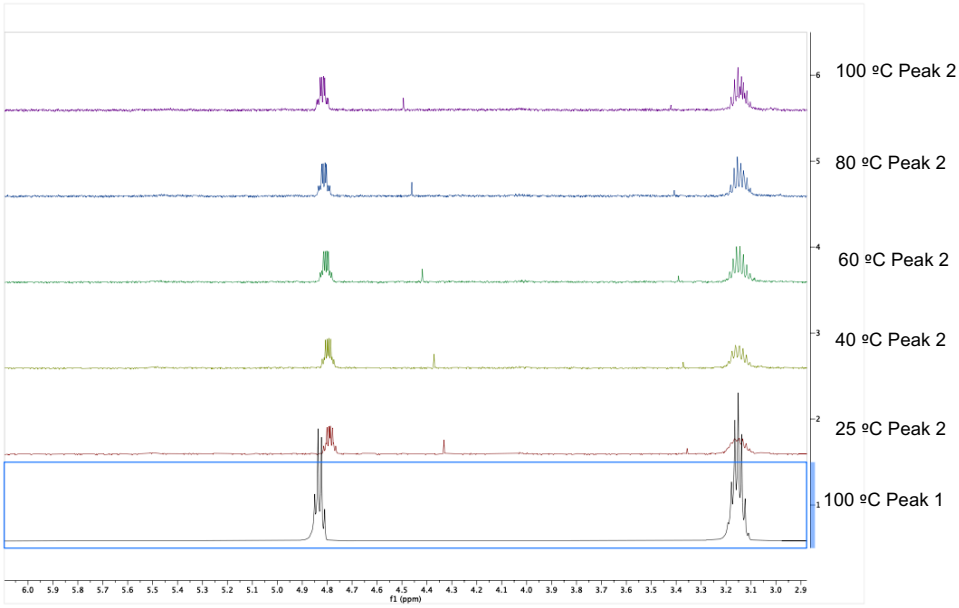

Aliphatic region:

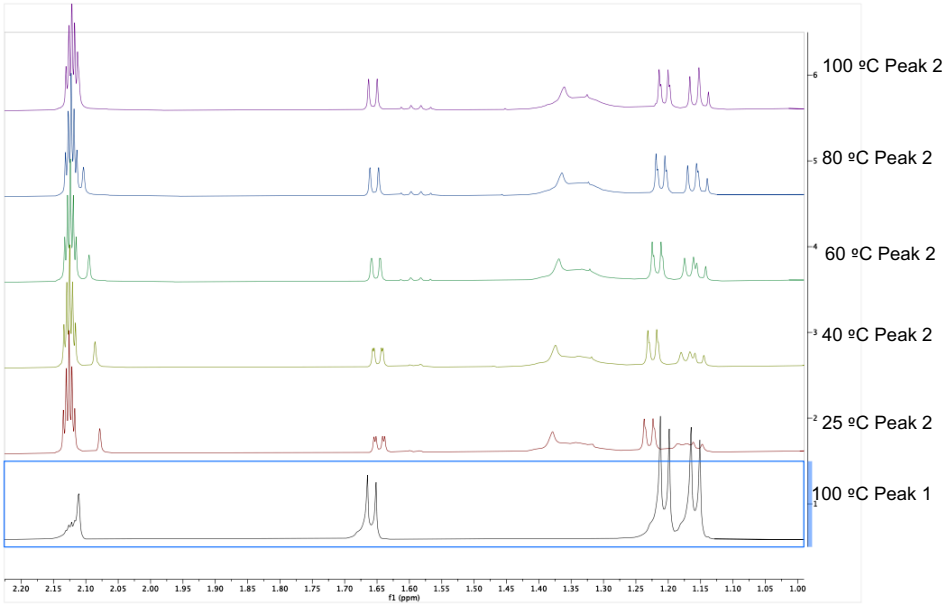

3.4.7. Diacetoxylated product

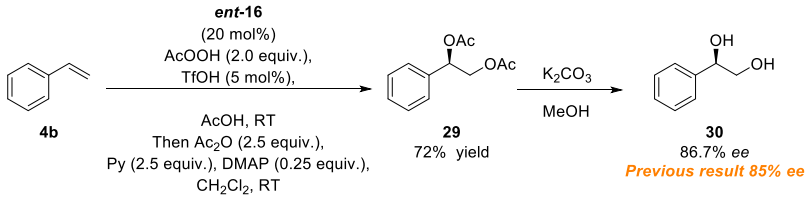

Following the described procedure, a round-bottomed flask with a stir bar was charged with iodine(I)-catalyst ***ent*-16** (71.5 mg, 0.1 mmol, 10 mol%) and a 0.01 M solution of TfOH in AcOH (5 mL, 0.05 mmol, 5 mol%) was added. After addition of AcOOH (36 % in AcOH, 0.254 g, 2 mmol, 2 equiv.) the reaction mixture was stirred for 1 h at room temperature. Then a solution of styrene (0.104 g, 0.11 mL, 1 mmol, 1 equiv.) in 7.5 mL AcOH was added slowly via syringe pump over 6 h. After complete addition the reaction mixture was allowed to continue stirring for 1 h at room temperature and then H_2O, brine and CH_2Cl_2 were added. After extraction of the aqueous phase with DCM the combined organic phases were dried over anhydrous Na_2SO_4 and concentrated in vacuo. The crude product was dissolved in 2.5 mL CH_2Cl_2 and Ac_2O (255.0 g, 2.5 mmol, 2.5 equiv.), pyridine (0.198 g, 2 mmol, 2.5 equiv.) and DMAP (0.031 g, 0.25 mmol, 0.25 equiv.) were added. After stirring at room temperature for 5 h, aqueous HCl (3 M) and H_2O were added and the aqueous phase was extracted with DCM. After drying over anhydrous Na_2SO_4 and removal of the solvent under reduced pressure, the crude product was purified by flash column chromatography on silica gel using Hex/EtOAc mixtures, giving **29** (0.155 g, 70% yield). In order to determine the enantiomeric excess, the products were converted into the corresponding diols. The products were dissolved in MeOH (0.1 M) and K_2CO_3 (1.5 equiv) was added followed by stirring at room temperature for 4 h. MeOH was removed under reduced pressure after acidification with 3 M aqueous HCl.

After extraction with CH_2Cl_2, the combined organic phases were dried over anhydrous Na_2SO_4 and concentrated under reduced pressure. The crude product were purified by flash column chromatography on silica gel using Hex/EtOAc mixtures to obtain **30** and then submitted to chiral HPLC analysis, 86.7% *ee*. NMR data in accordance with literature.[134]

(R)-1-phenylethane-1,2-diyl diacetate (29)

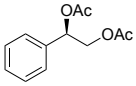

^{1}H-NMR (400 MHz; Chloroform-*d*): δ 7.41 – 7.30 (m, 5H), 6.01 (dd, *J* = 7.9, 4.0 Hz, 1H), 4.35 (dd, *J* = 11.9, 4.0 Hz, 1H), 4.30 (dd, *J* = 11.9, 7.9 Hz, 1H), 2.11 (s, 3H), 2.06 (s, 3H).

^{13}C-NMR (100 MHz; Chloroform-*d*): δ = 170.6, 170.2, 136.6, 128.9, 128.7, 126.8, 73.6, 66.2, 21.2, 20.8.

(R)-1-phenylethane-1,2-diol (30)

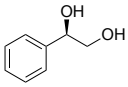

^{1}H-NMR (500 MHz; Chloroform-*d*): δ = 7.36 – 7.29 (m, 5H), 4.83 (dd, *J* = 8.3, 3.6 Hz, 1H), 3.77 (dd, *J* = 11.5, 3.6 Hz, 1H), 3.67 (dd, *J* = 11.5, 8.3 Hz, 1H), 2.68 (br. s, 1H), 2.26 (br. s, 1H).

^{13}C-NMR (125 MHz; Chloroform-*d*): δ = 140.5, 128.7, 128.1, 126.2, 74.7, 68.2.

HPLC (OD-H, *iso*-Propanol/*n*-hexane = 5/95, flow rate = 0.7 mL/min, l = 254 nm) T_R = 26.8 min (major), 29.1 min (minor), 86.7 % *ee*.

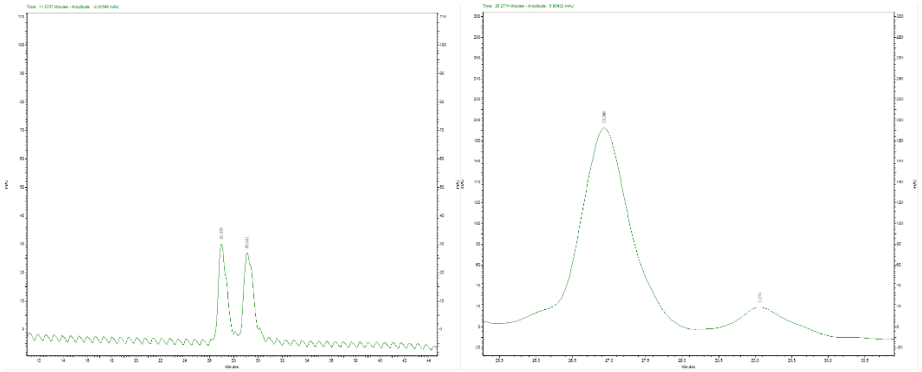

3.4.8. Dearomatization products

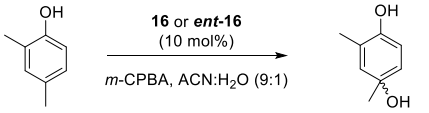

31 **32**
95%, 50% *ee*

Following an adapted procedure, into a Pyrex tube equipped with a stir bar was placed **31** (1 mmol, 1 equiv.) and chiral iodine(I) **16** or ***ent*-16** (0.1 mmol, 10 mol%) in a mixture of MeCN/TFE/H_2O (0.16 M, 8:1:1). Then, *m*-CPBA (1.8 mmol, 1.8 equiv.) was added and the mixture was stirred at –5 °C until no further progress was observed. The reaction was quenched with sat. aq $NaHCO_3$ solution (20 mL) and sat. aq $Na_2S_2O_3$ solution (20 mL). The layers were separated and the aqueous phase was extracted with CH_2Cl_2 (3 × 10 mL). The combined organic layers were dried (Na_2SO_4) and filtered and the solvent was removed under reduced pressure. The crude product was purified by flash column chromatography (silica gel, *n*-hexane/EtOAc, 85:15) to afford quinol **32** in 95% yield. Spectroscopic data matched the reported signals.[112]

(R)-4-hydroxy-2,4-dimethylcyclohexa-2,5-dien-1-one (32)

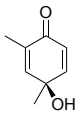

^{1}H-NMR (400 MHz, Chloroform-*d*) δ 6.85 (dd, *J* =10.1, 3.2 Hz, 1H), 6.67 – 6.64 (m, 1H), 6.11 (d, *J* = 10.1 Hz, 1H), 2.17 – 2.10 (br, 1H), 1.87 (s, 3H), 1.46 (s, 3H).

^{13}C-NMR (101 MHz, Chloroform-*d*) δ 186.0, 151.8, 147.4, 133.7, 127.0, 67.5, 26.8, 15.6.

SFC (IA, CO_2/Ethanol, 95/5, 3 mL/min, l = 240 nm) T_R= 1.78 min (*major*), 2.33 (*minor*), 50.3% *ee*.

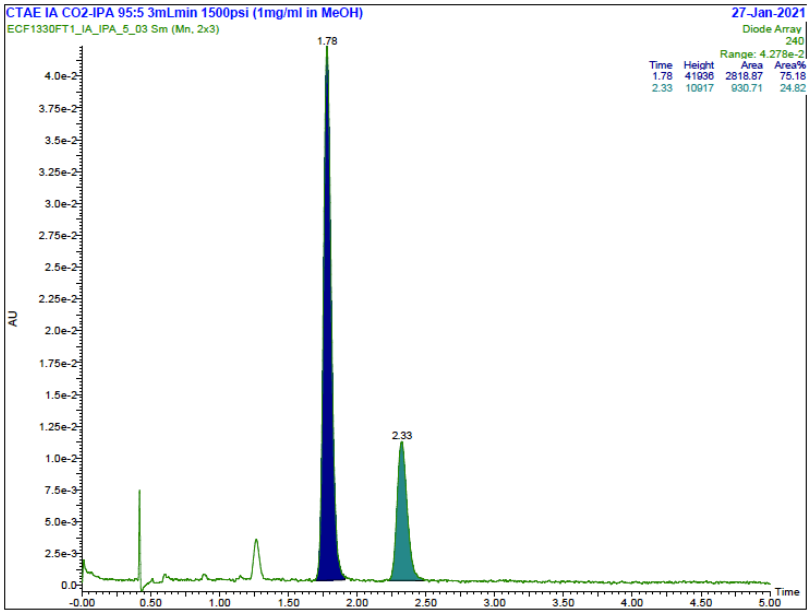

3.4.9. Diamine Products

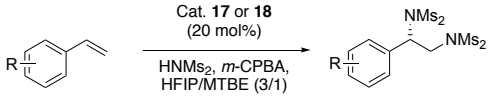

4 20

Following an adapted procedure, In a sealed pyrex tube, styrene (1 mmol) was added to a mixture of $HNMs_2$ (2.5 equiv.), catalyst **17** or **18** (0.2 equiv.) and *m*-CPBA (1 equiv.) in HFIP (0.9 mL) and MTBE (2.6 mL) at -5 ºC. After 24 h of reaction, another portion of *m*-CPBA (1 equiv.) was added and the final mixture was stirred for additional 24 h. After a total of 48 h reacting, the mixture was quenched with $NaHCO_3$ and extracted with CH_2Cl_2 (3x), dried over Na_2SO_4 and evaporated under reduced pressure. The final products **20** were purified by chromatography (silica gel, *n*-hexane/ethyl acetate, 85/15, v/v to 2/1, v/v) to give the pure diaminated product.

(S)-N,N'-(1-Phenylethane-1,2-diyl)bis(N-(methylsulfonyl)methanesulfonamide) (20a)

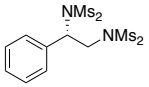

Using catalyst **17**: 0.317 g (71% yield), 98.99% *ee*

Using catalyst **18**: 0.327 g (74% yield), 99.19% *ee*

All spectral data matched the reported signals. [135]

^{1}H-NMR (400 MHz, Chloroform-*d*): δ = 7.64 – 7.60 (m, 2H), 7.46 – 7.40 (m, 3H), 5.91 (dd J = 5.3, 6.7 Hz, 1H), 4.79 (dd, J = 5.3, 15.3 Hz, 1H), 4.57 (dd, J = 6.8, 15.3 Hz, 1H), 3.84 – 3.30 (bs, 3H), 3.24 (s, 6H), 2.87 – 2.25 (bs, 3H).

^{13}C-NMR (100 MHz, Chloroform-*d*): δ = 133.8, 129.8, 130.2, 129.1, 63.4, 50.8, 44.5, 43.2.

HPLC (IB, ethanol/n-hexane = 20/80, flow rate = 0.7 mL/min, l = 254 nm) T_R = 15.4 min (major), 18.6 min (minor). 99.0% *ee* (cat. **17**); 99.2% *ee* (cat. **18**).

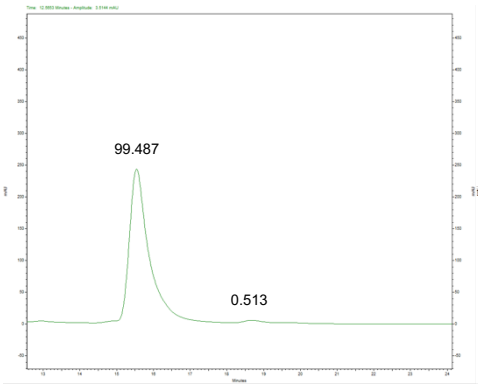

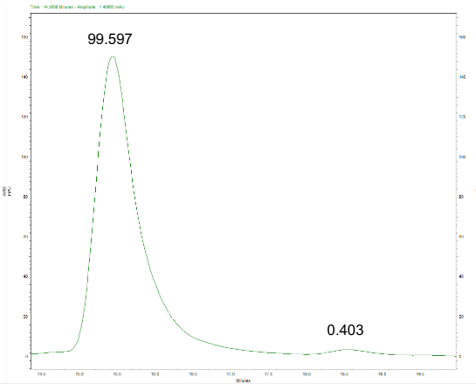

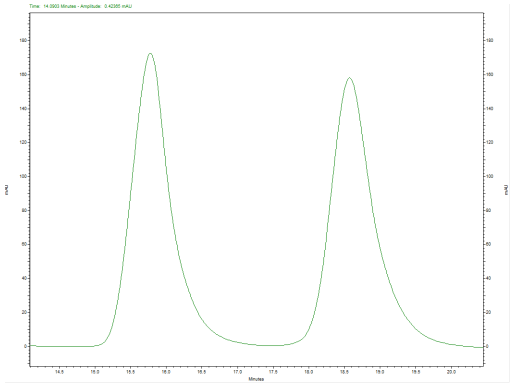

(S)-N,N'-(1-([1,1'-Biphenyl]-4-yl)ethane-1,2-diyl)bis(N-(methylsulfonyl)methanesulfonamide) (20b)

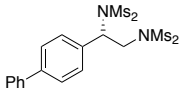

0.315 g (60% yield), 99.5% *ee*

All spectral data matched the reported signals.[135]

^{1}H-NMR (400 MHz, Chloroform-*d*): δ = 7.71 – 7.67 (m, 4H), 7.62 – 7.60 (m, 2H), 7.48 – 7.45 (m, 2H), 7.41 – 7.37 (m, 1H), 5.95 (dd, J = 5.4, 6.7 Hz, 1H), 4.83 (dd, J = 5.5, 15.3 Hz, 1H), 3.33 – 3.71 (bs, 3H), 4.60 (dd, J = 6.7, 15.4 Hz, 1H), 3.27 (s, 6H), 2.41-2.65 (bs, 3H).

^{13}C-NMR (100 MHz, Chloroform-*d*): δ = 142.5, 139.7, 132.6, 130.6, 127.6, 128.2, 129.1, 127.2, 63.3, 50.8, 44.5 (bs), 43.3.

HPLC (IB, ethanol/n-hexane = 20/80, flow rate = 0.7 mL/min, l = 254 nm) T_R = 21.0 min (major), 23.8 min (minor). 99.5% *ee*.

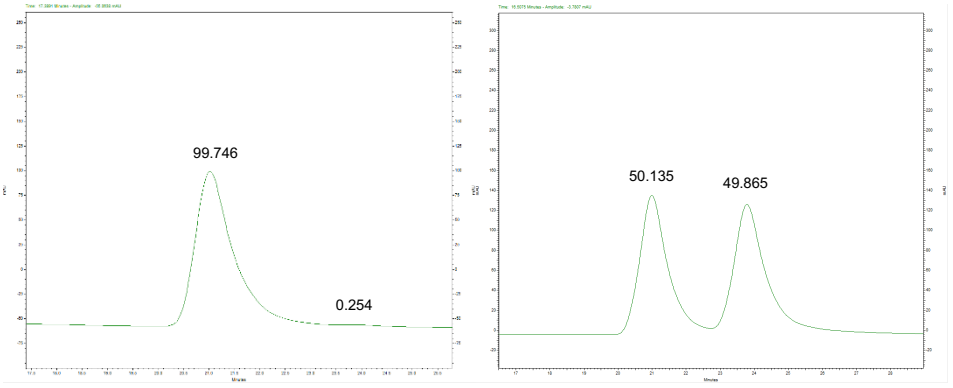

(*S*)-N,N'-(1-(2-Chlorophenyl)ethane-1,2-diyl)bis(N-(methylsulfonyl) methanesulfonamide) (20c)

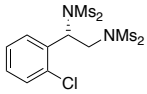

0.290 g (71% yield), 99.5% *ee.*

All spectral data matched the reported signals. [135]

^{1}H-NMR (400 MHz, Chloroform-*d*): δ 7.59 (dd, *J* = 2.3, 7.3 Hz, 1H), 7.49 – 7.46 (m, 1H), 7.40 – 7.33 (m, 2H), 6.24 – 6.20 (m, 1H), 4.80 – 4.73 (m, 1H), 4.42 – 4.37 (m, 1H), 3.44 (s, 6H), 3.32 – 2.38 (bs, 6H).

^{13}C-NMR (100 MHz, Chloroform-*d*): δ 135.9, 132.6, 131.2, 131.0, 130.4, 127.0, 59.1, 50.8, 42.6.

HPLC (IB, ethanol/n-hexane = 20/80, flow rate = 0.8 mL/min, l = 254 nm) T_R = 19.0 min (major), 20.6 min (minor). 99.5% ee.

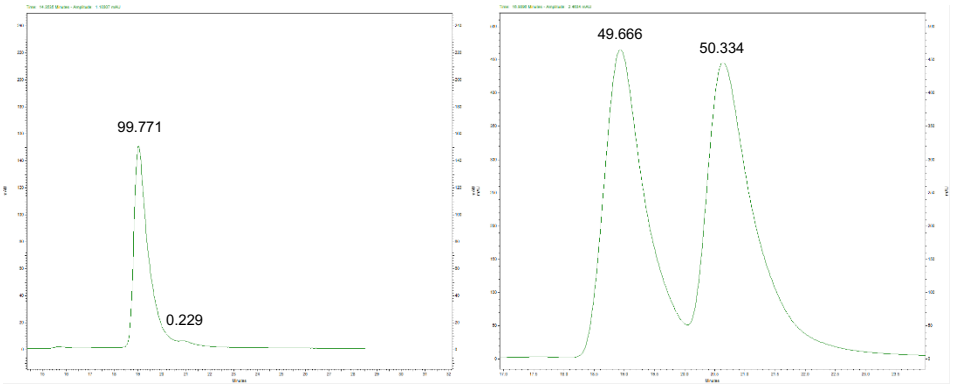

4. Chapter IV – C_1-Symmetry in aryliodine catalyzed diaminations: A proof of concept

Chapter IV – C_1-Symmetry in aryliodine catalyzed diaminations: A proof of concept

4.1. Introduction

Throughout this thesis many C_2-symmetric aryliodine(I) pre-catalysts have been mentioned. As already stated in section 1.4.2.1., another type of pre-catalysts are C_1-symmetric. While C_2-symmetric pre-catalysts have two identical arms (and therefore a symmetry axis), C_1-symmetry means they are asymmetric in the sense that no symmetry elements are present in their structure (Figure 29). The latter can have no more substituents (they only have one side chain) or show other substitution (they have two side chains but different from one another).

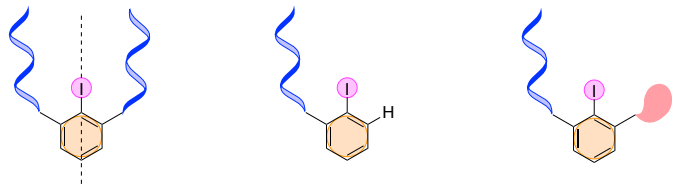

Figure 29. Symmetry and different designs for aryliodines(I)

Most of the C_2-symmetric pre-catalysts are generally more modular and their synthesis can be somewhat easier due to their structural symmetry.[100] However, many pre-catalysts have only one chiral centre that generates the chiral pocket for the desired transformation, or present unsymmetric structures.

This type of designs has been developed since the beginning of enantioselective I(III)-mediated reactions, with a broad range of structural motifs. One of the first ones came from Wirth in 1997 (Figure 30a, see Scheme 17).[83] Olofsson also synthesized in 2010 another diaryliodonium salt with a very similar structure (Figure 30b),[192] and finally, Fujita designed three different groups of C_1-symmetric aryliodines used respectively in oxylactonizations (See Schemes 20 and 21) and diacetoxylation of alkenes (Figure 30).[193] The basic difference between the three Fujita's reagents dwells in the different functionalization in the 6-

position of the aryl core, the alkylated chain in α to the carbonyl and the ester group.

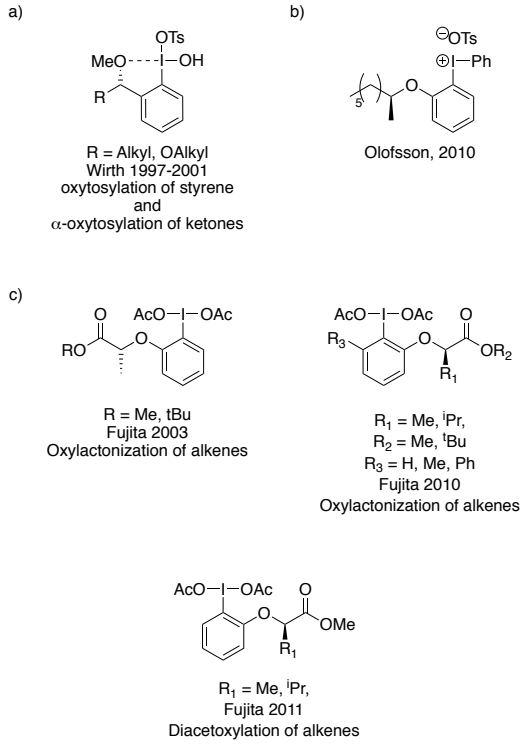

Figure 30. Examples of C_1-symmetric I(III) reagents from Wirth, Olofsson and Fujita

Although the first attempts at using this design were not very successful, the diacetoxylation of alkenes in 2011 yielded *ee* up to 96%, showing their potential to generate an effective chiral pocket.

4.1.1. Chiral C_1-symmetric aryliodine (I) pre-catalysts

From 2007, several pre-catalysts have been developed with one chiral centre, starting with the work of Wirth, who continued using a similar structure than seen in Figure 30. These pre-catalysts were applied to the α-oxygenation of ketones and accomplished yields of up to 42%.[115,194,195]

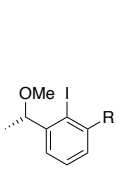

2007
α-oxytosylation of ketones
Up to 40% *ee*

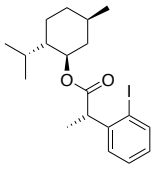

2008
α-oxytosylation of ketones
Up to 42% *ee*

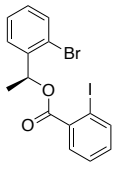

2010
α-oxytosylation of ketones
α-oxylactonization of ketones
Up to 26% *ee*

Figure 31. Pre-catalysts with one chiral centre from Wirth between 2007-2010

An enantioselective intramolecular diamination was also developed in 2014 by the same authors. The pre-catalyst used was based on the previous structures mentioned above, and contained a pyridine moiety in close proximity of the iodine(I) centre in order for the active I(III) species to coordinate with. The yields were moderate to good and up to 86% *ee* was obtained in the diamination.[196]

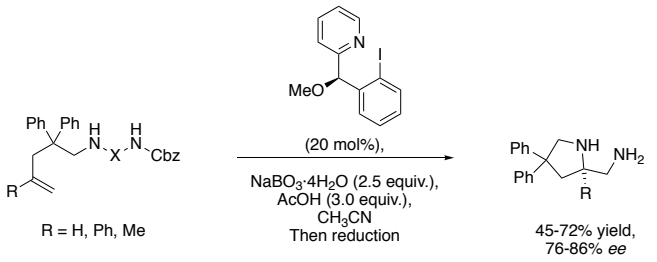

Scheme 101. Intramolecular asymmetric diamination by Wirth in 2014

Chapter IV – C_1-Symmetry in aryliodine catalyzed diaminations: A proof of concept

Legault has also developed several C_1-symmetric aryliodines(I), all of them with a common feature: the presence of a chiral oxazoline derived from a 1- or 1,1-substituted chiral aminoalcohols. The preparation of these species was simpler than other pre-catalyst as a first amidation of an acyl chloride gives an amide which will cyclize to yield the oxazoline moiety. This cyclization can be performed by different conditions, being Mitsunobu reaction one of the most used to synthesize these pre-catalysts (Scheme 102).

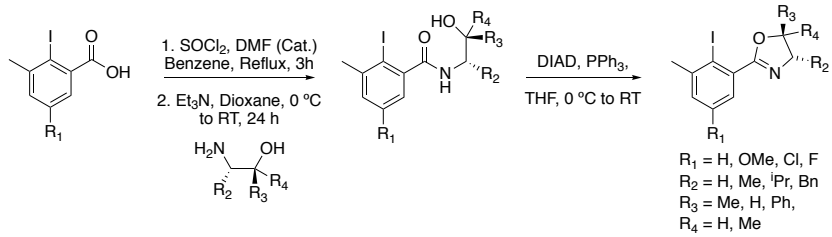

Scheme 102. Synthesis of oxazoline-based pre-catalysts

The first of this series was developed in 2012 and applied to the oxytosylation of ketones, which yielded up to 80% yield and 54% *ee* (Scheme 103).[197]

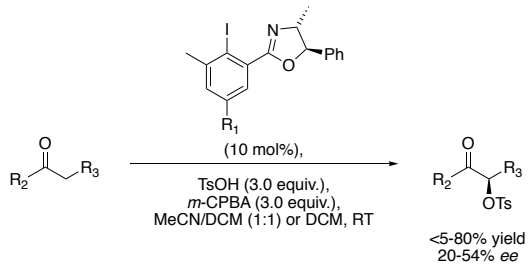

Scheme 103. α- Tosylation of ketones using the oxazoline-based aryliodines(I)

Chapter IV – C_1-Symmetry in aryliodine catalyzed diaminations: A proof of concept

In 2013, other pre-catalysts were synthesized, bearing a wide variety of moieties in the oxazoline core. Due to the bulkiness of the aminoalcohols used, the synthetic approach to these pre-catalysts was changed. Instead of using an acid as the starting point, it was transformed to the aldehyde and condensed with the aminoalcohol, and the oxazoline was obtained after treatment with NBS. The main limitation of these pre-catalysts resides in the low enantiodifferentiation for the oxytosylation of ketones, with a maximum of 34% *ee* (Scheme 104).[198]

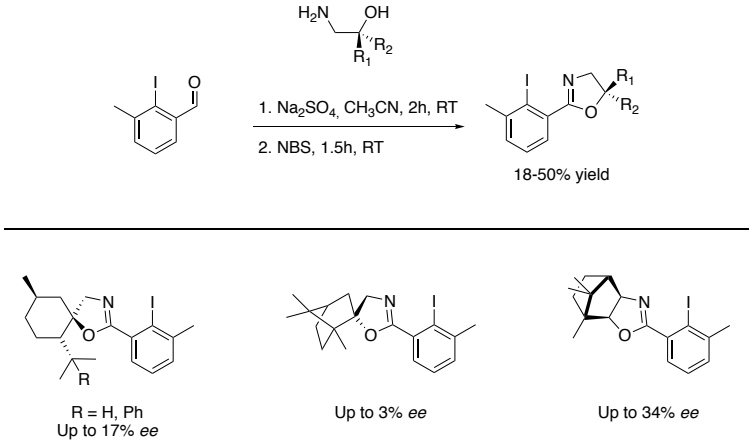

Scheme 104. Synthesis and application of bulky oxazoline pre-catalysts in the oxytosylation of ketones

During the same time, Moran also developed several pre-catalysts with a C_1-symmetry, based on the previous work from Wirth. The chiral chains were introduced either by Mitsunobu reaction, esterification or amidation reactions. The newly developed pre-catalysts were tried in both the α-oxygenation of ketones and the cyclization 5-oxo-5-phenylpentanoic acid, with much higher *ee* in the second case (51% *ee*) than in the first (18% *ee*).

The structure which gave higher enantioinduction in both cases was the derivative containing (1*S*,2*S*) pseudoephedrine (Scheme 39 and Scheme 105).[118]

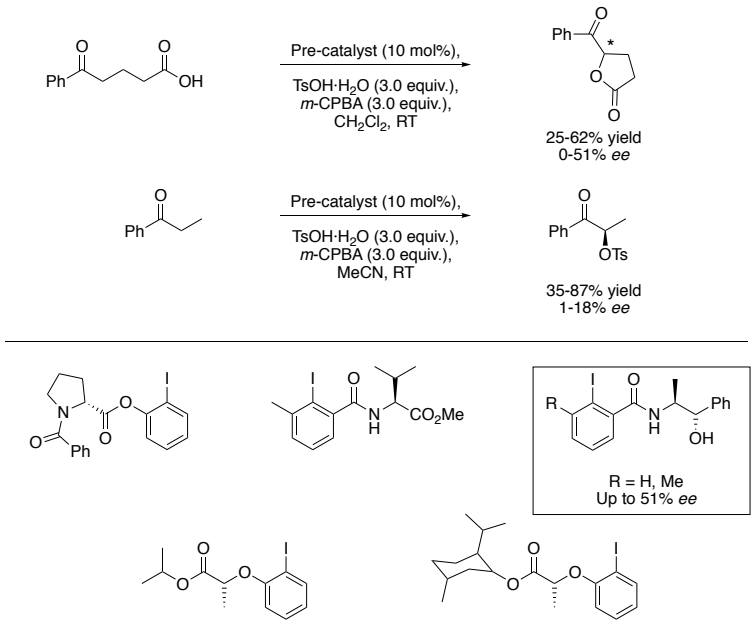

Scheme 105. Application of Moran's pre-catalysts in the oxytosylation of ketones and the cyclization 5-oxo-5-phenylpentanoic acid

In 2017, Pericàs and Nachtsheim synthesized a family of pre-catalysts which provided up to 86% *ee* when submitted to Kita's dearomatization. The synthesis of this aryliodines was started with the Grignard addition of ethynylmagnesium bromide to 2-iodobenzaldehyde. The racemic alcohol obtained was submitted to CALB (*Candida antarctica* lipase B), which could acetylate the (*R*)-enantiomer, leaving the (*S*)-enantiomer in 47% and >99.9% *ee*. Then, an azide-alkyne cycloaddition using different azides and a final protection of the alcohol with various silyl groups yielded a wide variety of pre-catalysts (Scheme 106).[199]

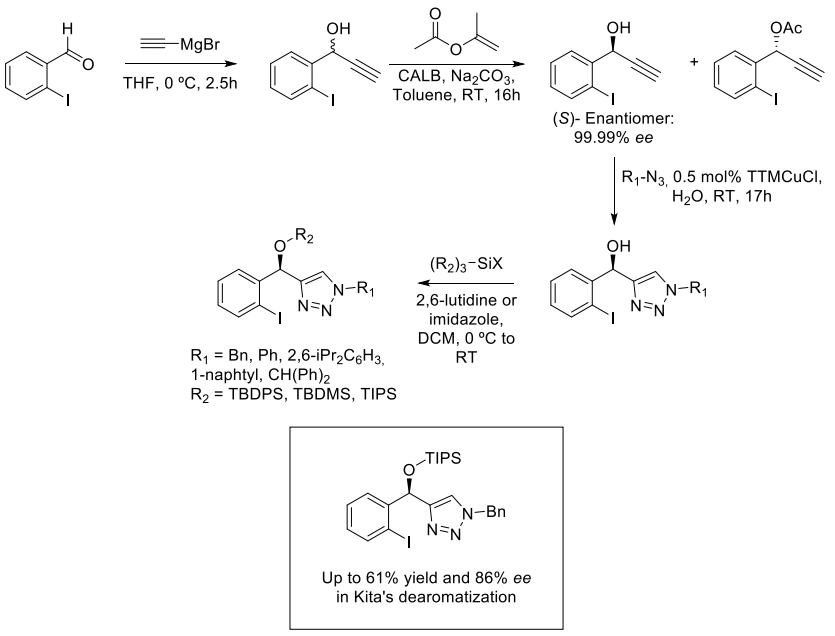

Scheme 106. Synthesis of triazole-based pre-catalysts

Finally, one relevant contribution for this project was developed by Gilmour in 2021. While studying the 1,2-difluorination of α-CF_3-styrenes yielding a pentafluorinated isopropyl group, his group developed C_1-symmetric pre-catalysts. These gave much lower yields and *ee* in the products than the original pre-catalyst.

In their study, the mentioned symmetry was obtained by simply using a monoalkylated aryl core instead of a double alkylated structure (thus using a phenol instead of a resorcinol).

While the C_2-symmetric pre-catalysts yielded pentafluorinated products in up to 88% yield and 90% *ee*, the pre-catalysts with only one “arm” could not surpass 52% yield and 48% *ee* (Scheme 107). Therefore, the authors concluded that the C_2-symmetry of the pre-catalyst is a requirement to induce high yields and enantiomeric excesses.[200]

Chapter IV – C_1-Symmetry in aryliodine catalyzed diaminations: A proof of concept

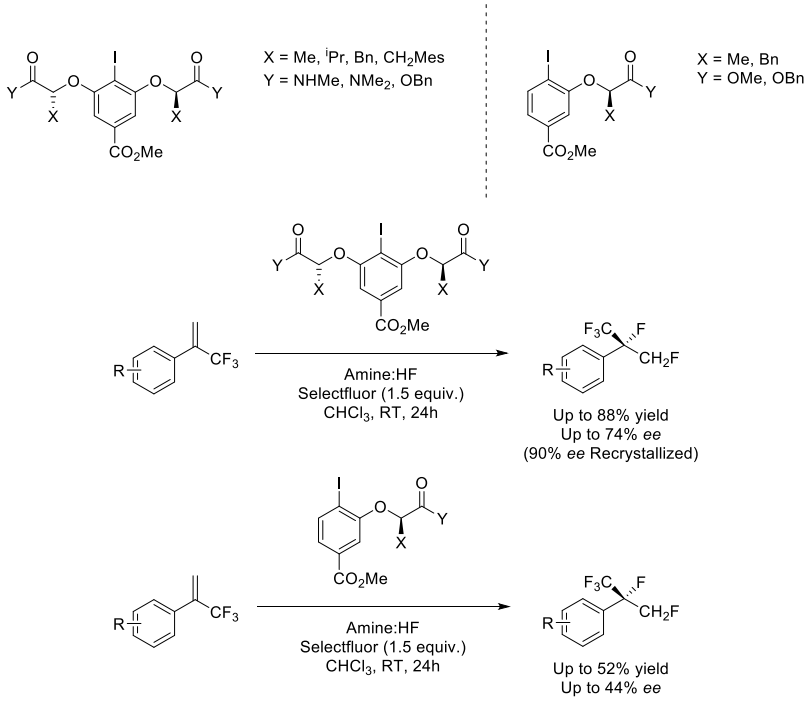

Scheme 107. Application of C_2 and C_1-Symmetric pre-catalysts

4.1.2. Proof of concept

The last project of this thesis is a proof of concept. In this case, we wanted to demonstrate the viability of a C_1-symmetric pre-catalyst, that it could yield a high *ee* of the products and finally compare it with pre-catalysts.

As seen throughout the introduction of this chapter, not all pre-catalysts are able to provide good enantiodifferentiation. Therefore, the main feature of any developed catalyst for styrene difunctionalisation dwells in its ability to differentiate between the two enantiotopic faces of a given substrate. This fact has proven to be the key to enantioselectivity induction.

Chapter IV – C_1-Symmetry in aryliodine catalyzed diaminations: A proof of concept

The whole design rationale to date resides in the structural disposition of the pre-catalysts so they create an efficient chiral pocket in their I(III) intermediate species. Some of the most studied designs have been previously developed in our lab in 2016 and 2017,[134,135] being both their I(I) and I(III) species thoroughly examined. It was found that the ligands in the I(III) species relied on stabilization by the chiral chains and noncovalent interactions (Figure 32).

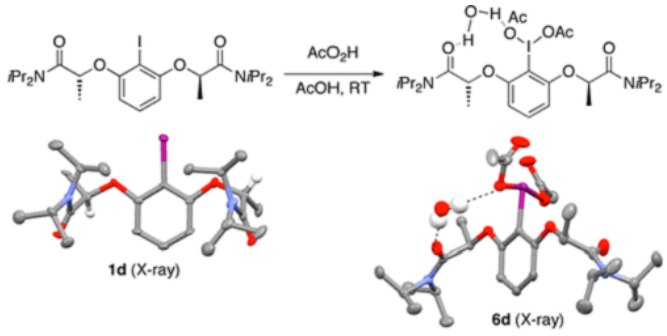

Figure 32. I(III) species of the Muñiz pre-catalyst showing a molecule of water for noncovalent interactions

Remarkably, the chiral pocket formed in the active species of these catalysts consists in a helical-type structure which blocks one of the faces of the styrene substrate (See Section 2.1.3). The asymmetric outcome of the transformation depends on the effectiveness of this obstruction, and this is the crucial feature to produce higher *ee* in the product.

Our focus was put on how to accomplish the same type of induction. This fact brought us to the idea of noncovalent interactions, and a suitable design for a catalyst structure.

The initial principle to obtain a C_1-symmetric pre-catalyst was to modify the chiral backbone so noncovalent interactions could also play a role in the overall enantioselective outcome of the transformation.

This modification would consist in the suppression of one of the two stereogenic centres of the Muñiz pre-catalyst.

Chapter IV – C_1-Symmetry in aryliodine catalyzed diaminations: A proof of concept

Given the insight from the racemic and asymmetric diaminations,[176] we envisioned a pre-catalyst with one chiral side-chain, as in the usual Muñiz pre-catalyst.[135] However, it would have one big difference: the other side-chain would be analogous to the one from the achiral pre-catalyst in Chapter II (Scheme 108).

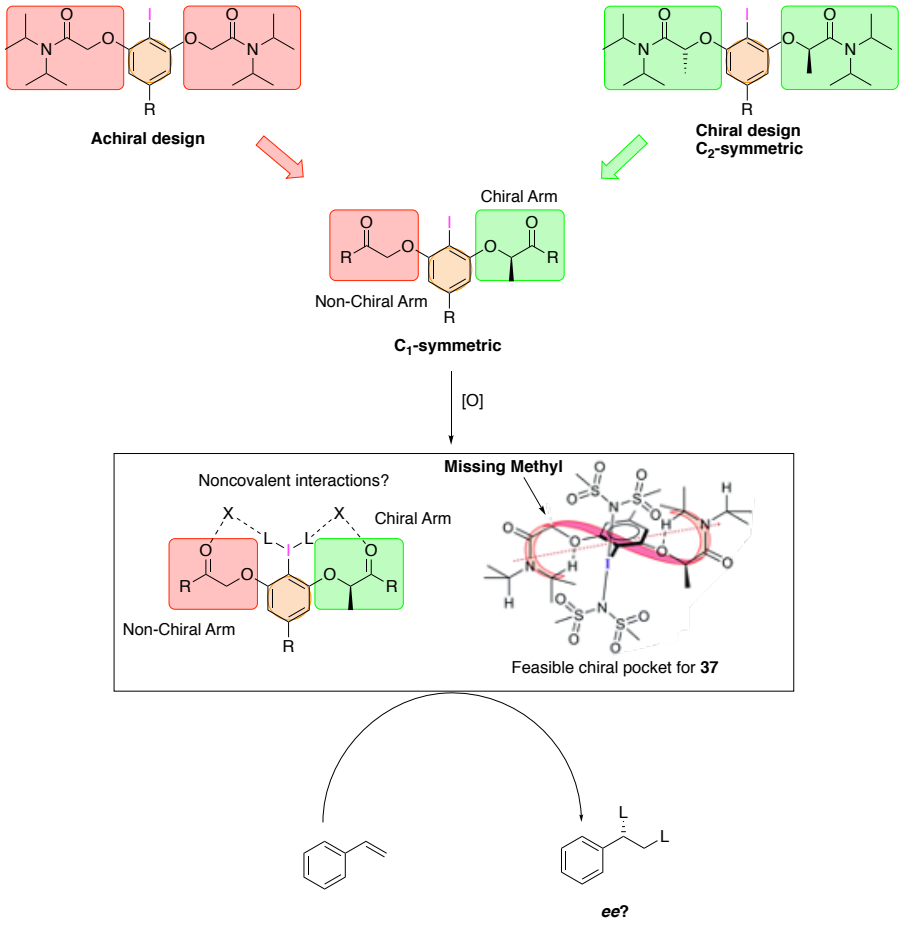

Scheme 108. Pre-catalyst design for the proof of concept

4.2. Results and discussion

4.2.1 Pre-catalyst synthesis

The synthesis of the desired pre-catalyst was envisioned, starting with a first mono-*O*-alkylation of resorcinol **3c** with commercially available methyl bromoacetate **38**. Afterwards, a Mitsunobu reaction would yield diester **35**. This way, both terminal moieties of the intermediates would have the same functional groups (For other unsuccessful routes, see experimental part, Section 4.4.2).

A saponification and subsequent amidation would give pre-catalyst **37** (Scheme 109).

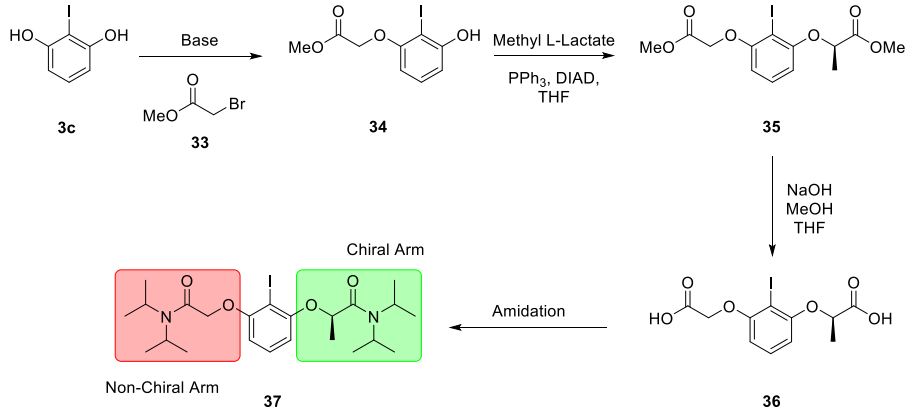

Scheme 109. Synthetic route to C_1-symmetric pre-catalyst **42** based on compound **17**

The reaction between **3c** and **38** was performed in several conditions. Decomposition was mostly observed when using NaH, but when K_2CO_3 was used instead a change in the reactivity was noticed. Even though the double *O*-alkylated product was always the major product of the reaction, **34** could be isolated in up to 45% yield (Table 8, Entry 4).

To overcome the excessive formation of **38**, an excess of **3c** and Cs_2CO_3 was added.

Chapter IV – C_1-Symmetry in aryliodine catalyzed diaminations: A proof of concept

The best conditions were obtained when heating the base and **3c** in acetone at 60 ºC for 30 min. then, **33** was added and stirred at 60 ºC for 30 min. more (Entry 4).

When the reaction was left for more than 30 minutes, formation of compound **38** and a decrease of the desired compound **34** was observed by TLC and GCMS (Entry 3).

Table 8. Screening for mono O-alkylation of **3c** with **33**

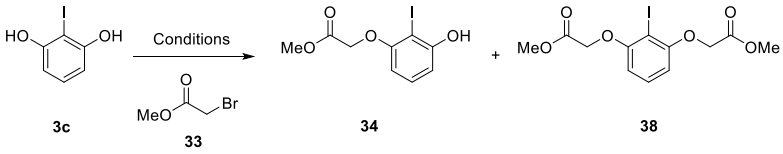

3c **33** **34** **38**

Entry	Conditions	**39** Yield	**43** Yield
1	**3c** (4.0 equiv.), NaH (4.0 equiv., 30 min.), DME, RT 30 min.	-	-
2	**3c** (4.0 equiv.), K_2CO_3 (4.0 equiv., 1 h), Dry DMF, RT, 18h	10%	50%
3	**3c** (4.0 equiv.), K_2CO_3 (4.0 equiv., 1 h), Dry Acetone, 60 ºC, 2h	33%	54%
4	**3c** (4.0 equiv.), K_2CO_3 (4.0 equiv., 30 min), Dry Acetone, 60 ºC, 30 min.	45%	50%

After the optimization to obtain **34**, the next step was to submit it to the Mitsunobu reaction with methyl L-lactate, in order to introduce the chiral side-chain. Given that only one of the alcohols was going to be functionalized, the equivalents of all the reagents were recalculated to half. Diester **35** was obtained in up to 93% yield after column chromatography (Scheme 110).

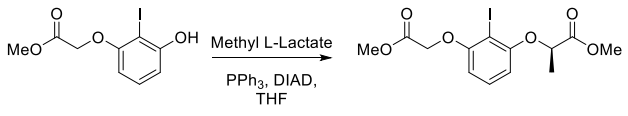

34 **35**
93% yield after column cromatography

Scheme 110. Mitsunobu reaction to obtain **35**

Saponification of **35** with the usual procedure, using NaOH in a 1:1 mixture of MeOH and THF also resulted in the conversion of **35** to the diacid **36**. In this case, the yield was as high as 94%, which is comparable to the one obtained when synthesizing **16**-**18** (Scheme 111).

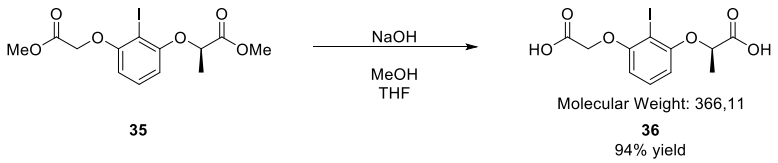

Scheme 111. Saponification of **35** to give diacid **36**

As for the final amidation reaction, which yielded pre-catalyst **37**, was initially performed with Et_3N as an auxiliary base, given that the role of Et_3N was not yet known. As stated above, this fact provokes racemization of the chiral centre of the catalyst (in this case only the contrary enantiomer can be obtained). Pre-catalyst **37** was initially obtained in 80% yield and 85% *ee* (Scheme 112).

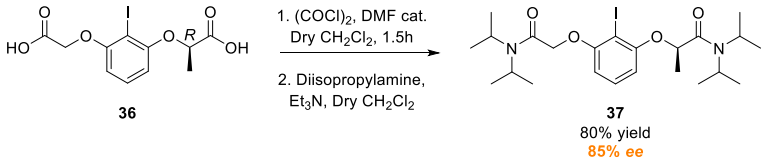

Scheme 112. Formation of **37** using Et_3N

The formation of ***rac*-37** should follow the same path as seen in Scheme 91, considering that the new achiral side-chain could also undergo ketene formation, even though this fact had no stereochemical consequences (Scheme 113). Racemization of the chiral side-chain was observed with a minimum of 7.50% formation of the opposite enantiomer from **37**.

Chapter IV – C_1-Symmetry in aryliodine catalyzed diaminations: A proof of concept

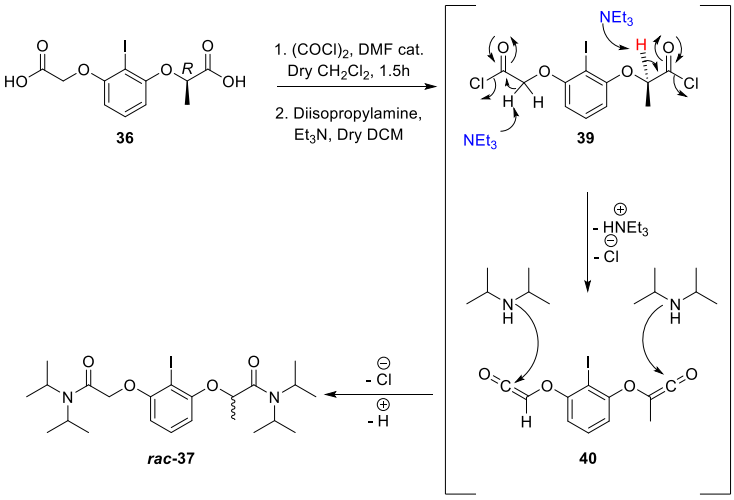

Scheme 113. Formation of ***rac*-37** according to our insights from Chapter III

When synthesizing the compound without the use of triethylamine, a yield of 70% and >99% *ee* was obtained, proving again the generality of the chemistry developed in Chapter III (Scheme 114).

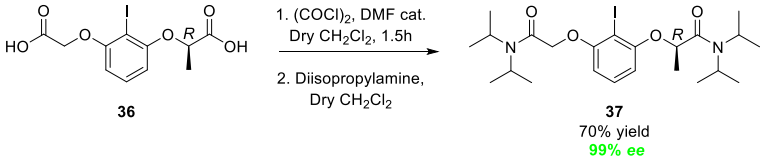

Scheme 114. Formation of **37** without using Et_3N

The synthesis of a C_1-symmetric pre-catalyst that could catalyze the diacetoxylation of alkenes was also explored. A similar procedure as for **37** was followed. In the final amidation step, 2,6-diisopropylaniline was used as a nucleophile, obtaining 91% yield of the pre-catalyst **37'** (Scheme 115).

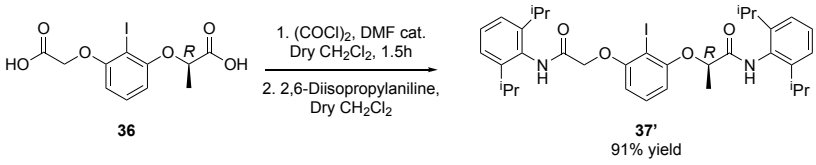

Scheme 115. Synthesis of pre-catalyst **37'**

The *meso*-form of 2,6-diisopropylaniline-containing C_2-symmetric pre-catalyst **16** was never observed. This fact brought us to not expect racemization in this case either, but further synthesis of the racemic pre-catalyst and analysis by SFC should confirm our hypothesis.

4.2.3. First catalytic trials

Once pre-catalysts **37** and **37'** were synthesized, their catalytic activity was tried in the styrene substrate. When comparing the results obtained following the same methodology as for **18**, a comparable yield was observed.

In terms of enantioinduction 84% *ee* was obtained of the corresponding diamine, showing that **37** could be a suitable pre-catalyst for the diamination of styrenes (Scheme 116).

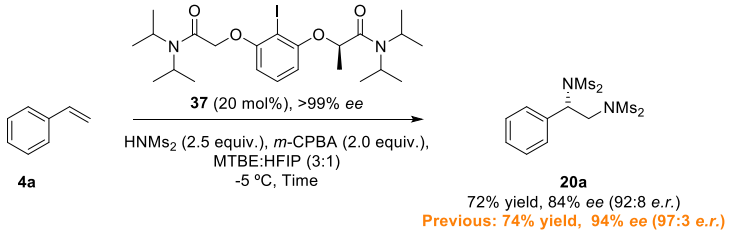

Scheme 116. Repetition of the diamination of **4a** with enantiopure pre-catalyst **37**

When submitting **37'** to the diacetoxylation reaction, the yield was moderate – 59% compared to the 71% obtained previously. The maximum *ee* obtained was 58%, which made us turn our attention towards diaminations instead of diacetoxilation reactions (Scheme 117). The development of this reaction with a C_1-symmetric pre-catalyst would require a thorough optimization, given that it is still far from the result obtained with **16** (85% *ee*).

Chapter IV – C_1-Symmetry in aryliodine catalyzed diaminations: A proof of concept

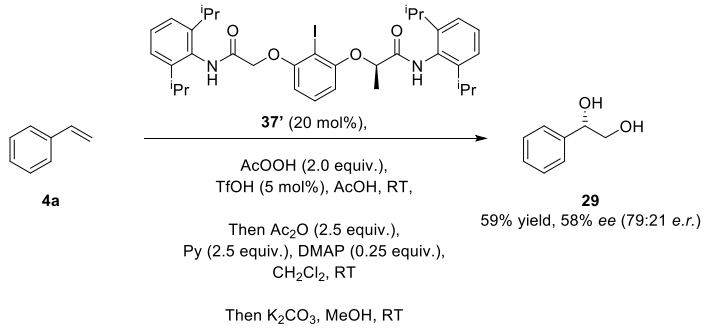

Scheme 117. Diacetoxylation reaction producing up to 58% *ee*

4.2.4. Scope

Several substituted styrenes were submitted to the reaction with **37** following the optimized procedure found in the last section. The yields were moderate 35-72%, and to our surprise, the *ee* went from 28% to a maximum of 90% (95:5 *e.r.*) (Scheme 118).

When observing the yields, the substrates followed the two expected trends **18** also followed: steric hindrance and electronic density in the substrate limit the conversion of the reaction.

In the case of steric hindrance, it can be observed that bulky substituents such as *para*-^{t}Bu in **20h** and naphthalene **20l** present reduced yields, 45 and 35% respectively. It could also be the case in **20d**, which presents only a 42% yield, given the proximity between the chlorine and the alkene moiety that will be difunctionalized. *Para*- substitution did not present this problem for the substrates tried in the reaction.

When looking into the electronic effect of the substituents, in general both electron-rich styrenes such as **20k** and electron-poor arenes such as **20f** were tolerated. Some electron-donating moieties like *p*-Methyl (**20m**) produce a lesser amount of product than more electron-withdrawing moieties like *p*-CF_3 (**20f**).

Chapter IV – C_1-Symmetry in aryliodine catalyzed diaminations: A proof of concept

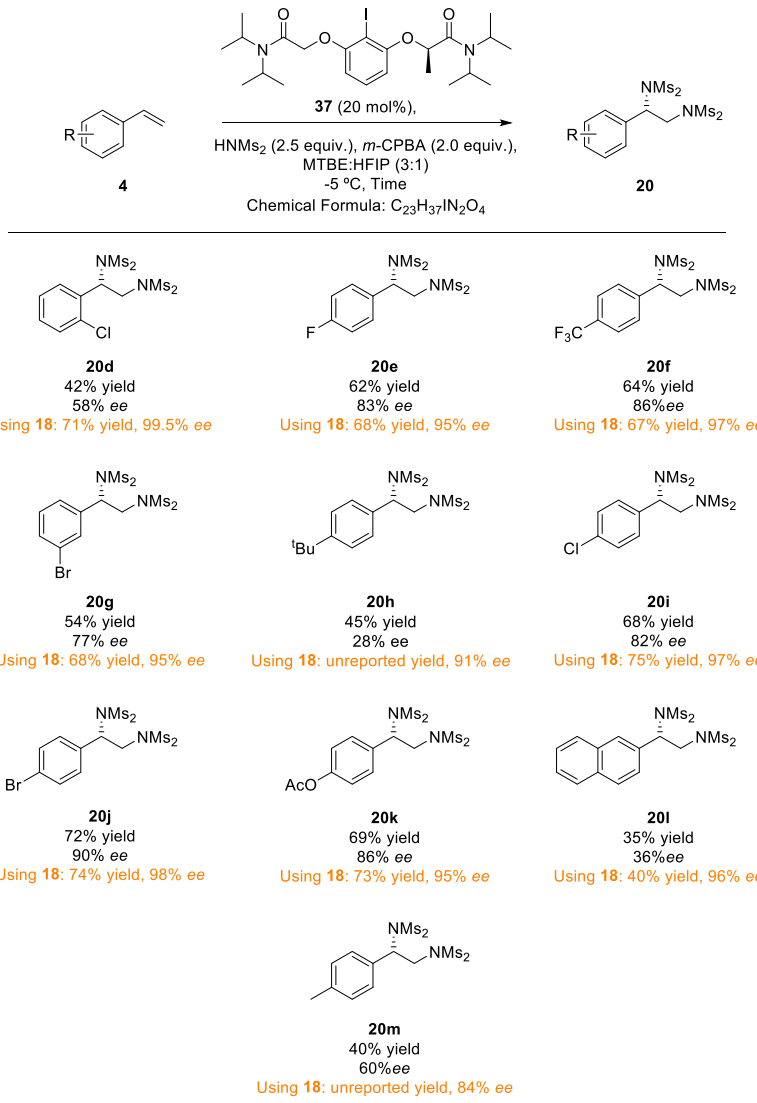

Scheme 118. Scope of the asymmetric diamination reaction using **37** as pre-catalyst

When a substrate bore a more EDG or EWG than the ones exposed above, the styrenes gave little or no conversion to their corresponding diamines.

For example, on the one hand electron-demanding *meta*-Nitrostyrene **20n** gave no conversion, and by-products were observed instead. On the other hand, electron-rich *para*-methoxystyrene **20q** also did not yield the

expected diamine. Other moieties such as the ones in **20o** or **20r** did not yield more than 20 or 10% yield respectively (Figure 33).

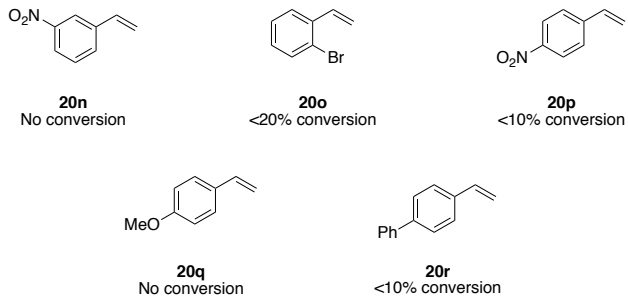

20n No conversion | **20o** <20% conversion | **20p** <10% conversion

20q No conversion | **20r** <10% conversion

Figure 33. Styrenes giving low or no product formation

The yields of the diamination reactions are comparable in most cases when using **37** and **18**. Even if many of the obtained diamines do not surpass the 6-7% difference in yields, products such as *ortho*-chlorinated **20d** gave a much larger difference. As stated above, this fact can be due to steric hindrance when using pre-catalyst **37**. In general, the trend for the yields of diamines **20** is maintained using **37** and **18** (Figure 34).

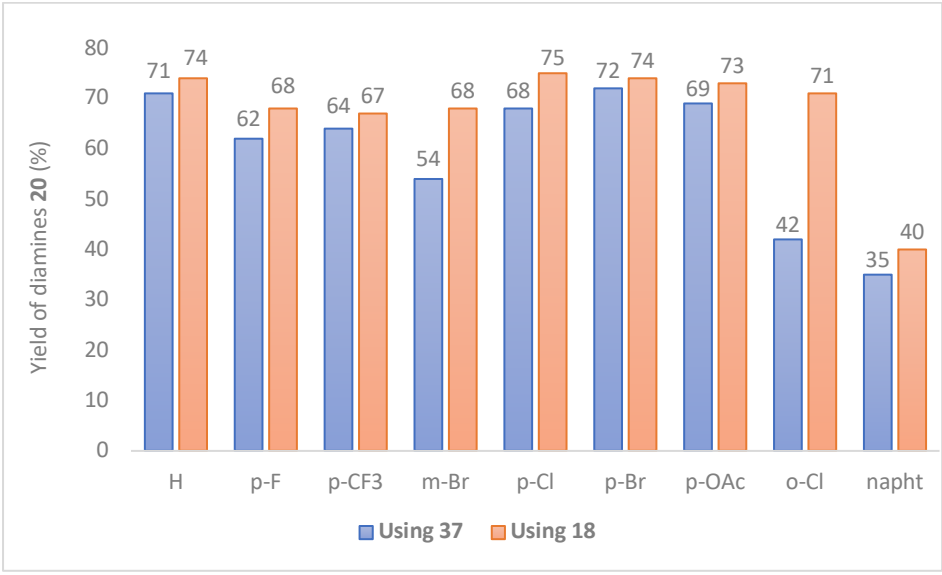

Figure 34. Yield comparison using **37** and **18**

In terms of *ee*, a close relationship between the yield and the enantioinduction was observed. In general, reactions with lower yield produced a lesser enantioenriched diamine, and higher yield transformations were in general associated with higher enantioinduction. Therefore, the steric and electronic effect mentioned above also play a role in the enantioinduction of this reaction.

While the lowest enantiomeric excess observed was 28% *ee* for **20h**, which has a bulky *para*-^{t}Bu substituent, the highest one observed was the 90% *ee* from substrate **20j**. Comparing *ee* for **20d** and **20g** shows that *meta*-substitution is better tolerated than *ortho*- substitution.

When examining the enantiodifferentiation obtained with **18** and **37**, one can observe that the difference between the *e.r.* values of the *S*-diamines obtained with **37** are similar. In fact, taking the 7 best substrates, this difference does not exceed 10% and goes as low as 3.5% for substrate **20j** (Figure 35 top). The higher difference is observed with substrate **20h** (95.5:4.5 *e.r.* with **18** to 64:36 *e.r.* using **37**).

When turning the *e.r.* values into *ee* the difference is clearer. Even though, most of the products keep a high percentage of their original *ee* (Figure 35 bottom).

With this results in hand, one can state that pre-catalyst **37** is more sensitive to steric bulkiness or changes in the substitution than pre-catalyst **18**. This can be due to a more flexible chiral pocket than in the case of **18**, which does not allow for as many changes in the reactive centres of the transformation. This fact could also be anticipated from the original design, given that the newly introduced achiral side-chain cannot hold such a steady position as the lactate-based side-chain.

Chapter IV – C_1-Symmetry in aryliodine catalyzed diaminations: A proof of concept

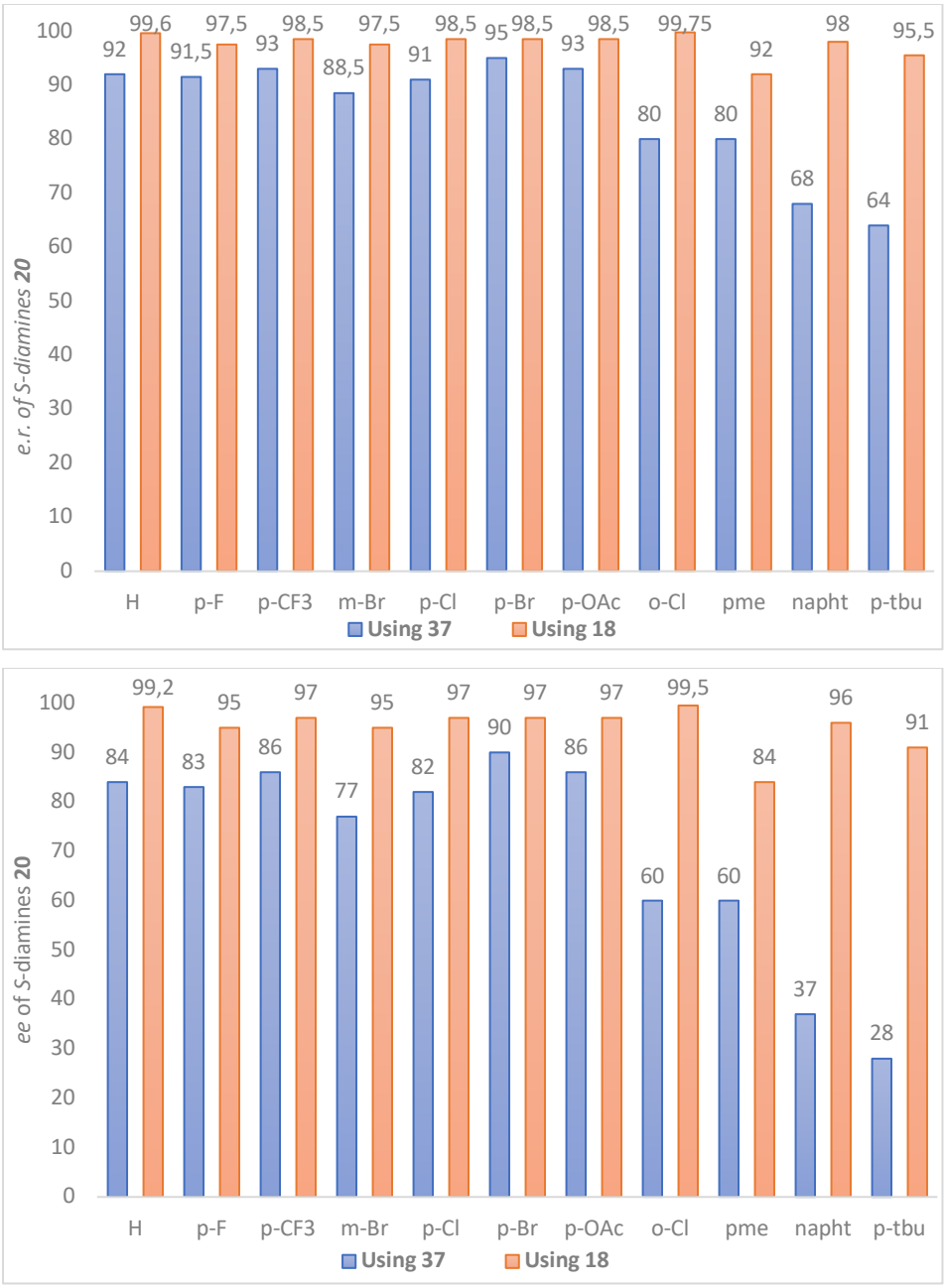

Figure 35. *e.r.* and *ee* for substrates **20** using **37** and **18** as pre-catalysts

4.2.5. Structural information and synthesis of I(III)

Both pre-catalysts **37** and **37'** were crystallized and analyzed by X-Ray diffraction. As expected, no relevant pre-organization was observed in their crystal structures (Figure 36).

When observing the crystal structure of **37**, a parallel display of both arms was found (Figure 36a). This fact is due to the type of packing observed in the obtained crystal, so no insight can be extracted to help understand the catalytic activity of this pre-catalyst. The same happened for the crystal of **37'**, as noncovalent interactions are not present in the crystal structure (Figure 36b).

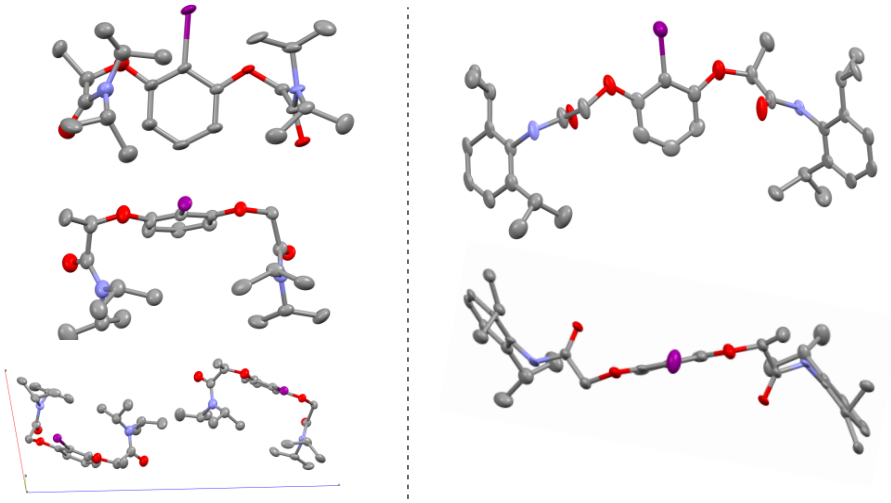

a) **37** b) **37'**

Figure 36. a) X-ray from **37** b) X-ray from **37'**

Chapter IV – C_1-Symmetry in aryliodine catalyzed diaminations: A proof of concept

To try to gain information on the active species in the catalytic cycle, the synthesis of the I(III) diacetate species of **37** was tried. Our group has already relied on the information from these species when oxidizing **16** and **18** to their corresponding I(III) diacetates.[134,135]

The reason behind this was that for a chiral pre-catalyst such as **37**, the diaminated version of the I(III) (diamidoiodane (III)) has never been isolated or crystallized.However, many conclusions can be drawn when observing the analogous Ar*I(OAc)$_2$.

All trials to synthesize and isolate the diacetoxy-I(III) compound derived from **37** were unsuccessful.

Many oxidation procedures were used, from the more classical $NaBO_3$ to the most recent oxidation of aryliodines using selectfluor and acetic acid by Wirth.[180] The low conversion and the presence of **37** prevented a full characterization of **41**.

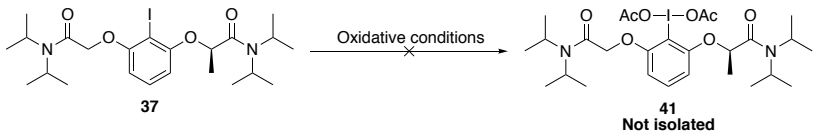

37 **41** **Not isolated**

Scheme 119. Unsuccessful synthesis of **41**

In view of the problematic synthesis of **41** the synthesis of analogous I(III) **41'** was also tried. It was rationalized that if any relevant structural information obtained from **41'** could help understand the action of C_1-symmetric pre-catalysts.

Trying several conditions (Table 10) it could be observed that the oxidation of this pre-catalyst was easier than **37**. Other oxidants like $NaClO{\cdot}5H_2O$, PIDA or DMP did not generate **41'**. The best results were obtained using Wirth's procedure for I(III) formation using Selectfluor, but the starting material was still observed by NMR.

Table 9. Screening for the oxidation of **37'**

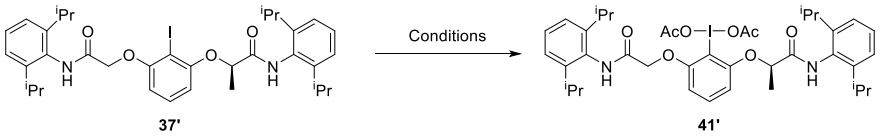

37' **41'**

Entry	Conditions	Crude NMR ratio **41':37'**
1	$NaBO_3 \cdot 4H_2O$ (16.0 equiv.), AcOH, RT, 16h	<1:1
2	$NaBO_3 \cdot 4H_2O$ (16.0 equiv.), AcOH, 45 ºC, 16h	<2:1
3	$NaClO \cdot 5H_2O$ (5.0 equiv.), AcOH, RT, 12h	<2.5:1
4	$NaClO \cdot 5H_2O$ (5.0 equiv.), AcOH, 50 ºC, 12h	<1:1
5	PIDA (2.0 equiv.), AcOH, RT, 12h	-
6	PIDA (10.0 equiv.), AcOH, RT, 12h	-
7	DMP (5.0 equiv.), AcOH, RT,12h	-
8	AcOOH (4.0 equiv.), AcOH, RT, 16h	3:1
9	Selectfluor (5.0 equiv.), Dry CH_3CN, RT,7h	4:1

The purification of **41'** by column chromatography, precipitation or washing was not possible as lactate-based I(III) compounds normally decompose when in contact with SiO_2 or other stationary phases.

Finally, crystallization was tried with a wide variety of polar protic and aprotic solvents, in combination with apolar solvents. Unfortunately, no crystals could be obtained from any of the trials.

Identification of **41'** was performed by NMR signal comparison with similar I(III). The signals corresponding to the proton of the secondary amide are more deshielded, as observed for many of this structures before (Figure 37).[180]

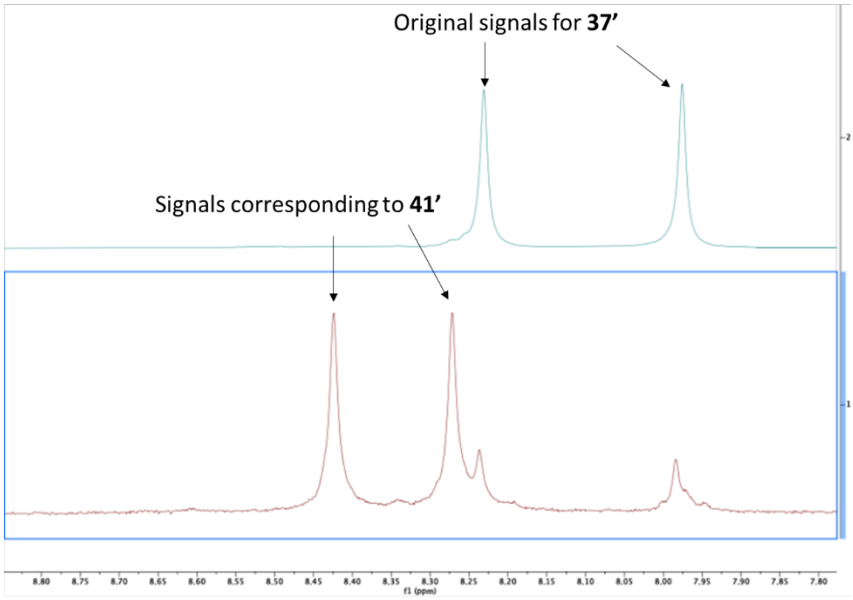

4.3. Conclusions

To conclude, we can state that the proof of concept was successful when looking at the yields and *ee* obtained when using **37** as a pre-catalyst for diamination. It is the first C_1-symmetric pre-catalyst based on the previous Muñiz pre-catalyst used in a reaction. Its design was based on our previous insight for these reactions and applied to the diamination and diacetoxylation reactions. Even though the diamination reaction yielded moderate yields and up to 90% *ee*, it was not the case of the diacetoxylated product.

The loss of enantiodifferentiation extracted from the scope demonstrates that even if **37** has half of the original chiral centres than **18**, its chiral pocket is still effective, with a minimum *e.r.* loss of 3.5%. Bulky or electronically disfavoured moieties were not as tolerated, as the minimum *ee* for a product was 28%. This fact could indicate that this chiral pocket is much more sensitive than in the case of **18** when the enantiodifferentiation takes place.

As for the noncovalent interactions within the catalytic environment of **37**, no experimental insight could be obtained. Both **41** and **41'** could not be crystallized and analyzed by X-ray diffraction or fully characterized.

4.4. Experimental part

4.4.1. General remarks

All solvents were commercially available and were used as received. Column chromatography was performed with silica gel (Merck, type 60, 0.063-0.2 mm). NMR data were recorded in deuterated solvents at 23 ºC on a Bruker Advance 400 Ultra Shield (400 MHz for ^{1}H, 100 MHz for ^{13}C and 376 MHz for ^{19}F) and Bruker 300 Ultrashield (300 MHz for ^{1}H and 75 MHz for ^{13}C) spectrometers. IR spectra were taken in a Bruker Alpha instrument in the solid or liquid state. Chemical shifts (δ) are reported in parts per million (ppm) and referenced to residual solvent. The following calibrations were used: $CDCl_3$ δ = 7.26 and 77.16 ppm. Coupling constants (*J*) are reported in Hertz (Hz). HPLC measurements were carried out on a Knauer Wellchrome (injection valve A0258, pump K-100, solvent organizer K-1500, UV-detector K-2600, detection at 220 or 254 nm) or on a Waters ACQUITY UPC2 SYSTEM (PDA photodiode array detector). The respective chiral stationary phase and exact conditions are specified for each individual compound within the compound characterization section. Thin layer chromatography (TLC) was carried out using Merck TLC Silicagel 60 F254 aluminum sheets; components were visualized by UV light (λ = 254 nm) and stained with permanganate dip. *m*-CPBA (≤77% purity) was purchased from Sigma Aldrich and used as received. The following compounds were commercially available and used as received: 4- fluorostyrene, 4-chlorostyrene, 4-bromostyrene, 4-tert-butylstyrene, 4-(trifluoromethyl)styrene, 4-vinylbiphenyl, 3-bromostyrene, 4-methoxystyrene, 4-acetoxystyrene, 4-methylstyrene, 4-vinylbiphenyl, 2-clorostyrene, 2-vinylnaphtalene, 1-Nitro-4-vinylbenzene, 1-Nitro-3-vinylbenzene, styrene, resorcinol, orcinol monohydrate, methyl bromoacetate.

4.4.2. Trials for pre-catalyst synthesis

The first route tried to pre-catalysts suitable for diamination and diacetoxylation started with a first mono O-alkylation of iodoorcinol **3c'** with **3d** or **3d'**. Then, the usual Mitsunobu procedure would be applied to obtain mono-esters **43**, which would be converted to pre-catalysts **45** by saponification, chlorination of the acid and amidation with diisopropylamine or 2,6-diisopropylaniline.

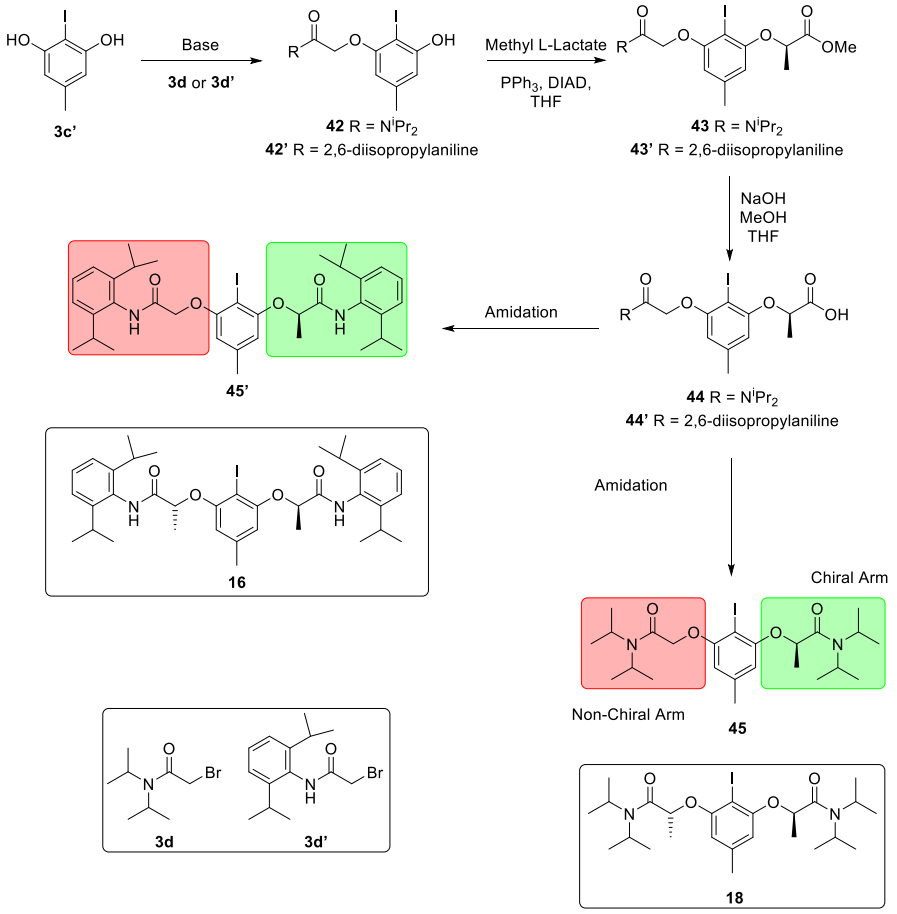

This route was discarded for the low yield of the first reaction. While the first trials with NaH and Py as bases did not yield any product and mostly decomposition was observed, trials with K_2CO_3 gave traces of the desired

mono-ester **42**. The double O-alkylated product **46** was formed always in a higher proportion, hampering the formation and isolation of **33**. Even though many bases and conditions were tried (See Table 10), the yield of **42** never went above 10%. The change in dryness of the reagents or solvents, temperature and base did not result in a clear product formation.

Table 10. Screening for mono O-alkylation of **3c'** with **3d** (Ratio 1:1). The reaction was left with the bases for 1h and controlled by TLC after addition of **3d**.

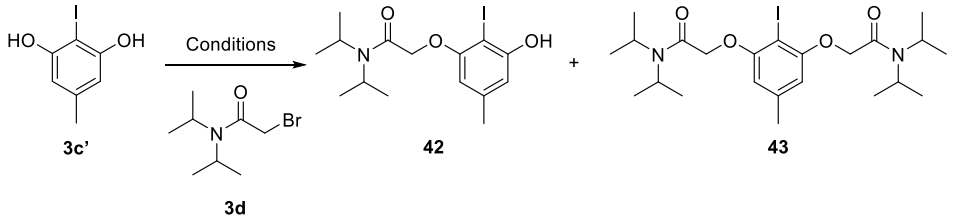

3c' 3d 42 43

Entry	Conditions	**33** Yield (%)	**37** Yield (%)
1	Py, DCM, RT	-	-
2	NaH (1.2 equiv.), DME, 0 ºC	-	-
3	NaH (1.0 equiv.), DME, 0 ºC to RT	-	-
4	NaH (1.2 equiv.), Dry DMF, RT	-	-
5	K_2CO_3 (1.2 equiv.), Acetone, RT	Traces	10%
6	K_2CO_3 (1.2 equiv.), Dry Acetone, RT	<5%	15%
7	K_2CO_3 (1.2 equiv.), Dry Acetone, 60 ºC	10%	20%

The same effect was observed when submitting **3c'** to reaction with **3d'** to obtain analogous pre-catalyst **45'** (based on pre-catalyst **16**). In this case, the reaction yielded 15% of the desired alcohol **42'**, but 66% of the di-alkylated species **46'** (Scheme 120).

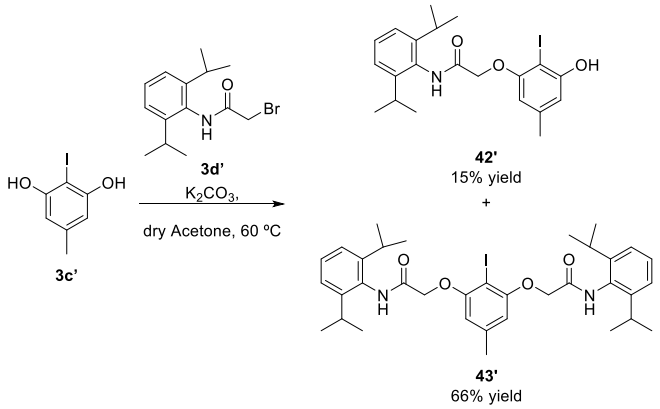

Scheme 120. O-alkylation of **3c'** using **3d'**

After these results, it was decided to use the starting material **3c** instead of **3c'**, which ultimately lead to the synthesized pre-catalysts **37** and **37'**. From the conclusions of Chapter III it can be extracted that luckily, pre-catalysts **17** and **18** have very comparable activities (See Chapter III).

4.4.3. Synthesis of 37 and 37'

Methyl 2-(3-hydroxy-2-iodophenoxy)acetate (34)

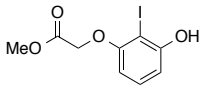

2-iodobenzene-1,3-diol (3.064 g, 12.984 mmol, 4.0 equiv.) was dissolved in 54 mL dry acetone under an argon atmosphere. Anhydrous K_2CO_3 (4.230 g, 12.984 mmol, 4.0 equiv.) was added slowly and the reaction mixture was stirred for 30 min at 60 °C. Methyl bromoacetate **33** (497 mg, 3.246 mmol, 1.0 equiv.) was then added dropwise and the reaction mixture was stirred for 30 min. at 60 ºC. The reaction mixture was filtered through cotton and concentrated under reduced pressure. Purification by flash column chromatography (5:1→4:1 Hex/EtOAc) afforded pure **34** as an off-white solid (576 mg, 1.872 mmol, 45 %).

R_f: 0.44 (2:1 Hex/EtOAc).

^{1}H-NMR (400 MHz; $CDCl_3$): δ = 7.16 (dd≈t, J = 8.2 Hz, 1H), 6.70 (dd, J = 8.2, 1.2 Hz, 1H), 6.27 (dd, J = 8.2, 1.2 Hz, 1H), 5.54 (s, 1H), 4.70 (s, 2H), 3.81 (s, 3H) ppm.

^{13}C-NMR (100 MHz; $CDCl_3$): δ = 168.9, 157.4, 156.6, 130.3, 109.0, 104.1, 78.8, 66.4, 52.5 ppm.

HRMS: calculated for $C_9H_9INaO_4^+$: 330.9438, found: 330.9438 ($[M+Na]^+$).

IR (ATR): $\tilde{\nu}$ = 3419, 1734, 1596, 1575, 1457, 1439, 1379, 1327, 1304, 1280, 1259, 1216, 1105, 1019, 977, 944, 772, 749, 703, 600, 549 cm^{-1}.

m.p.: 115-117 °C.

Methyl (*R*)-2-(2-iodo-3-(2-methoxy-2-oxoethoxy)phenoxy)propanoate (35)

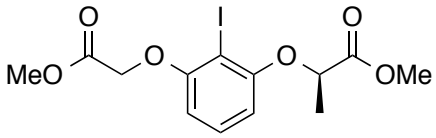

Methyl 2-(3-hydroxy-2-iodophenoxy)acetate **34** (430 mg, 1.396 mmol, 1 eq), methyl (*S*)-lactate (174 mg, 1.675 mmol, 1.2 eq), triphenylphosphine (439 mg, 1.675 mmol, 1.2 eq) and diisopropyl azodicarboxylate (339 mg, 1.675 mmol, 1.2 eq) were stirred under an argon atmosphere in 7 mL dry THF for 16 h at room temperature. Work-up and purification by flash column chromatography (DCM) afforded pure **35** as a colourless oil (514 mg, 1.304 mmol, 93 %).

R_f: 0.55 (2:1 Hex/EtOAc).

^{1}H-NMR (400 MHz; $CDCl_3$): δ = 7.17 (dd≈t, J = 8.3 Hz, 1H), 6.37-6.41 (m, 2H), 4.77 (q, J = 6.8 Hz, 1H), 4.70 (s, 2H), 3.80 (s, 3H), 3.75 (s, 3H), 1.70 (d, J = 6.8 Hz, 3H) ppm.

^{13}C-NMR (100 MHz; $CDCl_3$): δ = 172.2, 169.0, 158.5, 158.4, 129.8, 107.2, 106.2, 80.1, 74.4, 66.6, 52.5, 52.5, 18.7 ppm.

HRMS: calculated for $C_{13}H_{15}INaO_6^+$: 416.9806, found: 416.9812 ($[M+Na]^+$).

IR (ATR): $\tilde{\nu}$ = 2953, 1753, 1735, 1586, 1460, 1435, 1376, 1263, 1205, 1130, 1107, 1053, 1021, 999, 976, 847, 763, 701, 639, 622 cm^{-1}.

(*R*)-2-(3-(Carboxymethoxy)-2-iodophenoxy)propanoic acid (36)

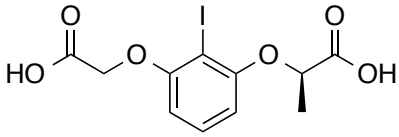

Methyl (*R*)-2-(2-iodo-3-(2-methoxy-2-oxoethoxy)phenoxy)propanoate (450 mg, 1.142 mmol, 1 eq) and aqueous NaOH (2 M, 3.2 mL, 6.393 mmol, 5.6 eq) were stirred in 6 mL THF/MeOH (1:1) for 4 h at room temperature. Work-up afforded pure **36** as a white solid (385 mg, 1.052 mmol, 92 %).

^{1}H-NMR (400 MHz; DMSO-d_6): δ = 7.22 (dd≈t, J = 8.3 Hz, 1H), 6.49 (d, J = 8.2 Hz, 1H), 6.43 (d, J = 8.3 Hz, 1H), 4.85 (q, J = 6.7 Hz, 1H), 4.75 (s, 2H), 1.55 (d, J = 6.7 Hz, 3H) ppm.

^{13}C-NMR (100 MHz; DMSO-d_6): δ = 172.6, 169.8, 157.9, 157.6, 129.7, 105.9, 105.4, 78.8, 72.8, 65.6, 18.3 ppm.

HRMS: calculated for $C_{11}H_{10}IO_6^-$: 364.9528, found: 364.9522 ([M-H]$^-$).

IR (ATR): $\tilde{\nu}$ = 2989, 2918, 1704, 1588, 1465, 1424, 1312, 1257, 1227, 1187, 1025, 898, 769, 703, 687, 649, 620, 578 cm^{-1}.

m.p.: >157 °C (decomp.).

(R)-2-(3-(2-(diisopropylamino)-2-oxoethoxy)-2-iodophenoxy)-N,N-diisopropylpropanamide (37)

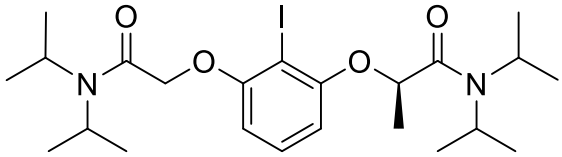

(*R*)-2-(3-(Carboxymethoxy)-2-iodophenoxy)propanoic acid **36** (350 mg, 0.956 mmol, 1 equiv.), oxalyl chloride (425 mg, 3.346 mmol, 3.5 equiv.) and a catalytic amount of DMF were stirred in 10 mL dry DCM for 1.5 h at room temperature under an argon atmosphere. The reaction mixture was concentrated *in vacuo* and redissolved in 5 mL dry DCM. Diisopropylamine (678 mg, 3.824 mmol, 4.0 equiv.) was added and the mixture was stirred for 1h at room temperature under an argon atmosphere. The reaction mixture was quenched by addition of aqueous HCl 3M (4 mL). Purification by flash column chromatography (DCM→10:1 DCM/MeOH) afforded pure as a white foam (468 mg, 0.685 mmol, 70 %).
R_f: 0.50 (2:1 Hex/EtOAc).
^{1}H-NMR (500 MHz, $CDCl_3$) δ 7.16 (t, J = 8.3 Hz, 1H), 6.60 (dd, J = 8.4, 1.0 Hz, 1H), 6.54 (dd, J = 8.4, 1.0 Hz, 1H), 4.84 (q, J = 6.9 Hz, 1H), 4.67 (s, 2H), 4.57 – 4.49 (m, 1H), 4.24 (s, 1H), 3.39 (s, 1H), 3.34 – 3.27 (m, 1H), 1.67 (d, J = 6.9 Hz, 3H), 1.39 (dd, J = 16.4, 6.8 Hz, 9H), 1.29 (d, J = 6.8 Hz, 3H), 1.19 (dd, J = 6.5, 3.5 Hz, 9H), 0.91 (d, J = 6.5 Hz, 3H) ppm.
^{13}C-NMR (126 MHz, $CDCl_3$) δ 169.66, 166.52, 158.43, 157.90, 130.14, 106.41, 105.85, 78.31, 78.02, 70.91, 48.99, 47.77, 46.59, 46.33, 21.21, 21.19, 21.05, 20.73, 20.66, 20.44, 20.04, 18.07 ppm.
HRMS: calculated for $C_{23}H_{37}IN_2NaO_4^+$: 555.1685, found: 555.1690 ($[M+Na]^+$).
IR (ATR): $\tilde{\nu}$ = 3378, 2961, 2929, 2868, 1689, 1587, 1499, 1459, 1382, 1362, 1332, 1254, 1238, 1096, 1022, 934, 797, 764, 752, 703, 658, 634, 551, 517, 489 cm^{-1}.

m.p.: 80-82 °C.

SFC (ID, CO_2/Ethanol, 80/20, 3 mL/min, l = 210 nm) T_R= 2.02 min (*R*), 2.95 (*S*), 99% *ee*.

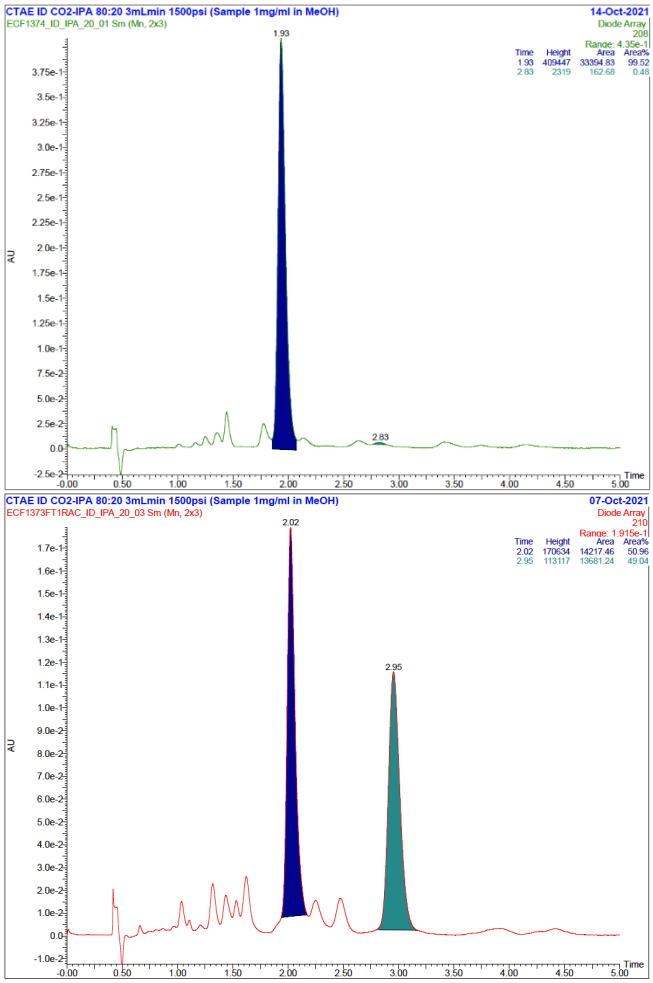

(*R*)-*N*-(2,6-Diisopropylphenyl)-2-(3-(2-((2,6-diisopropylphenyl)amino)-2-oxoethoxy)-2-iodophenoxy)propanamide (42)

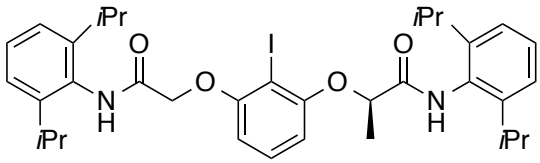

(*R*)-2-(3-(Carboxymethoxy)-2-iodophenoxy)propanoic acid **36** (350 mg, 0.956 mmol, 1 eq), oxalyl chloride (425 mg, 3.346 mmol, 3.5 eq) and a catalytic amount of DMF were stirred in 10 mL dry DCM for 3 h at room temperature under an argon atmosphere. The reaction mixture was concentrated *in vacuo* and the crude product, 2,6-diisopropylaniline (678 mg, 3.824 mmol, 4 eq) were stirred in 5 mL dry DCM for 16 h at room temperature under an argon atmosphere. Work-up and purification by flash column chromatography (DCM→10:1 DCM/MeOH) afforded pure **37'** as a white solid (596 mg, 0.871 mmol, 91 %).

R_f: 0.42 (2:1 Hex/EtOAc).

^{1}H-NMR (400 MHz; $CDCl_3$): δ = 8.23 (s, 1H), 7.98 (s, 1H), 7.42 (dd≈t, *J* = 8.3 Hz, 1H), 7.27-7.37 (m, 2H), 7.22 (d, *J* = 7.7 Hz, 2H), 7.18 (d, *J* = 7.7 Hz, 2H), 6.73 (dd≈d, *J* = 7.9 Hz, 1H), 6.66 (dd, *J* = 8.4, 1.0 Hz, 1H), 5.07 (q, *J* = 6.7 Hz, 1H), 4.74-4.84 (m, 2H), 3.12 (hept, *J* = 6.8 Hz, 2H), 2.88-3.05 (m, 2H), 1.81 (d, *J* = 6.7 Hz, 3H), 1.06-1.28 (m, 24H) ppm.

^{13}C-NMR (100 MHz; $CDCl_3$): δ = 170.6, 166.7, 157.5, 157.1, 146.3, 131.0, 130.1, 130.1, 128.9, 128.8, 123.8, 123.7, 107.6, 106.6, 79.9, 76.4, 68.4, 29.0, 28.8, 23.9, 23.8, 18.8 ppm.

HRMS: calculated for $C_{35}H_{45}IN_2NaO_4^+$: 707.2316, found: 707.2300 ($[M+H]^+$).

IR (ATR): $\tilde{\nu}$ = 3378, 2961, 2929, 2868, 1689, 1587, 1499, 1459, 1382, 1362, 1332, 1254, 1238, 1096, 1022, 934, 797, 764, 752, 703, 658, 634, 551, 517, 489 cm^{-1}.

m.p.: 80-82 °C.

4.4.4. Diacetoxylation of styrenes

The followed procedure is described in section 3.4.7. but using **37'** instead of **16** as pre-catalyst.

(S)-1-Phenylethane-1,2-diyl diacetate (29)

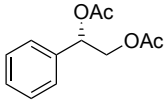

Following the general procedure, work-up and purification by flash column chromatography (Hex/EtOAc 15:1 to 10:1) afforded pure 29 (31.4 mg, 0.141 mmol, 71 %).

^{1}H-NMR (400 MHz; CDCl3): δ = 7.30-7.40 (m, 5H), 6.02 (dd, J = 7.9, 4.0 Hz, 1H), 4.34 (dd, J = 11.9, 4.0 Hz, 1H), 4.29 (dd, J = 11.9, 7.9 Hz, 1H), 2.12 (s, 3H), 2.06 (s, 3H) ppm.

^{13}C-NMR (100 MHz; CDCl3): δ = 170.7, 170.2, 136.6, 128.8, 128.7, 126.8, 73.5, 66.2, 21.2, 20.9 ppm.

(S)-1-Phenylethane-1,2-diol (30)

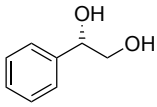

^{1}H-NMR (500 MHz; CDCl3): δ = 7.29-7.37 (m, 5H), 4.83 (dd, J = 8.2, 3.6 Hz, 1H), 3.77 (dd, J = 11.5, 3.6 Hz, 1H), 3.67 (dd, J = 11.5, 8.2 Hz, 1H), 2.68 (br. s, 1H), 2.26 (br. s, 1H) ppm.

^{13}C-NMR (125 MHz; CDCl3): δ = 140.6, 128.7, 128.2, 126.2, 74.8, 68.2 ppm.

HPLC: CHIRALCEL® OD-H, Hex/iPrOH = 90:10, 1 mL/min, t_R = 34.9 min (minor), 37.5 min (major), 58% ee.

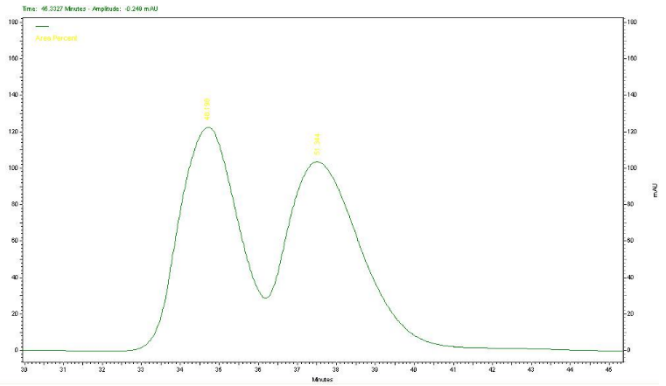

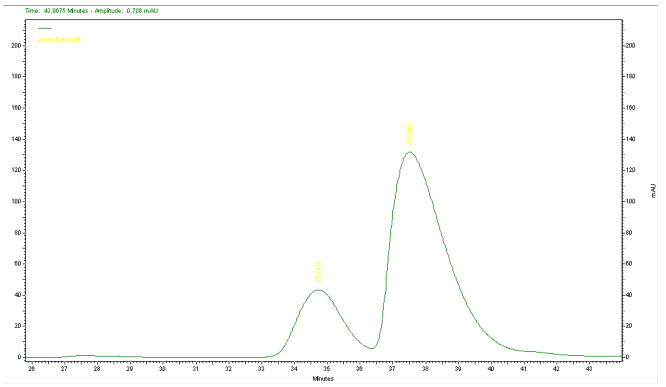

4.4.5. General procedure for the diamination of styrenes

In a sealed pyrex tube, styrene (0.1 mmol) was added to a mixture of $HNMs_2$ (2.5 equiv), **42** (0.2 equiv.) and *m*-CPBA (2 equiv.) in HFIP (0.09 mL) and MTBE (0.26 mL) at -5 ºC. After 48 h of reaction, the mixture was quenched with $NaHCO_3$ and extracted with DCM (3x), dried over Na_2SO_4 and evaporated under reduced pressure. The final crude product was S12 purified by chromatography (silica gel, n-hexane/ethyl acetate, 85/15, v/v to 2/1, v/v) to give the pure diaminated product.

4.4.6. Characterization and Chromatograms of diamines 20

(*S*)-*N*,*N*'-(1-Phenylethane-1,2-diyl)bis(*N*-(methylsulfonyl)methanesulfonamide) (20a)

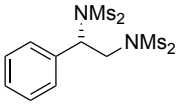

Isolated as a white foam in 72% yield.

^{1}H-NMR (400 MHz, $CDCl_3$): δ = 7.60-7.64 (m, 2H), 7.40-7.46 (m, 3H), 5.91 (dd *J* = 5.3, 6.7 Hz, 1H), 4.79 (dd, *J* = 5.3, 15.3 Hz, 1H), 4.57 (dd, *J* = 6.8, 15.3 Hz, 1H), 3.30-3.84 (bs, 3H), 3.24 (s, 6H), 2.25-2.87 (bs, 3H) ppm.

^{13}C-NMR (100 MHz, $CDCl_3$): δ = 133.9, 130.2, 129.8, 129.2, 63.5, 50.8, 44.5, 43.3 ppm.

HPLC: Chiralpak-IB, 0.8 mL/min, Hexanes/EtOH, 80/20, v/v, t_R = 16.7 min (*S*-enantiomer), 19.5 min (*R*-enantiomer), 84% *ee.*

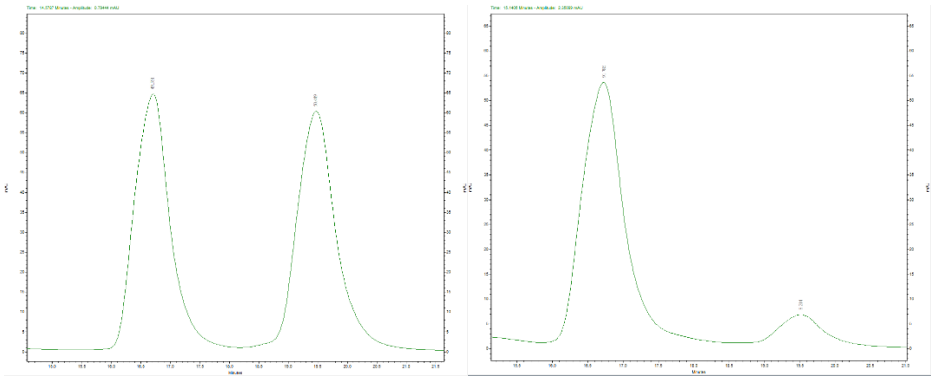

(*S*)-*N*,*N*'-(1-(2-Chlorophenyl)ethane-1,2-diyl)bis(*N*-(methylsulfonyl)

Chapter IV – C_1-Symmetry in aryliodine catalyzed diaminations: A proof of concept

methanesulfonamide) (20d)

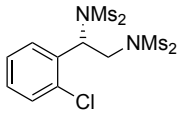

Isolated as white foam in 42% yield. Spectroscopic data in accordance with literature.

^{1}H-NMR (400 MHz, $CDCl_3$): δ = 7.59 (dd, *J* = 2.3, 7.3 Hz, 1H), 7.46-7,49 (m, 1H), 7.33-7.40 (m, 2H), 6.20-6.24 (m, 1H), 4.73-4.80 (m, 1H), 4.37-4.42 (m, 1H), 3.44 (s, 6H), 2.38-3.32 (bs, 6H) ppm.

^{13}C-NMR (100 MHz, $CDCl_3$): δ = 135.9, 132.6, 131.2, 131.0, 130.4, 127.0, 59.1, 50.8, 42.6, ppm.

HPLC: Chiralpak-IB, 0.8 mL/min, Hexanes/EtOH, 80/20, v/v, t_R = 22.9 min (*S*-enantiomer), 25.7 min (*R*-enantiomer). 58% *ee*.

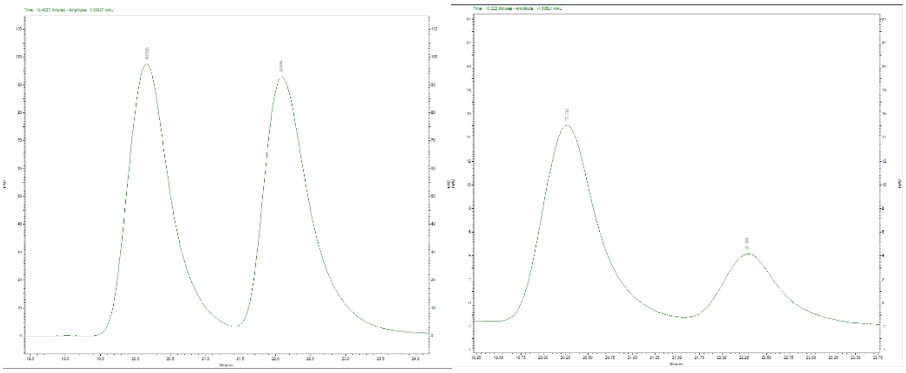

(*S*)-*N*,*N*'-(1-(4-Fluorophenyl)ethane-1,2-diyl)bis(*N*-(methylsulfonyl) methanesulfonamide) (20e)

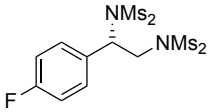

Isolated as white foam in 62% yield. Spectroscopic data in accordance with literature.

^{1}H-NMR (400 MHz, $CDCl_3$): δ = 7.61-7.66 (m, 2H), 7.12-7.17 (m, 2H), 5.88 (pst, *J* = 6.0 Hz, 1H), 4.76 (dd, *J* = 5.6, 15.4 Hz), 4,52 (dd, *J* = 6.5, 15.4 Hz, 1H), 3.28-3.76 (bs, 3H), 3.24 (s, 6H), 2.31-2.87 (bs, 3H) ppm.

^{13}C-NMR (100 MHz, $CDCl_3$): δ = 163.2 (d, *J* = 251.0 Hz), 132.2 (d, *J* = 8.3 Hz), 129.8 (d, *J* = 3.5 Hz), 116.2 (d, *J* = 21.5 Hz), 62.8, 50.9, 44.6, 43.3 ppm.

^{19}F-NMR (376 MHz, CDCl3): δ = -110.3 ppm.

HPLC: Chiralpak-IB, 0.8 mL/min, Hexanes/EtOH, 80/20, v/v, t_R = 16.2 min (*S*-enantiomer), 20.4 min (*R*-enantiomer), 83% *ee*.

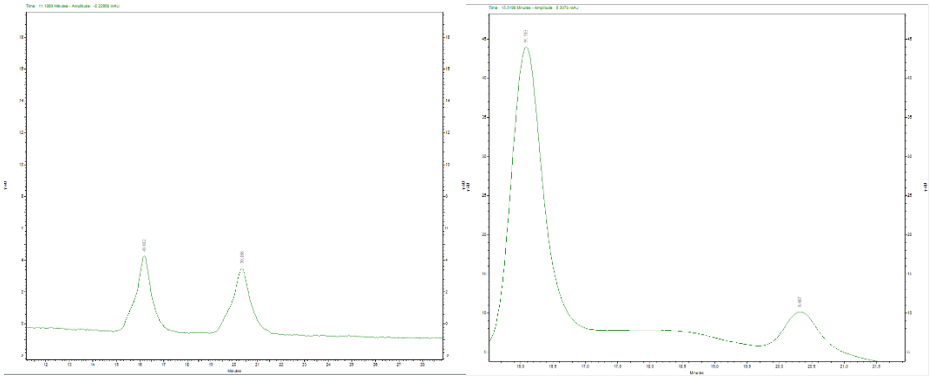

Chapter IV – C_1-Symmetry in aryliodine catalyzed diaminations: A proof of concept

(*S*)-*N*,*N*'-(1-(4-Bromophenyl)ethane-1,2-diyl)bis(*N*-(methylsulfonyl) methanesulfonamide) (20f)

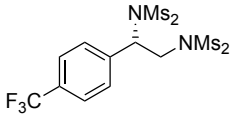

Isolated as white foam in 64% yield. Spectroscopic data in accordance with literature.[7]

^{1}H-NMR (400 MHz, CDCl3): δ = 7.76-7.79 (m, 2H), 7.71-7.73 (m, 2H), 5.93 (dd, *J* = 5.3, 6.6 Hz, 1H), 4.77 (dd, *J* = 5.2, 15.3 Hz, 1H), 4.60 (dd, *J* = 6.7, 15.3 Hz, 1H), 3.31-3.75 (bs, 3H), 3.28 (s, 6H), 2.29-2.90 (bs, 3H) ppm.

^{13}C-NMR (100 MHz, $CDCl_3$): δ = 138.0,132.0 (q, *J* = 33.0 Hz), 130.6, 126.1 (d, *J* = 3.7 Hz), 123.7 (q, *J* = 272.5 Hz), 62.8, 50.4, 44.6, 43.3 ppm.

^{19}F-NMR (376 MHz, CDCl3): δ = -63.0 ppm.

HPLC: Chiralpak-IB, 0.8 mL/min, Hexanes/EtOH, 80/20, v/v, t_R = 14.8 min (*S*-enantiomer), 23.4 min (*R*-enantiomer). 86% *ee*.

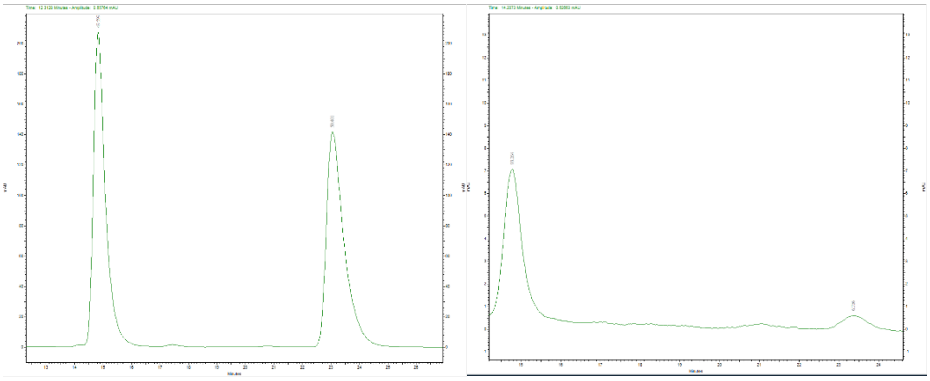

(*S*)-*N*,*N*'-(1-(3-Bromophenyl)ethane-1,2-diyl)bis(*N*-(methylsulfonyl) methanesulfonamide) (20g)

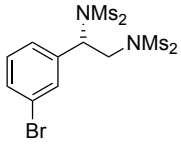

Isolated as white foam in 54% yield. Spectroscopic data in accordance with literature.

^{1}H-NMR (400 MHz, $CDCl_3$): δ = 7.75 (s, 1H), 7.56 (d, *J* = 8.1 Hz, 2H), 7.32 (t, *J* = 7.9 Hz, 1H), 5.84 (pst, *J* = 6.2 Hz, 1H), 4.69 (dd, *J* = 5.0, 15.3 Hz, 1H), 4,57 (dd, *J* = 6.9, 15.3 Hz, 1H), 3.33-3.78 (bs, 3H), 3.28 (s, 6H), 2.30-3.93 (bs, 3H) ppm.

^{13}C-NMR (100 MHz, $CDCl_3$): δ = 136.2, 133.1, 133.0, 130.6, 128.7, 123.1, 62.7, 50.5, 44.6,43.2 ppm.

HPLC: Chiralpak-IB, 0.8 mL/min, Hexanes/EtOH, 80/20, v/v, t_R = 15.7 min (*S*-enantiomer), 17.5 min (*R*-enantiomer). 77% *ee*.

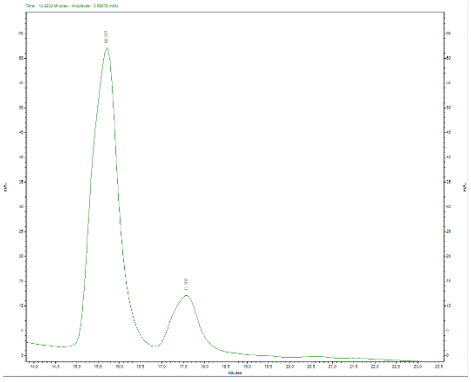

(1-(4-(tert-Butyl)phenyl)ethane-1,2-diyl)bis(N-(methylsulfonyl) methanesulfonamide) (20h):

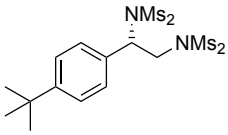

Isolated as a white solid in 45% yield. Spectroscopic data in accordance with literature.

^{1}H-NMR (500 MHz, CDCl3): δ = 7.52 (m, 2H), 7.44 (m, 2H), 5.88 (dd, J = 5.2, 6.8 Hz, 1H), 4.75(dd, J = 5.2, 15.3 Hz, 1H), 4.57 (dd, J = 6.8, 15.3 Hz, 1H), 3.28- 3.78 (bs, 3H), 3.24 (s, 6H), 2.19-3.10 (bs, 3H), 1.31 (s, 9H) ppm.

^{13}C-NMR (125 MHz, CDCl3): δ = 153.2, 130.7, 129.8, 125.9, 63.2, 50.8, 44.5 (bs), 43.2, 34.9,31.3 ppm.

HPLC: Chiralpak-IB, 1.0 mL/min, hexanes/EtOH, 80/20, v/v, t_R = 12.1 min (Senantiomer), 16.8 min (R-enantiomer). 28% *ee*.

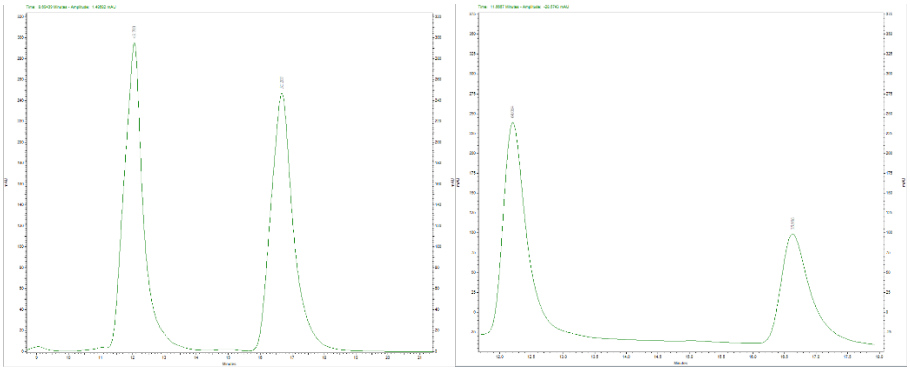

N,N'-(1-(4-Chlorophenyl)ethane-1,2-diyl)bis(N-(methylsulfonyl) methanesulfonamide) (20i):

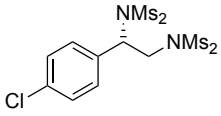

Isolated as a white solid in 68% yield. Spectroscopic data in accordance with literature.

^{1}H-NMR (300 MHz, CDCl3): δ = 7.58 (d, J = 8.5 Hz, 2H), 7.42 (d, J = 8.6 Hz, 2H), 5.85 (pst, J = 6.0 Hz, 1H), 4.75 (dd, J = 5.5, 15.3 Hz, 1H), 4.52 (dd, J = 6.5, 15.3 Hz, 1H), 3.30-3.94 (bs, 3H), 3.25 (s, 6H), 2.23-2.98 (bs, 3H) ppm.

^{13}C-NMR (75 MHz, CDCl3): δ = 136.0, 132.4, 131.6, 129.4, 62.8, 50.7, 44.5 (bs), 43.3 ppm.

HPLC: Chiralpak-IB, 1.0 mL/min, hexanes/EtOH, 80/20, v/v, t_R = 16.5 min (Senantiomer), 22.1 min (R-enantiomer). 82% *ee*.

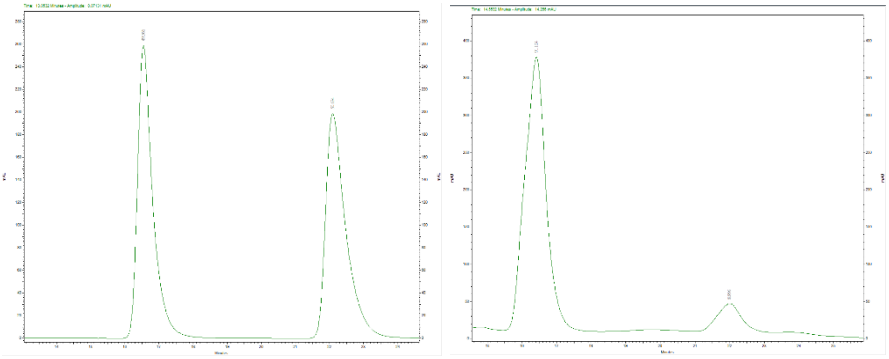

Chapter IV – C_1-Symmetry in aryliodine catalyzed diaminations: A proof of concept

N,N'-(1-(4-bromophenyl)ethane-1,2-diyl)bis(N-(methylsulfonyl) methanesulfonamide) (20j):

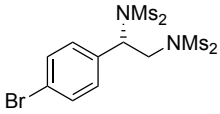

Isolated as a white foam in 72% yield. Spectroscopic data in accordance with literature.

^{1}H-NMR (400 MHz, CDCl3): δ = 7.57-7.59 (m, 2H), 7.49-7.52(m, 2H), 5.83 (pst, J = 6.0 Hz, 1H), 4.74 (dd, J = 5.5, 15.3 Hz, 1H), 4.52 (dd, J = 6.5, 15.3 Hz, 1H), 3.25 (s, 6H),3.29-3.74 (bs, 3H), 2.29-2.92 (bs, 3H) ppm.

^{13}C-NMR (100 MHz, CDCl3): δ = 132.9, 132.4, 131.8, 124.2, 62.9, 50.6, 44.6, 43.3 ppm.

HPLC: Chiralpak-IB, 0.8 mL/min, Hexanes/EtOH, 80/20, v/v, t_R = 17.8 min (S-enantiomer), 24.3 min (R-enantiomer). 90% ee.

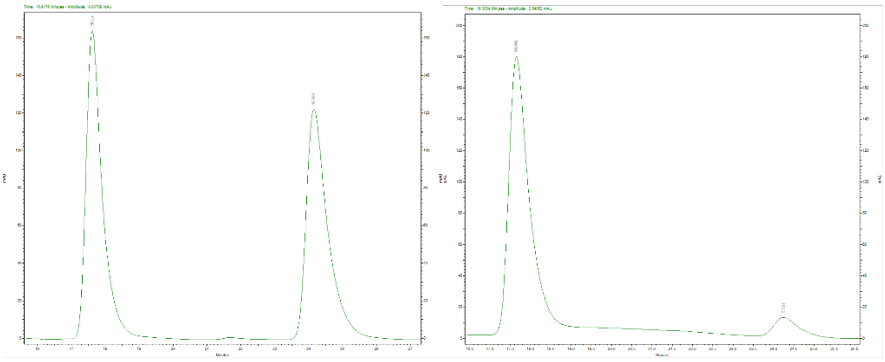

N,N'-(1-(4-bromophenyl)ethane-1,2-diyl)bis(N-(methylsulfonyl) methanesulfonamide) (20k):

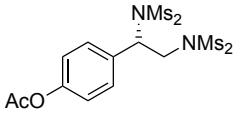

Isolated as a white foam in 69% yield. Spectroscopic data in accordance with literature.

^{1}H-NMR (400 MHz, $CDCl_3$): δ = 7.64 (dd, *J* = 8.5 Hz, 2H), 7.16 (d, *J* = 8.5 Hz, 2H), 5.88-5.91 (m, 1H), 4.76 (dd, *J* = 5.5, 15.3 Hz, 1H), 4.53 (dd, *J* = 6.7, 15.5 Hz, 1H), 3.10-3.80 (bs, 3H), 3.23 (s, 6H), 2.35-3.00 (bs, 3H), 2.29 (s, 3H) ppm.

^{13}C-NMR (125 MHz, $CDCl_3$): δ = 169.1, 151.5, 131.4, 131.3, 122.4, 62.9, 50.7, 44.5 (bs), 43.2, 21.2, ppm.

HPLC: Chiralpak-IB, 0.8 mL/min, Hexanes/EtOH, 80/20, v/v, t_R = 19.8 min (*S*-enantiomer), 26.5 min (*R*-enantiomer). 86% *ee*.

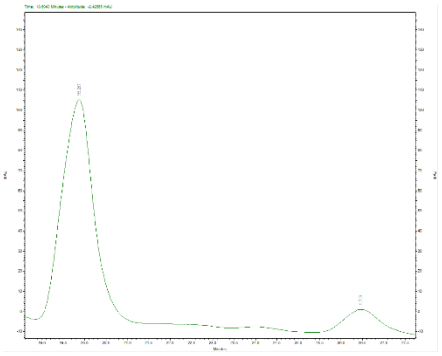

Chapter IV – C_1-Symmetry in aryliodine catalyzed diaminations: A proof of concept

N,N'-(1-(Naphthalen-2-yl)ethane-1,2-diyl)bis(N-(methylsulfonyl) methanesulfonamide) (20l):

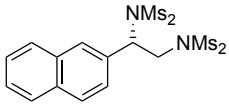

Isolated as a white solid in 35% yield. Spectroscopic data in accordance with literature.

^{1}H-NMR (400MHz, CDCl3): δ = 8.10 (s, 1H), 7.91 (d, J = 7.9 Hz, 2H), 7.80-7.90 (m, 1H), 7.70 (dd, J = 1.9, 8.6 Hz, 1H), 7.50-7.60 (m, 2H), 6.07 (pst, J = 6.0 Hz, 1H), 4.95 (dd, J = 5.3, 15.3 Hz, 1H), 4.67 (dd, J = 6.7, 15.3 Hz, 1H), 2.90-4.00 (bs, 3H), 3.25 (s, 6H), 1.85-2.90 (bs, 3H) ppm.

^{13}C-NMR (100MHz, CDCl3): δ = 133.4, 132.9, 130.9, 129.9, 129.1, 128.7, 127.8, 127.6, 127.1, 127.0, 63.6, 50.9, 44.6, 43.3 ppm.

HPLC: Chiralpak-IB, 0.7 mL/min, hexanes/EtOH, 80/20, v/v, t_R = 36.8min (*S*-enantiomer), 39.0 min (R-enantiomer). 36% *ee*.

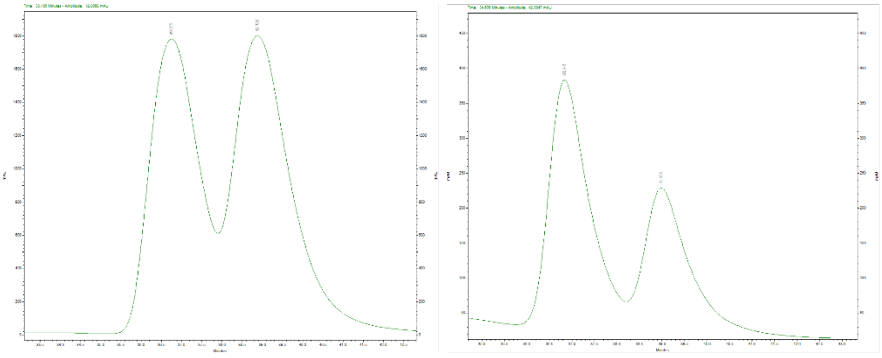

N,N'-(1-(Naphthalen-2-yl)ethane-1,2-diyl)bis(N-(methylsulfonyl) methanesulfonamide) (20m):

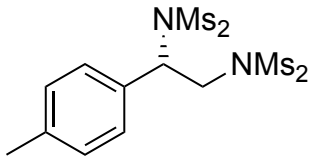

Isolated as a white foam in 40% yield. Spectroscopic data in accordance with literature.

^{1}H-NMR (400 MHz, $CDCl_3$): δ = 7.64 (dd, *J* = 8.5 Hz, 2H), 7.16 (d, *J* = 8.5 Hz, 2H), 5.88-5.91 (m, 1H), 4.76 (dd, *J* = 5.5, 15.3 Hz, 1H), 4.53 (dd, *J* = 6.7, 15.5 Hz, 1H), 3.10-3.80 (bs, 3H), 3.23 (s, 6H), 2.35-3.00 (bs, 3H),2.29 (s, 3H) ppm.

^{13}C-NMR (125 MHz, $CDCl_3$): δ = 169.1, 151.5, 131.4, 131.3, 122.4, 62.9, 50.7, 44.5 (bs), 43.2, 21.2 ppm.

HPLC: Chiralpak-IB, 0.8 mL/min, Hexanes/EtOH, 80/20, v/v, t_R = 14.5 min (*S*-enantiomer), 17.20 min (*R*-enantiomer). 60% *ee*.

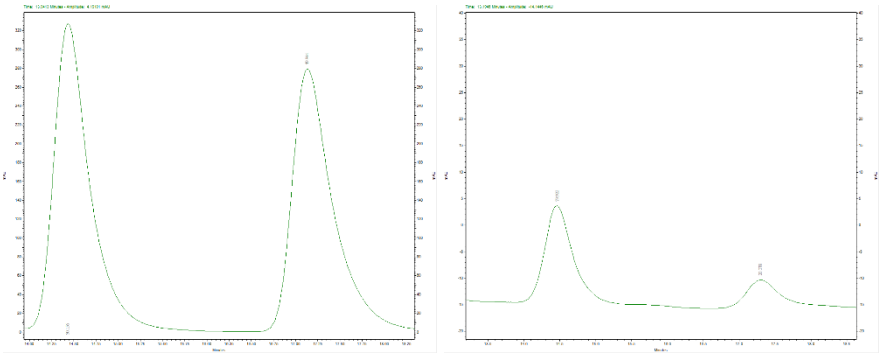

4.4.7. X-Ray Analysis of pre-catalysts 37 and 37'

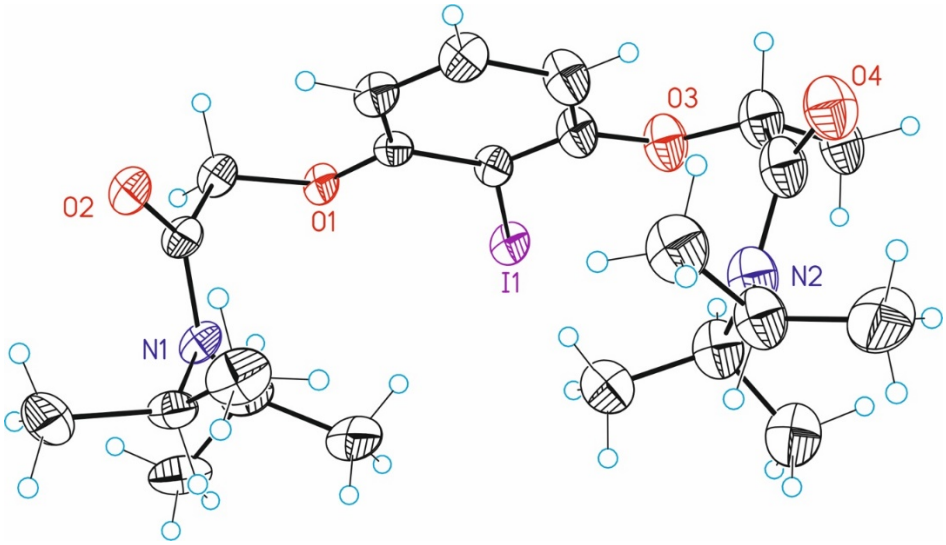

Table 11. Crystal data and structure refinement for **37**.

Identification code	mo_ECF1265FT2-05	
Empirical formula	C24 H37.55 Cl3 I N2 O4	
Formula weight	651.36	
Temperature	100(2)K	
Wavelength	0.71073 Å	
Crystal system	monoclinic	
Space group	P 21	
Unit cell dimensions	a = 8.4470(8)Å	a= 90°.
	b = 8.2569(8)Å	b = 98.838(3)°.
	c = 21.498(2)Å	g = 90°.
Volume	1481.6(3) Å3	
Z	2	
Density (calculated)	1.460 Mg/m3	
Absorption coefficient	1.381 mm-1	
F(000)	663	

Crystal size	0.050 x 0.050 x 0.020 mm^3
Theta range for data collection	1.917 to 25.392°.
Index ranges	-10<=h<=10,-9<=k<=9,-25<=l<=25
Reflections collected	5327
Independent reflections	5327[R(int) = ?]
Completeness to theta	=25.392° 99.2%
Absorption correction	Multi-scan
Max. and min. transmission	0.74 and 0.57
Refinement method	Full-matrix least-squares on F2
Data / restraints / parameters	5327/ 270/ 465
Goodness-of-fit on F2	1.043
Final R indices [I>2sigma(I)]	R1 = 0.0576, wR2 = 0.1289
R indices (all data)	R1 = 0.0787, wR2 = 0.1391
Flack parameter	x =0.01(3)
Largest diff. peak and hole	1.376 and -0.658 e.Å-3

Chapter IV – C_1-Symmetry in aryliodine catalyzed diaminations: A proof of concept

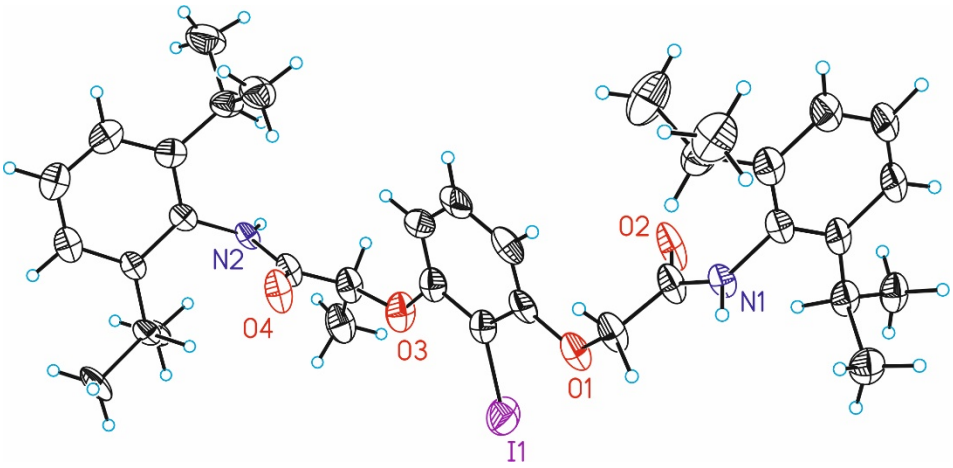

Table 12. Crystal data and structure refinement for **37'**.

Identification code	mo_ecf1168c1_b_0m
Empirical formula	C35 H45 I N2 O4
Formula weight	684.63
Temperature	100(2)K
Wavelength	0.71073 Å
Crystal system	triclinic
Space group	P -1
Unit cell dimensions	a = 9.624(5)Å α= 92.467(11)°.
	b = 10.533(5)Å β = 97.648(12)°.
	c = 17.245(8)Å γ = 98.756(12)°.
Volume	1708.7(14) $Å^3$
Z	2
Density (calculated)	1.331 Mg/m^3
Absorption coefficient	0.975 mm^{-1}
F(000)	708
Crystal size	0.100 x 0.010 x 0.010 mm^3
Theta range for data collection	1.960 to 18.993°.

Index ranges	-8<=h<=8,-9<=k<=9,-15<=l<=15
Reflections collected	7644
Independent reflections	2645[R(int) = 0.0668]
Completeness to theta =18.993°	96.5%
Absorption correction	Multi-scan
Max. and min. transmission	0.74 and 0.58
Refinement method	Full-matrix least-squares on F^2
Data / restraints / parameters	2645/ 444/ 416
Goodness-of-fit on F^2	1.512
Final R indices [I>2sigma(I)]	R1 = 0.0887, wR2 = 0.2161
R indices (all data)	R1 = 0.1109, wR2 = 0.2237
Largest diff. peak and hole	1.895 and -0.970 e.Å^{-3}

Chapter IV – C_1-Symmetry in aryliodine catalyzed diaminations: A proof of concept

5. Chapter V – Overall Conclusions

A practical, racemic diamination of styrenes was developed based on the previous insights from the asymmetric reaction. An effective pre-catalyst was designed for the transformation, taking into account that the use of a pre-catalyst with two side-chains in the 2 and 6-positions is a requirement for this reaction. Additionally, new amine nucleophiles such as tosylamides were introduced with good yields. The kinetic profile of the racemic reaction was also studied in the course of the pre-catalyst selection.

Next, an upscaled procedure for the synthesis of Ishihara-Muñiz pre-catalysts was developed. While doing so, the formation of a *meso*-species of the catalyst was detected. The first step of the project was to find a way to avoid said formation, which was performed without using an auxiliary base in the final step of the synthesis. After obtaining the pre-catalysts in a high enantiomeric excess, they were tried in their respective reactions, which produced a higher stereochemical outcome in the case of the Muñiz pre-catalyst **18**. Moreover, another pre-catalyst **17** was synthesized that yielded similar *ee* but its synthesis is cheaper given that is derived from resorcinol instead of orcinol. The diamines obtained by this method are >99% *ee* and represent the highest one ever reported for these compounds.

Finally, in a proof-of-concept project, an aryliodine **42** was designed to demonstrate that C_1-symmetric pre-catalyst based on the insights from the first two chapters could induce high *ee* in the diamination of styrenes. This design outperforms most of the reported asymmetric aryliodines(I) in other reactions within I(I/III) catalysis.

Chapter V – Overall Conclusions

After performing a substrate scope, it could be concluded that the loss of enantioinduction and yield is more acute when sterical or electronic effects are present in the substrates. Nevertheless, most of the enantioinduction is still observed after catalyzing with a structure that has only one stereogenic centre instead of two.

Chapter V - Overall Conclusions

6. References

(1) Saibabu Kotti, S. R. S.; Timmons, C.; Li, G. Vicinal Diamino Functionalities as Privileged Structural Elements in Biologically Active Compounds and Exploitation of Their Synthetic Chemistry. *Chemical Biology and Drug Design*. 2006, pp 101–114. https://doi.org/10.1111/j.1747-0285.2006.00347.x.

(2) Lucet, D.; Le Gall, T.; Mioskowski, C. The Chemistry of Vicinal Diamines. *Angewandte Chemie - International Edition*. October 16, 1998, pp 2580–2627. https://doi.org/10.1002/(SICI)1521-3773(19981016)37:19<2580::AID-ANIE2580>3.0.CO;2-L.

(3) György, P.; Melville, D. B.; Burk, D.; Du Vigneaud, V. The Possible Identity of Vitamin H with Biotin and Coenzyme R. *Science*. American Association for the Advancement of Science March 8, 1940, pp 243–245. https://doi.org/10.1126/science.91.2358.243.

(4) Fernandez-Mejia, C. Pharmacological Effects of Biotin. In *Journal of Nutritional Biochemistry*; J Nutr Biochem, 2005; Vol. 16, pp 424–427. https://doi.org/10.1016/j.jnutbio.2005.03.018.

(5) Barber, A.; Gottschlich, R. Novel Developments with Selective, Non-Peptidic Kappa-Opioid Receptor Agonists Review Central & Peripheral Nervous Systems Novel Developments with Selective, Non-Peptidic Kappa-Opioid Receptor Agonists. *Expert Opin. Investig. Drugs* **1997**, *6* (10), 1351–1368. https://doi.org/10.1517/13543784.6.10.1351.

(6) Camilleri, M. Novel Pharmacology: Asimadoline, a κ-Opioid Agonist, and Visceral Sensation. *Neurogastroenterology and Motility*. September 2008, pp 971–979. https://doi.org/10.1111/j.1365-2982.2008.01183.x.

(7) Abelson, M. B.; Allansmith, M. R.; Friedlaender, M. H. Effects of Topically Applied Ocular Decongestant and Antihistamine. *Am. J. Ophthalmol.* **1980**, *90* (2), 254–257. https://doi.org/10.1016/S0002-9394(14)74864-0.

References

(8) Keiser, J.; Utzinger, J. Efficacy of Current Drugs against Soil-Transmitted Helminth Infections: Systematic Review and Meta-Analysis. *JAMA - Journal of the American Medical Association*. April 23, 2008, pp 1937–1948. https://doi.org/10.1001/jama.299.16.1937.

(9) Anttila, S. A. K.; Leinonen, E. V. J. A Review of the Pharmacological and Clinical Profile of Mirtazapine. *CNS Drug Reviews*. Neva Press Inc. September 1, 2001, pp 249–264. https://doi.org/10.1111/j.1527-3458.2001.tb00198.x.

(10) Lewis, V. Undertreatment of Menopausal Symptoms and Novel Options for Comprehensive Management. *Current Medical Research and Opinion*. Taylor & Francis November 2009, pp 2689–2698. https://doi.org/10.1185/03007990903240519.

(11) Davies, B. E. Pharmacokinetics of Oseltamivir: An Oral Antiviral for the Treatment and Prophylaxis of Influenza in Diverse Populations. *The Journal of antimicrobial chemotherapy*. Oxford University Press 2010, p ii5. https://doi.org/10.1093/jac/dkq015.

(12) Ehrsson, H.; Wallin, I.; Yachnin, J. Pharmacokinetics of Oxaliplatin in Humans. *Med. Oncol.* **2002**, *19* (4), 261–265. https://doi.org/10.1385/MO:19:4:261.

(13) Yoon, T. P.; Jacobsen, E. N. Privileged Chiral Catalysts. *Science* **2003**, *299* (5613), 1691–1693. https://doi.org/10.1126/science.1083622.

(14) Jacobsen, E. N. Asymmetric Catalytic Epoxidation of Unfunctionalized Olefins. In *Catalytic Asymmetric Synthesis*; Ojima, I., Ed.; VCH: New York, 1993; Vol. 24, pp 159–202. https://doi.org/10.1080/00945719408001399.

(15) Jacobsen, E. N.; Zhang, W.; Muci, A. R.; Ecker, J. R.; Deng, L. Highly Enantioselective Epoxidation Catalysts Derived from l,2-Diaminocyclohexane. *J. Am. Chem. Soc.* **1991**, *113* (18), 7063–

7064. https://doi.org/10.1021/ja00018a068.

(16) Irie, R.; Noda, K.; Ito, Y.; Katsuki, T. Enantioselective Epoxidation of Unfunctionalized Olefins Using Chiral (Salen)Manganese(III) Complexes. *Tetrahedron Lett.* **1991**, *32* (8), 1055–1058. https://doi.org/10.1016/S0040-4039(00)74486-8.

(17) Zhang, W.; Loebach, J. L.; Wilson, S. R.; Jacobsen, E. N. Enantioselective Epoxidation of Unfunctionalized Olefins Catalyzed by (Saien)Manganese Complexes. *J. Am. Chem. Soc.* **1990**, *112* (7), 2801–2803. https://doi.org/10.1021/ja00163a052.

(18) Ohkuma, T.; Ooka, H.; Hashiguchi, S.; Ikariya, T.; Noyori, R. Practical Enantioselective Hydrogenation of Aromatic Ketones. *J. Am. Chem. Soc.* **1995**, *117* (9), 2675–2676. https://doi.org/10.1021/ja00114a043.

(19) Hashiguchi, S.; Fujii, A.; Takehara, J.; Ikariya, T.; Noyori, R. Asymmetric Transfer Hydrogenation of Aromatic Ketones Catalyzed by Chiral Ruthenium(II) Complexes. *J. Am. Chem. Soc.* **1995**, *117* (28), 7562–7563. https://doi.org/10.1021/ja00133a037.

(20) Gómez Aranda, V.; Barluenga, J.; Aznar, F. The Addition of Aromatic Amines to Alkenes in the Presence of Thallium(III) Acetate. *Synthesis (Germany)*. Georg Thieme Verlag July 1, 1974, pp 504–505. https://doi.org/10.1055/s-1974-23358.

(21) Chong, A. O.; Oshima, K.; Sharpless, K. B. Synthesis of Dioxobis(Tert-Alkylimido)Osmium(VIII) and Oxotris(Tert-Alkylimido)Osmium(VIII) Complexes. Stereospecific Vicinal Diamination of Olefins. *J. Am. Chem. Soc.* **1977**, *99* (10), 3420–3426. https://doi.org/10.1021/ja00452a039.

(22) Bäckvall, J. E. Stereospecific Palladium-Promoted Vicinal Diamination of Olefins. *Tetrahedron Lett.* **1978**, *19* (2), 163–166. https://doi.org/10.1016/S0040-4039(01)85073-5.

(23) Muñiz, K.; Nieger, M. A First Asymmetric Diamination of Olefins.

References

Synlett **2003**, No. 2, 211–214. https://doi.org/10.1055/s-2003-36799.

(24) Muñiz, K.; Nieger, M.; Mansikkamäki, H. Stereochemically Defined Osmium Centers from Asymmetric Diamination of Olefins: Mechanistic Implications for Osmium-Mediated Acrylate Functionalization. *Angew. Chemie - Int. Ed.* **2003**, *42* (48), 5958–5961. https://doi.org/10.1002/anie.200352244.

(25) Muñiz, K.; Nieger, M. Enantioselective Catalytic Diamination of Alkenes with a Bisimidoosmium Oxidant. *Chem. Commun.* **2005**, No. 21, 2729–2731. https://doi.org/10.1039/b502150b.

(26) Streuff, J.; Hövelmann, C. H.; Nieger, M.; Muñiz, K. Palladium(II)-Catalyzed Intramolecular Diamination of Unfunctionalized Alkenes. *J. Am. Chem. Soc.* **2005**, *127* (42), 14586–14587. https://doi.org/10.1021/ja055190y.

(27) Muñiz, K.; Iglesias, A.; Fang, Y. Platinum-Catalysed Aerobic 1,2-Aminooxygenation of Alkenes. *Chem. Commun.* **2009**, No. 37, 5591–5593. https://doi.org/10.1039/b912139k.

(28) Muñiz, K.; Streuff, J.; Hövelmann, C. H.; Núñez, A. Exploring the Nickel-Catalyzed Oxidation of Alkenes: A Diamination by Sulfamide Transfer. *Angew. Chemie - Int. Ed.* **2007**, *46* (37), 7125–7127. https://doi.org/10.1002/anie.200702160.

(29) Iglesias, A.; Muñiz, K. Oxidative Interception of the Hydroamination Pathway: A Gold-Catalyzed Diamination of Alkenes. *Chem. - A Eur. J.* **2009**, *15* (40), 10563–10569. https://doi.org/10.1002/chem.200901199.

(30) Muñiz, K.; Hövelmann, C. H.; Streuff, J. Oxidative Diamination of Alkenes with Ureas as Nitrogen Sources: Mechanistic Pathways in the Presence of a High Oxidation State Palladium Catalyst. *J. Am. Chem. Soc.* **2008**, *130* (2), 763–773. https://doi.org/10.1021/ja075041a.

(31) Muñiz, K.; Hövelmann, C. H.; Campos-Gómez, E.; Barluenga, J.; González, J. M.; Streuff, J.; Nieger, M. Intramolecular Diamination of Alkenes with Palladium(II)/Copper(II) Bromide and IPy2BF4: The Role of Halogenated Intermediates. *Chem. - An Asian J.* **2008**, *3* (4), 776–788. https://doi.org/10.1002/asia.200700373.

(32) Muñiz, K. Advancing Palladium-Catalyzed C-N Bond Formation: Bisindoline Construction from Successive Amide Transfer to Internal Alkenes. *J. Am. Chem. Soc.* **2007**, *129* (47), 14542–14543. https://doi.org/10.1021/ja075655f.

(33) Iglesias, Á.; Pérez, E. G.; Muñiz, K. An Intermolecular Palladium-Catalyzed Diamination of Unactivated Alkenes. *Angew. Chemie - Int. Ed.* **2010**, *49* (44), 8109–8111. https://doi.org/10.1002/anie.201003653.

(34) Muñiz, K.; Kirsch, J.; Chávez, P. Intermolecular Regioselective 1,2-Diamination of Allylic Ethers. *Adv. Synth. Catal.* **2011**, *353* (5), 689–694. https://doi.org/10.1002/adsc.201000813.

(35) Martínez, C.; Pérez, E. G.; Iglesias, Á.; Escudero-Adán, E. C.; Muñiz, K. Regioselective Intermolecular Diamination and Aminooxygenation of Alkenes with Saccharin. *Org. Lett.* **2016**, *18* (12), 2998–3001. https://doi.org/10.1021/acs.orglett.6b01368.

(36) Martínez, C.; Muñiz, K. Defined Palladium-Phthalimidato Catalysts for Improved Oxidative Amination. *Chem. - A Eur. J.* **2016**, *22* (22), 7367–7370. https://doi.org/10.1002/chem.201601128.

(37) Martínez, C.; Muñiz, K. Palladium-Catalyzed Vicinal Difunctionalization of Internal Alkenes: Diastereoselective Synthesis of Diamines. *Angew. Chemie - Int. Ed.* **2012**, *51* (28), 7031–7034. https://doi.org/10.1002/anie.201201719.

(38) Minakata, S.; Miwa, H.; Yamamoto, K.; Hirayama, A.; Okumura, S. Diastereodivergent Intermolecular 1,2-Diamination of Unactivated Alkenes Enabled by Iodine Catalysis. *J. Am. Chem. Soc.* **2021**, *143*

(11), 4112–4118. https://doi.org/10.1021/jacs.1c00228.

(39) Francis, D.; Nelson, A.; Marsden, S. P. Synthesis of β-Diamine Building Blocks by Photocatalytic Hydroamination of Enecarbamates with Amines, Ammonia and N−H Heterocycles. *Chem. – A Eur. J.* **2020**, *26* (65), 14861–14865. https://doi.org/10.1002/CHEM.202003562.

(40) Shen, T.; Lambert, T. H. Electrophotocatalytic Diamination of Vicinal C–H Bonds. *Science (80-.).* **2021**, *371* (6529), 620–626. https://doi.org/10.1126/SCIENCE.ABF2798.

(41) Musher, J. I. The Chemistry of Hypervalent Molecules. *Angew. Chemie Int. Ed. English* **1969**, *8* (1), 54–68. https://doi.org/10.1002/anie.196900541.

(42) Li, X.; Chen, P.; Liu, G. Recent Advances in Hypervalent Iodine(III)-Catalyzed Functionalization of Alkenes. *Beilstein Journal of Organic Chemistry*. 2018, pp 1813–1825. https://doi.org/10.3762/bjoc.14.154.

(43) Willgerodt, C. Ueber Einige Aromatische Jodidchloride. *J. für Prakt. Chemie* **1885**, *33* (1), 154–160. https://doi.org/10.1002/prac.18860330117.

(44) Varvoglis, A. (Anastasios). *Hypervalent Iodine in Organic Synthesis*; Academic Press, 1997.

(45) Zhdankin, V. V. Hypervalent Iodine(III) Reagents in Organic Synthesis. *Arkivoc* **2009**, No. 1, 1.

(46) Zhdankin, V. V. Organoiodine(V) Reagents in Organic Synthesis. *J. Org. Chem* **2011**, *76*, 1185. https://doi.org/10.1021/jo1024738.

(47) Stevenson, P. J.; Treacy, A. B.; Nieuwenhuyzen, M. *Preparation of Dess-Martin Periodinane-the Role of the Morphology of 1-Hydroxy-1,2-Benziodoxol-3(1H)-One 1-Oxide Precursor*; 1997; Vol. 2.

(48) Ireland, R. E.; Liu, L. An Improved Procedure for the Preparation of the Dess-Martin Periodinane. *Journal of Organic Chemistry*.

American Chemical Society 1993, p 2899. https://doi.org/10.1021/jo00062a040.

(49) Dess, D. B.; Martin, J. C. A Useful 12-I-5 Triacetoxyperiodinane (the Dess-Martin Periodinane) for the Selective Oxidation of Primary or Secondary Alcohols and a Variety of Related 12-I-5 Species. *J. Am. Chem. Soc.* **1991**, *113* (19), 7277–7287. https://doi.org/10.1021/ja00019a027.

(50) Altermann, S. M.; Richardson, R. D.; Page, T. K.; Schmidt, R. K.; Holland, E.; Mohammed, U.; Paradine, S. M.; French, A. N.; Richter, C.; Bahar, A. M.; Witulski, B.; Wirth, T. Catalytic Enantioselective α-Oxysulfonylation of Ketones Mediated by Iodoarenes. *European J. Org. Chem.* **2008**, No. 31, 5315–5328. https://doi.org/10.1002/ejoc.200800741.

(51) Charpentier, J.; Früh, N.; Togni, A. Electrophilic Trifluoromethylation by Use of Hypervalent Iodine Reagents. *Chemical Reviews*. American Chemical Society January 28, 2015, pp 650–682. https://doi.org/10.1021/cr500223h.

(52) Koser, G. F.; Ollevier, T.; Desyroy, V. [Hydroxy(Tosyloxy)Iodo]Benzene. In *Encyclopedia of Reagents for Organic Synthesis*; John Wiley & Sons, Ltd, 2004. https://doi.org/10.1002/047084289x.rh070.

(53) Moriarty, R. M.; Vaid, R. K.; Koser, G. F. [Hydroxy(Organosulfonyloxy)Iodo]Arenes in Organic Synthesis. *Synlett* **1990**, *1990* (7), 365–383. https://doi.org/10.1055/s-1990-21097.

(54) Wang, Z.; Herraiz, A. G.; del Hoyo, A. M.; Suero, M. G. Generating Carbyne Equivalents with Photoredox Catalysis. *Nat. 2018 5547690* **2018**, *554* (7690), 86–91. https://doi.org/10.1038/NATURE25185.

(55) Kaiho, T. *Iodine Chemistry and Applications*; Wiley Blackwell, 2014;

Vol. 9781118466. https://doi.org/10.1002/9781118909911.

(56) Zhdankin, V. V. *Hypervalent Iodine Chemistry: Preparation, Structure, and Synthetic Applications of Polyvalent Iodine Compounds*; 2014. https://doi.org/10.1002/9781118341155.

(57) Ochiai, M. Organic Synthesis Using Hypervalent Organoiodanes. In: Chemistry of Hypervalent Compounds; Akiba, K., Ed.; Wiley-VCH: New York, 1999; p 359.

(58) Okuyama, T.; Takino, T.; Sueda, T.; Ochiai, M. Solvolysis of Cyclohexenyliodonium Salt, a New Precursor for the Vinyl Cation: Remarkable Nucleofugality of the Phenyliodonio Group and Evidence for Internal Return from an Intimate Ion—Molecule Pair. *J. Am. Chem. Soc.* **1995**, *117* (12), 3360–3367. https://doi.org/10.1021/ja00117a006.

(59) Grushin, V. V.; Demkina, I. I.; Tolstaya, T. P. Unified Mechanistic Analysis of Polar Reactions of Diaryliodonium Salts. *J. Chem. Soc. Perkin Trans. 2* **1992**, No. 4, 505–511. https://doi.org/10.1039/p29920000505.

(60) Merritt, E. A.; Olofsson, B. Diaryliodonium Salts: A Journey from Obscurity to Fame. *Angewandte Chemie - International Edition*. November 16, 2009, pp 9052–9070. https://doi.org/10.1002/anie.200904689.

(61) Carroll, M. A.; Wood, R. A. Arylation of Anilines: Formation of Diarylamines Using Diaryliodonium Salts. *Tetrahedron* **2007**, *63* (46), 11349–11354. https://doi.org/10.1016/j.tet.2007.08.076.

(62) Sundalam, S. K.; Stuart, D. R. Base Mediated Synthesis of Alkyl-Aryl Ethers from the Reaction of Aliphatic Alcohols and Unsymmetric Diaryliodonium Salts. *J. Org. Chem.* **2015**, *80* (12), 6456–6466. https://doi.org/10.1021/acs.joc.5b00907.

(63) Milas, N. A.; Plesnicar, B. Formation of Di-t-Butyl Poly Oxides in the Reaction of t-Butyl Hydroperoxide with Iodosobenzene and

Iodosobenzene Diacetate in Methylene Chloride and in Diethyl Ether at - 80 to + 5°. *J. Am. Chem. Soc.* **1968**, *90* (16), 4450–4453. https://doi.org/10.1021/ja01018a044.

(64) Magnus, P.; Lacour, J.; Weber, W. Direct N-Alkyl Azidonation of N,N-Dialkylarylamines with the Iodosylbenzene/Trimethylsilylazide Reagent Combination. *J. Am. Chem. Soc.* **1993**, *115* (20), 9347–9348. https://doi.org/10.1021/ja00073a084.

(65) Kita, Y.; Tohma, H.; Takada, T.; Mitoh, S.; Fujita, S.; Gyoten, M. A Novel and Direct Alkyl Azidation of p -Alkylanisoles Using Phenyl Iodine(III) Bis(Trifluoroacetate) (PIFA) and Trimethylsilyl Azide. *Synlett* **1994**, *1994* (6), 427–428. https://doi.org/10.1055/s-1994-22875.

(66) Fontana, F.; Minisci, F.; Yong, M. Y.; Lihua, Z. A Novel and Mild Source of Carbon-Centered Radicals by Iodosobenzene Diacetate (IBDA) and Sodium Azide from Alcohols, Ethers, Aldehydes, Amides and Alkyl Iodides. *Tetrahedron Lett.* **1993**, *34* (15), 2517–2520. https://doi.org/10.1016/S0040-4039(00)60456-2.

(67) Wiedenfeld, D.; Breslow, R. Directed Formation of Carbon-Bromine and Carbon-Sulfur Bonds by Tandem Radical Chain Reactions. *J. Am. Chem. Soc.* **1991**, *113* (23), 8977–8978. https://doi.org/10.1021/ja00023a074.

(68) Wang, Y.; Chen, B.; He, X.; Gui, J. Bioinspired Synthesis of Nortriterpenoid Propindilactone G. *Cite This J. Am. Chem. Soc* **2020**, *142*, 5007–5012. https://doi.org/10.1021/jacs.0c00363.

(69) Kita, Y.; Tohma, H.; Inagaki, M.; Hatanaka, K.; Yakura, T. A Novel Oxidative Azidation of Aromatic Compounds with Hypervalent Iodine Reagent, Phenyliodine(III) Bis(Trifluoroacetate) (PIFA) and Trimethylsilyl Azide. *Tetrahedron Lett.* **1991**, *32* (34), 4321–4324. https://doi.org/10.1016/S0040-4039(00)92160-9.

(70) Kita, Y.; Tohma, H.; Hatanaka, K.; Takada, T.; Fujita, S.; Mitoh, S.;

Sakurai, H.; Oka, S. Hypervalent Iodine-Induced Nucleophilic Substitution of Para-Substituted Phenol Ethers. Generation of Cation Radicals as Reactive Intermediates. *J. Am. Chem. Soc.* **1994**, *116* (9), 3684–3691. https://doi.org/10.1021/ja00088a003.

(71) Tohma, H.; Morioka, H.; Takizawa, S.; Arisawa, M.; Kita, Y. Efficient Oxidative Biaryl Coupling Reaction of Phenol Ether Derivatives Using Hypervalent Iodine(III) Reagents. *Tetrahedron* **2001**, *57* (2), 345–352. https://doi.org/10.1016/S0040-4020(00)00941-8.

(72) Wang, X.; Studer, A. Iodine(III) Reagents in Radical Chemistry. *Acc. Chem. Res.* **2017**, *50* (7), 1712–1724. https://doi.org/10.1021/acs.accounts.7b00148.

(73) Ochiai, M.; Takaoka, Y.; Nagao, Y. Hypervalent Alkenyliodonium Tetrafluoroborates. Evidence for Generation of Alkylidenecarbenes via Base-Induced α-Elimination. *J. Am. Chem. Soc.* **1988**, *110* (19), 6565–6566. https://doi.org/10.1021/ja00227a048.

(74) Ochiai, M.; Kunishima, M.; Tani, S.; Nagao, Y. Generation of [β-(Phenylsulfonyl)Alkylidene]Carbenes from Hypervalent Alkenyl- and Alkynyliodonium Tetrafluoroborates and Synthesis of 1-(Phenylsulfonyl)Cyclopentenes. *J. Am. Chem. Soc.* **1991**, *113* (8), 3135–3142. https://doi.org/10.1021/ja00008a049.

(75) Pribram, R. Ueber Das Optische Drehungsvermögen Des Jodoniumtartrates. *Justus Liebigs Ann. Chem.* **1907**, *351* (1–3), 481–485. https://doi.org/10.1002/jlac.19073510139.

(76) Merkushev, E. B.; Novikov, A. N.; Makarchenko, S. S.; Moskal'chuk, A. S.; Glushkova, V. V.; Kogai, T. I.; Polyakova, L. G. Organic Compounds of Polyvalent Iodine. Simple Synthesis of (Diacyloxyiodo)Benzenes. *J. Org. Chem. USSR (Engl. Transl.)* **1975**, *12*, 1246–1249.

(77) Imamoto, T.; Koto, H. Asymmetric Oxidation of Sulfides to Sulfoxides with Trivalent Iodine Reagents. *Chem. Lett.* **1986**, *15*

(6), 967–968. https://doi.org/10.1246/cl.1986.967.

(78) Ray, D. G.; Koser, G. F. Iodinanes with Iodme(III)-Bound Homochiral Alkoxy Ligands: Preparation and Utility for the Synthesis of Alkoxysulfonium Salts and Chiral Sulfoxides. *J. Am. Chem. Soc.* **1990**, *112* (14), 5672–5673. https://doi.org/10.1021/ja00170a059.

(79) Ray, D. G.; Koser, G. F. Iodinanes with Chiral Ligands. Synthesis and Structure of Iodine(III) Dibenzoyl Tartrates. *Journal of Organic Chemistry*. American Chemical Society February 1, 1992, pp 1607–1610. https://doi.org/10.1021/jo00031a054.

(80) Koposov, A. Y.; Boyarskikh, V. V.; Zhdankin, V. V. Amino Acid-Derived Lodobenzene Dicarboxylates: Reagents for Oxidative Conversion of Alkenes to Amino Acid Esters. *Org. Lett.* **2004**, *6* (20), 3613–3615. https://doi.org/10.1021/ol0484714.

(81) Ochiai, M.; Takaoka, Y.; Masaki, Y.; Nagao, Y.; Shiro, M. Synthesis of Chiral Hypervalent Organoiodinanes, Iodo(III)Binaphthyls, and Evidence for Pseudorotation on Iodine. *J. Am. Chem. Soc.* **1990**, *112* (14), 5677–5678. https://doi.org/10.1021/ja00170a063.

(82) Ochiai, M.; Kitagawa, Y.; Takayama, N.; Takaoka, Y.; Shiro, M. Synthesis of Chiral Diaryliodonium Salts, 1,1'-Binaphthyl-2-Yl(Phenyl)Iodonium Tetrafluoroborates: Asymmetric α-Phenylation of β-Keto Ester Enolates [8]. *Journal of the American Chemical Society*. American Chemical Society October 6, 1999, pp 9233–9234. https://doi.org/10.1021/ja992236c.

(83) Wirth, T.; Hirt, U. H. Chiral Hypervalent Iodine Compounds. *Tetrahedron: Asymmetry* **1997**, *8* (1), 23–26. https://doi.org/10.1016/S0957-4166(96)00469-7.

(84) Urs H. Hirt, †; Bernhard Spingler, ‡ and; Thomas Wirth*, †. New Chiral Hypervalent Iodine Compounds in Asymmetric Synthesis. **1998**. https://doi.org/10.1021/JO980475X.

References

(85) Hirt, U. H.; Schuster, M. F. H.; French, A. N.; Wiest, O. G.; Wirth, T. Chiral Hypervalent Organo-Iodine(III) Compounds. *European J. Org. Chem.* **2001**, *2001* (8), 1569–1579. https://doi.org/10.1002/1099-0690(200104)2001:8<1569::AID-EJOC1569>3.0.CO;2-T.

(86) Kiirti, L.; Herczegh, P.; Visy, J.; Simonyi, M.; Antus, S.; Pelter, A. New Insights into the Mechanism of Phenolic Oxidation with Phenyliodonium(in) Reagents. *J. Chem. Soc. - Perkin Trans. 1* **1999**, No. 4, 379–380. https://doi.org/10.1039/a809206k.

(87) Subramaniam, V. S. Kita Oxidation/Dearomatization. In *Catalysis from A to Z*; Wiley, 2020. https://doi.org/10.1002/9783527809080.cataz09456.

(88) Dohi, T.; Maruyama, A.; Takenaga, N.; Senami, K.; Minamitsuji, Y.; Fujioka, H.; Caemmerer, S. B.; Kita, Y. A Chiral Hypervalent Iodine(III) Reagent for Enantioselective Dearomatization of Phenols. *Angew. Chemie - Int. Ed.* **2008**, *47* (20), 3787–3790. https://doi.org/10.1002/anie.200800464.

(89) Fujita, M.; Okuno, S.; Lee, H. J.; Sugimura, T.; Okuyama, T. Enantiodifferentiating Tetrahydrofuranylation of But-3-Enyl Carboxylates Using Optically Active Hypervalent Iodine(III) Reagents via a 1,3-Dioxan-2-Yl Cation Intermediate. *Tetrahedron Lett.* **2007**, *48* (49), 8691–8694. https://doi.org/10.1016/j.tetlet.2007.10.015.

(90) Fujita, M.; Yoshida, Y.; Miyata, K.; Wakisaka, A.; Sugimura, T. Enantiodifferentiating Endo-Selective Oxylactonization of Ortho-Alk-l-Enylbenzoate with a Lactate-Derived Aryl-Λ3-Iodane. *Angew. Chemie - Int. Ed.* **2010**, *49* (39), 7068–7071. https://doi.org/10.1002/anie.201003503.

(91) Uyanik, M.; Yasui, T.; Ishihara, K. Enantioselective Kita Oxidative Spirolactonization Catalyzed by In Situ Generated Chiral

Hypervalent Iodine(III) Species. *Angew. Chemie* **2010**, *122* (12), 2221–2223. https://doi.org/10.1002/ange.200907352.

(92) Kong, W.; Feige, P.; De Haro, T.; Nevado, C. Regio- and Enantioselective Aminofluorination of Alkenes. *Angew. Chemie - Int. Ed.* **2013**, *52* (9), 2469–2473. https://doi.org/10.1002/anie.201208471.

(93) Farid, U.; Malmedy, F.; Claveau, R.; Albers, L.; Wirth, T. Stereoselective Rearrangements with Chiral Hypervalent Iodine Reagents. *Angew. Chemie Int. Ed.* **2013**, *52* (27), 7018–7022. https://doi.org/10.1002/anie.201302358.

(94) Mizar, P.; Wirth, T. Flexible Stereoselective Functionalizations of Ketones through Umpolung with Hypervalent Iodine Reagents. *Angew. Chemie - Int. Ed.* **2014**, *53* (23), 5993–5997. https://doi.org/10.1002/anie.201400405.

(95) Malmedy, F.; Wirth, T. Stereoselective Ketone Rearrangements with Hypervalent Iodine Reagents. *Chem. - A Eur. J.* **2016**, *22* (45), 16072–16077. https://doi.org/10.1002/chem.201603022.

(96) Brown, M.; Kumar, R.; Rehbein, J.; Wirth, T. Enantioselective Oxidative Rearrangements with Chiral Hypervalent Iodine Reagents. *Chem. - A Eur. J.* **2016**, *22* (12), 4030–4035. https://doi.org/10.1002/chem.201504844.

(97) Ochiai, M.; Takeuchi, Y.; Katayama, T.; Sueda, T.; Miyamoto, K. Iodobenzene-Catalyzed α-Acetoxylation of Ketones. In Situ Generation of Hypervalent (Diacyloxyiodo)Benzenes Using m-Chloroperbenzoic Acid. *J. Am. Chem. Soc.* **2005**, *127* (35), 12244–12245. https://doi.org/10.1021/ja0542800.

(98) Dohi, T.; Maruyama, A.; Yoshimura, M.; Morimoto, K.; Tohma, H.; Kita, Y. Versatile Hypervalent-Iodine(III)-Catalyzed Oxidations with m-Chloroperbenzoic Acid as a Cooxidant. *Angew. Chemie - Int. Ed.* **2005**, *44* (38), 6193–6196.

https://doi.org/10.1002/anie.200501688.

(99) Richardson, R. D.; Wirth, T. Hypervalent Iodine Goes Catalytic. *Angewandte Chemie - International Edition*. July 3, 2006, pp 4402–4404. https://doi.org/10.1002/anie.200601817.

(100) Flores, A.; Cots, E.; Bergès, J.; Muñiz, K. Enantioselective Iodine(I/III) Catalysis in Organic Synthesis. *Adv. Synth. Catal.* **2019**, *361* (1), 2–25. https://doi.org/10.1002/adsc.201800521.

(101) Dohi, T.; Takenaga, N.; Nakae, T.; Toyoda, Y.; Yamasaki, M.; Shiro, M.; Fujioka, H.; Maruyama, A.; Kita, Y. Asymmetric Dearomatizing Spirolactonization of Naphthols Catalyzed by Spirobiindane-Based Chiral Hypervalent Iodine Species. *J. Am. Chem. Soc.* **2013**, *135* (11), 4558–4566. https://doi.org/10.1021/ja401074u.

(102) Uyanik, M.; Yasui, T.; Ishihara, K. Hydrogen Bonding and Alcohol Effects in Asymmetric Hypervalent Iodine Catalysis: Enantioselective Oxidative Dearomatization of Phenols. *Angew. Chemie Int. Ed.* **2013**, *52* (35), 9215–9218. https://doi.org/10.1002/anie.201303559.

(103) Uyanik, M.; Yasui, T.; Ishihara, K. Chiral Hypervalent Organoiodine-Catalyzed Enantioselective Oxidative Spirolactonization of Naphthol Derivatives. *J. Org. Chem.* **2017**, No. Iii, acs.joc.7b01941. https://doi.org/10.1021/acs.joc.7b01941.

(104) Murray, S. J.; Ibrahim, H. Asymmetric Kita Spirolactonisation Catalysed by Anti-Dimethanoanthracene-Based Iodoarenes. *Chem. Commun.* **2015**, *51* (12), 2376–2379. https://doi.org/10.1039/C4CC09724F.

(105) Dohi, T.; Sasa, H.; Miyazaki, K.; Fujitake, M.; Takenaga, N.; Kita, Y. Chiral Atropisomeric 8,8′-Diiodobinaphthalene for Asymmetric Dearomatizing Spirolactonizations in Hypervalent Iodine Oxidations. *J. Org. Chem.* **2017**, *82* (22), 11954–11960.

https://doi.org/10.1021/acs.joc.7b02037.

(106) Jain, N.; Xu, S.; Ciufolini, M. A. Asymmetric Oxidative Cycloetherification of Naphtholic Alcohols. *Chem. - A Eur. J.* **2017**, *23* (19), 4542–4546. https://doi.org/10.1002/chem.201700667.

(107) Harned, A. M. Asymmetric Oxidative Dearomatizations Promoted by Hypervalent Iodine(III) Reagents: An Opportunity for Rational Catalyst Design? *Tetrahedron Lett.* **2014**, *55* (34), 4681–4689. https://doi.org/10.1016/J.TETLET.2014.06.051.

(108) Uyanik, M.; Sasakura, N.; Mizuno, M.; Ishihara, K. Enantioselective Synthesis of Masked Benzoquinones Using Designer Chiral Hypervalent Organoiodine(III) Catalysis. *ACS Catal.* **2017**, *7* (1), 872–876. https://doi.org/10.1021/acscatal.6b03380.

(109) Zhang, D. Y.; Xu, L.; Wu, H.; Gong, L. Z. Chiral Iodine-Catalyzed Dearomatizative Spirocyclization for the Enantioselective Construction of an All-Carbon Stereogenic Center. *Chem. - A Eur. J.* **2015**, *21* (29), 10314–10317. https://doi.org/10.1002/chem.201501583.

(110) Quideau, S.; Lyvinec, G.; Marguerit, M.; Bathany, K.; Ozanne-Beaudenon, A.; Buffeteau, T.; Cavagnat, D.; Chénedé, A. Asymmetric Hydroxylative Phenol Dearomatization through In Situ Generation of Iodanes from Chiral Iodoarenes and m -CPBA. *Angew. Chemie* **2009**, *121* (25), 4675–4679. https://doi.org/10.1002/ange.200901039.

(111) Volp, K. A.; Harned, A. M. Chiral Aryl Iodide Catalysts for the Enantioselective Synthesis of Para-Quinols. *Chem. Commun.* **2013**, *49* (29), 3001. https://doi.org/10.1039/c3cc00013c.

(112) Muñiz, K.; Fra, L. Enantioselective 4-Hydroxylation of Phenols under Chiral Organoiodine(I/III) Catalysis. *Synth.* **2017**, *49* (13), 2901–2906. https://doi.org/10.1055/s-0036-1588808.

(113) Hashimoto, T.; Shimazaki, Y.; Omatsu, Y.; Maruoka, K. Indanol-

Based Chiral Organoiodine Catalysts for Enantioselective Hydrative Dearomatization. *Angew. Chemie - Int. Ed.* **2018**, *57* (24), 7200–7204. https://doi.org/10.1002/anie.201803889.

(114) Uyanik, M.; Yasui, T.; Ishihara, K. Hypervalent Iodine-Catalyzed Oxylactonization of Ketocarboxylic Acids to Ketolactones. *Bioorg. Med. Chem. Lett.* **2009**, *19* (14), 3848–3851. https://doi.org/10.1016/J.BMCL.2009.03.148.

(115) Farooq, U.; Schäfer, S.; Shah, A. U. H. A.; Freudendahl, D. M.; Wirth, T. Synthesis of New Enantiomerically Pure Organoiodine Catalysts and Their Application in the α-Functionalization of Ketones. *Synthesis (Stuttg).* **2010**, No. 6, 1023–1029. https://doi.org/10.1055/s-0029-1218640.

(116) Richardson, R. D.; Page, T. K.; Altermann, S.; Paradine, S. M.; French, A. N.; Wirth, T. Enantioselective α-Oxytosylation of Ketones Catalysed by Iodoarenes. *Synlett* **2007**, No. 4, 538–542. https://doi.org/10.1055/s-2007-967960.

(117) Yu, J.; Cui, J.; Hou, X. Sen; Liu, S. S.; Gao, W. C.; Jiang, S.; Tian, J.; Zhang, C. Enantioselective α-Tosyloxylation of Ketones Catalyzed by Spirobiindane Scaffold-Based Chiral Iodoarenes. *Tetrahedron Asymmetry* **2011**, *22* (23), 2039–2055. https://doi.org/10.1016/j.tetasy.2011.12.003.

(118) Rodríguez, A.; Moran, W. J. Chiral Aryl Iodide-Catalyzed Enantioselective α-Oxidation of Ketones. *Synthesis (Stuttg).* **2012**, *44* (8), 1178–1182. https://doi.org/10.1055/s-0031-1290590.

(119) Guilbault, A. A.; Legault, C. Y. Drastic Enhancement of Activity in Iodane-Based α-Tosyloxylation of Ketones: Iodine(III) Does the Hypervalent Twist. *ACS Catal.* **2012**, *2* (2), 219–222. https://doi.org/10.1021/cs200612s.

(120) Brenet, S.; Berthiol, F.; Einhorn, J. 3,3-Diiodo-BINOL-Fused Maleimides as Chiral Hypervalent Iodine(III) Organocatalysts.

European J. Org. Chem. **2013**, No. 36, 8094–8096. https://doi.org/10.1002/ejoc.201301329.

(121) Basdevant, B.; Legault, C. Y. Enantioselective Iodine(III)-Mediated Synthesis of α-Tosyloxy Ketones: Breaking the Selectivity Barrier. *Org. Lett.* **2015**, *17* (19), 4918–4921. https://doi.org/10.1021/acs.orglett.5b02501.

(122) Beaulieu, S.; Legault, C. Y. Mechanistic Insights on the Iodine(III)-Mediated α-Oxidation of Ketones. *Chem. - A Eur. J.* **2015**, *21* (31), 11206–11211. https://doi.org/10.1002/chem.201501177.

(123) Levitre, G.; Dumoulin, A.; Retailleau, P.; Panossian, A.; Leroux, F. R.; Masson, G. Asymmetric α-Sulfonyl- and α-Phosphoryl-Oxylation of Ketones by a Chiral Hypervalent Iodine(III). *J. Org. Chem.* **2017**, *82* (22), 11877–11883. https://doi.org/10.1021/acs.joc.7b01597.

(124) Suzuki, S.; Kamo, T.; Fukushi, K.; Hiramatsu, T.; Tokunaga, E.; Dohi, T.; Kita, Y.; Shibata, N. Iodoarene-Catalyzed Fluorination and Aminofluorination by an Ar-I/HF·pyridine/MCPBA System. *Chem. Sci.* **2014**, *5* (7), 2754–2760. https://doi.org/10.1039/C3SC53107D.

(125) Pluta, R. K.; Krach, P. E.; Cavallo, L.; Falivene, L.; Rueping, M. Metal-Free Catalytic Asymmetric Fluorination of Keto Esters Using a Combination of Hydrogen Fluoride (HF) and Oxidant: Experiment and Computation. *ACS Catal.* **2018**, acscatal.7b03118. https://doi.org/10.1021/acscatal.7b03118.

(126) Jobin-Des Lauriers, A.; Legault, C. Y. Iodine(III)-Mediated Oxidative Hydrolysis of Haloalkenes: Access to α-Halo Ketones by a Release-and-Catch Mechanism. *Org. Lett.* **2016**, *18* (1), 108–111. https://doi.org/10.1021/acs.orglett.5b03345.

(127) Wu, H.; He, Y. P.; Xu, L.; Zhang, D. Y.; Gong, L. Z. Asymmetric Organocatalytic Direct C(Sp2)-H/C(Sp3)-H Oxidative Cross-Coupling by Chiral Iodine Reagents. *Angew. Chemie - Int. Ed.*

2014, *53* (13), 3466–3469. https://doi.org/10.1002/anie.201309967.

(128) Sreenithya, A.; Patel, C.; Hadad, C. M.; Sunoj, R. B. Hypercoordinate Iodine Catalysts in Enantioselective Transformation: The Role of Catalyst Folding in Stereoselectivity. *ACS Catal.* **2017**, *7* (6), 4189–4196. https://doi.org/10.1021/acscatal.7b00975.

(129) Shimogaki, M.; Fujita, M.; Sugimura, T. Enantioselective Oxidation of Alkenylbenzoates Catalyzed by Chiral Hypervalent Iodine(III) to Yield 4-Hydroxyisochroman-1-Ones. *European J. Org. Chem.* **2013**, No. 31, 7128–7138. https://doi.org/10.1002/ejoc.201300959.

(130) Fujita, M.; Mori, K.; Shimogaki, M.; Sugimura, T. Total Synthesis of (12R)- and (12S)-12-Hydroxymonocerins: Stereoselective Oxylactonization Using a Chiral Hypervalent Iodine(Iii) Species. *RSC Adv.* **2013**, *3* (39), 17717. https://doi.org/10.1039/c3ra43230k.

(131) Alhalib, A.; Kamouka, S.; Moran, W. J. Iodoarene-Catalyzed Cyclizations of Unsaturated Amides. *Org. Lett.* **2015**, *17* (6), 1453–1456. https://doi.org/10.1021/acs.orglett.5b00333.

(132) Gelis, C.; Dumoulin, A.; Bekkaye, M.; Neuville, L.; Masson, G. Chiral Hypervalent Iodine(III) Catalyst Promotes Highly Enantioselective Sulfonyl-and Phosphoryl-Oxylactonizations. *Org. Lett.* **2017**, *19* (1), 278–281. https://doi.org/10.1021/acs.orglett.6b03631.

(133) Wöste, T. H.; Muñiz, K. Enantioselective Vicinal Diacetoxylation of Alkenes under Chiral Iodine(III) Catalysis. *Synth.* **2016**, *48* (6), 816–827. https://doi.org/10.1055/s-0035-1561313.

(134) Haubenreisser, S.; Wöste, T. H.; Martínez, C.; Ishihara, K.; Muñiz, K. Structurally Defined Molecular Hypervalent Iodine Catalysts for Intermolecular Enantioselective Reactions. *Angew. Chemie - Int. Ed.* **2016**, *55* (1), 413–417.

https://doi.org/10.1002/anie.201507180.

(135) Muñiz, K.; Barreiro, L.; Romero, R. M.; Martínez, C. Catalytic Asymmetric Diamination of Styrenes. *J. Am. Chem. Soc.* **2017**, *139* (12), 4354–4357. https://doi.org/10.1021/jacs.7b01443.

(136) Wang, Q.; Zhong, W.; Wei, X.; Ning, M.; Meng, X.; Li, Z. Metal-Free Intramolecular Aminofluorination of Alkenes Mediated by PhI(OPiv)2/Hydrogen Fluoride–Pyridine System. *Org. Biomol. Chem.* **2012**, *10* (43), 8566. https://doi.org/10.1039/c2ob26664d.

(137) Mennie, K. M.; Banik, S. M.; Reichert, E. C.; Jacobsen, E. N. Catalytic Diastereo- and Enantioselective Fluoroamination of Alkenes. *J. Am. Chem. Soc.* **2018**, *140* (14), 4797–4802. https://doi.org/10.1021/jacs.8b02143.

(138) Woerly, E. M.; Banik, S. M.; Jacobsen, E. N. Enantioselective, Catalytic Fluorolactonization Reactions with a Nucleophilic Fluoride Source. *J. Am. Chem. Soc.* **2016**, *138* (42), 13858–13861. https://doi.org/10.1021/jacs.6b09499.

(139) Molnár, I. G.; Gilmour, R. Catalytic Difluorination of Olefins. *J. Am. Chem. Soc.* **2016**, *138* (15), 5004–5007. https://doi.org/10.1021/jacs.6b01183.

(140) Banik, S. M.; Medley, J. W.; Jacobsen, E. N. Catalytic, Diastereoselective 1,2-Difluorination of Alkenes. *J. Am. Chem. Soc.* **2016**, *138* (15), 5000–5003. https://doi.org/10.1021/jacs.6b02391.

(141) Haj, M. K.; Banik, S. M.; Jacobsen, E. N. Catalytic, Enantioselective 1,2-Difluorination of Cinnamamides. *Org. Lett.* **2019**, *21* (13), 4919–4923. https://doi.org/10.1021/ACS.ORGLETT.9B00938.

(142) Banik, S. M.; Medley, J. W.; Jacobsen, E. N. Catalytic, Asymmetric Difluorination of Alkenes to Generate Difluoromethylated Stereocenters. *Science (80-.).* **2016**, *353* (6294), 51–54. https://doi.org/10.1126/science.aaf8078.

(143) Scheidt, F.; Schäfer, M.; Sarie, J. C.; Daniliuc, C. G.; Molloy, J. J.;

Gilmour, R. Enantioselective, Catalytic Vicinal Difluorination of Alkenes. *Angew. Chemie Int. Ed.* **2018**, *57* (50), 16431–16435. https://doi.org/10.1002/ANIE.201810328.

(144) Muñiz, K. Promoting Intermolecular C-N Bond Formation under the Auspices of Iodine(III). *Acc. Chem. Res.* **2018**, *51* (6), 1507–1519. https://doi.org/10.1021/acs.accounts.8b00137.

(145) Hadjiarapoglou, L.; Spyroudis, S.; Varvoglis, A. Phenyliodine(III) Bis[Phtalimidate]: A Novel Polyvalent Iodine Compound. *Synthesis (Stuttg).* **1983**, *3*, 207–208.

(146) Papadopoulou, M.; Varvoglis, A. ChemInform Abstract: PHENYLIODINE(III) BISIMIDATES, A NOVEL CLASS OF TRIVALENT IODINE COMPOUNDS. *J. Chem. Res.* **1983**, *14* (27), 66–67. https://doi.org/10.1002/chin.198327238.

(147) Moriarty, R. M.; Khosrowshahi, J. S. A Versatile Synthesis of Vicinal Diazides Using Hypervalent Iodine. *Tetrahedron Lett.* **1986**, *27* (25), 2809–2812. https://doi.org/10.1016/S0040-4039(00)84648-1.

(148) Röben, C.; Souto, J. A.; González, Y.; Lishchynskyi, A.; Muñiz, K. Enantioselective Metal-Free Diamination of Styrenes. *Angew. Chemie Int. Ed.* **2011**, *50* (40), 9478–9482. https://doi.org/10.1002/ANIE.201103077.

(149) Souto, J. A.; González, Y.; Iglesias, A.; Zian, D.; Lishchynskyi, A.; Muñiz, K. Iodine(III)-Promoted Intermolecular Diamination of Alkenes. *Chem. - An Asian J.* **2012**, *7* (5), 1103–1111. https://doi.org/10.1002/asia.201101025.

(150) Souto, J. A.; Martínez, C.; Velilla, I.; Muñiz, K. Defined Hypervalent Iodine(III) Reagents Incorporating Transferable Nitrogen Groups: Nucleophilic Amination through Electrophilic Activation. *Angew. Chemie Int. Ed.* **2013**, *52* (4), 1324–1328. https://doi.org/10.1002/anie.201206420.

(151) Lishchynskyi, A.; Muñiz, K. An Approach to the Regioselective

Diamination of Conjugated Di- and Trienes. *Chem. - A Eur. J.* **2012**, *18* (8), 2212–2216. https://doi.org/10.1002/chem.201103435.

(152) Souto, J. A.; Zian, D.; Muñiz, K. Iodine(III)-Mediated Intermolecular Allylic Amination under Metal-Free Conditions. *J. Am. Chem. Soc.* **2012**, *134* (17), 7242–7245. https://doi.org/10.1021/JA3013193.

(153) Souto, J. A.; Becker, P.; Iglesias, Á.; Muñiz, K. Metal-Free Iodine(III)-Promoted Direct Intermolecular C–H Amination Reactions of Acetylenes. *J. Am. Chem. Soc.* **2012**, *134* (37), 15505–15511. https://doi.org/10.1021/JA306211Q.

(154) Purkait, N.; Okumura, S.; Souto, J. A.; Muñiz, K. Hypervalent Iodine Mediated Oxidative Amination of Allenes. *Org. Lett.* **2014**, *16* (18), 4750–4753. https://doi.org/10.1021/OL502179Z.

(155) Prévost, C. Prévost Trans-Dihydroxylation. *Compt. Rend.* **1933**, *196*, 1129–1131. https://doi.org/10.1007/978-3-319-03979-4_222.

(156) Funes-Ardoiz, I.; Sameera, W. M. C.; Romero, R. M.; Martínez, C.; Souto, J. A.; Sampedro, D.; Muñiz, K.; Maseras, F. DFT Rationalization of the Diverse Outcomes of the Iodine(III)-Mediated Oxidative Amination of Alkenes. *Chem. – A Eur. J.* **2016**, *22* (22), 7545–7553. https://doi.org/10.1002/CHEM.201600415.

(157) Romero, R. M.; Souto, J. A.; Muñiz, K. Substitution Effects of Hypervalent Iodine(III) Reagents in the Diamination of Styrene. *J. Org. Chem.* **2016**, *81* (14), 6118–6122. https://doi.org/10.1021/acs.joc.6b01070.

(158) Sreenithya, A.; Hadad, C. M.; Sunoj, R. B. Hypercoordinate Iodine for Catalytic Asymmetric Diamination of Styrene: Insights into the Mechanism, Role of Solvent, and Stereoinduction †. **2019**. https://doi.org/10.1039/c9sc01513b.

(159) Ram, R. N.; Soni, V. K. Synthesis of α-Functionalized Trichloromethylcarbinols. *J. Org. Chem.* **2015**, *80* (17), 8922–8928. https://doi.org/10.1021/ACS.JOC.5B01547.

References

(160) Yoshimura, A.; Nemykin, V. N.; Zhdankin, V. V. O-Alkoxyphenyliminoiodanes: Highly Efficient Reagents for the Catalytic Aziridination of Alkenes and the Metal-Free Amination of Organic Substrates. *Chem. – A Eur. J.* **2011**, *17* (38), 10538–10541. https://doi.org/10.1002/CHEM.201102265.

(161) Yoshimura, A.; Zhdankin, V. V. Advances in Synthetic Applications of Hypervalent Iodine Compounds. *Chem. Rev.* **2016**, *116* (5), 3328–3435. https://doi.org/10.1021/acs.chemrev.5b00547.

(162) Zhu, C.; Yoshimura, A.; Ji, L.; Wei, Y.; Nemykin, V. N.; Zhdankin, V. V. Design, Preparation, X-Ray Crystal Structure, and Reactivity of o-Alkoxyphenyliodonium Bis(Methoxycarbonyl)Methanide, a Highly Soluble Carbene Precursor. *Org. Lett.* **2012**, *14* (12), 3170–3173. https://doi.org/10.1021/ol301268j.

(163) Cots, E.; Flores, A.; Romero, R. M.; Muñiz, K. A Practical Aryliodine(I/III) Catalysis for the Vicinal Diamination of Styrenes. *ChemSusChem* **2019**, *12* (13), 3028–3031. https://doi.org/10.1002/cssc.201900360.

(164) Yoshimura, A.; Yusubov, M. S.; Zhdankin, V. V. Synthetic Applications of Pseudocyclic Hypervalent Iodine Compounds. *Org. Biomol. Chem.* **2016**, *14* (21), 4771–4781. https://doi.org/10.1039/c6ob00773b.

(165) Zhou, B.; Haj, M. K.; Jacobsen, E. N.; Houk, K. N.; Xue, X. S. Mechanism and Origins of Chemo- and Stereoselectivities of Aryl Iodide-Catalyzed Asymmetric Difluorinations of β-Substituted Styrenes. *J. Am. Chem. Soc.* **2018**, *140* (45), 15206–15218. https://doi.org/10.1021/jacs.8b05935.

(166) Marsh, G. P.; Parsons, P. J.; McCarthy, C.; Cornique, X. G. An Efficient Synthesis of Nitroalkenes by Alkene Cross Metathesis: Facile Access to Small Ring Systems. *Org. Lett.* **2007**, *9* (14), 2613–2616. https://doi.org/10.1021/ol070557k.

(167) Yokoyama, A.; Maruyama, T.; Tagami, K.; Masu, H.; Katagiri, K.; Azumaya, I.; Yokozawa, T. One-Pot Synthesis of Cyclic Triamides with a Triangular Cavity from Trans-Stilbene and Diphenylacetylene Monomers. *Org. Lett.* **2008**, *10* (15), 3207–3210. https://doi.org/10.1021/ol801083r.

(168) Joucla, L.; Cusati, G.; Pinel, C.; Djakovitch, L. Heterogeneously Pd/C Catalysed Procedure for the Vinylation of Aryl Bromides. *Appl. Catal. A Gen.* **2009**, *360* (2), 145–153. https://doi.org/10.1016/j.apcata.2009.03.016.

(169) Bertini, V.; Alfei, S.; Pocci, M.; Lucchesini, F.; Picci, N.; Iemma, F. Monomers Containing Substrate or Inhibitor Residues for Copper Amine Oxidases and Their Hydrophilic Beaded Resins Designed for Enzyme Interaction Studies. *Tetrahedron* **2004**, *60* (50), 11407–11414. https://doi.org/10.1016/j.tet.2004.09.083.

(170) Wang, X.; Studer, A. Iodine(III) Reagents in Radical Chemistry. *Acc. Chem. Res.* **2017**, *50* (7), 1712–1724. https://doi.org/10.1021/acs.accounts.7b00148.

(171) Noyori, R. *Asymmetric Catalysis in Organic Synthesis*, 2nd editio.; Wiley & sons, Chichester, 1994. https://doi.org/10.1002/recl.19961150216.

(172) Zhou, Q.-L.; Wiley InterScience (Online service). *Privileged Chiral Ligands and Catalysts*; Wiley-VCH Verlag, 2011.

(173) Jacobsen, E. N.; Pfaltz, A.; Yamamoto, H. *Comprehensive Asymmetric Catalysis*; Springer, 1999.

(174) Zhdankin, V. V.; Stang, P. J. Chemistry of Polyvalent Iodine. *Chem. Rev.* **2008**, *108* (12), 5299–5358. https://doi.org/10.1021/cr800332c.

(175) Zhdankin, V. V. *Hypervalent Iodine Chemistry : Preparation, Structure, and Synthetic Applications of Polyvalent Iodine Compounds*; Wiley, 2013.

(176) Cots, E.; Flores, A.; Romero, R. M.; Muñiz, K. A Practical Aryliodine(I/III) Catalysis for the Vicinal Diamination of Styrenes. *ChemSusChem* **2019**, *12* (13), 3028–3031. https://doi.org/10.1002/cssc.201900360.

(177) Yusubov, M. S.; Zhdankin, V. V. Iodine Catalysis: A Green Alternative to Transition Metals in Organic Chemistry and Technology. *Resour. Technol.* **2015**, *1* (1), 49–67. https://doi.org/10.1016/j.reffit.2015.06.001.

(178) Romero, R. M.; Wöste, T. H.; Muñiz, K. Vicinal Difunctionalization of Alkenes with Iodine(III) Reagents and Catalysts. *Chem. – An Asian J.* **2014**, *9* (4), 972–983. https://doi.org/10.1002/ASIA.201301637.

(179) Claraz, A.; Masson, G. Asymmetric Iodine Catalysis-Mediated Enantioselective Oxidative Transformations. *Org. Biomol. Chem.* **2018**, *16* (30), 5386–5402. https://doi.org/10.1039/c8ob01378k.

(180) Hokamp, T.; Wirth, T. Hypervalent Iodine(III)-Catalysed Enantioselective α-Acetoxylation of Ketones. *Chem. - A Eur. J.* **2020**, *26* (46), 10417–10421. https://doi.org/10.1002/chem.202000927.

(181) Zhong, W.; Liu, S.; Yang, J.; Meng, X.; Li, Z. Metal-Free, Organocatalytic Syn Diacetoxylation of Alkenes. *Org. Lett.* **2012**, *14* (13), 3336–3339. https://doi.org/10.1021/ol301311e.

(182) Shimazaki, Y.; Wata, C.; Hashimoto, T.; Maruoka, K. Enantioselective Hydrative Para-Dearomatization of Sulfonanilides by an Indanol-Based Chiral Organoiodine Catalyst. *Asian J. Org. Chem.* **2021**, *10* (7), 1638–1642. https://doi.org/10.1002/ajoc.202100152.

(183) Deng, X.-J.; Liu, H.-X.; Zhang, L.-W.; Zhang, G.-Y.; Yu, Z.-X.; He, W. Iodoarene-Catalyzed Oxyamination of Unactivated Alkenes to Synthesize 5-Imino-2-Tetrahydrofuranyl Methanamine Derivatives.

J. Org. Chem **2021**, *86*, 2021. https://doi.org/10.1021/acs.joc.0c02047.

(184) Wu, F.; Kaur, N.; Alom, N.-E.; Li, W. Chiral Hypervalent Iodine Catalysis Enables an Unusual Regiodivergent Intermolecular Olefin Aminooxygenation. *JACS Au* **2021**. https://doi.org/10.1021/jacsau.1c00103.

(185) Wata, C.; Hashimoto, T. Organoiodine-Catalyzed Enantioselective Intermolecular Oxyamination of Alkenes. *J. Am. Chem. Soc.* **2021**, *143*, 1745–1751. https://doi.org/10.1021/jacs.0c11440.

(186) Uyanik, M.; Ishizaki, S.; Ishihara, K.; Zarate, C. Synthesis of Chiral Organoiodine Catalyst for Enantioselective Oxidative Dearomatization Reactions: N,N'-(2S,2'S)-(2-Iodo-1,3-Phenylene)Bis(Oxy)Bis(Propane-2,1-Diyl)Bis(2,4,6-Trimethylbenzamide). *Org. Synth.* **2021**, *98*, 1–27. https://doi.org/10.15227/orgsyn.098.0001.

(187) Uyanik, M.; Ishizaki, S.; Kazuaki Ishihara. Chiral Organoiodine-Catalyzed Enantioselective Oxidative Dearomatization of Phenols. *Org. Synth.* **2021**, *98*, 28–50. https://doi.org/10.15227/orgsyn.098.0028.

(188) Yoshida, Y.; Kanashima, Y.; Mino, T.; Sakamoto, M. Asymmetric Syntheses and Applications of Planar Chiral Hypervalent Iodine(V) Reagents with Crown Ether Backbones. *Tetrahedron* **2019**, *75* (28), 3840–3849. https://doi.org/10.1016/j.tet.2019.06.008.

(189) Miller, L. L.; Johnson, J. R. The Structure of Wedekind's Ketenium Compounds. *J. Org. Chem.* **1936**, *1* (2), 135–140. https://doi.org/10.1021/jo01231a001.

(190) Jones, F. M.; Arnett, E. M. Thermodynamics of Ionization and Solution of Aliphatic Amines in Water. In *Progress in Physical Organic Chemistry*; Streitwieser Jr., A., Taft, R. W., Eds.; John Wiley and Sons Ltd., 2007; Vol. 11, pp 263–322.

https://doi.org/10.1002/9780470171905.ch4.

(191) Eiji Takashiro, H.; Matsumoto, T.; Suzuki, K. Total Synthesis of the Gilvocarcins. *J. Am. Chem. Soc.* **1994**, *116* (3), 1004–1015. https://doi.org/10.1021/ja00082a023.

(192) Jalalian, N.; Olofsson, B. Design and Asymmetric Synthesis of Chiral Diaryliodonium Salts. *Tetrahedron* **2010**, *66* (31), 5793–5800. https://doi.org/10.1016/J.TET.2010.05.004.

(193) Fujita, M.; Wakita, M.; Sugimura, T. Enantioselective Prévost and Woodward Reactions Using Chiral Hypervalent Iodine(III): Switchover of Stereochemical Course of an Optically Active 1,3-Dioxolan-2-Yl Cation. *Chem. Commun.* **2011**, *47* (13), 3983–3985. https://doi.org/10.1039/C1CC10129C.

(194) Richardson, R. D.; Page, T. K.; Altermann, S.; Paradine, S. M.; French, A. N.; Wirth, T. Enantioselective α-Oxytosylation of Ketones Catalysed by Iodoarenes. *Synlett* **2007**, *2007* (4), 538–542. https://doi.org/10.1055/s-2007-967960.

(195) Altermann, S. M.; Richardson, R. D.; Page, T. K.; Schmidt, R. K.; Holland, E.; Mohammed, U.; Paradine, S. M.; French, A. N.; Richter, C.; Bahar, A. M.; Witulski, B.; Wirth, T. Catalytic Enantioselective α-Oxysulfonylation of Ketones Mediated by Iodoarenes. *European J. Org. Chem.* **2008**, *2008* (31), 5315–5328. https://doi.org/10.1002/ejoc.200800741.

(196) Mizar, P.; Laverny, A.; El-Sherbini, M.; Farid, U.; Brown, M.; Malmedy, F.; Wirth, T. Enantioselective Diamination with Novel Chiral Hypervalent Iodine Catalysts. *Chem. - A Eur. J.* **2014**, *20* (32), 9910–9913. https://doi.org/10.1002/chem.201403891.

(197) Guilbault, A. A.; Basdevant, B.; Wanie, V.; Legault, C. Y. Catalytic Enantioselective α-Tosyloxylation of Ketones Using Iodoaryloxazoline Catalysts: Insights on the Stereoinduction Process. *J. Org. Chem.* **2012**, *77* (24), 11283–11295.

https://doi.org/10.1021/jo302393u.

(198) Thérien, M. È.; Guilbault, A. A.; Legault, C. Y. New Chiral Iodooxazoline Catalysts for the I(III)-Mediated α-Tosyloxylation of Ketones: Refining the Stereoinduction Model. *Tetrahedron: Asymmetry* **2013**, *24* (19), 1193–1197. https://doi.org/10.1016/J.TETASY.2013.08.002.

(199) Hempel, C.; Maichle-Mössmer, C.; Pericàs, M. A.; Nachtsheim, B. J. Modular Synthesis of Triazole-Based Chiral Iodoarenes for Enantioselective Spirocyclizations. *Adv. Synth. Catal.* **2017**, *359* (17), 2931–2941. https://doi.org/10.1002/ADSC.201700246.

(200) Meyer, S.; Häfliger, J.; Schäfer, M.; Molloy, J. J.; Daniliuc, C. G.; Gilmour, R. A Chiral Pentafluorinated Isopropyl Group via Iodine(I)/(III) Catalysis. *Angew. Chemie Int. Ed.* **2021**, *60* (12), 6430–6434. https://doi.org/10.1002/ANIE.202015946.